



UNIVERSITY OF SOUTHERN QUEENSLAND

**Sustainable Hybrid Composite Sandwich Panel with
Natural Fibre Composites as Intermediate Layer**

A dissertation submitted by

JAUHAR FAJRIN

B.Eng., The University of Mataram, Indonesia, 1997
MSc(Eng), The University of Liverpool, United Kingdom, 2001

For the award of the degree of

Doctor of Philosophy

School of Civil Engineering and Surveying
Faculty of Health, Engineering and Sciences
December 2013

Abstract

Providing accommodation in a large scale at relatively affordable price has always been a challenging task not only for government but also for housing industry. There are two key factors in order to solve these two challenges. The first factor is to reduce the self-weight of the structure to maintain affordable prices. In building construction, the self-weight of a structure represents a large proportion of the total load on a structure. The adoption of appropriate material results in the reduction of element cross section, size of foundation and supporting elements thereby reduces the overall cost of the housing construction. The second factor is to utilize the panelised housing system to encourage the mass production of houses. With this construction system, a house can be built faster than stick-built homes. In most cases, panelised homes can be assembled in a matter of days which means that lesser labour is needed and more homes can be built. Other advantages of panelised homes are such as the system can eliminate costing delays, less weather damage during construction and also precision engineered to highest quality.

This research has been carried out to meet these challenges, which is aimed at developing a new type of hybrid composite sandwich wall panel that might be manufactured as modular panelised system. The typical sandwich panel used in building application commonly consists of metal skins and soft core. Although oriented strand board (OSB) is commonly employed for the skin of sandwich structure in structural insulated panels (SIPs), the observed shortcomings of this typical skin such as mould build-up and disintegration in the presence of flood water have reduced their usage. In this study, metal based skins of thin flat aluminium sheets were adopted. Metal skins are actually preeminent choice for their many advantages, but the price is always a concern. Consequently, reducing the thickness of the skin as much as possible is the only way to keep a competitive and reasonable overall cost. However, using thinner skins may result in the early failure of sandwich structure, such as face wrinkling or indentation. The sustainable hybrid concept offered in this research has been considered as a practical solution where an intermediate layer made from natural fibres composites (NFC) laminate was introduced.

In this regard, the research work has focused on four main stages to observe the suitability of natural fibre composites to be incorporated into the hybrid sandwich panels:

1. A validation of the concept of hybrid sandwich structure using a statistical based experiment approach.
2. An investigation of the mechanical properties of natural fibre composites that particularly prepared using vacuum bagging method.
3. An examination of structural behaviour of the hybrid sandwich panels under flexural and in-plane shear testing that includes a comparative analysis of the relative performance of hybrid and conventional sandwich panels, and also developing theoretical models to predict the behaviour of the developed hybrid sandwich panels.
4. A significance analysis of the experiment results using statistical software (Minitab 15) for both flexural and in-plane shear testing.

The investigation results throughout these four research work stages have provided clear evidence that, for structural application, natural fiber composite could be best employed as the intermediate layer of a hybrid sandwich panels.

Certification of Dissertation

I certify that the ideas, experimental works, results, analysis and conclusions reported in this dissertation are entirely my own effort, except where otherwise acknowledged. I also certify that the work is original and has not been previously submitted for any award, except otherwise acknowledged.

..... / /
Signature of Candidate

Endorsed:

..... / /
Signature of Principal Supervisor

..... / /
Signature of Associate Supervisor

..... / /
Signature of Associate Supervisor

Acknowledgements

I would like to express my deepest gratitude to my principal supervisors, A/Professor Yan Zhuge, for her excellent guidance, caring, patience and constant support throughout these years. She has been involved in all aspects of the study and I have learnt many things from her rich academic experience. I would like to thank to my associate supervisor Professor Frank Bullen for valuable advices and various useful suggestions regarding all the research works and also for his patiently corrected my writing both publication papers and the dissertation chapters. I would also like to thank A/Professor Hao Wang, my associate supervisor, for providing me with excellent atmosphere for doing research and also financial supports. A few informal discussions with him at the centre have also enriched my knowledge about academic networking and research collaboration. I also would like to express my great thank to the panel chairs for the confirmation of candidature; Professor Alan Kin-Tak Lau, Dr. Sourish Banerjee and Dr. Weena Lokuge.

I greatly appreciate the sponsorship from the Government of Indonesia, which made this PhD research possible. A huge thank also I would like to offer to Dr. Budi Indarsih, The director of the postgraduate sponsorship at The University of Mataram, for her wise advices and supports all the way through the years spent in this study.

I would like to acknowledge financial and technical support from the Faculty of Health, Engineering and Sciences and The Centre of Excellence in Engineered Fibre Composites (CEEFC). Also, I would like to say my warmest thanks to the technicians, Wayne Crowell and Mohan Trada, for their help and assistance during the experimental works. I am also very thankful for the administrative supports from Martin Geach. Amongst my fellow postgraduate students, I would like to say my special thanks to Mazed, Ghayana, Chamila, Zhang, Eris, Adriana, Ernesto, Sindy and Khrisna. They were good mates and were always willing to help and give their best. Many thanks to Professor Thiru Aravinthan, Dr. Allan Manalo, Dr. Mainul Islam, Dr. Jayantha Epaarachchi, Dr. Fransisco Cardona, for occasional valuable discussions.

I would also like to thank my parents; H. Mustafa and Hj. Siti Hafisah, and also father and mother in law; H. Muhammad and Hj. Siti Aminah, they were always supporting me and encouraging me with their best wishes. And last but not the least, many of the hours spent in the studying and writing up this dissertation that would otherwise have been spent with Suryani, Jasmine and Fadel - my lovely wife and children. My gratitude for their sacrifices cannot be measured. Lastly, to those whom I failed to mention but have been a great part of this research work, thank you very much indeed.

Associated Publications

Journals

Fajrin, J., Zhuge, Y., Bullen, F., Wang, H. (2011). The implementation of statistical inference to study the bending strength of sustainable hybrid sandwich panel composite, *Advanced Material Research*, Vols.250-253 (2011), pp 956-961.

Fajrin, J., Zhuge, Y., Bullen, F., Wang, H. (2011). Flexural strength of sandwich panel with lignocellulosic composites intermediate layer - a statistic approach, *International Journal of Protective Structure (IJPS)*, Vol. 2/No 4, December 2011., 453-464.

Fajrin, J., Zhuge, Y., Bullen, F., Wang, H. (2013). Hybrid sandwich panel with natural fibre composite intermediate layer: Manufacturing process and significance analysis, *Malaysian Journal of Civil Engineering (MJCE)*, Vol. 25/Special Issue (1), 2013, 95-111.

Fajrin, J., Zhuge, Y., Bullen, F., Wang, H. (2013). Significance analysis of flexural behaviour of hybrid sandwich panels, *Open Journal of Civil Engineering*, 2013, 3, 1-7, <http://dx.doi.org/10.4236/ojce.2013.33B001> Published Online September 2013 (<http://www.scirp.org/journal/ojce>)

Refereed Conference Proceedings

Fajrin, J., Zhuge, Y., Bullen, F., Wang, H. (2011). The implementation of statistical inference to study the bending strength of sustainable hybrid sandwich panel composite, 2011 International conference on Civil Engineering, Architecture and Building Materials (CEABM 2011) in Haikou, China, 18-20 June 2011.

Fajrin, J., Zhuge, Y., Bullen, F., Wang, H. (2012). New Concept for Optimal Application of Natural Fibre Reinforced Plastic (NFRP) in Building Construction, 8th Asia Pacific Structural Engineering & Construction Conference (APSEC 2012) and 1st International Conference on Civil Engineering Research (ICCER 2012), Joint conference Malaysia-Indonesia, Surabaya, 2-4 October 2012, pp 378-385.

Fajrin, J., Zhuge, Y., Bullen, F., Wang, H. (2013). Significance analysis of flexural behaviour of hybrid sandwich panels, 2013 Conference on Civil Engineering and Safety (CCES 2013), Beijing, China, 20-22 September 2013.

Table of Contents

List of Figures	viii
List of Tables	xiv
Notations	xvii
Chapter 1 Introduction	1
1.1. Some Benefits of Composite Sandwich Panels	1
1.1.1. Earthquake resistance	2
1.1.2. Structural insulated panels	3
1.1.3. Recent enhancements	4
1.2. The Utilization of Green Materials in Composites for Building Applications	5
1.3. The Application of the Hybrid Concept	5
1.4. Statistical Based Experimental Approach	6
1.5. Research Objectives and Scope	8
1.6. Dissertation Structure	9
1.7. Summary	10
Chapter 2 A Review of Composite Sandwich Panels and Sustainable Green Composites	12
2.1. General	12
2.2. The Structure of Sandwich Panels	13
2.2.1. Alternative structures and materials for sandwich panels	15
2.2.2. The Application of Sandwich Panel within the Building Industry	22
2.3. Sustainable Green Composites	26
2.3.1. Natural fibre composites (NFCs)	28
2.3.2. Wood plastic composites (WPC)	34
2.3.3. Lignocellulosic composites	35
2.3.4. The Application of Sustainable Green Composites in Building Structure	37
2.4. The Wide Spectrum of Hybrids	39
2.5. Chapter Conclusion	43
Chapter 3 Research Concept and Validation Process Using Statistical Experimental Design	45
3.1. Introduction	45
3.2. The Research Concept	45
3.2.1. Basic concept of sandwich panel	47
3.2.2. The hybrid sandwich panel model	56
3.3. Concept for Research Validation Process	60
3.3.1. Statistical experimental design	60
3.3.2. Simple comparative experiments	62
3.3.3. Single factor experiment	64
3.4. Validation process	67
3.4.1. Validation process using simple comparative experiment	67

3.4.2.	Validation process using single factor experiment	74
3.5.	Chapter Conclusions	83
Chapter 4	Preparation, Fabrication and Characterization of Natural Fibre Composites for Hybrid Sandwich Panel	85
4.1.	Introduction	85
4.2.	Natural Fibre Preparation and Chemical Treatment	86
4.2.1.	Natural fibre preparation	86
4.2.2.	Chemical treatment	87
4.3.	Manufacturing Natural Fibre Using Vacuum Bagging Method	92
4.4.	Characterization of Natural Fibre Composites	97
4.4.1.	Tensile test	99
4.4.2.	Flexural test	111
4.4.3.	Compression test	120
4.4.4.	Shear test	126
4.5.	General Discussions	133
4.6.	Chapter Conclusions	139
Chapter 5	Flexural Behaviour of Sustainable Hybrid Sandwich Panel	141
5.1.	General	141
5.2.	Flexural Test for Composite Sandwich Structure	142
5.3.	Sample Preparation	143
5.4.	Experimental Program	147
5.5.	Testing Results and Discussions	148
5.5.1.	Comparison of ultimate load	149
5.5.2.	Comparison of load-deflection behaviour	150
5.5.3.	Theoretical and experimental deflections	159
5.5.4.	Comparison of load-strain behaviour	164
5.5.5.	Comparison of mode of failure	167
5.6.	Chapter Conclusions	174
Chapter 6	Development of A Testing Rig for The Diagonal In-Plane Shear Test of Sandwich Panels	176
6.1.	General	176
6.2.	Shear Test for Composite Sandwich Panels	176
6.2.1.	Type of diagonal shear test	177
6.2.2.	Diagonal tension shear test of sandwich panels	180
6.3.	Investigation on Various Shear Testing Rig Designs	188
6.3.1.	Hardwood testing rig	188
6.3.2.	Assessment of different types of testing rig using small-scale prototypes	189
6.4.	Design of the Steel Testing Rig	193
6.4.1.	Testing rig preparation	193
6.4.2.	Trial testing with MDF board specimen	193
6.4.3.	Failure patterns	195
6.4.4.	Trial testing with sandwich panel specimen	197
6.5.	Chapter Conclusions	200

Chapter 7	The In-Plane Shear Behaviour of Sustainable Hybrid Sandwich Panels	201
7.1.	General	201
7.2.	Theoretical concept of diagonal tension shear test	201
7.3.	Sample preparation	205
7.4.	Experimental Program	208
7.5.	Testing Results and Discussions	210
7.5.1.	Comparison of ultimate load, in-plane shear load and shear stress	210
7.5.2.	Comparison of load-deflection behaviour	214
7.5.3.	Comparison of failure modes	218
7.5.4.	Comparison of load-strain behaviour	222
7.5.5.	The interpretation of diagonal shear test results	229
7.5.6.	Theoretical evaluation of shear strength of sandwich panels	232
7.5.7.	Comparison analysis between theoretical model and experiment results	236
7.6.	Chapter Conclusions	239
Chapter 8	Significance Analysis of The Flexural and In-Plane Shear behaviour of Hybrid Sandwich Panels	241
8.1.	General	241
8.2.	Significance and Statistical Analysis in Composite Research	241
8.3.	Significance Analysis for Flexural Behaviour of Hybrid Sandwich Panels	243
8.3.1.	Experiment results	243
8.3.2.	Analysis and discussions	246
8.4.	Significance Analysis for In-Plane Shear Behaviour of Hybrid Sandwich Panels	253
8.4.1.	Experiment results	253
8.4.2.	Analysis and discussions	254
8.5.	Chapter Conclusions	259
Chapter 9	Summary, Conclusions and Recommendations	261
9.1.	Summary	261
9.2.	Conclusions	263
9.3.	Recommendations	266
	References	268
	Appendix A	A-1
	Appendix B	B-1
	Appendix C	C-1
	Appendix D	D-1

List of Figures

Chapter 2 A Review of Composite Sandwich Panels and Sustainable Green Composites

<i>Figure</i>	<i>Figure Title</i>	<i>Page</i>
Figure 2.1.	<i>Left:</i> Typical form of sandwich panel structure (Zenkert, 1995). <i>Right:</i> Examples of structural sandwich panel elements (Davies, 2001)	13
Figure 2.2.	<i>Top-left:</i> Sandwich panel with fibrous core (Zhou and Stronge, 2005). <i>Bottom-left:</i> Sandwich panel with honeycomb core (Abbadi et al, 2009). <i>Right:</i> Sandwich panel with Kagome lattice core (Fan et al, 2007)	17
Figure 2.3.	Figure 2.3. <i>Upper:</i> Sandwich panel with Alporas core (Styles et al, 2007). <i>Bottom:</i> Sandwich panel with prismatic core (Wei et al, 2006).	19
Figure 2.4.	<i>Upper:</i> Sandwich panel with concrete core (Benayoune et al, 2006). <i>Bottom:</i> Sandwich panel with corrugated skin (Grenestedt and Reany, 2007).	21
Figure 2.5.	<i>Left:</i> Typical form of structural insulated panels (Mullens and Arif, 2006). <i>Right:</i> Metal SIP for building construction (MCA, 2010).	24
Figure 2.6.	Life-cycle phases relate to the flow of materials through the life of building (Kim and Rigdon, 1998).	27
Figure 2.7.	<i>Upper:</i> Composite structural panels with soy-oil resin (Dweib et al, 2004). <i>Bottom:</i> Cellular beam (Burgueno et al, 2005)	38
Figure 2.8.	<i>Upper:</i> Sandwich panel with shear keys (Mitra, 2009). <i>Bottom:</i> Sandwich panel with reinforcing tube inserts (Mamalis et al, 2002).	40
Figure 2.9.	<i>Left:</i> Sandwich panel with internal sheet (Jiang and Shu, 2005) <i>Right:</i> Sandwich panel with intermediate layer (Mamalis et al, 2008)	41

Chapter 3 Research Concept and Validation Process Using Statistical Experimental Design

<i>Figure</i>	<i>Figure Title</i>	<i>Page</i>
Figure 3.1.	Typical stress distribution in sandwich panel: (<i>top</i>) conventional sandwich panel, and (<i>bottom</i>) hybrid sandwich panel with intermediate layer	46
Figure 3.2.	Long and cross sections of sandwich panel loaded in 3-point bending	48
Figure 3.3.	The cross section in shear analysis for homogeneous beam	51
Figure 3.4.	Sketch of sandwich beam cross section for shear analysis	52
Figure 3.5.	(A) The shear stress in the faces and the complete shear stress distribution across the depth of the sandwich. (B) The corresponds simplified shear stress distribution in sandwich beam	53

Figure 3.6.	Basic assumption in ordinary beam theory	54
Figure 3.7.	New type of deformation due to core shear.	54
Figure 3.8.	Long and cross sections of hybrid sandwich panel loaded in 3-point bending	56
Figure 3.9.	<i>Left:</i> MTS Alliance RT/10 testing machine connected to computer device. <i>Right:</i> Sample set-up under three-point bending loads scheme.	68
Figure 3.10.	Bending stress (MPa) and improvement (%) of sandwich panel	70
Figure 3.11.	Strength to weight ratio (KNm/kg) and density (gr/cm ³) of sandwich panel	71
Figure 3.12.	Typical failure patterns of unmodified sandwich panel (<i>above</i>) and modified sandwich panel (<i>bottom</i>)	72
Figure 3.13.	Specimen preparation and flexural testing	75
Figure 3.14.	Bending stress (MPa) of sandwich panel beam tested under single factor experimental design	77
Figure 3.15.	Strength to weight ratio (<i>specific strength</i>) of sandwich structures for two different sample categories based on core used	78
Figure 3.16.	<i>Left:</i> Typical failure patterns of sandwich panels with balsa core. <i>Right:</i> sandwich panel with polystyrene core	79

Chapter 4 Preparation, Fabrication and Characterization of Natural Fibre Composites for Hybrid Sandwich Panel

<i>Figure</i>	<i>Figure Title</i>	<i>Page</i>
Figure 4.1.	Natural fibres incorporated in this research	86
Figure 4.2.	Chemicals used for the alkali treatment of natural fibres	90
Figure 4.3.	Step-by step of alkali treatment of natural fibres	91
Figure 4.4.	Final drying of natural fibres	92
Figure 4.5.	The combination of resin and hardener system used in this research	93
Figure 4.6.	Typical parts of vacuum bagging system (www.omeco.com)	94
Figure 4.7.	The equipment for vacuum bagging process used in this research	95
Figure 4.8.	Process of fabricating natural fibre composite laminates with vacuum bagging method in this research	96
Figure 4.9.	Natural fibre based panels and MDF panel prepared for mechanical characterization testing	98
Figure 4.10.	Setting-up testing machine for tensile test of NFCs	99
Figure 4.11.	The dot-plot diagram of the tensile strength of NFCs and MDF	103
Figure 4.12.	The dot-plot diagram of the tensile modulus of NFCs and MDF	106
Figure 4.13.	The dot-plot diagram of the Poisson's ratio of NFCs and MDF	107
Figure 4.14.	Typical load-extension graphs of different MDF	108
Figure 4.15.	Typical load-extension graphs of different NFCs	109
Figure 4.16.	Typical tensile failure patterns of different NFCs	110
Figure 4.17.	Setting-up for flexure test	112
Figure 4.18.	The dot-plot diagram of the flexural strength of NFCs	115
Figure 4.19.	The dot-plot diagram of the flexural modulus of NFCs	117
Figure 4.20.	Typical stress-strain graphs of different NFCs in flexure	118
Figure 4.21.	Typical flexure failure patterns of different NFCs	119

Figure 4.22.	Setting-up for compression test of NFCs	120
Figure 4.23.	The dot-plot diagram of the compressive strength of NFCs	123
Figure 4.24.	Typical compression failure patterns of different NFCs	124
Figure 4.25.	Typical load-crosshead graphs of different NFCs in compression	125
Figure 4.26.	Setting-up for shear test of NFCs	127
Figure 4.27.	The dot-plot diagram of the shear strength of NFCs	129
Figure 4.28.	Typical load-crosshead graphs of different NFCs in shear	131
Figure 4.29.	Typical shear failure patterns of different NFCs	132
Figure 4.30.	Shear and tensile strength of HDPE/Henequen fibre (80/20 v/v) composite (Franco and Gonzales, 2005)	133
Figure 4.31.	The average tensile strength values of different NFCs and MDF	133
Figure 4.32.	The average tensile modulus values of different NFCs and MDF	134
Figure 4.33.	The average Poisson's ratio values of different NFCs and MDF	135
Figure 4.34.	The average flexural strength values of different NFCs	137
Figure 4.35.	The average flexural modulus values of different NFCs	138
Figure 4.36.	The average shear strength values of different NFCs	139
Figure 4.37.	The average compression strength values of different NFCs	139

Chapter 5 Flexural Behaviour of Sustainable Hybrid Sandwich Panel

<i>Figure</i>	<i>Figure Title</i>	<i>Page</i>
Figure 5.1.	Sandwich panel fabrication process	145
Figure 5.2.	The schematic illustration of the flexural test for medium scale specimens	147
Figure 5.3.	The schematic illustration of the flexural test for large scale specimens	147
Figure 5.4.	The actual set up of flexural test	148
Figure 5.5.	The average maximum load carrying capacity and deflection against the type of intermediate layer of medium scale sandwich panels	150
Figure 5.6.	The average maximum load carrying capacity and deflection against the type of intermediate layer of large scale sandwich panels	150
Figure 5.7.	Load-deflection graphs of medium scale CTR specimens	151
Figure 5.8.	Load-deflection graphs of medium scale JFC specimens	152
Figure 5.9.	Load-deflection graphs of medium scale HFC specimens	153
Figure 5.10.	Load-deflection graphs of representative specimens for CTR, JFC and HFC in medium scale specimens	154
Figure 5.11.	Load-deflection graphs of large scale CTR specimens	155
Figure 5.12.	Load-deflection graphs of large scale JFC specimens	156
Figure 5.13.	Load-deflection graphs of large scale MDF specimens	156
Figure 5.14.	Load-deflection graphs of large scale MDF specimens	157
Figure 5.15.	Deformation due to core shear under third point loading scheme	159
Figure 5.16.	Load-strain relationship for medium scale sandwich panels	164
Figure 5.17.	Load-strain relationship for large scale sandwich panels	166
Figure 5.18.	Failure mechanisms of medium scale CTR specimen	168
Figure 5.19.	Failure mechanisms of medium scale JFC specimen	169
Figure 5.20.	Failure mechanisms of medium scale HFC specimen	170

Figure 5.21.	Failure mechanisms of large scale CTR specimen	171
Figure 5.22.	Failure mechanisms of large scale JFC specimen	172
Figure 5.23.	Failure mechanisms of large scale MDF specimen	173

Chapter 6 Development of A Testing Rig for The Diagonal In-Plane Shear Test of Sandwich Panels

<i>Figure</i>	<i>Figure Title</i>	<i>Page</i>
Figure 6.1.	Diagonal tension test using deformable square panel (Castenie et al, 2004)	178
Figure 6.2.	<i>Left:</i> Diagonal compressions shear testing arrangement. <i>Right:</i> actual testing (Ismail et al, 2010)	179
Figure 6.3.	<i>Left:</i> Testing arrangement. <i>Right:</i> actual testing set-up (Kuenzi et al, 1962)	180
Figure 6.4.	<i>Above:</i> Testing arrangement. <i>Bottom:</i> actual testing (Morgenthaler et al, 2005)	181
Figure 6.5.	<i>Left:</i> Panel shear test of plywood using compressive loading. <i>Right:</i> using tensile loading (Youngquist and Kuenzi, 1961)	182
Figure 6.6.	<i>Left:</i> Photoelastic model in position for loading. <i>Right:</i> isochromatic pattern for model showing the constant maximum stress for each fringe (Bryan, 1961)	183
Figure 6.7.	Shear test fixture described by De-Iorio et al (2002)	184
Figure 6.8.	<i>Left:</i> Testing arrangement. <i>Right:</i> actual testing (Bi and Coffin, 2006)	184
Figure 6.9.	<i>Left:</i> Testing arrangement. <i>Right:</i> actual testing (Hossain and Wright, 1998)	185
Figure 6.10.	<i>Left:</i> Testing arrangement. <i>Right:</i> actual testing (Kim et al, 2006)	186
Figure 6.11.	<i>Left:</i> Basic assumption. <i>Right:</i> Actual testing (Mosalam et al, 2008)	187
Figure 6.12.	Test results of the test using hardwood testing rig	188
Figure 6.13.	Testing set-up and failure mechanisms of the test with hardwood testing rig	189
Figure 6.14.	Front and side view of each prototype of testing rig	190
Figure 6.15.	The bar-chart of the testing results for each frame prototype	191
Figure 6.16.	Load-extension graph of the testing results for each frame prototype	191
Figure 6.17.	Failure mechanism for each frame prototype	192
Figure 6.18.	Proposed steel testing rig with the specimen inside	193
Figure 6.19.	The setting-up of the trial test with MDF board specimens	194
Figure 6.20.	The bar-chart of the trial test results with MDF panels	195
Figure 6.21.	The load-deflection curves of the trial test results with MDF panels	195
Figure 6.22.	Post-test failure patterns of corner-cut MDF panels	196
Figure 6.23.	Post-test failure patterns of whole MDF panels	196
Figure 6.24.	Bar-chart of trial tests with different conditions	197
Figure 6.25.	Load-extension graphs of trial tests with different conditions	198
Figure 6.26.	Failure mechanisms at the first and second trial of the test	199
Figure 6.27.	Failure mechanisms at the third and fourth trial of the test	199

Chapter 7 The In-Plane Shear Behaviour of Sustainable Hybrid Composite Sandwich Panels

<i>Figure</i>	<i>Figure Title</i>	<i>Page</i>
Figure 7.1.	Geometrical analysis of the picture frame (Mohammed et al, 2000)	201
Figure 7.2.	Schematic of the picture frame (Cao et al, 2008)	203
Figure 7.3.	Schematic of the diagonal tension test (Hossain and Wright, 1998)	204
Figure 7.4.	Schematic of testing set up as per ASTM 564 (ASTM, 1997)	204
Figure 7.5.	Special equipment and process of cutting EPS core for shear panel. (A) Volt-ampere, (B) Supporting frame, (C) Eye bolts, (D) and (E) Hot wire.	206
Figure 7.6.	Fabrication process for shear panel specimens	207
Figure 7.7.	Schematic illustration of diagonal tension shear test	208
Figure 7.8.	Actual test set-up for sandwich panel under diagonal tension shear test	209
Figure 7.9.	The configuration of strain gauges placement throughout the panels	210
Figure 7.10.	The average ultimate diagonal load and vertical deformation against the type of intermediate layer of sandwich panel	212
Figure 7.11.	The average ultimate in-plane shear load and shear displacement against the type of intermediate layer of sandwich panel	213
Figure 7.12.	The average shear stress and shear angle against the type of intermediate layer of sandwich panel	214
Figure 7.13.	Diagonal load-vertical extension of CTR specimens	215
Figure 7.14.	. Diagonal load-vertical extension of JFC specimens	216
Figure 7.15.	Diagonal load-vertical extension of MDF specimens	217
Figure 7.16.	Diagonal load-vertical extension of representative specimens for CTR, JFC and MDF sandwich panel	218
Figure 7.17.	Shear failure mechanism of CTR specimens	219
Figure 7.18.	Failure mechanism of sandwich panel under compression buckling load	219
Figure 7.19.	Shear failure mechanism of JFC specimens	220
Figure 7.20.	Shear failure mechanism of MDF specimens	221
Figure 7.21.	Load-strain (front side) relationship of representative of CTR specimens	222
Figure 7.22.	Load-strain (back side) relationship of representative of CTR specimens	223
Figure 7.23.	Load-extension graph of specimen CTR-2-12 and its mode of failure	224
Figure 7.24.	Load-strain (front side) relationship of representative of JFC specimens	224
Figure 7.25.	Load-strain (back side) relationship of representative of JFC specimens	225
Figure 7.26.	Load-extension graph of specimen JFC-1-12 and its mode of failure	226
Figure 7.27.	Load-strain (front side) relationship of representative of MDF specimens	226

Figure 7.28.	Load-strain (back side) relationship of representative of MDF specimens	227
Figure 7.29.	Load-extension graph of specimen MDF-1-12 and its mode of failure	228
Figure 7.30.	Load-strain relationship of different sandwich panels category	228

Chapter 8 Significance Analysis of Flexural and In-Plane Shear behaviour of Hybrid Sandwich Panels

<i>Figure</i>	<i>Figure Title</i>	<i>Page</i>
Figure 8.1.	Dot-plot diagram for medium scale samples under flexural test	244
Figure 8.2.	Dot-plot diagram for large scale samples under flexural test	244
Figure 8.3.	Dot-plot diagram for the in-plane shear test results	254
Figure 8.4.	The power curve of flexural test with medium scale specimens	259

List of Tables

Chapter 2 A Review of Composite Sandwich Panels and Sustainable Green Composites

<i>Table</i>	<i>Table Title</i>	<i>Page</i>
Table 2.1.	Mechanical properties of wood based material (Duggal, 2008)	37
Table.2.2.	The simulation results obtained by Mamalis et al (2008)	42

Chapter 3 Research Concept and Validation Process Using Statistical Experimental Design

<i>Table</i>	<i>Table Title</i>	<i>Page</i>
Table 3.1.	Experimental arrangements for simple comparative experiment (<i>small size</i>)	68
Table 3.2.	Experimental arrangements for simple comparative experiment (<i>large size</i>)	68
Table 3.3.	Bending strength (MPa) small size sandwich panel beam	69
Table 3.4.	Bending strength (MPa) larger size sandwich panel beam	69
Table 3.5.	Computer output using Minitab 15 software for the Two-Sample <i>t</i> -test	73
Table 3.6.	Summary of Two-Sample <i>t</i> -test results for all samples categories	74
Table 3.7	Experimental arrangements for single factor analysis	74
Table 3.8.	The result of single factor experiment	76
Table 3.9.	Computer output using Minitab 15 for the analysis of variance (Anova)	80
Table 3.10.	Summary of the Tukey's test result using Minitab 15	82
Table 3.11.	The result of Dunnet's test using Minitab 15	82
Table 3.12.	The summary of Fisher's test result using Minitab 15	83

Chapter 4 Preparation, Fabrication and Characterization of Natural Fibre Composites for Hybrid Sandwich Panel

<i>Table</i>	<i>Table Title</i>	<i>Page</i>
Table 4.1	Alkali treatment to different types of natural fibres-chemical composition and treatment time and temperature condition	88
Table 4.2.	Alkali treatment to different types of natural fibres-pre-post treatment and concluding remarks (references as per Table 4.1)	89
Table 4.3.	Properties of resin system (www.fgi.com.au)	93
Table 4.4.	Testing standards used for mechanical characterization of NFCs	98
Table 4.5.	Tensile properties of jute natural fibre composite	101
Table 4.6.	Tensile properties of sisal natural fibre composite	101
Table 4.7.	Tensile properties of hemp fibre and bamboo based composite	102
Table 4.8.	Tensile properties of medium density fibre (MDF)	102
Table 4.9.	Tensile strength and tensile modulus of different natural fibre composites from several literatures	111
Table 4.10.	Flexural properties of jute natural fibre composite	113
Table 4.11.	Flexural properties of sisal natural fibre composite	114
Table 4.12.	Flexural properties of hemp and bamboo natural fibre composite	114

Table 4.13.	Flexural strength and flexural modulus of different natural fibre composites from several literatures	119
Table 4.14.	Compressive properties of jute natural fibre composite	121
Table 4.15.	Compressive properties of sisal natural fibre composite	122
Table 4.16.	Compressive properties of bamboo based and hemp natural fibre composite	122
Table 4.17.	Compressive strength and compressive modulus of different natural fibre composites from several literatures	126
Table 4.18.	Shear properties of jute natural fibre composite	128
Table 4.19.	Shear properties of sisal natural fibre composite	128
Table 4.20.	Shear properties of bamboo based composite	128
Table 4.21.	Shear properties of hemp natural fibre composite	129
Chapter 5 Flexural Behaviour of Sustainable Hybrid Sandwich Panel		
<i>Table</i>	<i>Table Title</i>	<i>Page</i>
Table 5.1.	Properties of aluminium skin and EPS core	144
Table 5.2.	Experimental arrangements for flexural testing (<i>medium scale</i>)	146
Table 5.3.	Experimental arrangements for flexural testing (<i>large scale</i>)	146
Table 5.4.	Theoretical and experimental deflection values of medium scale sandwich panels for 50 and 100 N load.	161
Table 5.5.	Theoretical and experimental deflection values of large scale sandwich panels for 50 and 100 N load.	162
Chapter 6 Development of A Testing Rig for The Diagonal In-Plane Shear Test of Sandwich Panels		
<i>Table</i>	<i>Table Title</i>	<i>Page</i>
Table 6.1.	The configuration of small-scale testing rig prototypes	190
Chapter 7 The In-Plane Shear Behaviour of Sustainable Hybrid Composite Sandwich Panels		
<i>Table</i>	<i>Table Title</i>	<i>Page</i>
Table 7.1.	Sample arrangements for in-plane shear testing	207
Table 7.2.	Diagonal tension shear test results	211
Table 7.3.	Experimental results interpretation for CTR specimens	230
Table 7.4.	Experimental results interpretation for JFC specimens	231
Table 7.5.	Experimental results interpretation for MDF specimens	231
Table 7.6.	Comparison of the average results for different specimen groups	231
Table 7.7.	Predicted results using Modified-Kuenzi Model (Approach-1)	237
Table 7.8.	Predicted results using Modified-Kuenzi Model (Approach-2)	237
Table 7.9.	Predicted results using Modified-Hoff-Mautner Model	238
Table 7.10.	Predicted results using Modified-Mamalis Model	238
Table 7.11.	Predicted results using Classical Euler shear stress model	239
Chapter 8 Significance Analysis of Flexural and In-Plane Shear behaviour of Hybrid Sandwich Panels		
<i>Table</i>	<i>Table Title</i>	<i>Page</i>
Table 8.1.	Failure loads of medium scale samples under flexural test	243
Table 8.2.	Failure loads of large scale samples under flexural test	243

Table 8.3.	The results of normalization process for medium scale samples	245
Table 8.4.	The results of normalization process for large scale samples	245
Table 8.5.	Analysis of variance table for single-factor experimental design	246
Table 8.6.	Analysis of variance table for single-factor experimental design	247
Table 8.7.	Analysis of variance results for medium scale sandwich panel obtained by statistical software Minitab 15	247
Table 8.8.	The results of Tukey's test for medium scale sandwich panels obtained by statistical software Minitab 15	249
Table 8.9.	The results of Dunnet's test for medium scale sandwich panels obtained by statistical software Minitab 15	250
Table 8.10.	The results of Fisher's test for medium scale sandwich panels obtained by statistical software Minitab 15	250
Table 8.11.	The theoretical results of Anova for large scale sandwich panels	251
Table 8.12.	Analysis of variance results for large scale sandwich panels obtained by statistical software Minitab 15	251
Table 8.13.	The results of Tukey's test for large scale sandwich panels obtained by statistical software Minitab 15	252
Table 8.14.	The results of Dunnet's test for large scale sandwich panels obtained by statistical software Minitab 15	252
Table 8.15.	The results of Fisher's test for large scale sandwich panels obtained by statistical software Minitab 15	252
Table 8.16.	Failure loads of specimens tested under in-plane shear loading scheme	253
Table 8.17.	Tabulated data for analysis of variance (Anova) for in-plane shear test	253
Table 8.18.	The theoretical results of ANOVA for in-plane shear test	254
Table 8.19.	Analysis of variance results for in-plane shear test obtained by statistical software Minitab 15	255
Table 8.20.	The results of Tukey's test for in-plane shear test obtained by statistical software Minitab 15	256
Table 8.21.	The results of Dunnet's test for in-plane shear test obtained by statistical software Minitab 15	257
Table 8.22.	The results of Fisher's test for in-plane shear test obtained by statistical software Minitab 15	257
Table 8.23.	Statistical power value of each testing arrangement	258

Notations

Roman Alphabets

<i>Notation</i>	<i>Description</i>
a	Length of a panel
A	Initial cross-sectional area of the specimen; Area of cross-section between the notches
A_c	Area of the cut off portion
$A_c z_c$	The first moment of area of the cut-off portion about the centroidal axis
b	Width of a panel; width of specimen; Plate's breadth
c	Foam core of thickness
d	Depth; Plate thickness
D	Stiffness; Plate rigidity
E	Young modulus
E_c	Young's modulus of the core
E_f	Young's modulus of the face; Flexural modulus of elasticity
E_i	Young's modulus of the intermediate layer
$(EI)_{eq}$	Equivalent flexural rigidity
$(EI)_{core}$	Flexural rigidity of the core
$(EI)_{intermediate\ layer}$	Flexural rigidity of the intermediate layer
F	Applied force; Load; Measured force
F_{max}	Maximum load
F_s	Shear force components
F_x	Pulling force
F_0	F-value
G_c	Shear modulus of the core
h	Thickness of the specimen; Effective depth
H	Thickness
H_0	Null hypothesis
H_1	Alternative hypothesis
k	The stiffness
k_s	Shear buckling coefficient
L	Initial distance between grips; Span length
L_{cr}	Buckling load factor
h	Thickness of specimen
f_1, f_2	Facings thickness
$MS_{treatments}$	Treatments mean square
MS_E	Error mean square
N_{cr}	Buckling load
$n_1 ; n_2$	Sample sizes
P	Load; P-value
q_f	Shear buckling stress

Q	Shear force
S	Core shear parameters
$S' ; S''$	Beam mid-point deflections
$S_1^2 ; S_2^2$	The two individual sample variances
SS_t	Total corrected sum squares
$SS_{\text{treatments}}$	Sum squares due to treatments (i.e. between treatments)
SS_E	Sum squares due to error (i.e. within treatments)
t	Thickness of faces; Plate's thickness
t_o	The t-value
t_c	foam core of thickness
t_f	face sheets with thickness
U	Panel shear rigidity, N
V	Shear force
v	Poisson's ratio
y_{ij}	The ijth observation
$\bar{y}_1 ; \bar{y}_2$	Sample means
y_{ij}	The jth observation from factor level i
z	Depth

Greek Alphabets

<i>Notation</i>	<i>Description</i>
Δ	Shear displacement
ΔS	Difference in deflection between S'' and S'
ΔL	Increase of the distance between grips; Difference in load
ε	Strain in the longitudinal direction
ε_l	longitudinal strain
ε_n	Strain in the normal direction, with $n = b$ (width) or h (thickness)
ε_t	Nominal tensile strain
ϵ_{ij}	Normal random variable associated with ijth observation
ϵ_{ij}	Random error component
$\varepsilon_f'' ; \varepsilon_f'$	Flexural strains, corresponds to the given values of flexural strain $\varepsilon_f' = 0,0005$ and $\varepsilon_f'' = 0,0025$
λ_f	Poisson's ratio of facings
γ	Shear angle
σ_1	Stress (MPa) measured at the strain value of $\varepsilon_1 = 0,0025$
σ_2	Stress (MPa) measured at the strain value of $\varepsilon_2 = 0,0025$
σ	Flexural stress
ϑ	Poisson's ratio, expressed in a dimensionless ratio with $n = b$ (width) or h (thickness) indicating the normal value chosen
μ_i	Mean of the response at the ith factor level
μ_1	Mean of the response at the first factor level
μ_2	Mean of the response at the second factor level
μ_i	Mean of the ith factor level or treatment.

μ	Parameter common to all treatments called the overall mean
τ	Shear stress
τ_{ave}	Average shear stress
τ_i	Parameter unique to the ith treatment called ith treatment effect
σ	Tensile stress
σ_c	Compressive strength

CHAPTER 1

INTRODUCTION

1.1. Some Benefits of Composite Sandwich Panels

Global increases in population, development and urbanization accompanied by a desire for improvement in living standard places ever heavier demands on sustainability. One of the greatest challenges for the future to engineer will be to provide adequate, innovative, affordable and sustainable housing. Unfortunately while demand for housing has increased, supply has lagged resulting in significant price increases, especially in urban areas. Providing appropriate accommodation in a large scale has always been a challenging task not only for government but also for the housing industry. The question of how to provide appropriate housing on a large scale at relatively affordable prices has occupied the minds of planners and governments for many years.

There are two key factors that must be considered in order to attempt to solve those challenges. The first factor is reducing the actual weight of the structures to maintain affordable prices. In building construction, the self-weight of a structure represents a large proportion of the total dead load, and hence the cost. The adoption of appropriate construction materials may result in the reduction of element cross section, size of foundation and supporting elements thereby reducing the overall cost. The second factor is the utilization of prefabricated panelised housing systems to encourage the mass production of houses. A panelised housing system is a form of construction in which the large majority of housing components are pre-fabricated at a factory and shipped to the site for erection. With such a construction system, a house can be built faster than the current framed on site homes. In most cases, panelised homes can be assembled in a matter of days which means that lesser labour is needed and more homes can be built within the same time/labour frame. Other advantages of panelised homes

are that the system can eliminate costing delays, sustain less weather damage during construction and also the ability to be precision engineered to the highest quality.

Composite sandwich panels that are capable of being manufactured rapidly and cheaply in large quantities meet all the requirements of the optimal building component. Previously, composite sandwich panels have been widely used in manufacturing industries such as aerospace, marine and automotive. Continued development has now allowed it to become a viable choice in other applications such as civil and building infrastructure, particularly for lightweight applications. The high strength to weight ratio is the most recognized advantage of composite sandwich panels. The lightweight properties of composite sandwich panel also have the advantage of making them easy to transport, and that they require fewer resources to manufacture. Excellent insulation properties can also be incorporated in the design making the composite sandwich panel a popular alternative option in modern lightweight structures.

1.1.1. Earthquake resistance

An additional advantage of composite sandwich panel, due to their lightweight properties, is that they have good resistance to earthquakes. The earthquake force is related to the mass of building and its acceleration which means that the heavier the building, the more the force is exerted. Reducing the mass of structures or buildings is the most important factor to decrease the risk of earthquake damage (Ergul et al, 2003). When composite sandwich panels are utilized in building construction, some experts claim that the built-construction is a green construction. The less waste generated during the construction process is the reason for this claim. Hong et al (2012), stated that the common wet type of construction process results in a considerable amount of industry wastes and hazardous material. He also said that the presence of hazardous waste material leads to heavy economic loss for society as well as increasing energy consumption and the occurrence of environmental issues. Some researchers relate the earthquake resistance housing to sustainability. Lewis (2003) stated that damage and destruction caused by natural hazards is the arch-indicator of non-sustainable development. Earthquake resistant building is thus seen as a prerequisite for sustainable housing.

The conventional form of sandwich structure consists of two thin stiff and strong face layers which are separated by a thick, lightweight and low density core material.

The face sheets are bonded to the core using structural adhesive to obtain a load transfer between the components. The face sheets will act together to carry external bending moment, while the primary purpose of the core is to resist shear and to stabilize the faces against buckling or wrinkling. The faces usually consist of thin and high performing material, such as composite laminates made from carbon or glass fibres, while the core material is a low density with relatively low performing material which results in high specific mechanical properties of the panel under favourable loadings. The choice of constituent materials depends mainly on the specific application and design criteria of the sandwich panel products (Davies, 2001).

The most outstanding benefit of this type of composite structure is its high strength and stiffness to weight ratio (Zenkert, 1995; Zhou and Stronge, 2005; Schwarts and Givli, 2007, Moreira and Rodriguez, 2009). On the other hand, this typical structure also has a few drawbacks; they suffer from strong stress concentration at the interfaces between the face sheets, the weak adhesive layer and the core, as a consequence of the distinctly different properties of these materials in contact (Icardi and Ferrero, 2009). The layered configuration of the sandwich panel, the considerable differences in the elastic properties between the face-sheets and the core, and the manufacturing process make the panel susceptible to defects in the form of debonding between the face-sheets and the core (Schwartz and Givli, 2007). Overall, the use of sandwich panel contributes to earthquake resistance.

1.1.2. Structural insulated panels

It is believed that the most successful application of composite sandwich panels in housing industry is in the form of structural insulated panels (SIPs). The panels are made by sandwiching a rigid insulation foam core between two facesheets, typically oriented strand board (OSB). Currently the more conventional timber stud wall system is being replaced by SIP construction. The possibilities for energy efficiency and long-term cost saving can be explored through the use of this innovative building system. SIPs can be used either as a complete wall structure or a wall component over timber framing. Besides providing excellent structural integrity, SIPs also ensure a high level of environmental sustainability. The finished product will require less energy to maintain and also will use fewer materials than a conventionally built home, emit less pollution and result in an improved living space. At the component level, SIPs can be

used to construct an energy efficient curtain or cladding wall over timber framing. However, SIPs can create a strong, energy efficient building envelope on itself (Andrews, 1992; Mullens and Arif, 2006).

1.1.3. Recent enhancements

A lot of research work has been done on improving the properties of sandwich panel composite. The enhancement efforts were done by either improving skin or core properties or even introducing new element inside to form a hybrid sandwich structure. The first category is the enhancement of face sheet materials which have been extensively investigated by many researchers (Rocca and Nanni, 2005; Benayoune et al, 2006; Grenestedt and Reany, 2007; Kampner and Grenestedt, 2008; Russo and Zuccarello, 2007 and Van Erp and Rogers, 2008). The most important attempt is the introduction of fibre composites skin which has major impact on the use of sandwich panel composite. Some enhancements in this area are the development of a glass fibre-reinforced polymer face sheets by Van Erp and Rogers (2008) and the introduction of corrugated skins by Grenestedt and Reany (2007).

In the second category, extensive works have been carried out on dealing with the issue of enhancing the properties of core materials; Zhou and Stronge (2005) introduced a fibrous core which was an irregular arrangement of independent fibres, Fan et al (2007) reported their work on using Kagome lattice cores reinforced by carbon fibres, while a honeycomb core attracted a lot of researchers' attention (Master and Evans, 1996; Meraghni et al., 1999; Khan, 2006; Baral et al, 2010; Liu and Zhao, 2007). In the third category; a few studies have also been carried out on introducing new element to improve the properties of composite sandwich panel. A model of polymer composite structure with intermediate layer was developed by Jiang and Shu (2005), in which an additional sheet, called internal sheet was introduced into the core. More recently, Mamalis et al (2008) reported their work on employing intermediate layers between the face sheets and the core, also to improve the properties of composite sandwich panel. The reason for the additional layer is obvious in that it reduces the mismatch between stress levels and material functionality.

1.2. The utilization of Green Materials in Composites for Building Application

The term of sustainable or sustainability has many definitions, adaptations and applications. The most common and widely accepted meaning can be adopted from the term of sustainable development which is defined as meeting the needs of the present without compromising the ability of the future generations to meet their own needs (WCED in UN-Habitat, 2008). The concept of green or sustainable building is being more widely adopted in the construction industry as the awareness of the need for environment protection continues to rise. The key principles relate to the ecological sustainability of building include the use of raw materials based on renewable resources, products that are easily recycled and that are economic during the construction process (Berge, 2009). The concept of sustainable material integrates a variety of strategies during design, construction and site operation.

In relation to the principles of sustainability, natural fibres are a major renewable resource material throughout the world and specifically in the tropics. According to a Food and Agriculture Organization (FAO) survey, natural fibres like jute, sisal, coir, and banana are abundantly available in developing countries such as India, Srilanka, Thailand, Indonesia, Bangladesh, Philippine, Brazil, and South Africa. Recent reports indicate that plant fibres can be used as reinforcement in polymer composite to replace more expensive and non-renewable synthetic fibres such as glass especially in low pressure laminating (Mathur, 2006).

Currently, natural fibre reinforced composites have drawn more attention as alternative building materials, especially as wood substitutes in the developing countries. The concept of using natural fibre as a building component is actually not a new idea since it has been used centuries ago for different applications. It is worth noting at this early stage in the dissertation that in this research, natural fibres have been prepared as a laminate sheet using advanced vacuum bagging method for use as an intermediate layer in a hybrid composite sandwich panel.

1.3. The Application of Hybrid Concept

Although many efforts have been made to utilize natural fibres for building components, most were found to be either structurally or economically unviable. A bio-based building component with higher structural performance is normally achieved at the

expense of significantly higher cost as a larger size is typically required. Similarly, reducing the size to maintain the cost will only produce a building component with lower structural performance that may not be competitive with conventional building materials. For instance, Singh and Gupta (2005) in Mohanti et al (2005) stated that manufacturing of single layered natural fibre based panels as the alternative for plywood failed to possess the desired structural properties. The specific strength, stiffness and dimensional stability were inadequate. In order to cope with this problem, he developed composite laminates from hybrid natural fibres prepared using different type of natural fibres such as sisal, jute, coir mats and unsaturated polyester, phenolic or polyurethane resins.

In order to deal with those shortcomings, Christian and Billington (2009) suggested modifying the shape of structural components to overcome the inherent large deflection performance of natural fibre composites due to their low modulus of elasticity. Alternatively, hybridization at both the constituent and structural levels was recommended by Drzal et al. (2004). A hybrid structure is a combination of two or more materials in a predetermined geometry and scale, optimally serving a specific engineering purpose. There has, however been a certain duality about the way in which hybrids are observed. For example, Ashby and Brechet (2003) stated that a sandwich structure is an example of a hybrid material that reflects duality, sometimes it is regarded as a structure that consists of two skins with a thick core layer in the middle, but occasionally it is also viewed as a bulk material that has its own global density, stiffness and strength.

The hybrid concept introduced in this thesis can be explained as follows. A natural fibre composite (NFC) laminate is placed as an intermediate layer in between an aluminium skin and an EPS core to produce a hybrid composite sandwich panel. This new structure is a combination of two components, composite sandwich panel with aluminium skins and EPS foam core as an integrated sandwich structure and intermediate layer laminates made of NFRP that resulting in a hybrid composite structure.

1.4. Statistical Based Experimental Approach

Generally, experimental works in civil engineering field are conducted based on standardized test procedures. In this typical experiment, all conditions are kept constant

except those under investigation. The variation in the conditions under investigation are then measured and recorded in standardized form to obtain immediately readable results (Horath, 1995). The reason why this typical method is frequently employed in civil engineering field is due to time and cost constraint. The weakness of this type of experiment, however, is that the conclusion drawn is only based on the descriptive statistics which only tell the reader an immediately result without proper analysis how significant the differences between the conditions under investigation and those are kept constant.

There has a comparable method in statistical based experiment to the above method that is called as single factor experiment. This typical experimental design is the most common approach employed by many researchers to explore the difference among more than two levels of a factor. Antony (2003) addressed this type of experiment as a One-Variable-At-a-Time (OVAT), where one variable is varying during the experiment and all the rest variables are fixed. A single factor analysis is a process of analysing data obtained from experiment with different levels of a factor, usually more than two levels of factor.

There are some distinct advantages and disadvantages of the two different experimentally approach. The advantages of using standardized test procedures is that this typical method only involves smaller number of specimens so that they are more time efficient, less costly while maintaining reasonable accuracy. The data obtained is only based on the simple descriptive statistics analysis that may include mean, median and standard deviation. The disadvantages include potential bias of the result due to fewer samples employed, which may lead to error in interpretation of results and decrease the ability to generalize the result beyond the samples actually analysed. On the other hand, time and cost are the main drawbacks of statistical based experiment as it needs more samples to be involved in the analysis. The most advantage of statistical based experiment is that it can provide more accurate results since both descriptive and inferential statistics analysis are involved. Inferential statistics analysis can be defined as a process of inferring characteristics about a population, from a sample drawn from that population (Hicks, 1982). This process usually involves testing a hypothesis using appropriate rules, with the outcome that the hypothesis is either accepted or rejected.

There is a problem with the implementation of standardized test procedures as different countries tend to define specific procedures for their own implementation. Much research has been undertaken on composite sandwich panels. Most of the research however, has only presented test results descriptively without fully testing the research hypothesis using statistical inference. It is not surprising that the results of many published papers differ widely. In this study, a statistically based experiment was employed thoroughly in order to provide not only descriptive statistics data but also testing a specific hypothesis with inferential statistics analysis to obtain more information about the experiments conducted.

There are a number of excellent software products to assist researchers in both design and analysis phase of experiment. Some of the software includes Design-Expert, JMP and Minitab (Montgomery, 2009). The last two software-packages are widely available for general-purpose statistical software packages that have good data analysis capabilities. In this work, a Minitab version 15 has been employed thoroughly to analyse the experiment results.

1.5. Research Objectives and Scope

As already hinted at the previous section, the main objective of this research was to develop a new type of hybrid composite sandwich structure with an intermediate layer made from sustainable material. The mechanical and structural properties of the new sandwich panel were extensively investigated. The research steps may be described as:

- 1) Validate the concept of hybrid sandwich structure using a statistical based experiment approach. The flexural behaviour of sandwich structure with various intermediate layers and core materials was investigated using simple comparative and single factor experiments and the results will be analysed with both descriptive and inferential statistics.
- 2) Fabricate and characterize the mechanical behaviour of natural fibre composites for the intermediate layer of hybrid composite sandwich panel.
- 3) Investigate the flexural behaviour of the new hybrid composite sandwich panel in medium and large scale experiment and developing an analytical model to predict the deflection of the panel.

- 4) Examine the behaviour of the hybrid composite sandwich panel under in-plane shear loading experimentally and analytically. This included the design and development of apparatus testing equipment and also developing theoretical models to predict the in-plane shear strength of the developed hybrid sandwich panels.
- 5) Analyse the significance improvement of the new hybrid panel compared to the conventional sandwich panel structure using inferential statistical analysis. All the results of flexural and in-plane shear experiments were analysed using Minitab 15 software packages.

The outcome from this research is a new hybrid composite sandwich panel that has better structural properties and is more sustainable than the existing available products. The great benefit of this hybrid is the capability of structure to carry more loads without significant additional cost. The research is also expected to reinforce the use of proper statistical analysis. The statistical experimental design used in this research outlines procedures for determining the significance of the experimental results.

1.6. Dissertation Structure

This dissertation is presented through nine chapters as follows.

- 1) The first chapter is an introduction that explained all about general information of the current situation, background, research concept, objectives and outline of the dissertation.
- 2) Chapter 2 provides a review of alternative structure and material for composite sandwich panel in building application. This chapter commences with some information of existing composite sandwich panel structure and materials and their application for structural and non-structural component in building structure. The review of composite sandwich panel with green sustainable material is then presented followed by an overview of recent development in the use of sustainable composite sandwich panels for building applications. The chapter is concluded with a discussion on the need for the new hybrid structure for sustainable composite sandwich panel.

- 3) Chapter 3 is concerned with research concept and its validation using statistical based experiments. The chapter contains details of the hybrid sandwich panel concept and general information about statistical based experiments and its framework for the analysis. Validation process using simple comparative experiment and single factor experiment were included.
- 4) Chapter 4 describes all the work dealing with the preparation, fabrication and characterization of natural fibre composites. Chemical treatment of the fibre, fabricating process using vacuum bagging process and characterization of different natural fibre composites are discussed.
- 5) Chapter 5 presents the flexural behaviour of sustainable hybrid composites panels. This chapter covers the experimental program, experimental results and observation, developing theoretical model to predict the deflection of the panel and comparison of the proposed theoretical equation with the results of experiment.
- 6) Chapter 6 discusses the evaluation of the in-plane shear behaviour of the sustainable hybrid sandwich panel. The design and development of appropriate in-plane shear equipment is included.
- 7) Chapter 7 concerns with the in-plane shear behaviour of sustainable hybrid composites panels. This chapter includes the experimental program, experimental results and observation, developing theoretical model to predict the shear strength of the panel and comparison of the proposed theoretical equation with the results of experiment.
- 8) Chapter 8 focuses on the “significance analysis” using inferential statistics analysis. The inferential statistics analyse of the flexural and in-plane shear behaviour of sustainable hybrid sandwich panel are comprehensively discussed in this chapter.
- 9) Chapter 9 includes summary, conclusions of the research and recommendations for future research.

1.7. Summary

The utilization of green sustainable material in building application has become a popular trend. Although it has been developed quite intensively, most outcomes do not

satisfy either structural or economic requirements. Introducing a hybridization concept at both material and structural level provides a significant improvement to overcome the nature large deflection performance of natural fibre composites due to their low modulus of elasticity while retaining cost effectiveness.

This research fills the gap that exists in the area of sustainable green composite sandwich panels which previously has mostly concentrated on the conventional structural form. The research presents a new concept of the utilization of sustainable green composites as a part of a hybrid composite sandwich panel to obtain a new type of sandwich panel with higher load bearing capacity.

CHAPTER 2

A REVIEW OF COMPOSITE SANDWICH PANELS AND SUSTAINABLE GREEN COMPOSITES

2.1. General

In the last three decades the use of composite sandwich panels has been extended from the very basic to within incredibly advanced structures. It was originally primarily used for aerospace structure but now it has become a viable choice for various application fields including the transportation and building industries. Composites are well known by their high strength to weight ratio characteristic that makes them attractive to almost all engineering fields. The structural sandwich construction is one of the first forms of composite structures to have attained broad acceptance and usage (Marshall, 1998; Peters, 1998). In aerospace industry, sandwich structures have been extensively applied for almost all commercial airliners, helicopters and nearly all military air and space vehicles. Cargo containers, navy ship interiors, small boats and yachts, automobile parts all make extensive use of sandwich construction. This type of composite structure has also been widely used in building construction for non-structural components, such as for relocatable shelters, interior partitions, doors and windows. The application in the building industries has now widened to structural application in which the sandwich panels serve as a load carrying member such as with structural insulated panels (SIPs).

This chapter explores the literatures around the different types of sandwich panel structures and its materials constituents that have been developed to date. Particular attention will be given to the sandwich structures that relate to the building structure, although in the early sections of this chapter all different types of sandwich panel will be briefly discussed. The information is provided in a concise format as much research has been undertaken. More relevant literature review will be embedded in the specific

chapters when deal with a particular testing of the new hybrid sandwich panel developed by the writer.

2.2. The Structure of Sandwich Panels

A structural sandwich panel, as explained in ASTM C 274 (ASTM, 2007), is a special form of a laminated composite comprising of a combination of different materials that are bonded together so as to utilize the properties of each separate component to the structural advantage of the whole assembly. The sandwich structure always follows the same pattern. A pair of thin and strong skins is separated by a lightweight and thick core which has adequate stiffness in a direction normal to the face of the panel (Davies, 2001). There are many possibilities for material combination for this typical structure which enables optimum design to be produced for particular applications. The facings can be made of steel, aluminium, wood, fibre plastic and in some cases may be concrete. The core may be balsa wood, wood, different type of foams or even paper.

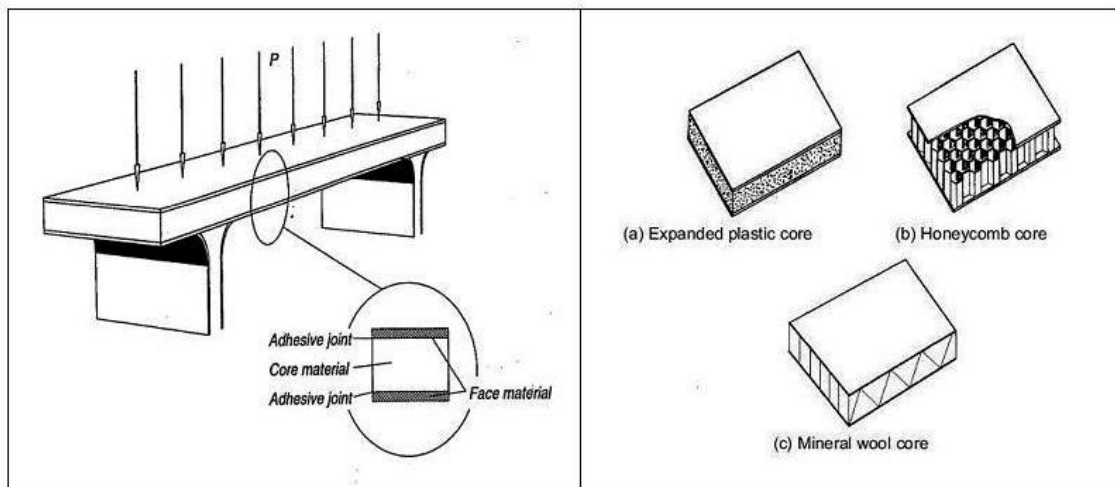


Figure 2.1. *Left*: Typical form of sandwich panel structure (Zenkert, 1995).

Right: Examples of structural sandwich panel elements (Davies, 2001)

There is a large range of material choices for sandwich panel structure. Zenkert (1995) stated that almost any structural material that is available in the form of thin sheet may be used to form the faces of sandwich panel. He also mentioned that the alternative of core materials has also increased dramatically in recent years since the introduction of different types of cellular plastics. However, the choice of core is also

dependent on the adhesive material used. For example, when polystyrene foam is used for a core, an ester-based adhesive, such as polyester or vinylester, cannot be used as foam will be dissolved by the styrene present in the adhesive resin.

The great advantage of this type of composite structure is its high strength and stiffness to weight ratio. The lightweight characteristics of this typical structure have the advantage of being very easy to transport, take fewer resource to manufacture and have excellent insulation properties. The advantages have ensured that structural sandwich panels have become important elements in modern lightweight building structures. More advantages outlined by Davies (2001) include excellent airtightness, capable of rapid erection, easy repair or replacement in case of damage, economical mass production and long life at low maintenance cost. Zenkert (1995) added further specific advantages such as high energy absorption, buoyancy and integration of functions such as thermal and acoustic insulation. In building applications, Davies (2001) explained that the combination of thin steel or aluminium facings with low density plastic or mineral wool cores in a sandwich structure have a particular combination of properties that make them ideal for use as walls and roofs. The combination of those two materials results in a sandwich panel that has higher load-bearing capacity, protection of the insulation against mechanical damage, weather protection, vapour barrier and corrosion protection.

Sandwich structures are widely used not only because they offer a high bending stiffness with minimum mass, but also because of their capability to be tailored to meet specific design requirements such as high damping properties and impact protection (Icardi and Ferrero, 2009). In recent years, they have been used as structural building components in many industrial and office buildings. Their use has now been extended to residential building construction due to their ability to improve both the structural and thermal performance of houses.

Although many authors considered a composite to consist of only two components, Zenkert (1995) stated that a sandwich structure consists of three main parts as illustrated in Figure 2.1; the skins, core and adhesive material. The skins will act together to carry external bending moment, while core resists shear loading and keep the skins separated and maintains a high section modulus. The other important role of core is also to stabilize the faces against buckling or wrinkling. The face sheets are

bonded to the core using a structural adhesive to obtain a shear load transfer between the components.

A more comprehensive explanation about the core and adhesive function is outlined by Davies (2001) who stated that the primary role of the core and its adhesive is to prevent the upper face slipping relative to the lower face. He also mentioned that the prevention of this undesirable performance requires a core with a sufficiently high shear modulus as well as adequate shear strength. In addition, Davies (2001) explained the core material and its adhesive play a critical role to restrain the upper face so that it does not suffer local buckling in compression, a phenomenon generally termed as wrinkling. Another reason why the mechanical properties of the core has critical role in the structural design is due to the fact that the stress at which wrinkling failure takes place is mainly dependent on the stiffness of the core.

Sandwich panels also have some weaknesses and limitations. The combination of two or more dissimilar materials has resulted in a complex phenomenon of failure mechanism (Mamalis et al, 2008). In addition, the design of structural elements made from sandwich composites is often a difficult task as reliable strength prediction requires the preliminary knowledge of the mechanical behaviour of the skins and core, as well as all peculiar damage mechanisms. Extensive works in this field have been carried out by many researchers to improve the structural behaviour of sandwich structure in which some researchers have studied successfully certain material combination either in the core or in the face layer to form a hybrid sandwich structures and some others have developed structural based solutions as discussed in the following section.

2.2.1. Alternative structures and materials for sandwich panels

As outlined in the previous section, sandwich panel possess several drawbacks that has limited their application. In order to address with the drawbacks, researchers have proposed a number of different concepts. The main concept presented is usually based on how to strengthen either the skin and/or the core. Some of the suggested improvements are discussed in the following section that consider both core and skin innovations.

Zhou and Stronge (2005) introduced a fibrous core sandwich that was thin and lightweight with face sheets separated by an irregular arrangement of independent fibres. The fibres had a random angle of fibre inclination and a range of initial curvatures. The through-thickness Young's modulus, initial compressive yield stress and fully plastic compressive stress of fibrous core structures were calculated. The conclusion drawn was that a large angle can increase the through-thickness Young's modulus, but at the expense of reducing the shear modulus. The best range of fibre angle of inclination depends on the specific application of the panel, as presented in Figure 2.2 (*top left*).

An experimental study on using Kagome lattice cores reinforced by carbon fibres for sandwich panel was reported by Fan et al. (2007). The sandwich panels were assembled with bonded laminate skins, as shown in Figure 2.2 (*right*). The mechanical behaviours of the sandwich panels were tested by out-of-plane compression, in-plane compression and three-point bending. Different failure modes of the sandwich structures were revealed. The experimental results showed that the carbon fibre reinforced lattice grids were much stiffer and stronger than foams and honeycombs. It was found that buckling and debonding dominate the mechanical behaviour of the sandwich structures, and that more compliant skin sheets had the potential to further improve the overall mechanical performance of the sandwich panels.

Sandwich panels with honeycomb cores were considered by many researchers (Master and Evans, 1996; Meraghni et al., 1999; Khan, 2006; Baral et al, 2010; Liu and Zhao, 2007). A honeycomb sandwich structure combines high flexural rigidity and bending strength with low weight. The idea of using honeycomb core is not an entirely new as it was developed as early as the 50's. One of pioneer study in this field was reported by Seidl (1956). The study was carried out at the Forest Product Laboratory, US Department of Agriculture, published as Report No 1918 (Seidl, 1956). The honeycomb core was prepared using corrugated paper of low resin content. The paper was pre-treated with resin in order to obtain a core that had good resistance to environmental effects such as damp or wet conditions. The resin used was phenol-formaldehyde type and the face sheet of the panels was made of different material such as veneer, plywood, hardboard, asbestos board and aluminium. Extensive testing on dry and wet condition showed that the performance of developed wall panels was

comparable to conventional house construction in term of bending strength and resistance to vertical loads. The thermal insulation was also relatively good and depended upon the density of the core.

Amongst the recent published works in this area was that by Abbadi et al, (2009) which examined the experimental and numerical outcomes around the utilization of honeycomb core for composite sandwich panel. The experimental testing was carried out via a four-point bending load. The typical honeycomb core sandwich panel tested is presented in Figure 2.2 (*bottom-left*). The sandwich panels were prepared using aluminium ($AlMg_3$) skins and the core were made either from aluminium sheets or aramide fibres folded and glued together forming a hexagonal cell structure. The honeycomb core is an opened cell with 2 different densities, 55 kg/m^3 and 85 kg/m^3 of aluminium and 48 kg/m^3 of aramide fibre with each density were replicates 4 times. The experimental part of this work concluded that the stiffness of sandwich panels increases as the overall density of the core raises. Similarly, the ultimate load rises with the increase in the density of the core. Other important finding was that the sandwich panels with an aramide core were more ductile than those with an aluminium core.

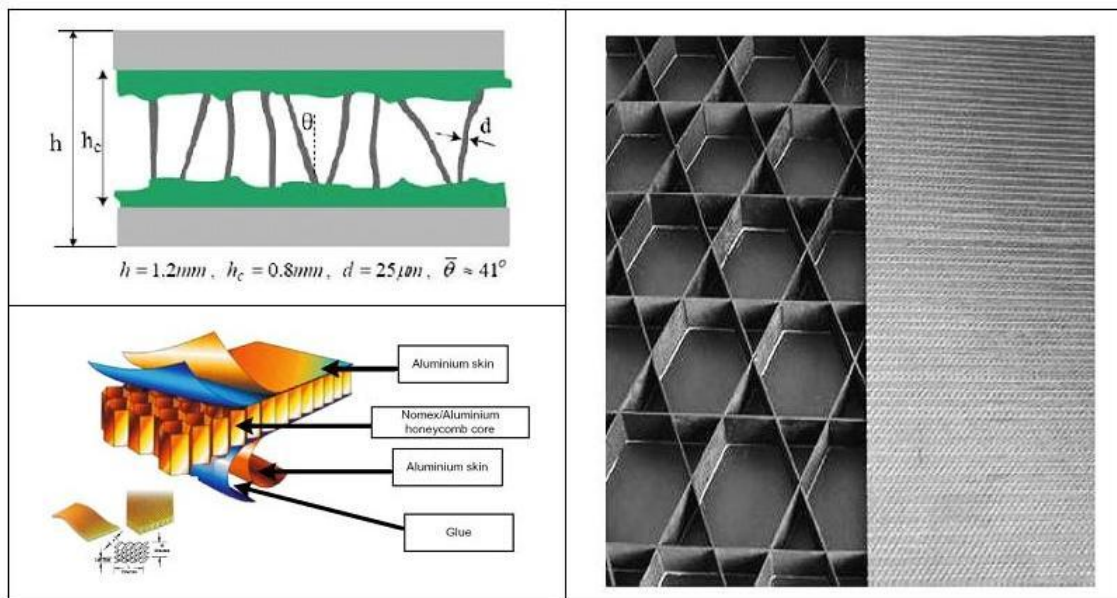


Figure 2.2. *Top-left*: Sandwich panel with fibrous core (Zhou and Stronge, 2005).
Bottom-left: Sandwich panel with honeycomb core (Abbadi et al, 2009).
Right: Sandwich panel with Kagome lattice core (Fan et al, 2007)

In 2008, He and Hu conducted a study that focused on the utilization of honeycomb core with particular focus on the weight ratio of the core. They found that the weight ratio range of honeycomb core, as deduced on the basis of optimum mechanical properties, offer a good foundation for the design of honeycomb sandwich panels. The optimum weight for the honeycomb core was 50–66.7% of the weight of the whole honeycomb sandwich panels, based on a theoretical analysis. The honeycomb sandwich panels were designed on that basis and the design results verified by good agreement between the theoretical and experimental outcomes.

Research on the utilization of carbon foam core was carried out by Sihm and Rice (2003) that aimed at examining the suitability of sandwich structure with ultra light-weight carbon foam core and laminate composite skins to be used in load-carrying structures. The tests were conducted under static and fatigue four-point bending load. The test results showed that the beams under static loadings behaved nearly linear elastically until the maximum failure loads, and then failed either in the yielding or in brittle mode following the post-failure behaviour of the carbon foam core.

Other type of core that frequently used in sandwich structure is wood based. Fernandez-Cabo et al (2010) reported the outcomes of their investigation on the development of sandwich structure that comprised of oriented strand board (OSB) skins and low-density wood fibre core. The sandwich panels were tested under shear and bending tests in small and full-scale with different densities. The results showed that density across a panel section was not constant. A quasi-linear behaviour was found for all the densities showing that a perfectly linear behaviour existed as the increasing of the density. The overall results of this work showed that the wood-based sandwich structure can be a viable solution for a cladding but included a recommendation that special care should be given to the selection of the facesheets due to the influence of hygro-thermal changes.

In order to overcome the shortcomings of polymer foam cores under high temperature, expanded metal mesh with foam infills have been introduced. The advantages of this typical core include good stiffness and strength to weight ratio, high impact energy absorption, good sound damping, electromagnetic wave absorption, thermal insulation and non-combustibility (Gibson, 2000; Styles et al, 2007). In addition, Styles et al (2007) reported on the use of aluminium foam core in a sandwich

structure. The core used was a closed cell aluminium foam commercially known as ALPORAS with a density of 0.23 g/cm^3 . The influence of core thickness on the deformation mechanism of the sandwich structure under four-point bending load was the focus of the investigation. The sandwich panels were prepared by placing a single ply of glass fibre/polypropylene pre-preg on either side of the aluminium foam core. The thickness of the core was varied to be 5, 10 and 20 mm, forming final panels with an average total thickness of 5.16, 10.19 and 20.47 mm. The results showed that samples with thinner core deformed through skin failure while the thicker panels failed due to indentation. In addition, the occurrence of core deformation increased with the core thickness.

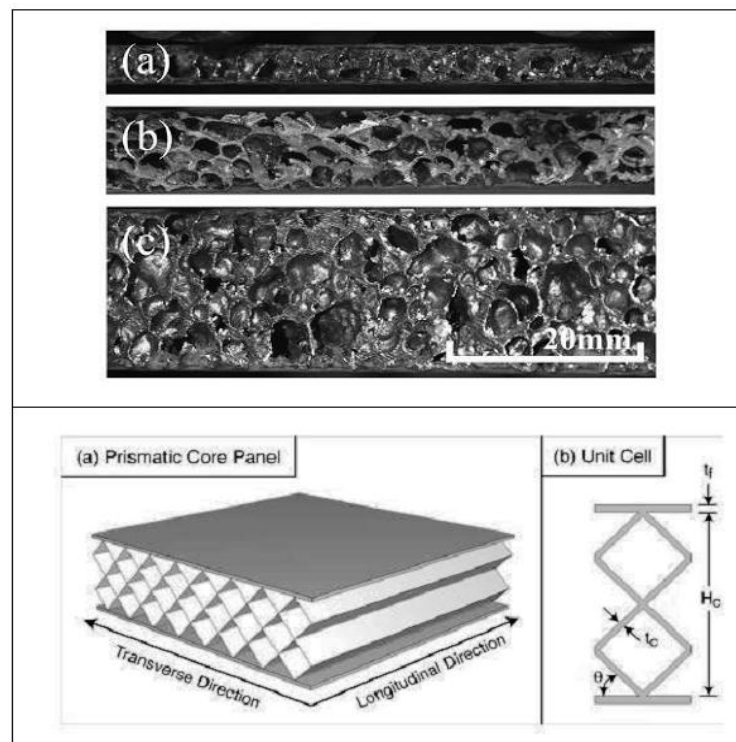


Figure 2.3. *Upper*: Sandwich panel with Alporas core (Styles et al, 2007).
Bottom: Sandwich panel with prismatic core (Wei et al, 2006).

Another effort to improve the performance of core was the use of a prismatic core (Lu et al, 2005). This typical core consists of a periodic array of diamond shaped prismatic cells. Wei et al, (2006) conducted an optimization study on the bending behaviour of the panels with this prismatic core. The panel with a prismatic core was compared to a corrugated core sandwich panel and a honeycomb core panel. It was concluded that when optimized solely for transverse loading, the prismatic core panels

outperformed those with corrugated core at lower loads and relatively comparable at high loads. Moreover, the corrugated core panel showed better performance when optimized solely for longitudinal loading. The overall comparison showed that the prismatic core panels performed similar to the corrugated core panels. While fabricating prismatic core incurred some additional cost, it was also noted that from structural point of view, the jointly optimized corrugated panels were competitive with honeycomb core panels particularly at higher load capacity.

Other research has focused on improving the properties of sandwich structures by enhancing the quality of facesheets. Skins improvement can be achieved by modification of material properties or geometrical shape. Sandwich panel with corrugated skins, as presented in Figure 2.4 (*bottom*), was introduced by Grenestedt and Reany (2007). They reported that corrugated skins could substantially increase the wrinkling strength of compression loaded sandwich specimens without increasing the weight. This type of sandwich had one or both face sheets corrugated to carry some of the loads usually carried by the core. A further study to this work was carried out by Kampner and Grenestedt (2007) in which finite element analysis and other analytical tools were used to point out some of the potentials as well as limitations of using corrugated skin to carry shear loads. It was found that employing corrugated skin improved shear carrying capability and offered weight saving, particularly for heavily loaded sandwich beams.

A newer generation of fibre composite sandwich panel was developed by Van Erp and Rogers (2008) that consisted of glass fibre-reinforced polymer face sheets and a modified phenolic core material. The flexural behaviour and collapse pattern of this sandwich composite beam was examined by Manalo et al (2009) in flatwise and edgewise positions. The experimental testing showed that the flatwise beam specimens collapsed in a sudden, brittle type. In edgewise position, the presence of fibre composite skins prevented the sudden failure of the beam. The overall conclusion that was drawn from the investigation was that this innovative composite sandwich structure was suitable for structural beam application.

Research on the development of precast concrete sandwich panels (PCSP) was reported by Benayoune et al (2006). The concept involved placing a layer of insulation in between two concrete layers that are called wythes. The concrete wythes skins are

connected by a concrete webs, steel connectors or the combination of them. The sandwich panels with various slenderness ratios were subjected to eccentric loads. The data of variation of strains across the insulation layers, strain in the shear connectors, crack appearance and propagation under increasing load and the deflection characteristics were recorded and analysed. Another parameter that was also studied on was the role of the shear connectors in transferring load from the skins to the core ensuring that the structure behaves as a composite. The results showed that the PCSP behaved in fully composite manner under the eccentric load until collapsed. The main conclusion was that the ultimate strengths were found to decrease non-linearly with the increase of the slenderness ratio.

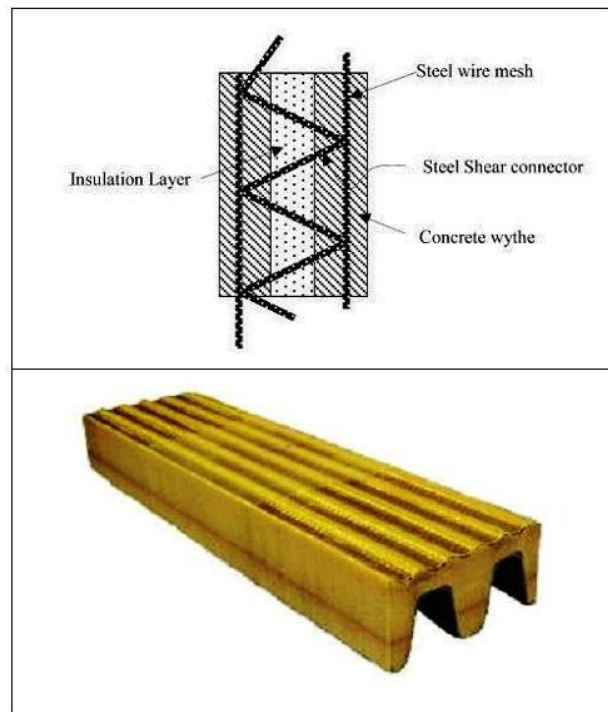


Figure 2.4. *Upper:* Sandwich panel with concrete core (Benayoune et al, 2006).
Bottom: Sandwich panel with corrugated skin (Grenestedt and Reany, 2007).

A sandwich structure with glass fibre reinforced plastics (GRFP) skins and PVC foam or polyester mat cores was developed by Russo and Zuccarello, (2007). This type of sandwich panel was specifically designed for marine construction. The research involves experimentally and numerically aspects with two different cores employed. The skins were 3 mm thick of fibre-glass laminates fabricated by a hand lay-up method. The two cores were a 4 mm thick thermosets polyester mat commercially known as COREMAT[®] and closed cell PVC foam called Divinycell[®]. The samples were a 16 mm

total thickness of sandwich panel with Divinycell[®] core and 10 mm for the COREMAT[®] core. The panels were tested using 3 and 4 points bending loads and shear, flatwise tensile and flatwise compressive tests were also conducted. This work concluded that the theoretical prediction of the strength and the actual failure mechanism of this type of sandwich structure were difficult, especially in the presence of prevalent shear loading. The eventual stress orthogonal to the middle plan of the sandwich structure strongly influenced the failure mode and strength. This particular stress results in an early skin-core delamination in sandwich structures with PVC core, and core shear-cohesive failure in the structures with polyester mat.

Other work in the area of using glass-fibre skins was carried-out by Rocca and Nanni (2005) which employed a fibre reinforced foam core. The core was closed-cell foam combined with dry fibres produced by WebCore Technologies. The thickness of the foam core was 76.3 mm (3 in) and glass reinforcement placed creating a hybrid stitched fibre reinforced foam core characterized by stitches in longitudinal direction and by contiguous webs in the transversal direction. The glass-fibre skin consisted of a pre-attached GFRP plus several layers of bi-directional E-glass fabric added during the fabrication with the final total thickness of the skin of about 6.35 mm. The sandwich panel was developed for the transportation industry. Static and dynamic fatigue tests focused on the ultimate capacity and the stiffness of the structure under compressive and flexural loadings. It was found that under static compressive load, the load-deformation curves were essentially linear with some ductility behaviour beyond the peak load. In the flexural test, it was observed that the bending stiffness corresponding to the fatigue conditioned beams were slightly higher than values obtained under static loading. It was also noted that the uniformity of composite structure had a direct effect on the overall performance so that particular care was required during the manufacturing process.

2.2.2. The application of sandwich panel within the building industry

The early application of composite sandwich structure in buildings structure was mostly for non-structural components. As mentioned earlier, those applications include relocatable shelters, interior partitions, doors and windows. There were some limitations at the early stage development of sandwich panels; one of them being the low quality of

the adhesives. The early production of sandwich panels, casein glue and urea-formaldehyde were extensively used with wood facings and cores (Marshall, 1998; Peters, 1998). He also explained that the continuous search for better adhesives subsequently resulted in the development of new higher quality adhesive such as rubber-phenolic and vinyl-phenolic. Since then, many further developments have been achieved including the development of sandwich panels for load carrying capacity in residential construction such as for roofs and walls. Perhaps the most successful application of sandwich panel in building construction is in the form of structural insulated panels (SIPs).

SIPs are a simple composite sandwich panel consisting of three layers. SIPs typically consist of two outer skins and an inner core of insulating material to form a monolithic unit using a structural grade adhesive (Tracy, 2000). Most structural insulated panels use oriented strand board (OSB) for their facings. Other materials that have been used for face sheets include plywood, fibre cement board and metal. The core of SIP is typically made from expanded polystyrene (EPS), extruded polystyrene (XPS), or polyurethane. However, virtually any bondable material could be used as a facing and any rigid insulation for the core. When acting separately, the insulating core and the face sheets are both non-structural and insubstantial components in themselves. When bonded together using structural adhesive under strictly controlled conditions, these materials act synergistically to form a composite material. SIPs can be used either as a complete wall structure or as a wall component. At the component level, SIPs can be used to construct an energy efficient curtain wall over timber framing. However, SIPs can create a strong, energy efficient building envelope in itself (Andrews, 1992; Mullens and Arif, 2006).

Construction with SIPs takes less time, money and labour while producing high performance, sustainable buildings. With SIP construction, homes and lightweight commercial buildings can be built more quickly, easily and cost effectively. At the first stage of construction process, lower energy cost might not be a significant thing, but for a whole life-service of a building the SIP is a good choice (Tracy, 2000). Kermany (2006) stated that the greatest benefit of SIP is that the structural support and the insulation are incorporated into a single system during the manufacturing process which enables a high quality, more accurate, thermal effectiveness and a greater level of

structural support to be achieved. A product guide issued by Structural Insulated Panel Association (SIPA) in 2007 indicates that a high density insulating core also enables the structures to be assembled with minimal framing. The more framing, the higher framing factor and the more energy lost due to thermal bridging. Framing factor is defined as the percentage of area in a wall assembly composed of sawn lumber. A typical SIP home averages a framing factor of only a 3%, while stick-framed homes averages a framing factor ranging from 15% to 25 percent%.

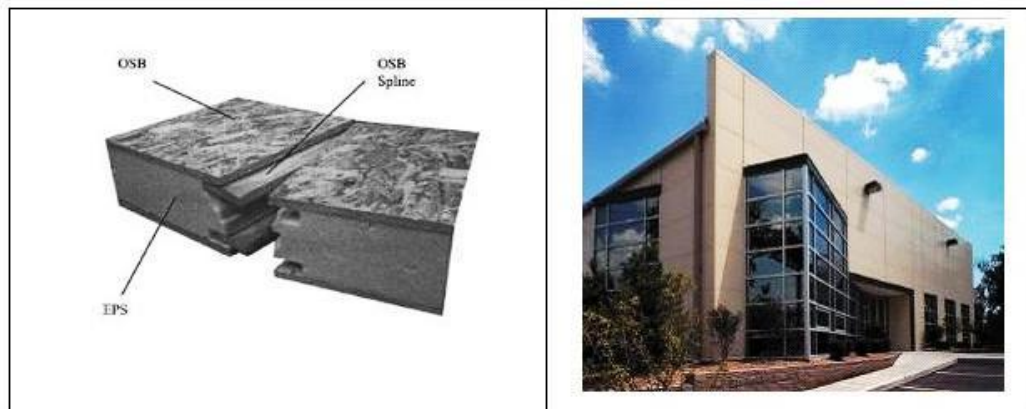


Figure 2.5. *Left:* Typical form of structural insulated panels (Mullens and Arif, 2006).
Right: Metal SIP for building construction (MCA, 2010).

A report prepared by The Federation of American Scientist for The Charles Pankow Foundation (Kelly, 2009), also stated that oriented strand board (OSB) facings are used for the vast majority of SIPs. OSB is an engineered wood product made from cross oriented layers of thin, rectangular wooden strips compressed and bonded together with wax and resin adhesives. OSB has been extensively tested as a load-bearing material and is commonly available in large sizes. Metal SIP manufacturers often use aluminium as a skin material. This structural panel system is used in both residential sites, such as carports or walkways, as well as industrial systems, such as in the construction of cold storage facilities.

Although the common type of SIP that consists of OSB skins and EPS core meets the requirements for structural applications, research on either improving the properties or introducing new constituent materials have been ongoing. The hurricane Katrina in New Orleans in 2005 damaged many houses built with OSB SIPs due to windborne missiles and this has been one motivation for research into better SIPs.

Several research efforts that relate to the development of new structural insulated panels are discussed below.

Kawasaki et al (2009) developed a wood-based sandwich panel with low-density fibreboard core for structural insulated walls and floors, with different face materials. The authors claimed that heat retention property of low-density fibreboard was superior to the current commercial insulators such as plastic foams and mineral wools. This claim was based on their work in 1998, in which ultra-low density fibreboard for core material was developed. In this work, some wood-based sandwich panels with low density fibre board core were fabricated with different thickness, core density and face materials. The elastic and shear moduli were determined after conducting four-point out-of-plane bending tests. The flexural rigidities of these panels were discussed extensively.

Vaidya et al (2010) developed an innovative composite structural insulated panel (CSIP) for exterior walls of a modularized structure. The face sheets of the CSIP consisted of E-glass fibres impregnated with polypropylene matrix and EPS foam core. Two primary testing schemes were conducted, i.e. uniaxial compressive loading and high velocity impact (HVI). The mode of failure observed under concentric load was buckling, while the eccentrically loaded panels failed by delamination between the core and the face sheets. For this eccentrically loaded test, panels failed at a load of 17 kN, which was 6.25 percent greater than the design load specified by American Plywood Association (APA) design guide (APA, 1998). The deflection at the design load was observed to be 3 mm which was less than the allowable deflection of 16.25 mm as obtained from ACI 318-05 (ACI, 2005). Under HCI, this CSIP could withstand the equivalent impact energy of 66.7 N of 5.1 cm x 10.2 cm wind missile travelling at a speed of 44.7 m/s which is the standard developed by Federal Emergency Management Agency (FEMA), FEMA 361 (Vaidya et al, 2000). A similar type of composite structural insulated panels (CSIPs) that consisted of orthotropic thermoplastic glass/polypropylene laminate as face sheets and EPS as a core was developed by Mousa and Uddin (2010). The CSIPs have a considerably high face sheets/core moduli ratio ($E_f/E_c=12.500$) compared to the ordinary sandwich construction. This investigation presented models for interfacial tensile stress and critical wrinkling in-plane stress associated with the debonding of CSIP. The models were validated using full-scale

experimental testing. The experimental testing was performed according to the ASTM E 72 standard (ASTM, 1997) which deals with testing panels for building application. All panels tested failed by face sheets debonding with a natural half-wavelength approximately equal to the core thickness.

2.3. Sustainable Green Composites

Green construction, also known as sustainable building, refers to a structure and using process that is environmentally responsible and resource-efficient throughout a building life-cycle. The process includes design, construction, operation, maintenance, renovation and demolition (Ji and Plainiotis, 2006). The primary objective of the green building practices is to reduce the environmental impact of buildings. Green building concept brings together practices and techniques that can reduce the impacts of a building and its surrounding aspects on the environment and the health of human life.

Although green or sustainability can be associated with all aspects of buildings such as design and energy efficiency, material efficiency, operations and maintenance efficiency and waste reduction, the current section will specifically emphasize on the material aspects. The easiest way to begin incorporating sustainable design principles in buildings is by carefully selecting materials that are environmentally friendly to human health. The selection process of sustainable materials can be done through three phases as explained by Kim and Rigdon (1998). Firstly, understanding the environmental impacts of the material in the pre-building phase will lead to the wise selection of building materials. Some aspects that need to be considered are such as raw material procurement methods, manufacturing process and the transportation process. These aspects are incorporated in the pre-building phase that consists of extraction, processing packaging and shipping. The ecological damage related to the gathering of materials and the conversion process into building material that includes loss of wildlife habitat, erosion, and water and air pollution, has to be considered as well. Secondly, knowing the natural occurrence of material during the building phase is the next essential thing for the material selection. The building phase refers to the effective or useful life of a material that begins with the assembling process into a structure, includes the maintenance and repair of the material, and extends throughout the material's life as part of a building. Included in this consideration is the waste generated on a building

construction site. The critical aspect in this case is whether the waste can be reduced to the fewer amounts or the waste can be recycled. Thirdly, understanding what will occur to the building materials after their service life, or post-building phase, is the last crucial part on the selection process for sustainable categorization. The post-building phase started when the function of materials as a part of buildings has expired. At this stage, the material may be reused, recycled or discarded. The three subsequent processes can be schematically presented as shown in the Figure 2.6.

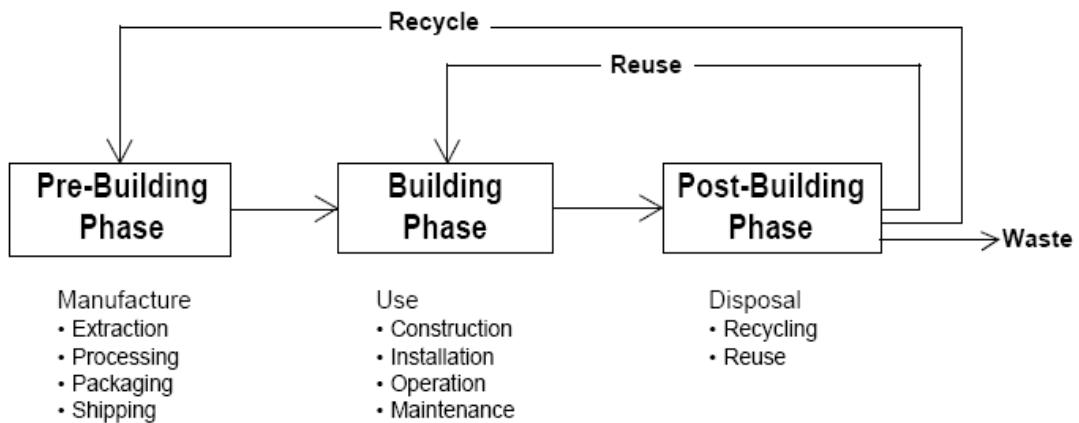


Figure 2.6. Life-cycle phases relate to the flow of materials through the life of building (Kim and Rigdon, 1998).

It is clear that the use of natural-based materials meets the prerequisites as a sustainable material. The less pre-processing prior to incorporation in building structure, lower embodied energy and toxicity, and easy to re-use or recycle has theoretically placed them as a renewable material. When natural-based materials are integrated in building products, the products become more sustainable. There are a number of reasons for the increase of awareness in natural-based such as recent concerns over declining petroleum supplies, increased government legislation, and a greater emphasis on sustainability and biodegradability (Staiger and Tucker, 2008; Pickering, 2008). More comprehensively, Hanninen et al, (2010) described the reasons as follows. Natural fibres have a potentially lower environmental burden than the man-made fibres. In addition, the ability of natural fibre to biodegrade naturally alleviates some of the potential problems associated with the disposal or recycling of man-made counterparts. Another aspect of potential reduction in environmental impact than can be provided by using natural fibre composites is the substitution of existing materials that delivers Sustainable Hybrid Composite Sandwich Panel with Natural Fibre Composites as Intermediate Layer

higher burden to the environment. Two particular examples are the replacement of treated timber with wood plastic composites (WPC) and the replacement of glass fibre reinforced polymer (GFRP) composites in automotive industry with natural fibre composites (NFC). In the later case, the lightweight of NFC is about 60% lighter than its GFRP composites counterpart and offers significant reduction of the weight of automotive products. From an automotive point of view, lower weight means less fuel consumption and reduced the CO₂ emissions.

Natural-based material composites are generally separated into two categories that distinguished by their materials origin. The composites derived from wood-based material are known as wood plastic composites (WPC) and those derived from non-wood materials are called as natural fibres composites (NFCs), or in some literatures called natural fibre reinforced polymer or plastics (NFRP) composites. They may contain natural fibres reinforced conventional polymer or the whole composites derived from both natural fibre reinforcement and bio-matrix. It has been argued that the first group of composites is not entirely biodegradable. Drzal et al, (2004) stated that the bio-composite derived from natural fibres and petroleum based thermoplastics or thermosets are not fully environmentally friendly as the matrix resins are not degradable while the bio-based content of the final composite products falls within the definition of bio-based materials. The following sections will explore composites derived from natural based materials.

2.3.1. Natural fibre composites (NFCs)

One of the most emerging natural-based products that have attracted attention are known as natural fibre reinforced plastics (NFRP) composites, or natural fibre composites (NFCs). As the name implies, the NFCs composite is a class of composite that contains natural fibres mixed with synthetic or bio resins that are inherently environmentally beneficial. Other advantages of NFC are well explained in many published papers dealing with this topic, Suddel and Rosemaund (2008) highlighted the advantages of using NFC: low density, low cost, high toughness, acceptable specific strength properties, good thermal properties, low embodied energy, reduced tool wear in the moulding process and better acoustic properties thereby reducing the noise, reduced

irritation to the skin and respiratory system, and they also have low energy requirement for processing.

There are three main categories of natural fibre composites (Suddel and Rosemaund, 2008). The first is composites in which the natural fibre serves as filler in commodity thermoplastic. The second is composites where longer fibres enhanced with compatibiliser and additives attain additional strength and toughness in thermoplastic. The third is composites where natural fibres are used with thermosetting resins as designed elements within engineered components.

In order to have a more comprehensive knowledge about NFCs, it is essential to have knowledge about their raw material, natural fibres. Natural fibres can be defined as bio-based fibres from vegetable and animal origin. This definition includes all natural cellulosic fibres and protein based fibres and excludes man-made cellulosic, wood fibre and synthetic materials (Van-Dam, 2008). Natural fibres are predominantly used as the replacement for conventional synthetic fibres, so they have to compete with these conventional materials in order to gain their own market. However the diverse application of natural fibres has recently increased significantly due to consumer awareness of environmental concerns and the interest in seeking alternatives for oil-based materials. Natural fibres are a major renewable resource material throughout the world specifically in the tropics. According to the FAO survey, natural fibres like jute, sisal, coir, and banana are abundantly available in developing countries such as India, Srilanka, Thailand, Indonesia, Bangladesh, Philippine, Brazil, and South African.

Natural Fibres

There are a number of natural fibres that currently commercially available for different uses. Four different natural fibres that employed in this research, which are jute, hemp, sisal and bamboo, are briefly discussed below.

Jute (*C. Capsularis*) is an annually grown natural fibre that is extracted from the stem of plants that belonging to the genus of *Corchorus*, family *Tiliceae*. It has a wide range of usage but mostly used for packaging material. It is also used for home textiles, decorative fabrics, shopping bags, blankets, etc. The utilization of jute has currently even widened to as floor coverings, insulation materials, geotextiles and jute-based composites. Jute is grown in the rainy seasons at temperature of 21-38⁰C with relative humidity of 65-95% (Rahman, 2010; Mussig, 2010).

Hemp (*Cannabis Sativa L.*) is defined as green, abundantly available and ubiquitous plant, economically valuable, possibly dangerous, and certainly mysterious in many ways. It is a multifunctional crop that can provide valuable raw material for non-wood industrial application. Hemp is normally grown from northern latitudes to tropical climates. The traditional uses of hemp are for making ropes, twines, bags and hard wearing fabrics. More recently, it is also used as a raw material for pulp and paper industry. The potential applications have now widened to include building industry to produce insulating products and automotive industry as interior parts (Amaducci, 2010; Mussig, 2010).

Sisal (*Agave Sisalana*) is a leaf fibre derived from a plant that most commonly referred to species of agave family. It is mainly cultivated for its fibre, which is extracted from the leaves. Sisal is considered to be indigenous to central and south America. Owing to its potential to grow under diverse ecological and climatic conditions, it has now widespread to Asian and African countries. The primarily uses of sisal are in ropes and twines industries. Sisal is also converted to yarn, string, bags, floor mats, wall coverings and handicrafts. The paper industry also uses the plant as a source of cellulose pulp. Currently, the applications have extended to automotive, furniture and building industry in the form of sisal-reinforced composites. In building industry, sisal is also seen as a potential candidate to replace asbestos in roofing material (Anandjiwala and John, 2010; Mussig, 2010).

Bamboo is a tree like plant that belongs to the family of Bambusoideae of the grass family Poaceae. Bamboo stalks are a typical material that possess continuously graded properties and are characterized by spatially varying microstructures created by non-uniform distributions of the constituents phases (Silva et al, 2006). Bamboo is a non-wood lignocellulosic material that has been widely used in tropical countries as a source of housing material, furniture and daily households uses such as for chopsticks, musical instruments and handicrafts. It is widely used for raw material for pulp and paper, plywood, medium density fibreboard, particle board and oriented strand board (Malanit et al, 2009). Bamboo has a long history in building applications and perhaps the oldest materials used for housing construction. It is an excellent building material for owing flexibility and versatility when treated properly. In the country where bamboo grows naturally, the price is relatively cheap and readily available. It is estimated that

more than one billion people live in bamboo house, mostly in developing countries. In addition, bamboo has been recognized as a sustainable building material due to their ecological and economical characteristic (Paudel and Lobovikov, 2003).

Uses of Natural Fibre Composites (NFCs)

The use of NFCs in a range of industrial applications has increased significantly over the last decades. Suddell and Rosemaund (2008) claimed that the construction industry constitutes the second largest sector to employ NFCs which includes light structural wall, insulation materials, floor and wall coverings, geotextiles and thatch roofing. Broadening the application of NFCs to include for load-carrying raises some challenges such as the lack of uniformity in bio-fibre properties, cost-effective surface treatment for bio-fibre, thermal and moisture sensitivity, low stiffness and impact resistance, uncontrolled bio-degradability (Drzal et al, 2004). Research in this area has mostly focused on how to improve the mechanical properties of the NFCs. Some of the relevant studies in this area are described below.

Jute is probably the most comprehensively studied natural material in the field of natural fibre reinforced composites. Many published papers dealing with different aspects of composites reinforced with jute fibre can be found very easily. Ray et al (2001) studied the dynamic mechanical and thermal analysis of alkali treated jute-vinylester composite. Saha et al (2000) reported their work on pre-treatment of jute fibres with acrylonitrile pre-treatment prior to incorporating into composites with polyester matrix. The resulting composites had some good properties such as tolerant against cold and boiling water, where water absorption and thickness swelling are much reduced compared to the composite reinforced with untreated fibres. Durability of jute fibre reinforced phenolic composites was investigated by Singh et al (2000). In this study, the physical and mechanical properties of jute-phenolic composites were carefully assessed under various conditions of humidity, hydrothermal, and weathering. The results showed that some biological damage in the form of fungal infestation appeared at the cut-edges of weathered composite samples. In addition, extensive disfigurement was noticed on all surfaces under high humidity and water immersion.

Mishra et al, (2002) studied the mechanical performance of jute-epoxy composites. The study was carried out by comparing the performance of composites obtained from untreated and chemically treated fibres. It was found that composites

reinforced with untreated fibres showed higher tensile strength but lower flexural and impact properties. A comparative study was carried out by Ahmed and Vijayarangan (2008) which focused on comparing the matrix used. An isothalic polyester resin and general purposes resin reinforced with jute fibres were compared in terms of their performance. The resulted composites were subjected to tension, compression, flexural, in-plane and inter-laminar shear loading schemes. It was concluded that the performance of composites constituted by isothalic polyester are greater than the one with general polyester. There has been also an ongoing work on the exploring natural fibres in composites conducted at the Centre of Excellence in Engineered Fibre Composites (CEEFC) at the University of Southern Queensland (USQ). Kabir et al (2010) reported their work on the evaluation of mechanical and thermal properties of untreated and chemically treated jute fibre reinforced polyester composites. They found that the composites produced from alkali treated jute-polyester showed higher flexural properties. The treatment with 7% NaOH showed best results. In addition, compressive properties of alkalinized fibres showed higher strain properties and the best result was given by 5% NaOH treatment.

Much research has been undertaken on the use of hemp as a natural fibre. Suardana et al (2011) evaluated the mechanical properties of hemp reinforced polypropylene composites with particular attention to the effect of chemical surface treatment of the fibres. Alkaline and Silane treatments were given to hemp fibres prior to incorporating them into composites with a polypropylene matrix. It was suggested that alkali treatment with 4% by weight resulted in higher mechanical properties. Alkali treatment seems the favourite choice of chemical treatment for all natural fibres. The alkali treatment might also promote the adhesive of fibre-matrix that resulted in enhanced thermal and mechanical properties (Mwaikambo and Ansell, 2002; Bledzki et al, 2002). In addition to the chemical treatment of natural fibres topic, it was recommended that using 35 wt% alkali treated hemp fibres modified with maleated PS compatibiliser enhanced the tensile strength and modulus of the resulted composites (Hokkens et al, 2002; Bledzki et al, 2002). Hemp composites board was also developed and showed sufficient strength to be used as building components (Pogorzelski and Firkowicz-Pogorzelska, 2000; Bledzki et al, 2002).

The potential for using sisal as reinforcement in composites has been studied by many researchers. Rong et al (2002) studied the role of interaction in sisal-epoxy composites and its influence on the impact performance of the composites. In this work, the sisal fibres were modified using different methods; alkali, acetylation, cyanoethylation, silane coupling agent and heat treatment prior to incorporating into epoxy resin matrix. Surface tensiometer and dynamic mechanics analysis were employed to investigate the interfacial interactions of the composites. The effect of such interactions to the impact properties was then obtained. Mechanical properties and morphology of sisal-epoxy composites was investigated by Oksman et al (2000). Unidirectional sisal fibres were used to reinforce epoxy resin through resin transfer moulding method. The results showed that the stiffness of composite was about 20 GPa compared to the stiffness of pure epoxy resin of 3.2 GPa. The tensile strength was also higher, 210 MPa compared to the value obtained by testing pure epoxy resin, 80 MPa.

In addition to those two studies, Fonseca et al (2004) evaluated mechanical properties of sisal-polyester composites. The work focused on the polyester matrix formulation. Three different polyester formulations were introduced; polyester modified with silane coupling agent, flame retardant system and the blend of the two materials. The obtained composites were then compared to the unmodified sisal-polyester composite. It was demonstrated that the flame retardant acted as a particulate reinforcement to the polyester matrix while the silane coupling agent acted as a plasticizer, and that the addition of the two materials tended to decrease the composites performance. In addition, silane and alkali treatments improved the wettability of the fibres resulting in better mechanical properties and good water resistance of sisal-epoxy composites (Bisanda et al, 2000; Bledzki et al, 2002). Using other thermosets composites, Singh et al (1996) evaluated the effect of chemical treatment to the sisal-polyester composites. Sisal fibre was chemically treated using organotitanate, zirconate, silane and N-substituted methacrylamide. The overall conclusion drawn was that the mechanical properties of resulted composites were improved significantly. It was also observed that the tensile decreased by 30 to 44% when exposed to humid conditions, and by 50 to 70% for flexural strength. The composites made of N-substitute treated-sisal fibre exhibited better properties when exposed under dry and wet conditions.

Although bamboo has been served as building material for thousands of years, its main utilization remains as a traditional material. The development of technological tools and methods has however created the opportunity of using bamboo as building materials at more advanced levels. One of promising areas is the utilization of bamboo to reinforce thermosets or thermoplastic composites. This has been significant in the area and some relevant aspects are outlined below.

The effect of environmental ageing the mechanical properties of bamboo-glass fibre reinforced polypropylene (PP) composites was observed by Thwe et al (2002), as reported in Bledzki et al (2002). Two compounds of composites were prepared using a compression moulding method; one was the PP reinforced by short bamboo fibre (BFRP) and the other one was reinforced with a hybrid of bamboo and glass fibre (BGRP). It was observed that the tensile and flexural modulus of BGRP were 12.5 and 10 greater than the BFRP, respectively. The tensile and flexural strength of BGRP was also noted to be higher than those of BFRP by 7 and 25%, respectively. The durability of bamboo-PP composites was much increased by hybridization with a small quantity of glass fibre.

Reddy et al (2010) evaluated the chemical resistance and tensile properties of epoxy/polycarbonate blend coated bamboo fibres. It was found that the coated fibres showed higher tensile strength than uncoated fibres and also had better resistance to acids and alkalis. Moreover, Ismail et al (2002) evaluated the effects of employing silane coupling agent on the curing characteristic and mechanical properties of bamboo fibre filled rubber composites. It was found that the scorch and cure time of bamboo-rubber composites decreased with the increased filler loading in the presence of silane coupling agent. They noted that the tensile strength, tensile modulus, tear strength and hardness increased with the addition of coupling agent.

2.3.2. Wood plastic composites (WPC)

Smith and Wolcott (2006) reported on wood derived composite material as a unique development in the wood products industry. They saw it as an emerging renewable material class based on performance, process, and product design innovation. It has been widely used in North America for a wide range of products such as automobile parts, interior door skins, appliances and furniture (Smith and Wolcott,

2006). The potential market for WPC has since expanded to the construction industry. Since 1990s, the market for WPC material has grown significantly, particularly in the applications where good weather resistance and low maintenance are required. The biggest market segment is in decking and railing products, fencing, door and window panels in residential construction market (Hanninen and Hughes, 2010; Mussig, 2010).

Commercial WPC are produced with formulations composed of wood flour, synthetic thermoplastic resins and additives that includes lubricants, inorganic fillers, coupling agents, stabilizers, and biocides in various combinations (Smith and Walcott, 2006). Unlike the typical fibre used in NFC which is a short or long individual fibre, the “fibres” used in WPC most often take the form of particulate or wood flour. Typically WPC for building applications contain at least 50% of wood particle, but it may vary between 30-70%. Pine, Maple and Oak are the commonly used wood species for producing wood flour. The commonly used binder in producing WPC panels is Polyurethane-based. The WPC products with this typical adhesive range from hardboard (HB), oriented strand board (OSB), medium density fibre board (MDF) and strawboard, particleboard (PB) and laminated veneer lumber (LVS) (www.plastemart.com).

There are two main reasons why WPC has found wide use in the residential industry. Firstly, it can be tailored to almost any desired design (Takatani et al, 2007). Secondly, almost all machinery tools, such as cutting and sewing machine, for processing conventional wood can also be used for WPC processing (Winandy et al, 2004). Another major driver is cost. Noting that research into WPC was initially stimulated by the desire to redirect waste fibre and plastics from landfill to form useful products. Being a once waste product mean that they can very competitively to their traditional timber counterpart.

2.3.3. Lignocellulosic composites

There has also other type of green composite known as lignocellulosic composites. Sometimes, this is included in the WPC class. A lignocellulosic material is any substance that contains both cellulose and lignin and wood, agricultural crops and agricultural residues are included in this category. A lignocellulosic composite is a composite product made from any combination of lignocellulosic materials. The term of

composite and reconstituted wood is frequently used to describe any wood product that is glued together to produce a wide range of final wood-based product from fibreboard to laminated beams and structural components (English et al, 1994; Gilbert, 1994). Traditional lignocellulosic composites can be categorized into three main groups based on particle size; veneer, particle and fibre based materials. Plywood and laminated veneer lumber (LVL) is a veneer-based material. The class of particle board includes waverboard, oriented strand board (OSB), chipboard and particleboard. Meanwhile, other wood-based products such as hardboard and medium density fibreboard (MDF) are categorized as fibre-based panel materials (English et al, 1994; Gilbert, 1994).

Wood based materials such as plywood, hardboard, fibreboard and chipboard are also categorized as sustainable materials and primarily used for interior purposes. They can also be used as external cladding with the use of waterproof gluing and appropriate surface treatment. However, experience so far has shown that external applications can be vulnerable in harsh climate conditions. Plywood is often exposed as internal cladding, while fibreboard and chipboard are almost exclusively used in underlay on either floor or walls. Fibreboards are produced in porous, semi hard and hard variations from through heating in wet process. Fibreboards produced in dry process are widely known as medium density fibre (MDF) and high density fibre (HDF). MDF boards are regularly used in the production of furniture (Berge, 2009). According to Duggal (2008), plywood is a wood panel glued under pressure from an odd number (usually 3 to 13) of layers/piles of veneers.

Plywood has good strength both along as well as across the grains. It has better splitting resistance due to the grains in adjacent veneers in cross direction as nailing can be done very safely even near the edge. Plywood has been extensively used for partitions, ceilings and doors. Chipboard comprised of a centre layer of coarse wood chips and sandwiching outer layers of finer wood chips are generally characterized by a high density. This high density can be ascribed primarily to the fact that the fibre in the centre layer are positioned parallel with the longitudinal axes of the chips, that is in a plane which extend substantially parallel to the plane of manufactured board, and that the chips during the compression step required to form glue joints between the chips are compressed to an appreciable extent such that the density of the board will be substantially higher than the intrinsic density of starting material. Hardboard is built up

of felting from wood or vegetable (wood waste, waste paper and agriculture waste). Hardboards typically have one surface smooth and the other one textured (Duggal, 2008).

Table 2.1. Mechanical properties of wood based material (Duggal, 2008)

No	Wood Based Material	Mechanical Properties			
		Bending Strength (MPa)	Compressive Strength (MPa)	Tensile Strength (MPa)	Modulus of Elasticity (MPa)
1	Plywood (Birch)	80	60	70	1.5×10^4
2	Plywood (Spruce)	35	35	30	1.1×10^4
3	Fibreboard (MDF)	35-45	-	-	$3.5-4.0 \times 10^3$
4	Chipboard	7.0-8.5	4.0-5.0	3.0-4.0	$1.2-1.9 \times 10^3$

2.3.4. The application of sustainable green composites in building structure

The concept of using sustainable green material such as natural fibre composites in building components has been reported since the early seventies. The construction of cheap primary school building using jute fibre reinforced polyester in Bangladesh (1972-73) under the support of CARE and UNIDO is considered as the first effort in the use of natural fibre composite in developing countries. In the 80s, building panels and roofing sheets made from bagasse/phenolic were installed in houses in Jamaica, Ghana and Philippines (Salyer and Usmani, 1982; Mathur, 2006). In another program, developmental work on low cost building materials based on henequen, palm and sisal fibres and unsaturated polyester resin had been undertaken as a co-operative research project between the Government of Mexico and UNIDO for appropriate utilization of natural resources (Belmares et al, 1981; Mathur, 2006). In the 90s, UNDP in association with the government of India supported a program to develop jute based composite and moulded products as wood substitutes in packaging building sectors (Mathur, 2006). The use of natural fibres as reinforcement in a cement matrix has also been practiced for developing cheap building materials such as panels, claddings, roofing sheets and tiles, slabs and beams. More recent efforts relating to the application of natural fibre reinforced plastics (NRFP) in building construction are as follow.

Burgueno et al (2005) reported their study which demonstrated that bio-composites could be used for load-bearing components by improving their structural efficiency through cellular material arrangements. Laboratory-scale periodic cellular beams and plates, as presented in Figure 2.7 (*bottom*), were made from industrial hemp and flax

fibres with unsaturated polyester resin. Material and structural performance were experimentally assessed and compared with results from short-fibre composite using micro-mechanics models and sandwich analyses. Short-term analytical evaluation of full-scale cellular bio-composite components indicated that they were comparable with components made from conventional materials.

Dweib et al (2004) manufactured a bio-based roof structure as demonstrated in Figure 2.7 (*upper*). Cellulose fibres were successfully mixed with soy oil-based resin to form composite structural panels. The cellular fibres were in the form of paper sheets made from recycled cardboard boxes. The panels were prepared using a modified vacuum assisted resin transfer molding (VARTM) process. Five different structural beams were manufactured and tested under four-point bending test to study the strength, stiffness and mode of failure in a pure bending mode. The results from the beam test showed that the stiffness and strength meet the requirements for roof construction.

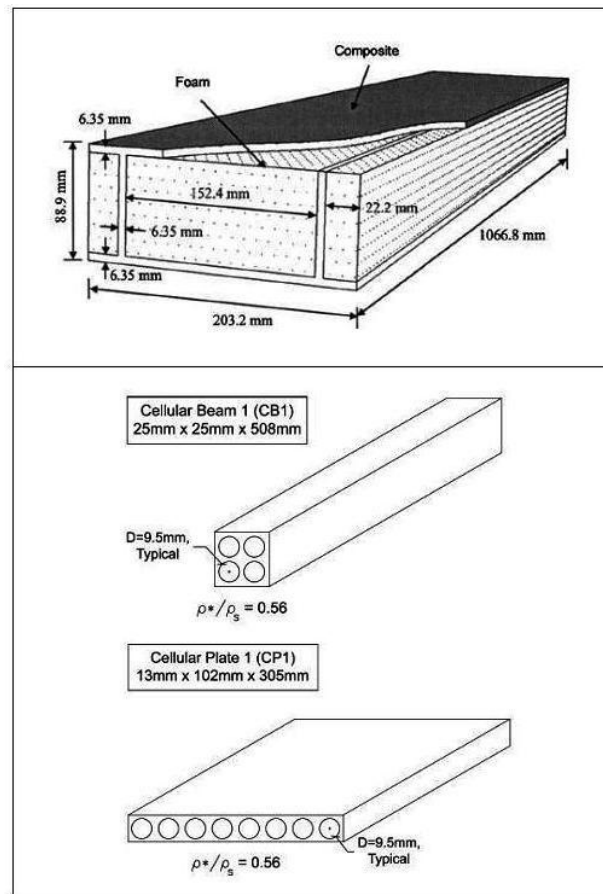


Figure 2.7. *Upper*: Composite structural panels with soy-oil resin (Dweib et al, 2004).
Bottom: Cellular beam (Burgueno et al, 2005)

Hu et al (2007) explained the advantages of this typical structure. Firstly, it has greater degree of structural integrity under wind and earthquake loads due to its monolithic structure. Secondly, the foam core used provides inherent insulation to the roof structure although it does not contribute much for structural and stiffness of the roof panel. Thirdly, as the panels are pre-fabricated model, it takes less time for the erection process that finally save time and money. Lastly, the panel has an integral weather protection layer that would eliminate the need for a shingles, and the maintenance and replacements associated with them.

Mehta et al (2005) proposed a novel processing method to prepare bio-composites for housing panels termed as bio-composites sheet molding compound panel (BCSMCP). Different types of natural fibres were mixed with unsaturated polyester resin to produce tested panels. The panel sheets were then tested under tensile, flexure and impact loads. It was claimed that the proposed method could produce a better bio-composites panel for housing applications. In addition, Uddin and Kalyankar (2011) developed a natural fibre reinforced polymeric structural insulated panels (NSIPs) for panelised construction. This structural sandwich panel is made of jute reinforced polypropylene laminate skins separated by expanded polystyrene (EPS) foam core. The laminate skins were prepared using compression molding process where fibre and matrices are subjected to predefine both pressure and temperature. Structural characterization was performed using flexural and low velocity impact (LVI) tests. Test results confirmed the potential of NSIPs concept to serve as an alternative to OSB SIPs and G/PP SIPs in structural application such as flooring and wall.

2.4. The Wide Spectrum of Hybrids

Having reviewed the many attempts to utilise sustainable green material in building structures, it is now apparent that the application of green materials for load carrying capacity members is not cost-effective. It becomes obvious that hybrid structure incorporating natural fibres is a possible solution. This section explores some of the existing hybrid structures.

Mitra (2009) proposed a sandwich panel with shear-key with the aim to increase the shear performance of sandwich composite panels. The shear-key is inserted in the PVC core and may be of any shape, size or material and the spacing in between the

shear-key may also of any configurations, as presented in Figure 2.8 (*upper*). The core material used was closed-cell semi-rigid PVC foam with a density of 100 kg/cm^3 with the commercial name of Divinycell H100. The skins were made of glass-fibre composite laminate, one was prepared with chopped strand mats and the other one was woven roving fibreglass mat, through a vacuum resin infusion methodology. The experimental investigation of in-plane shear response of sandwich panels was carried out as per recommendations of ASTM C 273 (ASTM, 2007). It was demonstrated by the experimental results that the introduction of shear-key has a positive effect on the initial in-plane shear stiffness and strength of the panels.

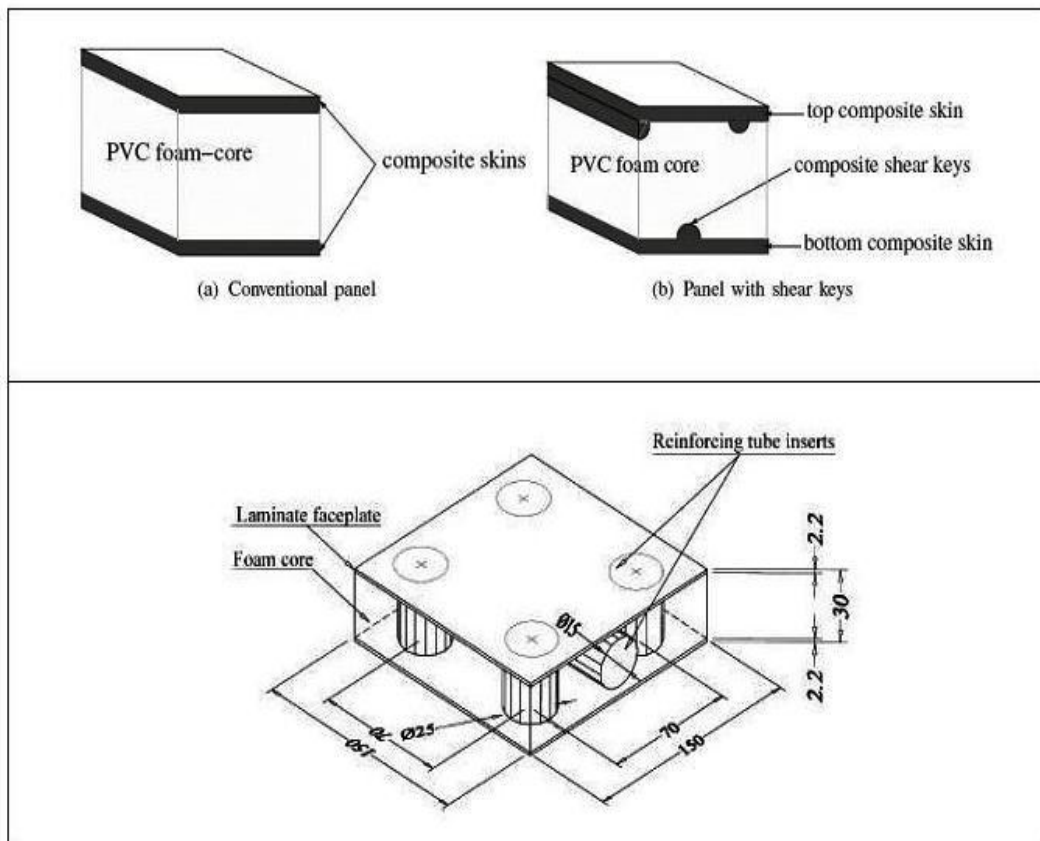


Figure 2.8. *Upper*: Sandwich panel with shear keys (Mitra, 2009).
Bottom: Sandwich panel with reinforcing tube inserts (Mamalis et al, 2002).

Another study with similar concept of strengthening core by inserting other constituent material was performed by Mamalis et al (2002). As seen in Figure 2.8 (*bottom*), several additional materials were inserted in the foam core connecting the external face plates in order to improve the structural crashworthiness properties. Such structures consist of foam or honeycomb core sandwiched between laminated face

skins. The inserted constituents may be in the form of tubes, cones or other types of inserts materials. In this investigation, the sandwich panels were reinforced with tube inserts placed in two different directions. Four tubes with diameter of 25 mm were transversely located to the sandwich panel plane and used as connecting elements between the skins and reinforcement to the whole structure. Another similar tube with the diameter of 15 mm was then placed longitudinally to the panel plane as additional reinforcement. The gap in around the faceplates and tubes was filled with syntactic foam core that made of closed-cell phenolic foam Contratherm, with the density equals to 130 kg/m^3 . The sandwich panels were subjected to compressive loading schemes that applied in edgewise and flatwise positions. The overall conclusion drawn from this work was that the use of internal reinforcement in the form of longitudinal and transversal fibre reinforced plastics tubes significantly improved the stiffness and the crash energy absorption features of the tested sandwich panels. The most common failure mode of sandwich panels subjected to the edgewise compressive load was a buckling of the faceplates and delamination between core and skins. Under flatwise loading direction, the collapse mechanism was initiated by the collapse of transverse tubes, then followed by the longitudinal reinforcement resulting in the delamination and fracture of the tubes that finally densification of foam core.

Researchers also studied the introduction of additional layers in the sandwich structure. Jiang and Shu (2005) reported their work on introducing an additional layer, called an internal sheet into the core of sandwich panel, as shown in Figure 2.9 (left). The investigation work was aimed at improving the resistance of sandwich structure to the local crush (impact load).

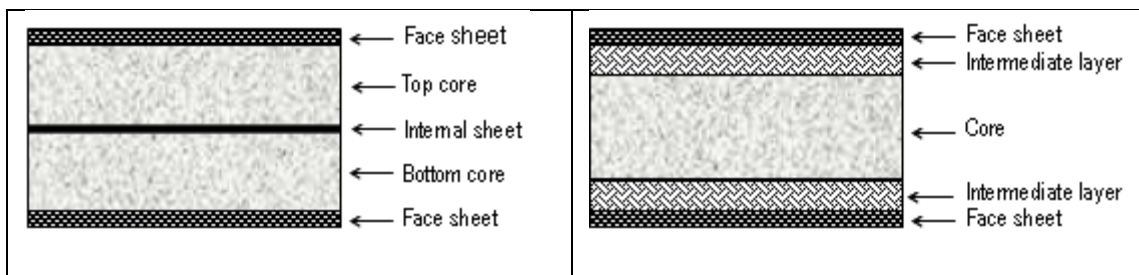


Figure 2.9. *Left:* Sandwich panel with internal sheet (Jiang and Shu, 2005)
Right: Sandwich panel with intermediate layer (Mamalis et al, 2008)

The authors studied the effects of internal sheets involved in a sandwich structure on local displacements of the core under impact loading. The investigation was carried Sustainable Hybrid Composite Sandwich Panel with Natural Fibre Composites as Intermediate Layer

out using simulation modelling with LS-DYNA3D software and was focused on the local displacement of a honeycomb core under three-point impact loading in various locations of internal sheet and of different levels of impact energy. The results showed that the local displacement of the core along the direction of the impact had been decreased significantly. The simulation results also revealed that the internal sheet introduced had no significant effects on the contact forces and the deflection of sandwich structure. Moreover, Mamalis et al (2008) introduced a concept of combining the advantages of metallic and polymeric materials while avoiding some of their major disadvantages. The schematic of this concept is presented in Figure 2.9 (*right*). Metal based materials were used as the skins in order to maximize the rigidity and extremely lightweight cores while introducing an intermediate layer made from composite materials or wood between the face sheets and the core. The simulation results from this study using finite element analysis are listed in the following table.

Table 2.2. The simulation results obtained by Mamalis et al (2008)

Case	Layers + thickness (mm)			Defl. (mm)	Failure modes				Weight (kg)	Cost (€)
	Face	IL	Core		FMB	FW	CS	Inden		
1	Steel:6	-	-	67.8	-	-	-	-	23.4	82
2	Al:8	-	-	80.1	-	-	-	-	11.2	45
3	GE:1.2	-	PVC: 25	57.0	18	6	18	5	2.7	27
4	GE: 3.6	-	PVC: 38	4.5	82	30	27	35	7.3	61
5	St:0.5	GE:	PVC: 25	12.9	8	178	18	78	6.7	42
6	Al:2/1	W: 4	PVC: 25	7.4	23	244	18	125	6.4	27
7	St: 0.5	GE: 1.2	PVC: 38	7.8	11	270	27	96	7.0	52
8	St: 0.8	GE: 1.2	PVC: 38	6.8	18	432	27	195	9.3	61
9	St: 0.5	GE: 1.2	PVC: 50	4.3	15	356	35	111	7.2	62
10	Al: 2/1	W: 4	PVC: 60	3.3	58	624	45	201	7.8	32

Notes: IL = intermediate layer; Al = aluminium; FMB = face micro buckling; FW = face wrinkling; CS = core shear; Inden = indentation; Defl = deflection

It was expected that the new hybrid sandwich beam could prevent the early failure of inundation or face wrinkling of face sheets due to the large differences between the structural properties of face sheets and core materials. Another problem is the relatively high price of good performance core used in the transportation industry. It was believed that using a low performance but cheap core material with the introduction of intermediate layers could be maintaining or even improving the properties of sandwich structure at lower cost. It was also noted by the authors that the final selection of the sandwich panel constituents was a compromise between the cost and the performance of

the material used. The introduction of intermediate layer allows the use of very cheap cores and also very thin face sheets. If a common material is chosen, for example wood, the introduction of an intermediate layer will reduce the cost significantly. In addition, the intermediate layer should be much stiffer than the core material, lightweight enough and preferably much thicker than the face sheets. Initially, a thin glass fibre/epoxy layer was used, but after several impact tests, thicker but lighter plywood was chosen in their research.

The research methodology used in their work was finite element analysis followed by experimental works for validation purpose. A typical panel, 100 cm long and 50 cm wide, had been analysed using finite element under linear central bending load of 6 kN in a typical three-point bending load case. The results reported on this work are summarized in Table 2.2. As it can be seen in the table, the geometrical size of the samples was not consistent. Case 1 and 2 were using single material configuration. The large deflection indicated that the single material panels cannot withstand the applied bending load. A glass fibre epoxy skins were combined with PVC core in the case 3 and 4. The results showed that a better structural performance was achieved when compared to Case 1 and 2. For the rest of the cases, intermediate layer made from glass fibre epoxy (GE), plywood (W) was introduced between metal skins (steel and aluminium) and PVC core. The deflection was reduced by more than four times when using a 1.2 mm glass fibre epoxy intermediate layer between 0.5 mm steel skins and 25 mm PVC core (case 5). The load capacity was increased to against the face wrinkling and indentation. The drawbacks, however, were the weight and cost increment. As a summary, this new hybrid concept has improved the structural capacity of sandwich structure at a reasonable cost.

2.5. Chapter Conclusion

From the literature review presented it can be seen that much research has been done by researchers worldwide. Many alternatives of sandwich construction may be obtained by combining different facing or core materials or even introducing other materials inside the conventional sandwich structure to form a hybrid structure. Although the choice of combinations is almost infinite in terms of material uses or structure configuration, the final decision made should be realistic in terms of whether

the outcomes meet the expected performance as desired by design. For examples, combining very strong and stiff laminate facesheets made of carbon fibre with very low density foam core is an unrealistic choice as the structure will fail due to core damage far before the face sheet reaches its optimum capacity. The introduction of a complicated sandwich structure, normally in the form of hybrid structure, with enhanced mechanical properties may raise the production cost significantly.

Regarding those two concerns, Marshal (1998) in Peters (1998) suggested two important considerations when designing sandwich structure. First, it is important to understand the fabrication sequence and methods. The cost of a sandwich structure is fundamentally fixed at the design stage and a considerable difference in cost can result from alternate solutions to the design problem. Second, properly choosing the core is also of equal importance. Several densities of core may be used in a single panel with each appropriate to the load carried in the area and adhesively bonded to its neighbour. In this case, it should be realized that connecting two cores together will need adequate amount of glue that may negate the weight saving obtained by employing low density core. Attaching glue to the sandwich structure is not only a direct cost title but also time consuming that may end up raising final production cost. In addition to those important recommendations, the ratio of cost to performance is a fundamental consideration when applying sandwich structure in building structure due to many competing types of construction have been crowded the market (Davies, 1998). The new hybrid sandwich panel proposed in this research has been designed while considering all those considerations. The new approach enables the structure to carry more loads at the expense of slightly increased in cost. The hybridization concept proposed is a reasonable way to increase load-bearing capacity of composite sandwich panel structure made of sustainable green material.

CHAPTER 3

RESEARCH CONCEPT AND VALIDATION PROCESS USING STATISTICAL EXPERIMENTAL DESIGN

3.1. Introduction

Research could be described as an organized effort on the part of a scientist (or other) to acquire knowledge about a natural or manufactured process (Kuehl, 2000). It was defined by Roscoe (1975) as being a systematic study of the relationships between variables. Brinberg (1982) described research as the interrelationships of conceptual, methodological, and substantive domains. He indicated that the conceptual domain includes concepts and ideas in abstract form and the methodological incorporates designs, strategies, measuring devices, and analytic techniques used to study a phenomenon or theory. The substantive domain deals with the events, processes and phenomenon which are being studied. This chapter explores the basic concept of the research reported in the dissertation and the validation process for confirming the significance of the outcomes for practical applications.

3.2. The Research Concept

The research work focused on introducing a new layer in between the skin and the core of a standard sandwich panel structure to form a hybrid structure. When a monolithic panel manufactured as a homogeneous material is subjected to a loading scheme, the typical stress distribution is a straight diagonal line from the top surface to the bottom as shown in Figure 3.1 (*top*). The stress distribution, however, will have a considerable transform at the top and bottom interface between the skin and core layers for sandwich structure, as shown in Figure 3.1 (*bottom*). Many authors have identified the stress discontinuity as a prime contributor for failure in sandwich panel. The idea of introducing an intermediate layer, which has intermediate properties between the skins

and core, is to reduce the problem. This concept can be best explained based upon the Hooke's laws which relate induced stress to the material's modulus of elasticity. When the intermediate layers are inserted, the abrupt step between the high and low stresses within the skins and core can be reduced because the elastic modulus of intermediate layers has a value between those of the skin and core. This configuration, of two layers of skins and intermediate layers at the top and bottom and the core in between theoretically generates a higher flexural strength for the sandwich panel. This concept can be explained by Figure 3.1.

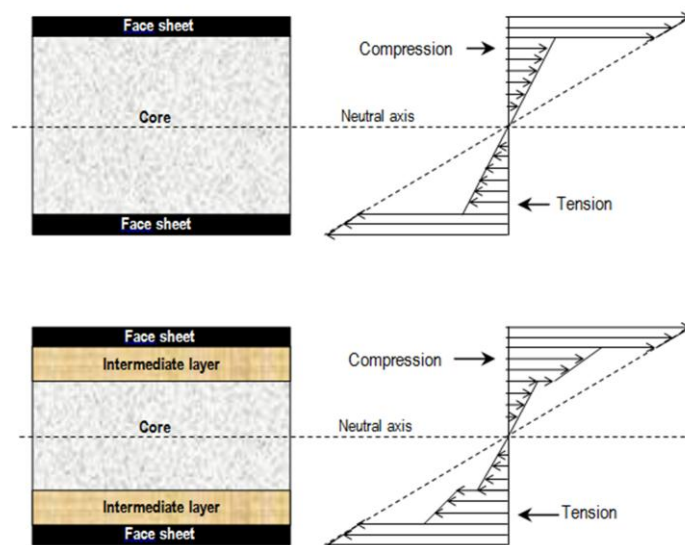


Figure 3.1. Typical stress distribution in sandwich panel: (*top*) conventional sandwich panel, and (*bottom*) hybrid sandwich panel with intermediate layer

For example in a metal face sandwich structure, the core possesses much less stiffness compared to the metal skins. The bending moment is distributed to the skins while the core carries almost all of the shear force. The core also provides a lateral support for the faces of sandwich structure which is extremely important especially when the sandwich structure employs thin metal faces. The thin metal face has low stability under compression and begins to fail immediately due to buckling. The lateral support from the core is activated when the face distorts in a wave-like pattern that induces stresses in the core material. The failure of the core or the bond can result in an immediate wrinkling failure of the face. Davies (2001) highlighted that in sandwich construction, the yield stress of skin material is of reduced concern because the load

carrying capacity of the structure is typically determined by wrinkling of the face in compression or by the shear failure of the core.

It thus becomes crucial to provide more lateral support for the face by introducing another layer that has intermediate properties between those of the faces and core. The current common approach to address the issue is either to increase the thickness of the faces or improves the quality of the core. Both approaches however may have significant impact on the overall cost. The price of skin material is normally expensive so that even slightly increasing the face thickness will significantly increase the cost. While the price of the core is much less than that of the skins, an increased thickness of the core can also result in higher overall cost. A basic theoretical analysis of a sandwich structure is provided in the following sections. This is followed by a more detailed theoretical exploration of hybrid sandwich panel structures.

3.2.1. Basic concept of sandwich panel

A sandwich typically consists of three elements which are the face sheets, core and adhesive. Every part of the panel has a specific function to enable the panel work as a unit. A sandwich beam of the same width and weight as a solid beam has a considerable higher stiffness due to its higher moment of inertia (Diab, 2009). The adhesive has an important role to ensure that faces and the core are fully bonded out but it is often neglected as a part the sandwich panel. The theoretical analysis presented here is adapted from different literatures but is largely based on the work of Zenkert (1995) who explicitly explained that the theoretical analysis in his book was a brief summary of what was earlier described by Allen (1969, 1966). In addition, a publication handout by Deshpande (2002) about the design of metallic foams has been very helpful.

Consider a sandwich beam of uniform width (b), with two equal face sheets of thickness t perfectly bonded to a foam core of thickness c . The beam is loaded in 3-point bending as shown in Figure 3.2 with a span L . Let E_f and E_c be the Young's moduli of the face sheets and core, respectively. The stress and deflections in a beam of this may be obtained by simple beam bending theory. In this initial stage of analysis the theory is based upon the assumption that cross-sections are plane and perpendicular to the longitudinal axis of the unloaded beam remain so when bending takes place. This

assumption leads to the well-known relationship between the bending moment and the curvature ($1/R$). The EI in this relation is the flexural rigidity.

$$\frac{M}{EI} = -\frac{1}{R} \dots\dots\dots 3.1$$

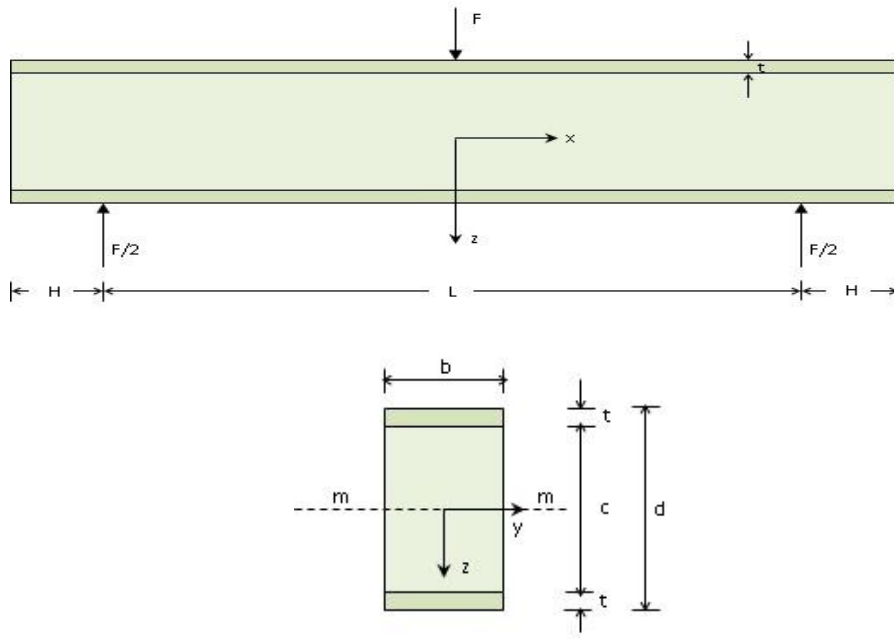


Figure 3.2. Long and cross sections of sandwich panel loaded in 3-point bending

For a sandwich beam, the equivalent flexural rigidity $(EI)_{eq}$ consists of the sum of the rigidities of the faces and core measured about the neutral axis, m-m, of the entire sections.

$$(EI)_{core} = E_c \cdot \frac{1}{12} bc^3 = \frac{1}{12} E_c bc^3 \dots\dots\dots 3.2$$

$$(EI)_{faces} = E_f \cdot I_f, \text{ about m-m} \dots\dots\dots 3.3$$

I_{faces} , can be calculated from the parallel axis theorem,

$$I_{faces} = 2 \left[I_{faces} + A \left(\frac{d}{2} \right)^2 \right] \dots\dots\dots 3.4$$

$$= 2 \left[\frac{1}{12} bt^3 + \frac{btd^2}{4} \right]$$

$$I_{faces} = \frac{1}{6} bt^3 + \frac{btd^2}{2} \dots\dots\dots 3.5$$

So that,

$$(EI)_{\text{faces}} = \frac{1}{6} E_f b t^3 + \frac{1}{2} E_f b t d^2 \quad \dots\dots\dots 3.6$$

Thus,

$$(EI)_{\text{eq}} = (EI)_{\text{faces}} + (EI)_{\text{core}} \quad \dots\dots\dots 3.7$$

$$= \frac{1}{6} E_f b t^3 + \frac{1}{2} E_f b t d^2 + \frac{1}{12} E_c b c^3$$

$$(EI)_{\text{eq}} = E_f \frac{b t^3}{6} + E_f \frac{b t d^2}{2} + E_c \frac{b c^3}{12} \quad \dots\dots\dots 3.8$$

The faces are usually thin compared with the core, i.e. $t \ll c$, and the first term of Equation 3.8 is therefore quite small and is less than 1% of the second value when:

$$\frac{d}{t} > 5.77 \quad \dots\dots\dots 3.9$$

As a result of material selection, the core usually has a much lower modulus than that of the face, i.e. $E_c \ll E_f$, the third term in Equation 3.8 is less than 1% if:

$$\frac{E_f}{E_c} \frac{t d^2}{c^3} > 16.7 \quad \dots\dots\dots 3.10$$

If the conditions in Equation 3.9 and Equation 3.10 are fulfilled, then the flexural rigidity of sandwich panel may reduce to:

$$(EI)_{\text{eq}} \approx E_f \frac{b t d^2}{2} \quad \dots\dots\dots 3.11$$

As indicated earlier, sandwich panel has a high stiffness because of its high moment of inertia. The stiffness of the above sandwich beam is given by:

$$k = \frac{F}{\delta} \quad \dots\dots\dots 3.12$$

Where:

- k : The stiffness
- F : The applied force
- δ : The displacement, which in this case is the deflection

The deflection of a homogeneous beam under 3-point bending load is,

$$\delta = \frac{F L^3}{48 E I} \quad \dots\dots\dots 3.13$$

For sandwich panel, this equation can be modified as

$$\delta = \frac{FL^3}{48(EI)_{eq}} \dots\dots\dots 3.14$$

Hence, by including Equation 3.14 into Equation 3.12, a stiffness of a sandwich panel can be obtained as follows.

$$k = \frac{48(EI)_{eq}}{L^3} \dots\dots\dots 3.15$$

Based on Equation 3.15, it can be seen that the higher flexural rigidity $(EI)_{eq}$, the higher beam stiffness. Using the sandwich concept the flexural rigidity and stiffness of a beam can be substantially enhanced, without much increase in weight.

Elastic stresses in sandwich panel

The stress in the faces and core may be determined by the use of ordinary beam theory, adapted to the composite nature of the cross-section. Because the sections remain plane and perpendicular to the longitudinal axis, the longitudinal strain at a point of z is given by

$$\epsilon_l = \frac{z}{R} \dots\dots\dots 3.16$$

The value of R can be obtained by rewriting Equation 3.1, and inserts the result into the Equation 3.16, which results in:

$$\epsilon_l = \frac{Mz}{(EI)_{eq}} \dots\dots\dots 3.17$$

This strain may be multiplied by the appropriate modulus of elasticity to give the bending stress at level z. For instance, the stresses in the faces and core are given by:

$$\sigma_f = \frac{Mz}{(EI)_{eq}} E_f \dots\dots\dots 3.18$$

For $\left[\frac{c}{2} \leq z \leq \frac{c+t}{2} \right]$; $\left[-\frac{c+t}{2} \leq z \leq -\frac{c}{2} \right]$

$$\sigma_c = \frac{Mz}{(EI)_{eq}} E_c \dots\dots\dots 3.19$$

For $\left[-\frac{c}{2} \leq z \leq \frac{c}{2} \right]$

Thus, the maximum face and core stresses are obtained with $z = \pm(c + t)/2$ and $z = \pm c/2$. Hence, the stresses vary linearly within each material constituent, but there is a jump in the stress at the face and core interface.

Shear stresses in sandwich panel

The shear stress(τ) in a homogeneous beam, as shown in Figure 3.3, at a depth z is defined by Equation 3.20.

$$\tau = \frac{Q}{bI} A_c z_c \dots\dots\dots 3.20$$

Where:

- Q : Shear force
- A_c : Are of the cut off portion
- A_cz_c : The first moment of area of the cut-off portion about the centroidal axis

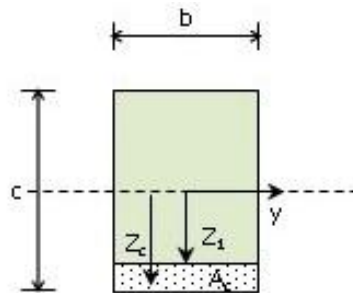


Figure 3.3. The cross section in shear analysis for homogeneous beam

For a sandwich beam, this equation is modified to take into account the moduli of elasticity of the different elements of the cross-section.

$$\tau = \frac{Q}{b(EI)_{eq}} \sum A_c z_c E \dots\dots\dots 3.21$$

Where the summation \sum is done for all parts of the section for which $z < z_1$. For example, to determine the shear stress at level z in the core of the sandwich, as shown in Figure 3.4, the procedure is as follows.

$$\begin{aligned} \sum A_c z_c E &= E_f \cdot A_f \cdot \frac{d}{2} + E_c \cdot A_c \cdot \left[\frac{1}{2} \left(\frac{c}{2} - z \right) + z \right] \dots\dots\dots 3.22 \\ &= E_f \cdot \frac{btd}{2} + E_c \cdot b \left(\frac{c}{2} - z \right) \left(\frac{c}{4} + \frac{z}{2} \right) \\ &= E_f \cdot \frac{btd}{2} + E_c \cdot b \left(\frac{c}{2} - z \right) \frac{1}{2} \left(\frac{c}{2} + z \right) \end{aligned}$$

$$\begin{aligned}
 &= E_f \cdot \frac{btd}{2} + \frac{E_c \cdot b}{2} \left(\frac{c}{2} - z \right) \left(\frac{c}{2} + z \right) \\
 &= E_f \cdot \frac{btd}{2} + \frac{E_c \cdot b}{2} \left(\frac{c^2}{4} + \frac{cz}{2} - \frac{cz}{2} - z^2 \right) \\
 \sum A_c b_c E &= \frac{E_f btd}{2} + \frac{E_c \cdot b}{2} \left(\frac{c^2}{4} - z^2 \right) \dots\dots\dots 3.23
 \end{aligned}$$

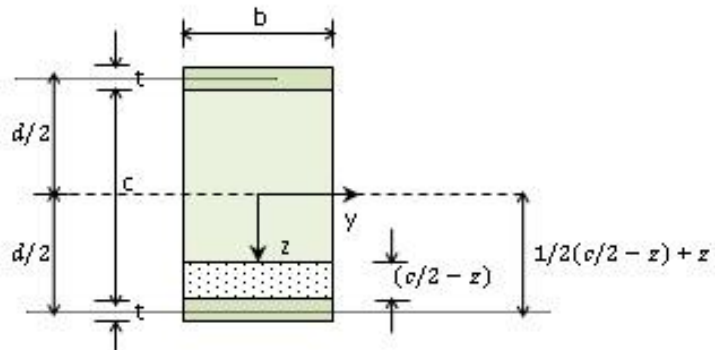


Figure 3.4. Sketch of sandwich beam cross section for shear analysis

Thus, as the shear stress in the core is defined as per Equation 3.21, then

$$\tau = \frac{Q}{b(EI)_{eq}} \left[\frac{E_f btd}{2} + \frac{E_c \cdot b}{2} \left(\frac{c^2}{4} - z^2 \right) \right] \dots\dots\dots 3.24$$

Eliminating the factor of b, gives the final equation to obtain shear stress in the core:

$$\tau = \frac{Q}{(EI)_{eq}} \left[\frac{E_f td}{2} + \frac{E_c}{2} \left(\frac{c^2}{4} - z^2 \right) \right] \dots\dots\dots 3.25$$

A similar expression may be obtained the shear stress in the faces and the complete of shear stress distribution across the depth of the sandwich is illustrated in Figure 3.5 (A). For a normal sandwich panel, $E_c \ll E_f$, so the second term in the equation 4.25 can be neglected and reduced to:

$$\tau = \frac{Q}{(EI)_{eq}} \cdot \frac{E_f td}{2} \dots\dots\dots 3.26$$

Considering Equation 3.11 where approximate $(EI)_{eq} = E_f btd^2/2$, the shear stress in the core can be simplified as follows.

$$\tau = \frac{Q}{E_f btd^2/2} \cdot \frac{E_f td}{2}$$

$$\tau = \frac{Q}{bd} \dots\dots\dots 3.27$$

The corresponding shear stress distribution in the sandwich beam is shown in Figure 3.5 (B).

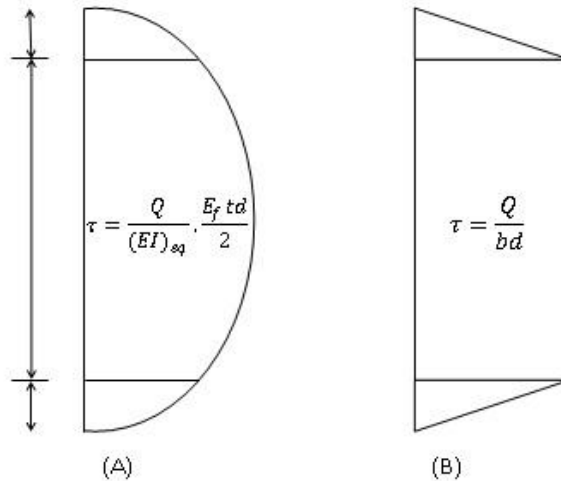


Figure 3.5. (A) The shear stress in the faces and the complete shear stress distribution across the depth of the sandwich. (B) The corresponding simplified shear stress distribution in the sandwich beam

Deflection of a sandwich panel

In a homogeneous material, the deflection due to shear is often neglected. For a sandwich panel, however, the core material is usually not rigid in shear and thus the deflection is not negligible in most cases. As it has been presented in previous equations, the deflection of sandwich panel can be obtained by adoption of the previous basic equation of beam deflection. Two previous subsequent equations, Equation 3.13 and Equation 3.14, showed how the basic beam deflection equation has been modified for a sandwich panel beam. Equation 3.15 shows that the increasing the separation of the face sheets increases the flexural rigidity and stiffness of a sandwich beam. While separation should be increased as much as possible, it may induce a shear mode of deformation that commonly neglected in ordinary beam analysis.

Recalling back at the assumption made for the ordinary beam bending theory, it was assumed that cross-sections that are plane and perpendicular to the longitudinal axis of the unloaded beam remain so when bending takes place. As it seen in Figure 3.6, the cross-section aa, bb, cc and dd has been slightly rotated but remain perpendicular to the

longitudinal axis of the deflected beam. The upper part of the beam is under compression and the lower part is under tension.

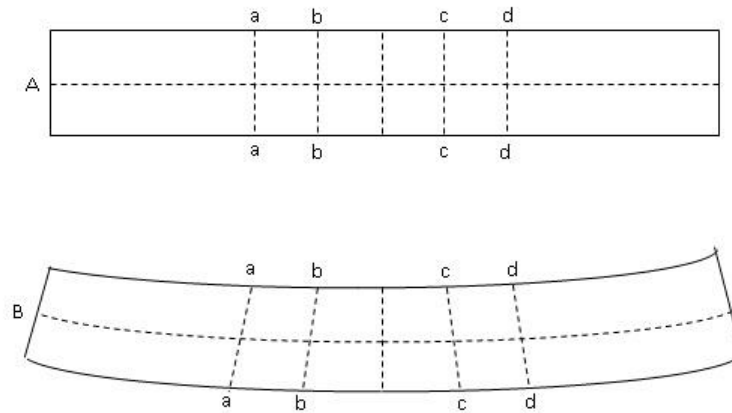


Figure 3.6. Basic assumption in ordinary beam theory

The shear stress in the core at any section has been defined by the Equation 3.27. This equation is associated with a shear strain.

$$\gamma = \frac{Q}{G_c b d} \dots\dots\dots 3.28$$

The above equation was provided by the following process.

$$G_c = \frac{\tau}{\gamma} \dots\dots\dots 3.29$$

$$\gamma = \frac{\tau}{G_c} \dots\dots\dots 3.30$$

$$\gamma = \frac{1}{G_c} \cdot \frac{Q}{bd} \dots\dots\dots 3.31$$

Where G_c is the shear modulus of the core material. This shear strain leads to a new kind of deformation as shown in the following figure.

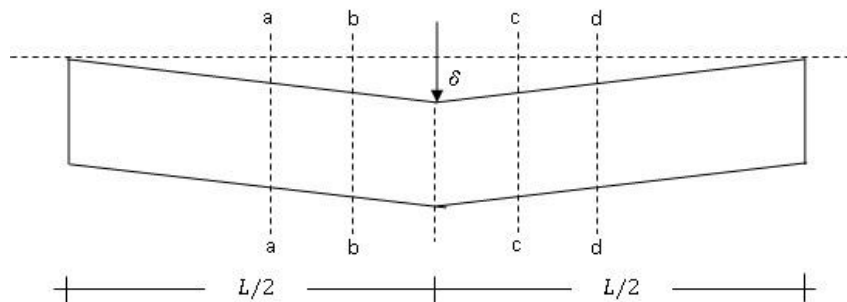


Figure 3.7. New type of deformation due to core shear.

As shown in the Figure 3.7, the points a, b, c, and d which lie on the centre line of the faces do not move horizontally but are displaced vertically. The deflection of the loading point due to this deformation mode is given by.

$$\frac{\delta}{L/2} = \gamma = \frac{Q}{G_c bd} \dots\dots\dots 3.32$$

$$\delta = \frac{Q \cdot L/2}{G_c bd} \dots\dots\dots 3.33$$

Since in 3-point bending load $Q = F/2$, then

$$\delta = \frac{F/2 \cdot L/2}{G_c bd} \dots\dots\dots 3.34$$

$$\delta = \frac{FL}{4 (G_c bd)} \dots\dots\dots 3.35$$

$$\delta = \frac{FL}{4(AG)_{eq}} \dots\dots\dots 3.36$$

The total deflection at the centre point of the beam due to the bending (Equation 3.14) and shear deformation (Equation 3.36) can be obtained by a linear superposition, which gives:

$$\delta = \frac{FL^3}{48(EI)_{eq}} + \frac{FL}{4(AG)_{eq}} \dots\dots\dots 3.37$$

This is a more appropriate equation for the deflection of sandwich panels and the equation for their stiffness also has to be modified. When considering the shear contribution in the deflection of sandwich panel, the stiffness of sandwich beam can be calculated based on the following equations.

$$k = \frac{F}{\frac{FL^3}{48(EI)_{eq}} + \frac{FL}{4(AG)_{eq}}} \dots\dots\dots 3.38$$

By rearranging this equation, the stiffness of sandwich beam can be obtained by the following equation.

$$k = \frac{48(EI)_{eq}}{L^3} + \frac{4(AG)_{eq}}{L} \dots\dots\dots 3.39$$

3.2.2. The Hybrid Sandwich Panel Model

The hybrid structure of the sandwich panel studied in this research is achieved by placing one more layer, which is called as an intermediate layer, between the core and the skins. The term hybrid arises from the fact that a new constituent has been incorporated in an ordinary sandwich panel structure which typically consists of only two elements, faces and core. By introducing this new layer the sandwich panel has now consists of three materials, that is skins, intermediate layers, and the core. The analysis of the behaviour of new hybrid sandwich panel is basically carried out by taking into account the contribution of this new element. However, the basic analysis remains the same as for the ordinary sandwich panel.

Consider a sandwich beam of uniform width (b), with two identical intermediate layer of thickness t_i perfectly bonded to the foam core of thickness t_c . The other two equal face sheets with thickness t_f are also perfectly bonded to the intermediate layer of the sandwich panel to create a hybrid form. The beam is loaded in 3-point bending as sketched in Figure 3.8 with a span L . Let E_f , E_i and E_c be the Young's moduli of the face sheets, intermediate layer and core, respectively. The stress and deflections in this hybrid sandwich beam may be obtained in a similar way as the ordinary sandwich beam.

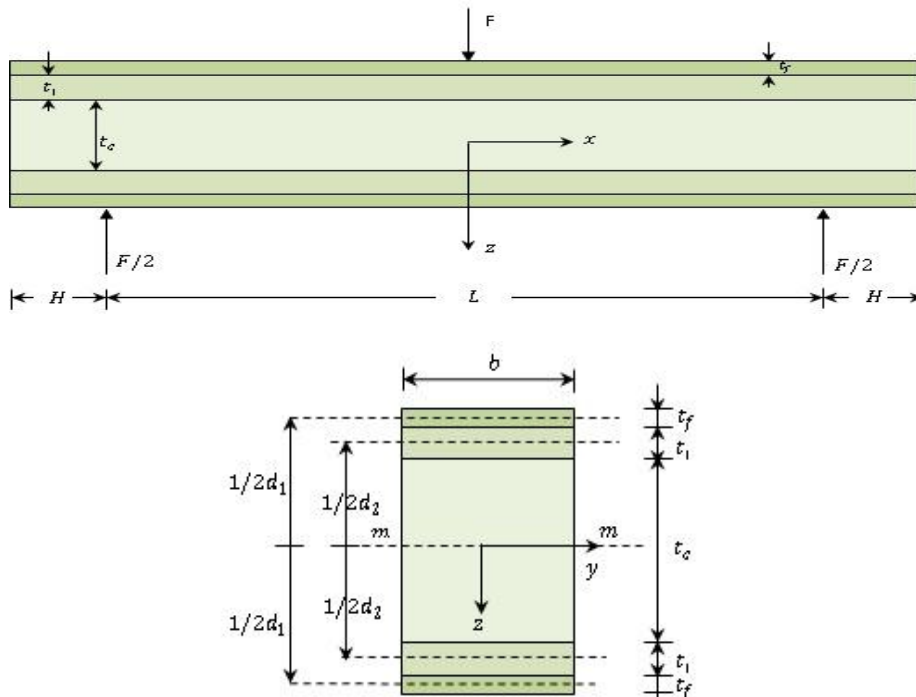


Figure 3.8. Long and cross sections of hybrid sandwich panel loaded in 3-point bending
Sustainable Hybrid Composite Sandwich Panel with Natural Fibre Composites as Intermediate Layer

For this hybrid sandwich beam, the equivalent flexural rigidity $(EI)_{eq}$ consists of the sum of the rigidities of the faces, intermediate layer and core measured about the neutral axis, m-m, of the entirely sections.

$$(EI)_{core} = E_c \cdot \frac{1}{12} bt_c^3 = \frac{1}{12} E_c bt_c^3 \quad \dots\dots\dots 3.40$$

$$(EI)_{intermediate\ layer} = E_i \cdot I_i, \text{ about m-m} \quad \dots\dots\dots 3.41$$

$$(EI)_{faces} = E_f \cdot I_f, \text{ about m-m} \quad \dots\dots\dots 3.42$$

I_{faces} , can be calculated from the parallel axis theorem,

$$I_{faces} = 2 \left[I_{faces} + A \left(\frac{d_1}{2} \right)^2 \right] \quad \dots\dots\dots 3.43$$

$$= 2 \left[\frac{1}{12} bt_f^3 + \frac{bt_f d_1^2}{4} \right]$$

$$I_{faces} = \frac{1}{6} bt_f^3 + \frac{bt_f d_1^2}{2} \quad \dots\dots\dots 3.44$$

So that,

$$(EI)_{faces} = \frac{1}{6} E_f bt_f^3 + \frac{1}{2} E_f bt_f d_1^2 \quad \dots\dots\dots 3.45$$

Using a similar way, $I_{intermediate\ layer}$, can also be calculated based on the parallel axis theorem,

$$I_{intermediate\ layer} = 2 \left[I_{intermediate\ layer} + A \left(\frac{d_2}{2} \right)^2 \right] \quad \dots\dots\dots 3.46$$

$$= 2 \left[\frac{1}{12} bt_i^3 + \frac{bt_i d_2^2}{4} \right]$$

$$I_{intermediate\ layer} = \frac{1}{6} bt_i^3 + \frac{bt_i d_2^2}{2} \quad \dots\dots\dots 3.47$$

So that,

$$(EI)_{intermediate\ layer} = \frac{1}{6} E_i bt_i^3 + \frac{1}{2} E_i bt_i d_2^2 \quad \dots\dots\dots 3.48$$

Hence,

$$(EI)_{eq} = (EI)_{faces} + (EI)_{intermediate\ layer} + (EI)_{core} \quad \dots\dots\dots 3.49$$

$$(EI)_{eq} = \frac{1}{6} E_f b t_f^3 + \frac{1}{2} E_f b t_f d_1^2 + \frac{1}{6} E_i b t_i^3 + \frac{1}{2} E_i b t_i d_2^2 + \frac{1}{12} E_c b t_c^3 \quad \dots \quad 3.50$$

Or, the above equation can be simplified as follows.

$$(EI)_{eq} = E_f \left[\frac{b t_f^3}{6} + \frac{b t_f d_1^2}{2} \right] + E_i \left[\frac{b t_i^3}{6} + \frac{b t_i d_2^2}{2} \right] + E_c \frac{b t_c^3}{12} \quad \dots \dots \dots \quad 3.51$$

As for the case for the ordinary sandwich panel, the contribution of the moment inertia of skin the stiffness of core might be neglected, but the moment inertia of intermediate layer should be taken into account as they have significant thickness. Hence, the above equation, Equation 3.50, may be reduced to:

$$(EI)_{eq} = \frac{1}{2} E_f b t_f d_1^2 + \frac{1}{6} E_i b t_i^3 + \frac{1}{2} E_i b t_i d_2^2 \quad \dots \dots \dots \quad 3.52$$

Following a similar procedure with the analysis for elastic stress distribution in ordinary sandwich beam, the stress at each layer of hybrid sandwich beam can be obtained by replacing the flexural rigidity of ordinary beam with the flexural rigidity of hybrid beam in Equation 3.51 or Equation 3.52, which gives:

$$\sigma_f = \frac{Mz}{(EI)_{eq}} E_f \quad \dots \dots \dots \quad 3.53$$

For $\left[\left(\frac{t_c}{2} + t_i \right) \leq z \leq \left(\frac{t_c}{2} + t_i + \frac{t_i}{2} \right) \right] \quad ; \quad \left[- \left(\frac{t_c}{2} + t_i + \frac{t_i}{2} \right) \leq z \leq - \left(\frac{t_c}{2} + t_i \right) \right]$

$$\sigma_i = \frac{Mz}{(EI)_{eq}} E_i \quad \dots \dots \dots \quad 3.53$$

For $\left[\frac{t_c}{2} \leq z \leq \left(\frac{t_c + t_i}{2} \right) \right] \quad ; \quad \left[- \left(\frac{t_c + t_i}{2} \right) \leq z \leq - \frac{t_c}{2} \right]$

$$\sigma_c = \frac{Mz}{(EI)_{eq}} E_c \quad \dots \dots \dots \quad 3.55$$

For $\left[- \frac{t_c}{2} \leq z \leq \frac{t_c}{2} \right]$

In a similar way to the previous analysis, the shear in the core of hybrid sandwich panel can be obtained by also taking into consideration the contribution of intermediate layer.

$$\begin{aligned}
 \sum A_c z_c E &= E_f \cdot A_f \cdot \frac{d_1}{2} + E_i \cdot A_i \cdot \frac{d_2}{2} + E_c \cdot A_c \cdot \left[\frac{1}{2} \left(\frac{t_c}{2} - z \right) + z \right] \quad \dots\dots\dots 3.56 \\
 &= E_f \cdot \frac{b t_f d_1}{2} + E_i \cdot \frac{b t_i d_2}{2} + E_c \cdot b \left(\frac{t_c}{2} - z \right) \left(\frac{t_c}{4} + \frac{z}{2} \right) \\
 &= E_f \cdot \frac{b t_f d_1}{2} + E_i \cdot \frac{b t_i d_2}{2} + E_c \cdot b \left(\frac{t_c}{2} - z \right) \frac{1}{2} \left(\frac{t_c}{2} + z \right) \\
 &= E_f \cdot \frac{b t_f d_1}{2} + E_i \cdot \frac{b t_i d_2}{2} + \frac{E_c \cdot b}{2} \left(\frac{t_c}{2} - z \right) \left(\frac{t_c}{2} + z \right) \\
 &= E_f \cdot \frac{b t_f d_1}{2} + E_i \cdot \frac{b t_i d_2}{2} + \frac{E_c \cdot b}{2} \left(\frac{t_c^2}{4} + \frac{t_c z}{2} - \frac{t_c z}{2} - z^2 \right)
 \end{aligned}$$

$$\sum A_c b_c E = E_f \cdot \frac{b t_f d_1}{2} + E_i \cdot \frac{b t_i d_2}{2} + \frac{E_c \cdot b}{2} \left(\frac{t_c^2}{4} - z^2 \right) \quad \dots\dots\dots 3.57$$

Thus,

$$\tau = \frac{Q}{b(EI)_{eq}} \left[\frac{E_f b t_f d_1}{2} + \frac{E_i b t_i d_2}{2} + \frac{E_c \cdot b}{2} \left(\frac{t_c^2}{4} - z^2 \right) \right] \quad \dots\dots\dots 3.58$$

By removing the factor of b, the final equation can be obtained as follows:

$$\tau = \frac{Q}{(EI)_{eq}} \left[\frac{E_f t_f d_1}{2} + \frac{E_i t_i d_2}{2} + \frac{E_c}{2} \left(\frac{t_c^2}{4} - z^2 \right) \right] \quad \dots\dots\dots 3.59$$

Finally, the deflection and stiffness of hybrid sandwich panel can be obtained in the similar way with the equations for ordinary sandwich panel. The deflection is the sum of deflection due to bending load and shear of the core, and subsequently the stiffness is the load divided by this deflection. By this process, the analogous equations below for the deflection and stiffness of ordinary beam are proposed for the hybrid sandwich panel with the value of flexural rigidities $(EI)_{eq}$ defined by Equation 3.51.

$$\delta = \frac{FL^3}{48(EI)_{eq}} + \frac{FL}{4(AG)_{eq}} \quad \dots\dots\dots 3.60$$

$$k = \frac{48(EI)_{eq}}{L^3} + \frac{4(AG)_{eq}}{L} \quad \dots\dots\dots 3.61$$

3.3. Concept for Research Validation Process

As indicated earlier, the concept of a hybrid sandwich panel with an intermediate layer was developed by Mamalis et al (2008). The research was targeted at developing a new hybrid sandwich panel for the transportation industry and emphasized cost-effective analysis as the main parameter. The research methodology used in their work was finite element analysis followed by experimental works for validation purposes, which is a common practice in engineering research. The work was carried out by comparing several possible choices of material combinations. Although the researchers claimed the outcome to be successful, the fact that the geometrical size of the samples was not consistently kept at the same level casts some doubt on the conclusions. Their original premise that an intermediate layer would be very beneficial is of course correct. There remains however a need to validate the premise using statistical experimental design.

3.3.1. Statistical experimental design

The term of “statistical experimental design” was introduced by Montgomery (2009). Other terms are used by statisticians such as “designed experiments” or “design of experiments” to describe the same process. In a designed experiment, the researchers make deliberate or purposeful changes in the controllable variables of the system or process, observe the resulting system output data, and then make an inference or decision about which variables are responsible for the observed changes in output performance. While all experiments may be considered to be designed experiments, some are poorly designed that may result in ineffective use of valuable resources. Statistically designed experiments allow efficiency and economy in the experimental process and also obtain scientific objectivity conclusions (Montgomery and Runger, 2003).

Statistically based experimental design techniques are particularly useful in engineering world for improving the performance of manufacturing process or in the development of new products (Montgomery and Runger, 2003). Some typical applications of statistically designed experiments in engineering include evaluation and comparison of basic design configurations, evaluation of different materials, and determination of key product design parameters that affect product performance. The

application of experimental design in engineering can result in products that are easier to manufacture, embrace better performance and entail less production time. The simple meaning of statistical experimental design is a set of experiments that follow the basic principles of statistical analysis. There are two main types of statistics analysis, descriptive and inferential statistics (Montgomery, 2009).

Roscoe (1975) defined descriptive statistics as a technique that enables the experimenter to describe with precision a collection of quantitative information in more concise and convenient terms than the original collection, in a fashion that makes for ease of interpretation. It is intended to facilitate the orderly communication and interpretation of disorganized mass of raw data. The counterpart of this statistic analysis, statistic inference, can be described as a collection of tools for making the best possible decisions in the face of uncertainty.

In a statistically based experiment, there are few important terms that need to be well understood before using it as a basis for experiment. They are such as treatments, factors, levels, variables and hypothesis. Treatments are the set of circumstances created for the experiments in response to research hypothesis and they are the focus of investigations (Kuehl, 2000). An important component of many treatments designs is the control treatment. A control treatment is a necessary benchmark treatment to evaluate the effectiveness of experimental treatments. A control treatment may represent the factor with no treatment or a standard practice to which the experimental method may be compared. In an engineering experiment, a standard practice is frequently used as a baseline or control. A factor is a particular group of treatments and several categories of each factor are termed as levels of factor. Variables, in most simple definition, are measurable characteristics that vary or can be changed. Roscoe (1975) classified variables into two broad categories namely independent and dependent. An independent variable is a factor that is manipulated in an experiment. It is a variable that stands alone and isn't changed by the other variables. Dependent variable is something that depends on other factors or independent variables. An independent variable is the variable that is changed in a scientific experiment to test the effects on the dependent variable. In other words, the independent variable is the variable that is varied or manipulated by the researcher, and the dependent variable is the response that is measured.

In this research, the treatment relates to the situation in which sandwich panels have an intermediate layer or not. There has been a single factor, the intermediate layer material that comprises two and four levels of a factor. In comparative experiment, there are two levels of factor that are compared to determine whether or not the introduction of an intermediate layer gives significant influence on enhancing the bending strength of the hybrid sandwich panel. Four levels of factor were used in single factor experiment in order to evaluate which type of intermediate layer produces the maximum bending strength. All other factors were kept constant, except the intermediate layer types. Further aspects of those two employed statistical experimental design are presented in the following sections.

3.3.2. Simple comparative experiments

Some basic statistics frameworks are presented in this section due to its significance use in this chapter and also in Chapter 8 for comparing the results with the results obtained by Minitab software. A simple comparative experiment is an experimental work that trying to compare two conditions or treatments whether or not they give equivalent results (Montgomery, 2009). In addition, Kuehl (2000) stated that the adjective comparative, in the simple comparative term, implies the establishment of more than one set of circumstances in the experiment, and that responses resulting from the differing circumstances will be compared with one another. In this type of statistical experimental design, a set up of trials is conducted to determine if changing in a single variable from one condition to another, while holding all others potential variables, has any effect on the response.

The proposed procedure on conducting simple comparative analysis described in this work is based on the process described by Montgomery (2009). Throughout the analysis, it is assumed that a completely randomized experimental design is used. In such design, the data are viewed as if they were a random sample from a normal distribution. Consider the two compared objects as two levels of a factor. Let $y_{11}, y_{12}, \dots, y_{1n_1}$ represent the n_1 observations from the first factor level and $y_{21}, y_{22}, \dots, y_{2n_2}$ represent the n_2 observations from the second factor level. The procedure for hypothesis testing in this analysis begins with describing a statistic model. A simple statistic model for such experiment is:

$$y_{ij} = \mu_i + \epsilon_{ij} \quad \left\{ \begin{array}{l} i=1, 2, \dots, a \\ j=1, 2, \dots, n_i \end{array} \right. \quad \dots \dots \dots \quad 3.62$$

Where:

- y_{ij} : The j th observation from factor level i
- μ_i : Mean of the response at the i th factor level
- ϵ_{ij} : Normal random variable associated with ij th observation

The next process is formulating the statistical for this typical analysis. The hypotheses for such analysis are:

$$H_0: \mu_1 = \mu_2 \quad \dots \dots \dots \quad 3.63$$

$$H_1: \mu_1 \neq \mu_2 \quad \dots \dots \dots \quad 3.64$$

Where:

- H_0 : Null hypothesis
- H_1 : Alternative hypothesis
- μ_1 : Mean of the response at the first factor level
- μ_2 : Mean of the response at the second factor level

The procedure of testing hypothesis are as follows; devise a procedure for taking a random sample, computing an appropriate test statistic, and then rejecting or failing to reject the null hypothesis. Part of this procedure is specifying the set of values called the critical region or rejection region for the test statistic that leads to the rejection of H_0 . Supposed that the variance of the two levels is equal then the appropriate test statistic to use for comparing two treatment means in the completely randomized design is:

$$t_0 = \frac{\bar{y}_1 - \bar{y}_2 - 0}{S_p \sqrt{\frac{1}{n_1} + \frac{1}{n_2}}} \quad \dots \dots \dots \quad 3.65$$

Where:

- \bar{y}_1 and \bar{y}_2 : Sample means
- n_1 and n_2 : Sample sizes

The value S_p is computed from S_p^2 , which is an estimate of the common variance,

$$S_p^2 = \frac{(n_1 - 1)s_1^2 + (n_2 - 1)s_2^2}{n_1 + n_2 - 2} \quad \dots \dots \dots \quad 3.66$$

Where:

- S_1^2 and S_2^2 : The two individual sample variances

To determine whether to reject H_0 or not, the value of t_0 would be compared with the t value obtained from the t distribution table. This test procedure is usually called the Two-Sample t -test. The H_0 will be rejected when the value of t_0 is

$$|t_0| > t_{\alpha/2, n_1+n_2-2} \dots\dots\dots 3.67$$

The other way to make a decision whether H_0 may or may not be rejected is by using P-values. The use of P-values has been widely accepted in practice. The P-value can be formally defined as the smallest level of significant that would lead to the rejection of the null hypothesis.

3.3.3. Single factor experiment

Single factor analysis is the most common approach employed by many researchers to explore the difference among more than two levels of a factor. Antony (2003) addressed this type of experiment as a One-Variable-At-a-Time (OVAT), where one variable is varying during the experiment and all the rest variables are fixed. Basically, there are two types of factor, quantitative and qualitative. A quantitative factor is a factor where some levels that can be quantified such as 0%, 10%, 20% and 30% are of interest. When the levels of a factor cannot be quantified such as different type of methods or materials, this kind of factor is classified as a qualitative factor.

A single factor analysis is a process of analyzing data obtained from experiment with different levels of a factor, usually more than two levels of factor. The appropriate procedure for testing the equality of several means is the analysis of variance or abbreviate as Anova. As the name implies, the Anova procedure attempts to analyze the variation in a set of responses and assign portions of this variation to each variable in a set of independent variables. The objective of the Anova is to identify important independent variables and determine how they affect the response (Wackerley, 2008). When only one factor is investigated, the process is called the one-way or single factor analysis of variance. The procedure for one-way Anova referred in this work is as described by Montgomery (2009) as follows.

Considers different levels, or treatments, of a single factor are being compared. The observed response from each treatment is a random variable. A simple linear statistic model for describing the observation results in such experiment is shown as follows.

$$y_{ij} = \mu_i + \epsilon_{ij} \quad \left\{ \begin{array}{l} i=1, 2, \dots, a \\ j=1, 2, \dots, n_i \end{array} \right. \quad \dots\dots\dots 3.68$$

Where

- y_{ij} : The ij th observation
- μ_i : Mean of the i th factor level or treatment.
- ϵ_{ij} : Random error component

The random error component, ϵ_{ij} , incorporates all sources of variability in the experiment including measurement, variability from uncontrolled factors, differences between the experimental units (such as test material, etc) to which the treatments are applied, and the noises in the process such as variability over time, effects of environmental variables. Equation 3.68 is called as a means model. Another alternative way to express the model for such data is to define:

$$\mu_i = \mu + \tau_i, \quad i=1, 2, \dots, a \quad \dots\dots\dots 3.69$$

So that Equation 3.68 becomes

$$y_{ij} = \mu + \tau_i + \epsilon_{ij} \quad \left\{ \begin{array}{l} i=1, 2, \dots, a \\ j=1, 2, \dots, n_i \end{array} \right. \quad \dots\dots\dots 3.70$$

Where

- μ : Parameter common to all treatments called the overall mean
- τ_i : Parameter unique to the i th treatment called i th treatment effect

The new equation provided is usually called as the effects model. The two models, means and effects model, are linear statistic model since the response variable, y_{ij} , is a linear function of the model parameters. Although both models are acceptable, the effects model is more broadly encounter in the experimental design literature. It was assumed that the experimental design is a completely randomized design. The objective in this design is to test and estimate the appropriate hypotheses about the treatment means. For hypothesis testing, the model errors are assumed to be normally and independently distributed. The null and alternative hypotheses for this statistical analysis are as follows.

$$H_0: \mu_1 = \mu_2 = \dots = \mu_a \quad \dots\dots\dots 3.71$$

$$H_1: \mu_i \neq \mu_j, \quad \text{for at least one pair } (i,j) \quad \dots\dots\dots 3.72$$

The analysis of variance (Anova) is derived from partitioning of total variability into its components parts. The total corrected sum of squares, which is used as a measure of overall variability in the data, is define as:

$$SS_T = \sum_{i=1}^a \sum_{j=1}^n (y_{ij} - \bar{y}_{...})^2 \dots\dots\dots 3.73$$

Note that the total corrected sum of squares may be written as:

$$\sum_{i=1}^a \sum_{j=1}^n (y_{ij} - \bar{y}_{...})^2 = n \sum_{i=1}^a \sum_{j=1}^n (\bar{y}_i - \bar{y}_{...})^2 + \sum_{i=1}^a \sum_{j=1}^n (y_{ij} - \bar{y}_i)^2 \dots\dots 3.74$$

The above equation states that the total variability in the data can be partitioned into a sum of squares of differences between the treatments means and the grand mean denoted as $SS_{treatments}$ and a sum of squares of differences of observation within a treatment from the treatment mean denoted SS_E . This statement can be written symbolically as:

$$SS_t = SS_{treatments} + SS_E \dots\dots\dots 3.75$$

Where:

- SS_t : Total corrected sum squares
- $SS_{treatments}$: Sum squares due to treatments (i.e. between treatments)
- SS_E : Sum squares due to error (i.e. within treatments)

There is also a partition of the number of degree of freedom that corresponds to the sum of squares in Equation 3.74. That is there are an = N observations; thus, SS_t has an – 1 degrees of freedom. There are a levels of the factor, So, $SS_{treatments}$ has a – 1 degrees of freedom. Also, within any treatment there are n replicates providing n – 1 degrees of freedom with which to estimate the experimental error. Since there are a treatments, the degrees of freedoms for error become a(n – 1). Therefore, the degrees of freedom partition is

$$an - 1 = a - 1 + a(n - 1) \dots\dots\dots 3.76$$

The ratio of $SS_{treatments}$ to the degree of freedom is called as the mean square for treatment, and may be written as follows.

$$MS_{treatments} = \frac{SS_{treatments}}{a-1} \dots\dots\dots 3.77$$

Now, if the null hypothesis is true, $MS_{\text{treatments}}$ is an unbiased estimator of σ^2 because $\sum_{i=1}^a \tau_i = 0$. However, if alternative hypothesis is true, $MS_{\text{treatments}}$ estimates σ^2 plus a positive term that incorporates variation due to the systematic difference in treatment means. It should be noted that the error mean square is defined as:

$$MS_E = \frac{SS_E}{(N - a)} \dots\dots\dots 3.78$$

The test statistic for the hypothesis of no differences in treatment means in analysis of variance is defined by the following equation.

$$F_0 = \frac{SS_{\text{treatments}}/(a - 1)}{SS_E/(N - a)} = \frac{MS_{\text{treatments}}}{MS_E} \dots\dots\dots 3.79$$

The H_0 hypothesis should be rejected and conclude that there are differences in the treatment means if:

$$F_0 > F_{\alpha, a-1, n-a} \dots\dots\dots 3.40$$

Or alternatively, a P-values approach can also be used for decision making.

3.4. Validation Process

3.4.1. Validation process using simple comparative experiment

Experimental program

In this experiment, modified sandwich panels (MB) containing intermediate layer were compared to the control of unmodified conventional sandwich panels (UB). Samples were prepared in two size categories, termed small and large. Each size categories was divided into two groups of samples based on the core used. Two types of core were used for small samples; polystyrene (EPS) and polyethylene (PE). While, the larger samples employed polystyrene (EPS) and balsa wood core. The arrangement of the experiment is shown in Table 3.1 and Table 3.2. The sandwich panels were made in accordance with ASTM C393-00 standard. According to this standard, the overall length of beam should be at least 25 times the thickness (t), span length of 20t for simply supported span, and 2t for the width. Hence, the large samples were prepared with the size of 312.5 x 25 x 12.5 mm and the small samples were 250 x 20 x 10 mm, with gauge length of 250 and 200 mm respectively. A 0.3 mm thickness of aluminium

sheet was used as the skin of all samples. The thicknesses of samples were kept constant at 12.5 mm for large beam samples and 10 mm for small beams.

Table 3.1. Experimental arrangements for simple comparative experiment (*small size*)

Samples group	Treatments	Role in sandwich structure	Material	Thickness (mm)
Group 1: Polystyrene (EPS) core	Unmodified Beams (UB)	Skin	Aluminium	0.3
		Intermediate layer	No IL	-
		Core	EPS	9.4
	Modified Beams (MB)	Skin	Aluminium	0.3
		Intermediate layer	Balsa wood	3
		Core	EPS	3.4
Group 2 : Polyethylene (PE) core	Unmodified Beams (UB)	Skin	Aluminium	0.3
		Intermediate layer	No IL	-
		Core	PE	9.4
	Modified Beams (MB)	Skin	Aluminium	0.3
		Intermediate layer	Balsa wood	3
		Core	PE	3.4

Table 3.2. Experimental arrangements for simple comparative experiment (*large size*)

Samples group	Treatments	Role in sandwich structure	Material	Thickness (mm)
Group 1: Polystyrene (EPS) core	Unmodified Beams (UB)	Skin	Aluminium	0.3
		Intermediate layer	-	-
		Core	EPS	11.9
	Modified Beams (MB)	Skin	Aluminium	0.3
		Intermediate layer	Plywood	3
		Core	EPS	5.9
Group 2 : Balsa wood core	Unmodified Beams (UB)	Skin	Aluminium	0.3
		Intermediate layer	None	-
		Core	Balsa wood	11.9
	Modified Beams (MB)	Skin	Aluminium	0.3
		Intermediate layer	Plywood	3
		Core	Balsa wood	5.9



Figure 3.9. *Left*: MTS Alliance RT/10 testing machine connected to computer device. *Right*: Sample set-up under three-point bending loads scheme.

All the components were bonded together using epoxy resin, Kinetix R246Tx thixotropic with Kinetix H160 hardener, as the adhesive. All specimens were tested using a MTS Alliance RT/10 testing machine with a maximum capacity of 10 kN under three-point bending scheme as per ASTM C 393-00. Samples in the small category were replicated 5 times, and 6 times for the large size. The test set-up for three-point bending load is shown in Figure 3.9.

Experimental results and discussions

The results of the simple comparative experiment are summarized in Table 3.3 and Table 3.4 which show the bending strength of all four different categories of samples. It can be noticed that there has a fluctuation in the distribution of individual data in the observed flexural strength. The presence of this fluctuation is normal for the data provided from such an experiment which implies that the response variable is a random variable, as it is commonly assumed in the statistical analysis. The fluctuation of observed data may arise from different sources such as material and sample preparation, human error or perhaps the performance of the testing machine.

Table 3.3. Bending strength (MPa) small size sandwich panel beam

Samples	Group 1: Polystyrene (EPS) core		Group 2: Polyethylene (PE) core	
	Modified Beam (MB)	Unmodified Beam (UB)	Modified Beam (MB)	Unmodified Beam (UB)
1	32.92	10.61	10.08	2.29
2	43.54	18.36	10.43	2.83
3	36.36	10.10	7.99	2.78
4	44.64		9.53	3.21
5	33.62		12.82	3.25
Average	38.22	13.02	10.17	2.87
Std Dev.	5.53	4.63	1.75	0.39
CV (%)	14.5	35.6	17.2	13.6

Table 3.4. Bending strength (MPa) larger size sandwich panel beam

Samples	Balsa core		Polystyrene (EPS) core	
	Modified Beam (MB)	Unmodified Beam (UB)	Modified Beam (MB)	Unmodified Beam (UB)
1	113.94	62.66	22.34	10.12
2	107.80	76.38	21.30	8.66
3	117.41	43.98	23.81	9.99
4	105.83	56.56	21.30	6.46
5	127.67	62.18	17.86	6.65
6	105.36	51.20	19.08	10.78
Average	113.00	58.83	20.95	8.78
Std Dev.	8.63	11.12	2.16	1.85
CV (%)	7.6	18.9	10.31	21.07

A quick visual assessment of these data gives the perception that the flexural strength of the modified beams (MB) is greater than the unmodified beams (UB). This impression is supported by comparing the average values of modified and unmodified beam sample presented in these tables. A clear illustration of the experiment results are presented in Figure 3.10 and Figure 3.11. As it can be observed from Figure 3.10, it is clearly shown that introducing intermediate layer has significantly increased the bending stress.

The bending stresses of all modified beam (MB) were notably higher than the unmodified beam (UB). The improvement ranges from 90% to around 250%, dependent on the type of the core material used. The lower strength of the core material the higher the improvement gained by introducing intermediate layer. When a low density (low strength) core material used such as polyethylene and polystyrene, early failure occurs due to localized compression. The introduction of intermediate layer results in improved bending strength but is not warranted when a very low core material such as polyethylene used as the core. The graph shows that, for small size samples, the maximum average bending strengths of modified sandwich panel with polystyrene and polyethylene were 10.17 MPa and 38.22 MPa, respectively. The correspond values for larger size samples were 20.95 MPa and 113 MPa for polystyrene (EPS) and Balsa wood cores, respectively.

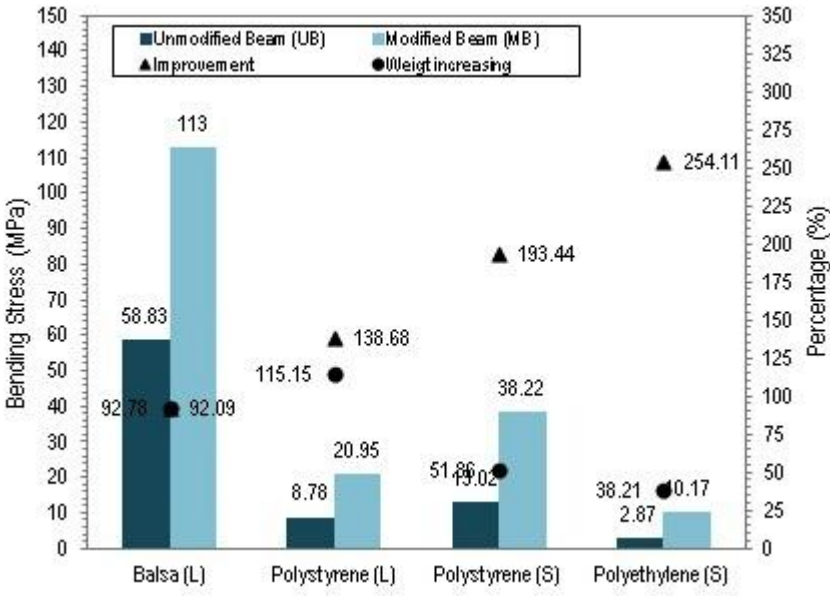


Figure 3.10. Bending stress (MPa) and improvement (%) of sandwich panel

The great advantage of using an intermediate layer is most apparent when a core material with high compressive strength is used. As shown in Figure 3.10, when balsa was used as the core material without intermediate layer; the bending stress of sandwich panel reached a value of 58.83 MPa which corresponds to the modulus of rupture of balsa wood. However, a considerable enhancement of bending strength to 113 MPa, which is 92.09% of improvement, is reached when intermediate layer was introduced in the panel. It also can be noticed in the figure that the improvement of bending strength due to introducing an intermediate layer will result in a substantial increase in the weight of sandwich panel. The range of weight increases varied from 40% to 100%. If a non-dimensional analysis is considered by using strength to overall density and/or weight ratios, which is termed material specific strength, the experimental results show that the specific strength of the two treatments were substantially similar for all large samples and higher for all small samples as illustrated in Figure 3.11.

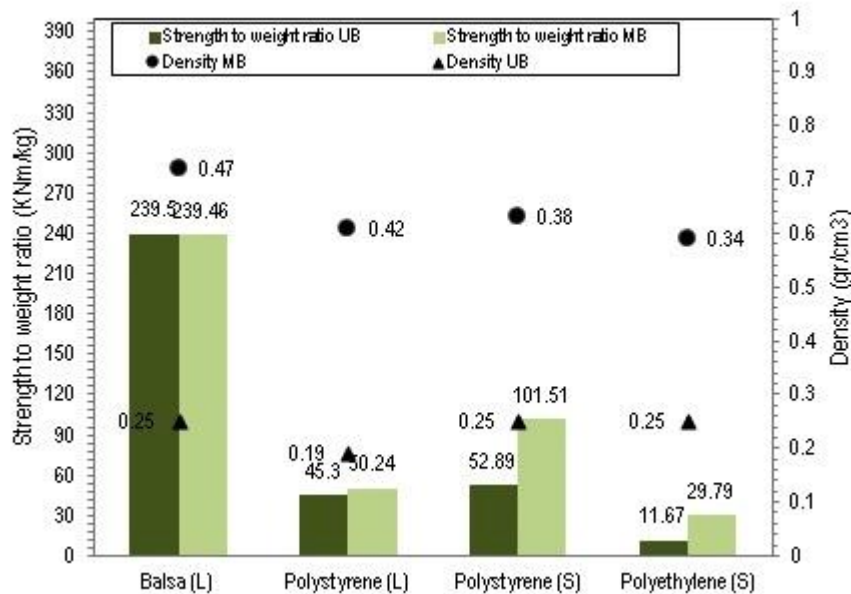


Figure 3.11. Strength to weight ratio (KNm/kg) and density (gr/cm³) of sandwich panel

The average specific strengths of modified and unmodified beam samples for specimens with balsa core were 238.5 and 239.5 KNm/kg, respectively. The values for samples with polyethylene cores were 11.67 and 29.79 KNm/kg, respectively. While such an improved strength to weight ratio is very good the product does not meet the minimum requirement for structural applications. The results are much higher than the specific strength of concrete, which is typically in the range of 8.3-16.6 KNm/kg and

approach the specific strength of other common metals such as aluminium alloy, steel alloy and titanium alloy (222, 254, and 288 KNm/kg, respectively). The density of modified beam samples was notably higher than the density of unmodified beam, but it is still much lower than the properties of common material like concrete, which are around 2.3 g/cm^3 . In some specific applications such as lightweight structure, specific strength is more important than other properties.

The failure patterns of the tested samples show how the modification concept using intermediate layers prevented early failure mechanisms due to wrinkling of the upper face, resulting in a higher bending capacity. Figure 3.12 shows that the unmodified beams collapsed mostly in the form of indentation or face wrinkling. Shear failure of the core and tensile failure at the bottom were the dominant failure mechanisms for the modified sandwich beam specimens. The results verified the earlier work of Mamalis et al (2008) which concluded that the introduction of an intermediate layer will improve the capability of a sandwich panel to resist early indentation and/or face wrinkling. The typical failure patterns of some specimens tested under flexural load are presented in the following figure.



Figure 3.12. Typical failure patterns of unmodified sandwich panel (*above*) and modified sandwich panel (*bottom*)

Significance analysis

In addition to the above discussion, which is actually a descriptive statistical analysis, an inferential statistical analysis was conducted to analysis any significant improvement obtained by the introduction of intermediate layer. Statistics software, Minitab-15 was employed to analyze the results of the experiments. As it has been mentioned earlier, this experiment was specifically designed to answer the question on

how significant the difference between two levels or treatments; control level and treatment level.

The result of inferential analysis of the large samples with balsa core, as a representative of four categories, is presented in Table 3.5. The result script from the Minitab15 software gives some important information. The most important information for statistical inference is the T-value and P-value. As it can be seen from the table, T-value of the test is 9.43, while the P-value is 0. The rule for making an inference or decision in this typical analysis is based on the statement that the H_0 hypothesis should be rejected when the T-value is higher than the T_α , which is obtained using t-distributions available in statistic books. With the level significance of 0.05 and the value of degree of freedom (DF) = 10, the statistic book gives the critical value of $T_\alpha=2.228$. As T-value = 9.43 exceeds the critical value, so the null hypothesis should be rejected at this level (0.05) which means that the bending stress of a modified sandwich panel with intermediate layer is significantly different than the unmodified panel. It can be said that the modification of a sandwich panel by incorporating an intermediate layer has significantly improved the flexural strength of sandwich panel.

Table 3.5. Computer output using Minitab 15 software for the Two-Sample *t*-test

Two-sample T for Modified Beam (MB) vs Unmodified Beam (UB)				
	N	Mean	StDev	SE Mean
Modified Beam (MB)	6	113.00	8.63	3.5
Unmodified Beam (UB)	6	58.8	11.1	4.5
Difference = mu (Modified Beam (MB)) - mu (Unmodified Beam (UB))				
Estimate for difference : 54.17				
95% CI for difference : (41.37, 66.98)				
T-Test of difference = 0 (vs not =): T-Value = 9.43 P-Value = 0.000 DF = 10				
Both use Pooled StDev = 9.9506				

The results of the analysis for other sample categories are presented in Table 3.6. In order to provide a T-value based t-distribution table (T_α), the degree of freedom should be used together with the chosen significance level (α). In this analysis it was decided to use the significance level of 95% ($\alpha = 0.05$). It is clearly demonstrated in Table 3.6 that the value of calculated T-value exceeds the value of T_α which means that the alternative hypothesis (H_1) is accepted and accordingly the null hypothesis (H_0) is rejected. In other words, the bending strength of the unmodified sandwich panels is significantly lower than that of the modified sandwich panels.

Table 3.6. Summary of Two-Sample *t*-test results for all samples categories

No	Categories	Minitab Analysis			$t_{\alpha/2, n_1+n_2-2}$
		T-value	P-Value	DF	
1	Balsa core (<i>large</i>)	9.43	0.000	10	2.228
2	Polystyrene core (<i>large</i>)	10.46	0.000	10	2.228
3	Polystyrene core (<i>small</i>)	6.58	0.001	6	2.447
4	Polyethylene core (<i>small</i>)	9.10	0.000	8	2.306

3.4.2. Validation process using single factor experiment

Experimental program

In this experiment, three different materials were employed for the intermediate layers; hardboard, medium density fiber (MDF) and plywood. With the inclusion of a control group that consists of an ordinary sandwich panel without intermediate layer, the experiment is carried out to test four levels of a factor. For the purposes of analysis, this factor was leveled as 0, 1, 2 and 3 as required by Minitab-15 software. Level 0 was the sample with no intermediate layer which used as the control level while level 1, 2 and 3 refer to as hardboard, MDF and plywood, respectively. The experimental arrangement of the single factor experiment is presented in Table 3.7.

Table 3.7. Experimental arrangements for single factor analysis

Samples group	Treatment levels	Role in sandwich structure	Material	Thickness (mm)
Group 1 (Balsa core)	Level 0	Skin	Aluminium	0.3
		Intermediate layer	No IL	-
		Core	Balsa wood	11.9
	Level 1	Skin	Aluminium	0.3
		Intermediate layer	Hardboard	3
		Core	Balsa wood	5.9
	Level 2	Skin	Aluminium	0.3
		Intermediate layer	MDF	3
		Core	Balsa wood	5.9
	Level 3	Skin	Aluminium	0.3
		Intermediate layer	Plywood	3
		Core	Balsa wood	5.9
Group 2 (EPS core)	Level 0	Skin	Aluminium	0.3
		Intermediate layer	No IL	-
		Core	EPS	11.9
	Level 1	Skin	Aluminium	0.3
		Intermediate layer	Hardboard	3
		Core	EPS	5.9
	Level 2	Skin	Aluminium	0.3
		Intermediate layer	MDF	3
		Core	EPS	5.9
	Level 3	Skin	Aluminium	0.3
		Intermediate layer	Plywood	3
		Core	EPS	5.9

As for the specimens for simple comparative experiment, the sandwich panel samples were fabricated in accordance with ASTM C 393-00 which is a standard test method for flexural properties of flat sandwich constructions. The samples were cut and shaped into the size of 312.5 x 25 x 12.5 mm for length, width and thickness, respectively. The span length was 250 mm and two types of core materials were employed; balsa wood and polystyrene (EPS). An aluminium sheet with the thickness of 0.3 mm was used as the skins for all samples. The overall thickness of sandwich panels was kept constant to 12.5 mm. This experiment was designed as a single factor with 4 levels. Each level was replicated 6 times; hence the total of samples tested was 48 beams. The processes for specimen preparation and the flexural testing are presented Figure 3.13.



Figure 3.13. Specimen preparation and flexural testing

Experimental results and discussions

Table 3.8 shows the flexural strength of four levels in single factor experiment. The data presented in the table indicates some differences in the average values of flexural strength. It also indicates the noise of the individual observation within a level as approximate by the coefficient of variation (CV) values. The average flexural strength of these treatments differs by a large amount when comparing each modified level to the control. However, a detailed analysis has to be made in order to provide more comprehensively findings.

In a single factor analysis, the comparison is not only made between each level and the control, but also between each factor levels. When a comparison is made between the modified samples, say between level 3 and level 4, the average flexural strength in these two samples differs by what seems to be a modest amount. Although there has a difference, it is not automatically implies that the two modified sandwich panel forms are significantly different. In the case of only a modest amount of difference encountered, the difference is perhaps due to the result of sampling fluctuation and the two sandwich panels' composition are really identical.

Table 3.8. The result of single factor experiment

Groups	Replications	Treatment Levels (based on intermediate layer used)			
		Level 1: No IL	Level 2: Hardboard IL	Level 3: MDF IL	Level 4: Plywood IL
Group 1 (Balsa core)	1	62.66	141.83	108.81	113.94
	2	76.38	151.84	136.69	107.80
	3	43.98	145.37	118.14	117.41
	4	56.56	164.37	124.02	105.83
	5	62.18	159.20	91.52	127.67
	6	51.2	139.35	125.98	105.36
Average		58.83	150.33	117.53	113
Stdv		11.12	9.95	15.71	8.63
CV (%)		18.90	6.62	13.36	7.64
Groups	Replications	Treatment Levels (based on intermediate layer used)			
		Level 1: No IL	Level 2: Hardboard IL	Level 3: MDF IL	Level 4: Plywood IL
Group 2 (EPS core)	1	10.12	13.66	20.01	22.34
	2	8.66	26.71	20.39	21.30
	3	9.99	17.15	25.50	23.81
	4	6.46	16.74	23.17	21.30
	5	6.65	27.75	24.64	17.86
	6	10.78	27.90	23.64	19.08
Average		8.78	21.65	22.89	20.95
Stdv		1.85	6.48	2.24	2.16
CV (%)		21.13	29.94	9.78	10.33

The data shown in Table 3.8, has been re-presented in the form of graphical data for more convenient and immediate notification. The bending strength of each level was plotted against the sample categories which is based upon the core used. The results are presented in the following figure.

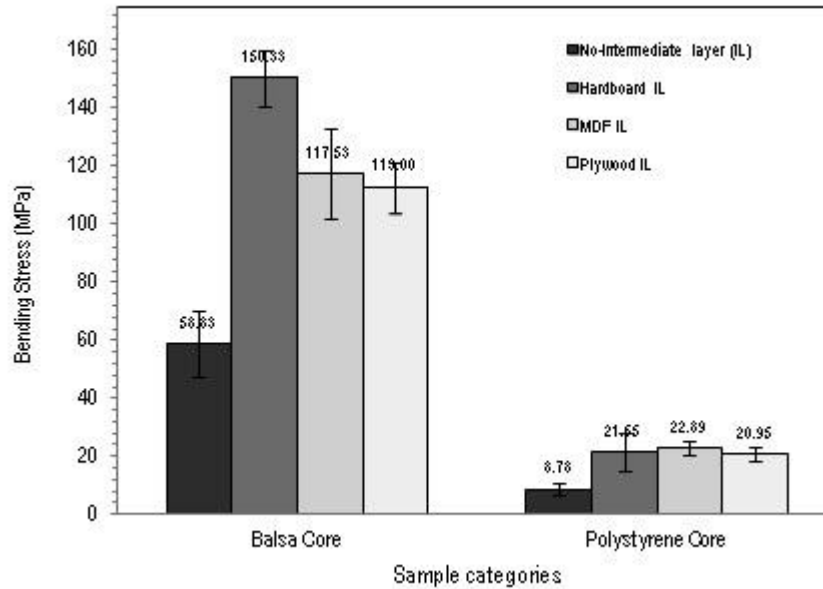


Figure 3.14. Bending stress (MPa) of sandwich panel beam tested under single factor experimental design

Figure 3.14 shows the bending stress of sandwich panels with different types of intermediate layer, hardboard, medium density fibre (MDF) and plywood against sandwich panel without intermediate layer. There are two categories of samples; one group of samples with a balsa core and the other group of samples with a polystyrene core. It is clearly demonstrated in this figure that the sandwich panels with an intermediate layer have superior bending stress capacity than the control group without an intermediate layer. The range of improvement contributed by the presence of an intermediate layer was around 100 – 150% for samples with a balsa core and 130-150% for samples with a polystyrene (EPS) core.

In addition, it is also evident that the core material plays a significant role in distributing some amount of bending stress in order to prevent a premature failure. The average bending stress for the sandwich panels with an intermediate layer and polystyrene core ranged from 20.95 – 21.65 MPa. This is quite far less than the capacity of the sandwich panel with an intermediate layer and balsa core, which was about 113 -

150 MPa. There are indeed other possible potential factors that can affect the bending stress of this new hybrid sandwich panel such as the interaction between the intermediate layer and the core material. The most important disadvantage of single factor experimental design is that it is unable to consider any possible interaction between the factors in the sample population. A factorial design of experiment could be a better way to overcome this limitation.

The introduction of intermediate layer in a sandwich structure will most likely incur a penalty regarding weight or cost, but the improvement achieved should compensate all those costs. If a specific strength or strength to weight ratio is considered as a parameter, incorporating an intermediate layer may reduce the specific strength up to 35% but also improve the strength up to 150%, as shown in Figure 3.15.

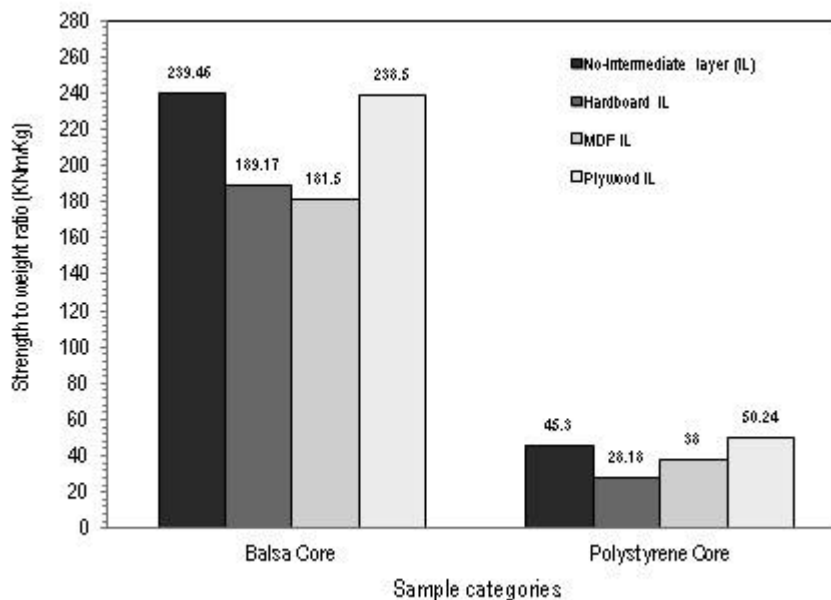


Figure 3.15. Strength to weight ratio (*specific strength*) of sandwich structures for two different sample categories based on core used

The figure shows that the specific strength of modified sandwich structures with hardboard and MDF intermediate layers are 189.17 and 181.5 KNm/Kg which is about 21% and 24.3 % less than the specific strength of unmodified sandwich structures. For the sandwich panel with the plywood intermediate layer the specific strength is almost similar to the unmodified one. Similar pattern is also observed by the sandwich structures with the polystyrene core. The specific strength of the modified sandwich structure with a plywood intermediate layer is higher than for the unmodified panel. The

use of hardboard and MDF as intermediate layers reduced the specific strength. Employing a plywood intermediate layer seems the most appropriate choice as it can improve the bending strength up to around 92.08% for a balsa core and 138.61% for a polystyrene core, while maintaining the similar specific strength as the unmodified sandwich structure. However, using plywood will increase cost as the price of plywood is almost double that of MDF and hardboard.

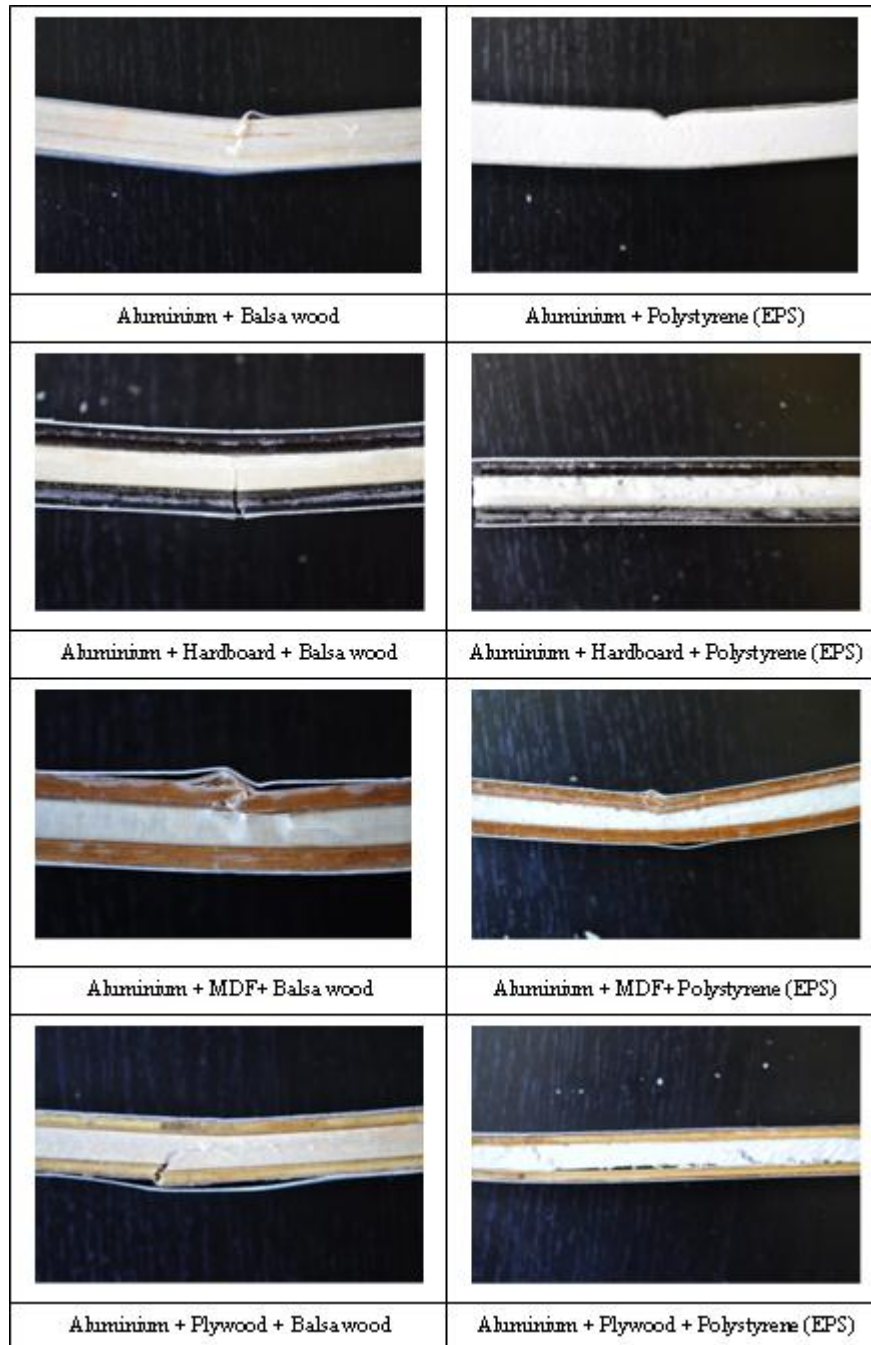


Figure 3.16. *Left:* Typical failure patterns of sandwich panels with balsa core.
Right: sandwich panel with polystyrene core

The typical failure modes seen in the sandwich panels are shown in Figure 3.16. The figure illustrates how the introduction of an intermediate layer has prevented the occurrence of premature failure modes. Sandwich panels with a balsa core and without an intermediate layer typically failed by wrinkling at the top skin. The addition of an intermediate layer provided some additional strength to the sandwich panel with failure occurs via mechanisms such as tensile, shear and delamination. A different mode of failure, indentation at the top skins, was encountered for the sandwich panel with polystyrene core. Core shear and delamination were the typical failure modes for the sandwich panels with polystyrene cores and with intermediate layers.

Significance analysis

The primary concern in this analysis is to find out the inference of how significant the difference among all means of factor levels and also between levels of factor. The appropriate procedure for testing the equality of several means as in this experiment is by performing analysis of variance (Anova). The results of Anova using Minitab are shown in Table 3.9. The rule of making a decision in this type of experiment is based on Equation 3.16; whenever the value of calculated F (F_0) exceeds the value of F table ($F_{\alpha,a-1,n-a}$) then a null hypothesis should be rejected and it can be concluded that the level means differ.

Table 3.9. Computer output using Minitab 15 for the analysis of variance (Anova)

One-way ANOVA: Bending stress versus Intermediate layer type

Source	DF	SS	MS	F	P
Intermediate layer type	3	25864	8621	63.41	0.000
Error	20	2719	136		
Total	23	28583			

S = 11.66 R-Sq = 90.49% R-Sq(adj) = 89.06%

Individual 95% CIs For Mean Based on Pooled StDev

Level	N	Mean	StDev	CI
0	6	58.83	11.12	(---*---)
1	6	150.33	9.95	(---*---)
2	6	117.53	15.71	(--*--)
3	6	113.00	8.63	(---*---)

-----+-----+-----+-----+-----+-----
 60 90 120 150

Pooled StDev = 11.66

For example, as presented in Table 3.9, the F-value obtained by Minitab, (F_0) = 63.41. If a significance level of 95% ($\alpha = 0.05$) is selected, 6 replications ($a = 6$) and 24

number of samples ($n = 24$) then from table F-distribution it can be found that $F_{(0.05;5,19)} = 2.74$. Because the value of $F_0 = 63.41 > 2.74$, H_0 will be rejected which means the level is different; that is, introducing intermediate layer significantly affects the bending stress of sandwich panel. A value of P is also very frequently used for drawing a conclusion; if the P-value is less than α (0.05, error tolerance level), it reflects that there has factor levels or treatments which have different means. It is clearly presented in Table 3.9 that the p-value of this analysis is very small as obtained by Minitab-15 analysis.

At the lower part of the Anova output, there has also information about the mean and standard deviation of all factor levels as well as their matrix. Based on the graph presented there, a rough decision of what factor levels differ can be obtained. But the decision that could be made would be subjected to unsatisfactorily for the research. Therefore, a pairwise comparison between all factor levels needs to be conducted. There are several possible test methods for this purpose such as Dunnet's test, Tukey's test and Fisher's test. Many statisticians prefer to use the Tukey method because it controls the overall error rate (Montgomery, 2009).

The Tukey's test compares all possible pairs of means and can be used to determine which means amongst a set of means differ from the rest. This typical test is normally conducted after Anova leads to a conclusion that there is evidence that the group means are different. The results are presented as a matrix showing the result of each pair as a confidence interval. If none of the Tukey confidence intervals equals zero, it indicates that all of the means are different. The output of Tukey's test for this experiment is summarized in Table 3.10.

Table 3.10 shows that for the first level comparison, there has no confidence interval contains zero, all results are positive numbers, which means that the level 1, 2 and 3 have a significant difference with level 0. All the confidence interval in the second process contains negative numbers, which means that level 1 has a large difference with level 2 and level 3. In the last step, the interval confidence is - 23.38 for the lower and +14.33 for the upper, which means there has a zero number in between the lower and upper confidence interval. This figure leads to a conclusion that there has no significant difference between level 2 and level 3. The results of this test are extremely important to drawing a conclusion, particularly the last one. Although the

mean bending strength of level 2 (117.53 MPa) and level 3 (113 MPa) could be considered to be different, the statistical analysis shows that those two means are basically similar.

Table 3.10. Summary of the Tukey’s test result using Minitab 15

Descriptions	Treatments	Confidence Interval		
		Lower	Centre	Upper
Comparison between level 0 to level 1, 2 and level 3	Level 0 vs Level 1	72.65	91.50	110.35
	Level 0 vs Level 2	39.85	58.70	77.55
	Level 0 vs Level 3	35.32	54.17	73.03
Comparison between level 1 to level 2 and 3	Level 1 vs Level 2	-51.65	-32.80	-13.95
	Level 1 vs Level 3	-56.18	-37.32	-18.47
Comparison between level 2 and 3	Level 2 vs Level 3	-23.38	-4.53	14.33

There are other kinds of pairwise comparison tests that usually conducted simultaneously with Tukey's test, such as Dunnett's test and Fisher’s test. They are basically similar to the Tukey’s test. The Dunnett's test is specifically designed for situations where all levels are to be pitted against one reference level. It is commonly used after Anova has rejected the hypothesis of equality of the means of the distributions. Its goal is to identify levels whose means are significantly different from the mean of reference level. The result of Dunnett’s test is presented in Table 3.11.

Table 3.11. The result of Dunnett’s test using Minitab 15

Dunnett's comparisons with a control				
Family error rate = 0.05				
Individual error rate = 0.0195				
Critical value = 2.54				
Control = level (0) of Intermediate layer type				
Intervals for treatment mean minus control mean				
Level	Lower	Center	Upper	
1	74.40	91.50	108.60	(-----*-----)
2	41.60	58.70	75.80	(-----*-----)
3	37.07	54.17	71.28	(-----*-----)
				-----+-----+-----+-----
				40 60 80 100

The Dunnett’s test only compares the control with the rest of factor levels. There are two possible ways to make judgment through this type of test. The first way is comparing the critical value of control level with other levels. As it can be seen in Table 3.11, the critical value of control (level 0) is 2.54. Meanwhile, the critical value of level 1, level 2 and level 3 was 91.5, 58.7 and 54.17, respectively. Those three critical values of levels were much higher than the critical value of control. This result confirms that

the bending stress of sandwich panel with intermediate layer is significantly higher than the conventional sandwich panel. The second way is by checking whether the confidence interval contains zero or not. The result in Table 3.11 shows that none of the three levels contains zero which means that they are substantially different. In addition, a Fisher's test is presented here for a comparison purpose. The Fisher's test is similar to the Tukey's test in term of goal and rules. The result of Fisher's test obtained using the Minitab 15 software is presented in the following table.

Table 3.12. The summary of Fisher's test result using Minitab 15

Descriptions	Treatments	Confidence Interval		
		Lower	Centre	Upper
Comparison between level 0 to level 1, 2, and 3.	Level 0 vs Level 1	77.46	91.50	105.54
	Level 0 vs Level 2	44.66	58.70	72.74
	Level 0 vs Level 3	40.13	54.17	68.22
Comparison between level 1 to level 2 and 3	Level 1 vs Level 2	-46.84	-32.80	-18.76
	Level 1 vs Level 3	-51.37	-37.32	-23.28
Comparison between level 2 and 3	Level 2 vs Level 3	-18.57	-4.53	9.52

As indicated in Table 3.12, for the first and second comparisons, none of the confidence interval contains zero number meaning that they are different to each other. However, the confidence interval in the third comparison includes a zero number between -18.57 and 9.52, which indicates that the level 2 and level 3 are not significantly different.

3.5. Chapter Conclusion

This chapter that explored the theoretical concept of the proposed hybrid sandwich panel and the validation of the research approach using statistical experimental design, several conclusions can be drawn from the previous analysis. Introducing an intermediate layer into the ordinary sandwich structure, that creates a hybrid sandwich panel, increases the flexural rigidity and correspondingly enhances the stiffness. Derivation of some important equations regarding the flexural rigidity and the stiffness of the new hybrid structure validates the research approach. The statistical experimental designs employed in this preliminary experiment have validated the previous claim of Mamalis et al (2008) that the introduction of intermediate layer significantly enhanced the mechanical properties of sandwich panel structure. The result of these preliminary experiments shows the potential of this new hybrid sandwich panel

composite to be developed further for potential use as a load-carrying component in building application. More detailed findings at this stage are as follows.

- 1) Based on the simple comparative experiment analysis it has been suggested that the introduction of intermediate layer significantly improved the bending strength of the new hybrid composite sandwich beams. The T-value of all four sample categories exceeded the corresponding values provided from relevant table *t*-distributions, verifying that the bending strength of the sandwich panels with intermediate layers are significantly higher than the unmodified sandwich panels. Both modified and unmodified composite sandwich beams exhibited excellent specific strengths at a level comparable to those of high strength metal alloys. The incorporation of natural based materials into the new hybrid composite sandwich panels has the potential to reduce costs while maintaining structural capacity with the additional benefits of improved fire resistance and insulation.
- 2) Single factor experiment has suggested that the introduction of intermediate layer, hardboard, medium density fibre (MDF) and plywood, has significantly improved the flexural strength of the sandwich panel. The results of statistics inferential analysis using software Minitab 15 confirmed that sandwich panels containing intermediate layer are significantly different to the conventional sandwich panel. The Tukey's and Fisher's test showed that all confidence levels were positive when compared other levels to the control (level 0). The result of Dunnet's test showed that the critical value of level 0 (control) was far less than those of other levels, which means that the bending stress of sandwich panel with intermediate layer is significantly different (higher) than conventional sandwich panel. Graphical descriptive statistics clearly demonstrated that the sandwich panels containing lignocellulosic composites intermediate layer have superior bending stress capacity than the control group with no intermediate layer. The range of improvement contributed by the presence of intermediate layer was around 100 – 150% for samples with a balsa core and 130-150% for samples with a polystyrene core. The result of this analysis shows the potential of lignocellulosic composite materials to be developed further for producing more sustainable hybrid sandwich panel.

CHAPTER 4

PREPARATION, FABRICATION AND CHARACTERIZATION OF NATURAL FIBRE COMPOSITES FOR HYBRID SANDWICH PANEL

4.1. Introduction

The previous chapters have demonstrated the excellent potential of hybrid sandwich panel as a new cost effective and innovative addition to the available spectrum of building elements. In the preliminary experiment discussed in Chapter 3, lignocellulosic composites that are readily available in the market were used for the intermediate layer. Although those materials demonstrate a good performance as the intermediate layer, they are originally designed and produced for different applications which are commonly for domestic uses such as for furniture and non-structural use in building construction. Currently the demand for them has also continuously increased and the market needs to supply other materials as the alternative. In this research, natural fibre composites (NFCs) were employed for the intermediate layer of the new developed hybrid sandwich panels.

In order to use these materials properly as a new constituent in sandwich panel structure, an adequate knowledge of mechanical properties and failure mechanism is required. This chapter focuses on the development of NFCs and includes details of material preparation, chemical treatment, fabrication process and experimental work on the characterization of their mechanical properties. The hybrid sandwich panel studied in this work consisted of aluminium skins, expanded polystyrene (EPS) core and NFCs intermediate layer. The properties of skins and core materials are well documented as they have been widely researched and in the building industry. The NFCs used for the intermediate layer had to have their basic properties determined experimentally as their mechanical properties are very sensitive to the fabrication process (Babu et al, 2009).

The natural fibres were chemically treated using alkali (NaOH) prior to being incorporated in the composite laminates. The laminates were fabricated using a vacuum bagging process and after curing for a week were cut to the required sizes for testing. The mechanical properties of NFCs were determined based on the ASTM and ISO standards as outlined below.

4.2. Natural Fibre Preparation and Chemical Treatment

4.2.1. Natural fibre preparation

Three types of natural fibres were used in this study, that is, jute, sisal and hemp that were all obtained from different sources. A chopped bamboo board (not fibre) was also used to prepare NFCs laminates. The natural fibres are all shown in Figure 4.1.



Figure 4.1. Natural fibres incorporated in this research

The Hessian jute fibre was purchased from Bunning's warehouse in Toowoomba. The fibres were available in a continuous roll and seem to be the most readily available natural fibres in current market. Hemp fibres were in the form of hemp mat that obtained from a Chinese supplier. Sisal fibres were sourced from a local trader in Lombok, Indonesia. The fibres were traditionally processed by the local farmer from *Agave Sisalana* leaves and then shipped to Australia for the specific purpose of this research. The chopped bamboo board were obtained from local Asian shops in Toowoomba and most probably shipped from the Philippines. Except for the hemp mat and the chopped bamboo, the jute and sisal fibres used in this research were chemically treated prior to further processing for NFC laminates fabrication. The sisal fibres were prepared in two forms of chopped and unidirectional fibres. The jute fibres were prepared in the form of woven fibres as originally purchased and were cut to required size prior to further processing.

4.2.2. Chemical treatment

It is well understood in composite mechanics that the main problem of using natural fibres to reinforce plastic matrix is the incompatibility of the two primary constituents and also the inherent high moisture absorption of fibre that may lead to the micro cracking and degradation of the composite laminates. In order to cope with this problem, various chemical treatments have been developed. The chemical treatments may or may not be applied together with pre and post treatment depended upon the final target quality of the NFCs. The methods for chemical treatments include alkaline, silane, acetylation, benzoylation, acrylation, maleated coupling agents, isocyanates and permanganate (Li et al, 2007).

Among the current available choices of chemical treatment method, alkali treatment is the most frequently used for natural fibres modification. This method is also known as mercerization, a process that removes a certain amount of lignin, wax and oils covering the surfaces of the fibre cell wall, depolymerizes cellulose and exposes the short length crystallites (Mohanty et al, 2001; Li et al, 2007) by using certain amount of sodium hydroxide (NaOH). Until now, there have been no standard procedures for the chemical treatment of NFCs and a large number of different procedures in term of chemical composition and processing steps are available in the literature. Even in a single specific method of using alkali treatment, many different

processes have been proposed and interestingly all those researchers claimed the effectiveness of their proposed approach. Some of the processes are summarized in Table 4.1.

Table 4.1 Alkali treatment to different types of natural fibres-chemical composition and treatment time and temperature condition

No	Fibre types	Percentage of Sodium Hydroxide (NaOH) used	Treatment Time and Temperature Condition	Authors/ Researchers
1	Sisal	2 %, Room temperature	2 hours Room temperature	Botaro et al (2010)
2	Alfa	1, 5 and 10%	24 and 48 hours 28 ⁰ C	Rokbi et al (2011)
3	Tossa jute	0-28%	30 minutes (0.5 hours) 20 ⁰ C	Gassan and Bledzki (1999)
4	Banana and Coconut husk	5, 10 and 15%	3 hours Room temperature	Ahad et al (2009)
5	Flax	1, 2 and 3%	20 minutes (0.33 hours) Room temperature	Weyenberg et al (2003)
6	Jute	5%	2, 4, 6 and 8 hours Room temperature	Ray et al (2001)
7	Hildegardia Populifolia	2%	30 minutes (0.5 hour)	Rajulu et al (2005)
8	Coir	2-10%	1 hours, 300 ⁰ C	Rout et al (2001)
9	Kenaf	5, 10 and 15%	2 hours, 25 ⁰ C	Cao et al (2007)
10	Banana	0.5 and 1%	30 minutes (0.5 hour)	Pothan et al (2002)

Table 4.1 shows the percentage of alkali or sodium hydroxide used for chemical treatment of different natural fibres. It is seen in the table that the percentage of NaOH used ranges from 0.5 to 28%, but mostly around 1-10%. The table also shows the treatment time and temperature pre-condition. The treatment time varies from 20 minutes to 48 hours. Although there is a range of pre-conditioned temperatures, the alkali treatment was frequently carried out under room temperature. In many tropical places, where most of the above cited researches were carried out, temperature of around 20⁰C to 30⁰C is considered as a room temperature.

Table 4.2 shows the pre and post treatment given to the natural fibres and some concluding remarks from different alkali treatments. Typically, the fibres were washed with fresh tap water, distilled water or demineralised water and then dried at room temperature prior to the chemical treatment. After the alkali treatment, the fibres were washed with distilled water and then dried either at room temperature or some pre-conditioned hot temperature. Several alkali treatments were followed by a neutralization process using sulphuric acid (H₂SO₄) or acetic acid (CH₃COOH).

Table 4.2. Alkali treatment to different types of natural fibres-pre-post treatment and concluding remarks (references as per Table 4.1)

No	Pre and Post Treatment	Concluding Remarks
1	<i>Pre-treatment:</i> Washed with distilled water, dried at room temperature for 48 hours, extracted with cyclohexane/ethanol for 48 hours. <i>Post-treatment:</i> Washed with distilled water, dried at $100 \pm 5^{\circ}\text{C}$	Treated samples have better interfacial adhesion, reduced water absorption capacity
2	<i>Pre-treatment:</i> N/A <i>Post treatment:</i> Washed with distilled water, dried at 60°C for 6 hours	Treatment with 10% NaOH over 24 hours improved the flexural strength and modulus about 60% and 62%, respectively. Longer treatment (48 hours) causes fibres to be stiffer and more brittle
3	<i>Pre-treatment:</i> Dewaxed using methanol-benzene (1:1) for 24 hours <i>Post treatment:</i> Washed with distilled water, neutralised using 2% sulfuric acid	Treatment increased the tensile strength and modulus of fibre to 120% and 150%, respectively
4	<i>Pre-treatment:</i> N/A <i>Post treatment:</i> Washed under running water, dried at room temperature for 2 days	Treatment has removed the impurities of fibres, increased surface roughness
5	<i>Pre-treatment:</i> N/A <i>Post treatment:</i> Washed with cold and acidified water, rinsed with cold water and oven dried at 80°C for 8 hours	Treatment increased the longitudinal bending strength and stiffness by 40% and 60%, respectively. Increased the longitudinal properties (strength and modulus) up to 30%. Transverse bending strength and stiffness increased by 200% and 500%, respectively.
6	<i>Pre-treatment:</i> N/A <i>Post treatment:</i> Washed with fresh water, neutralized with dilute acetic acid, washed with distilled water, dried in room temperature for 48 hours and oven dried at for 6 hours 100°C	Composites (35% fibre) prepared with 4 hours NaOH 5% has 20% higher flexural strength and 23% modulus than the control (untreated fibres)
7	<i>Pre-treatment:</i> N/A <i>Post treatment:</i> Washed with water and dried	Enhanced compression strength of composite by 7.5%, enhanced flexural modulus by 1.8%, decreased impact strength by 13.6%
8	<i>Pre-treatment:</i> Defatted/dewaxed process: Fibre scoured with hot detergent solution (2%) at 70°C for 1 hour, washed with distilled water and finally vacuum dried at 70°C . The fibres then extracted in a 1:2 mixture of ethanol and benzene (1:2) for 72 hours, followed by washing with distilled water and <i>Post treatment:</i> Washed with water and dried	2% Alkali improved tensile and flexural strength by 26 and 15%, respectively. 5% improves flexural strength by 17% and 10% decreased both tensile and flexural strength
9	<i>Pre-treatment:</i> N/A <i>Post treatment:</i> Washed several times with water, neutralized with dilute acetic acid, washed with water and oven dried at 70°C for 72 hours	Tensile strength of fibre treated at 140°C showed the highest result, the fracture strain of the fibre treated with 10 & 15% improved
10	<i>Pre-treatment:</i> N/A <i>Post treatment:</i> Washed with dilute acetic acid, oven dried at 70°C for 3 hours	Simple alkali treatment with 1% concentration was found to be the most effective

The chemicals used for the alkaline treatment in this research were obtained from different sources. The sodium hydroxide (NaOH) was purchased from Taiwan with the commercial name of Formosoda-P. This chemical is classified as a caustic soda with a purity of 99%. Distilled and demineralized water and also acetic acid (CH_3COOH) were obtained from a local supplier in Toowoomba, Australia. The chemicals used for the alkali treatment in this work are shown in Figure 4.2.



Figure 4.2. Chemicals used for the alkali treatment of natural fibres

The percentage of NaOH used in this research was 2% by weight (2% wt). The quantity of chemical used in this research was determined by considering all the information gained from the cited literatures shown in Table 4.1 and 4.2. As a pre-treatment, all fibres were washed with warm tap water and then dried at room temperature for 12 hours. The alkaline treatment was carried out by soaking natural fibres with 2% NaOH at ambient temperature for 4 hours. For the post treatment, the treated fibres were washed several times with warm tap water, neutralized with acetic acid and washed with demineralized water. The fibres were then allowed to dry for 3 days at room temperature. The step-by-step processes for the chemical treatment of natural fibres in this research are depicted in Figure 4.3.



Figure 4.3. Step-by step of alkali treatment of natural fibres

The last process on the preparation of natural fibres for manufacturing natural fibre composite (NFC) laminates was drying the fibres in an oven for 6 hours at 60⁰C as suggested by Rokbi et al (2011). The process is shown in Figure 4.4.



Figure 4.4. Final drying of natural fibres

4.3. Manufacturing Natural Fibre Using Vacuum Bagging Method

A vacuum bagging process was used for preparing natural fibre laminates. In a manual to the principles and practical application of vacuum bagging for laminating composite materials published by West System[®] Epoxy (2010), vacuum bagging (or vacuum bag laminating) is defined as a clamping method that uses atmospheric pressure to hold the adhesive or resin-coated components of a lamination in place until the adhesive cures. Vacuum bagging uses atmospheric pressure as a clamp to hold fibre and matrix together within an airtight envelope. A more simple description of vacuum bag moulding is the process that combines a manual method using hand-layup or spray-up on the open mould to produce a laminated component with a vacuum process after covering the laminated using polymeric sheet (Kaynak and Akgul, 2001; Akovali, 2001).

Several currently available modern adhesives that can be cured at room temperature have helped to make vacuum bag laminating techniques economically available by eliminating the need for much of the sophisticated and expensive equipment previously required for laminating. This method offers many advantages over other available method such as the possibility of controlling matrix content, producing custom shapes and allowing completion at the laminating process in one efficient operation. It

also delivers a firmly and evenly distributed pressure over the entire surfaces regardless of the nature or amount of material being laminated.

In this research, a modified low viscosity epoxy resin (R180) was used with a hardener (H180), shown in Figure 4.5, with a resin and hardener ratio of 100:20 by weight. Low viscosity combined with a fast cure makes this system ideal for marine and civil engineering application. The resin and hardener were purchased from Fibre Glass International (FGI) Ltd, Queensland Australia. The specifications of the resin system used for preparing NFC laminates are presented in the following table.

Table 4.3. Properties of resin system (*www.fgi.com.au*)

Resin R180	
Specification	
Viscosity (at 20 ⁰ C)	110-1500 Cps
Specific gravity	1.10 -1.10 kg/lit
Application	
Elastic modulus	2630 MPa
Flexural stress	30.6 MPa
Deflection at flexural stress	2.25 mm
Water absorption in 24 hours	0.3% ww
Hardener H180	
Specification	
Viscosity (at 20 ⁰ C)	100-300 Cps
Specific gravity	0.96 kg/lit
Typical properties (100:20 by wt)	
<i>Flexural properties (ASTM D790-90), 80 mm span at the rate of 2 mm.min</i>	
Tangent elastic modulus	3000 MPa
Modulus of rupture	93 MPa
<i>Compression properties (ASTM D695-91)</i>	
Elastic modulus	1340 MPa
Compressive stress	86 MPa



Figure 4.5. The combination of resin and hardener system used in this research

The process of fabricating NFC laminate using a vacuum bagging process is generally a combination of a hand lay-up process and applying pressure on the natural fibre composite laminate. The set-up is shown in Figure 4.6.

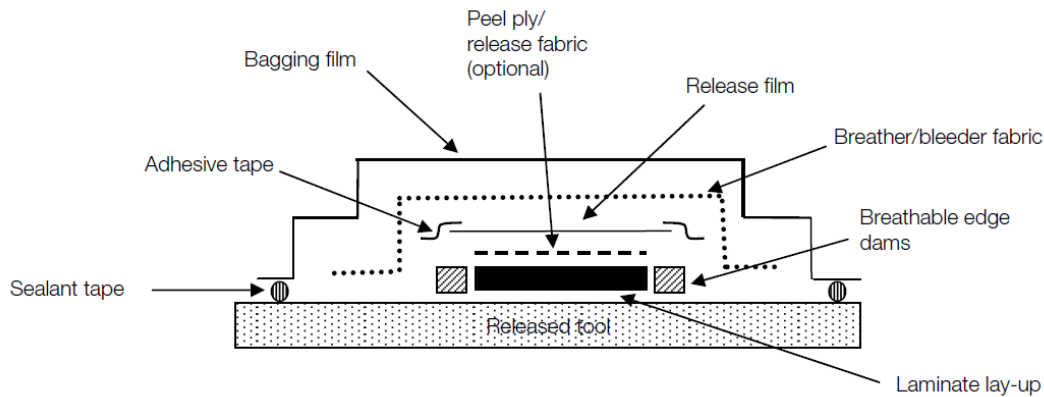


Figure 4.6. Typical parts of vacuum bagging system (www.omeco.com)

The vacuum bagging process that was used in this research is outlined below.

- 6) The process commenced by preparing all the materials to be laminated. The fibres were cut into the required shape and placed in the mould. At the same time, a release fabric, breathable material and vacuum bag were also cut to size. The vacuum bag was cut 20% larger than the mould dimensions.
- 7) The second step was to apply the mould release to the mould followed by applying a mastic sealant to the mould perimeter.
- 8) The surface of the mould base was then wetted with the mixed resin and the first layer of fibre mat was placed on the top of it. More resin was then poured on the top of the fibre mat and spread out prior to placing the subsequent fibre mat. This process was repeated several times until the required thickness was achieved.
- 9) The excess epoxy within the fibre mat was rolled out to make sure there had no pools of epoxy or air pockets within the fibre mat. When properly wetted, a pool of epoxy will appear around the edges of a thumb press.
- 10) A layer of release fabric was then placed over the laminate followed by a layer of breathable material. The release fabric will peel off the cured laminate leaving a fine textured surface. It will also absorb the excessive epoxy that can be removed after curing. The breathable polyester blanket allows the air to pass through the fibres to the port and absorbs excess epoxy that passes the release fabric.

- 11) The vacuum bag was then placed over the mould and sealed to the mould perimeter. The protective paper was then peeled from the mastic sealant starting at the corner of the mould. The edge of the bag has to be firmly pressed on to the mastic sealant while pulling the bag taut enough to avoid wrinkles.
- 12) The folds of excess bag were then sealed.
- 13) The vacuum line was connected and the vacuum pump turned on to evacuate air from the bag.
- 14) After curing, the vacuum bag, breather and release fabric were removed from the mould. The laminate was separated from the mould by inserting small wooden or plastic wedges between the edge of the laminate and the mould.

Once the laminates were cured, they were cut into the required size for mechanical properties characterization and for sandwich panel preparation for structural testing. The equipment for the vacuum bagging process used in this research is shown in Figure 4.7 and the step-by-step processes described above are shown in Figure 4.8.

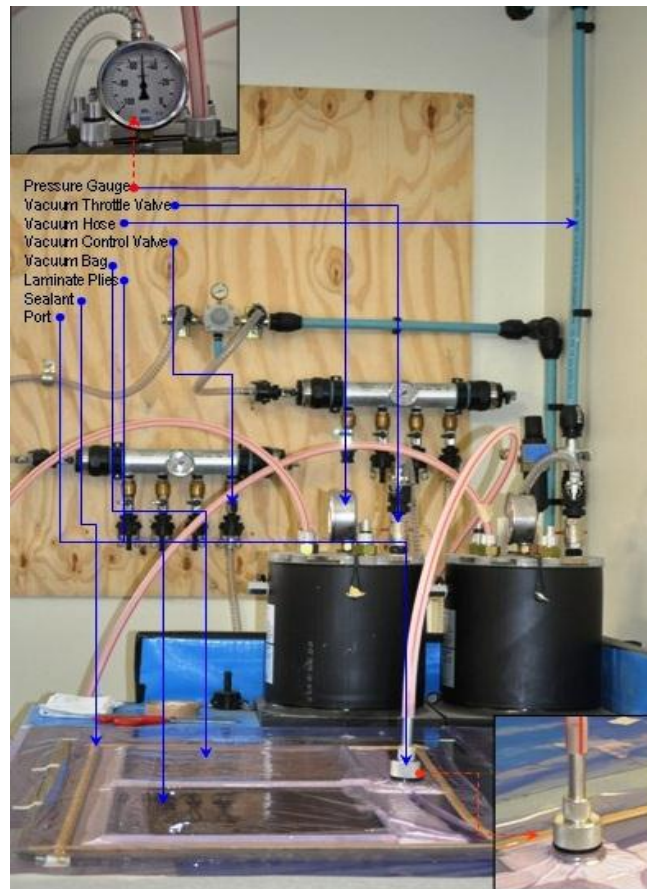


Figure 4.7. The equipment for vacuum bagging process used in this research.

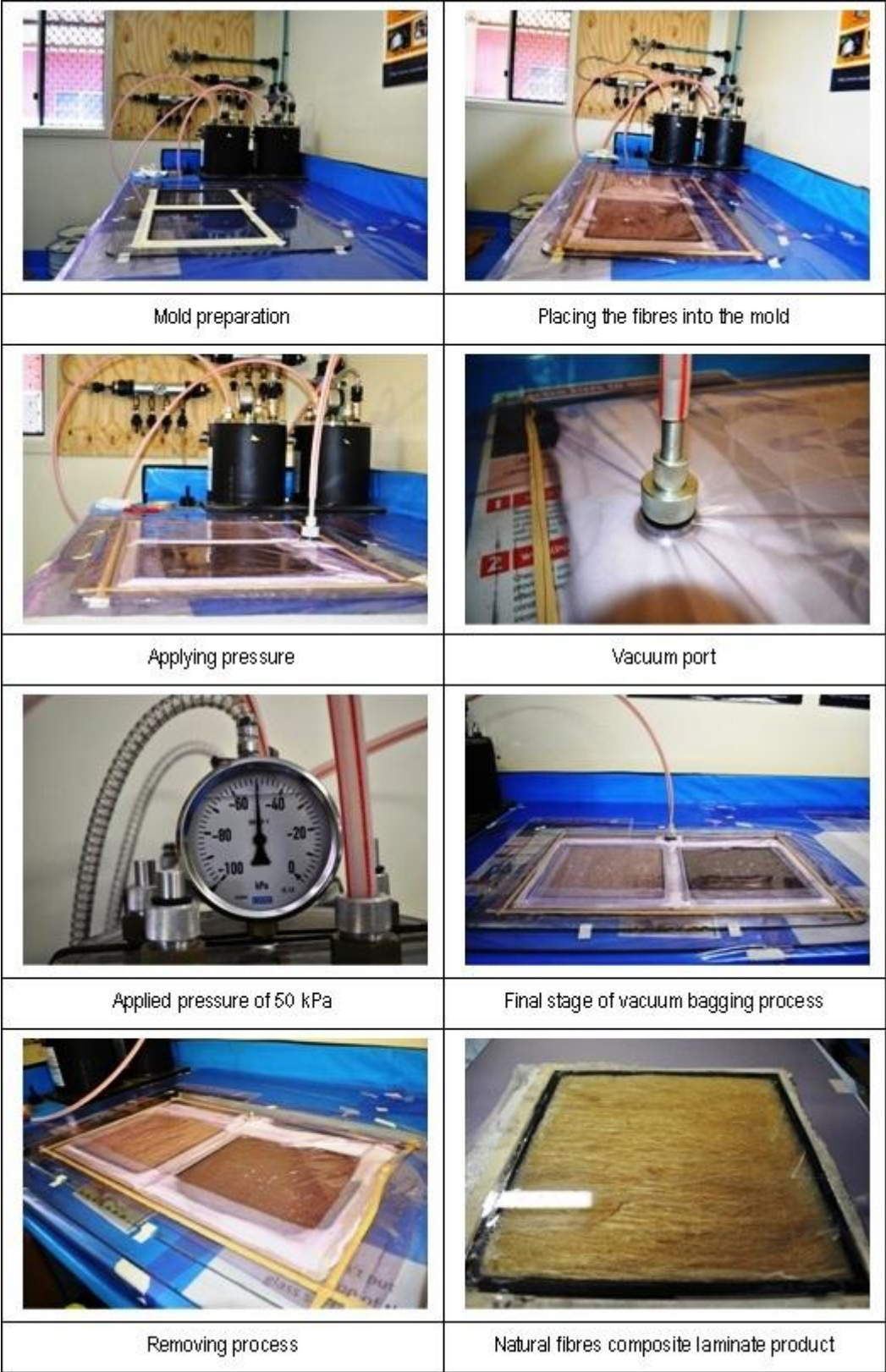


Figure 4.8. Process of fabricating natural fibre composite laminates with vacuum bagging method in this research

4.4. Characterization of Natural Fibre Composites

The hybrid sandwich panels studied in this research consists of aluminium skins, EPS core and NFCs intermediate layers. The skins and core materials were obtained from a well-established industrial supplier and their properties are readily available. Experimental testing was required to determine the basic mechanical properties of the NFCs. In this chapter section, the basic mechanical properties of NFCs will be presented and discussed.

Five different natural fibre composite panels were prepared using the process described in the previous section. Jute natural fibre composite (JNFC) was prepared in two different thicknesses, 3 mm and 5 mm. Hemp natural fibre composite and bamboo based composite were labelled as HNFC and BRNC, respectively. Sisal natural fibre composites were prepared as randomly oriented fibre and unidirectional oriented fibre and were labelled as SRNC and SUNC, respectively. Medium density fibre (MDF) panel was also prepared. All natural fibre based composite panels and the MDF panel prepared for this mechanical characterization test are shown in Figure 4.9. The JNFC laminate was prepared from a woven jute fibre. The laminate is categorised as a transverse isotropic material since their properties are similar in the parallel and transverse direction. Similarly, HNFC, BRNC and SRNC are also considered as transverse isotropic material as they were prepared from a randomly oriented fibre. The properties of laminate obtained from randomly oriented fibre are commonly not dependent on the direction. Meanwhile, the SUNC is considered as an orthotropic material due to their strength and stiffness are greater in a direction parallel to the fibres than in the transverse direction.

The experimental characterizations of NFCs for the intermediate layer were performed using tensile, compressive, flexural and shear tests. The tests were carried out as per the relevant ISO or ASTM standards for composite laminates. Although there are also comparable standards for the same mechanical testings of reinforced plastic materials, the listed standards below were commonly used in the CEEFC laboratory. It is also worth noting that the testing methods for natural fibre reinforced composites are mostly adopted from the available standard for reinforced plastic standards. Three to six specimens for each type of mechanical test had been prepared from the NFC laminates. The testing standards for each type of mechanical test are listed in Table 4.4.

Table 4.4. Testing standards used for mechanical characterization of NFCs

Type of test	Testing Standard	
	Code	Title
Tensile	BS EN ISO 527-2:1996	Plastics-determination of tensile properties
Compressive	ASTM D695-10	Standard test method for compressive properties of rigid plastics
Flexure	EN ISO 14125:1998	Fibre-reinforced plastic composites-Determination of flexural properties
Shear	ASTM D 5379/D5379 M-05	Standard test method for Shear properties of composite by the V-Notched beam method



Figure 4.9. Natural fibre based panels and MDF panel prepared for mechanical characterization testing

4.4.1. Tensile test

Tensile tests were carried out, as listed in Table 4.3, according to BS EN ISO 527-2:1996 using a MTS machine with a maximum load capacity of 100 kN. Three to six sets of specimens were prepared for each panel. An extensometer was also attached at the middle of specimen's gauge length in order to measure longitudinal and transverse deformation for the determination of Poisson's ratio. In order to prevent any damage to the testing equipment, the extensometer was removed from the specimen once the longitudinal strain reached 3000 microstrain. The machine was set-up to apply a pressure of 8 MPa at the gripping area in between the gauge length of the specimen. The testing speed applied was 2 mm/min. The tensile testing set up is shown in Figure 4.10.

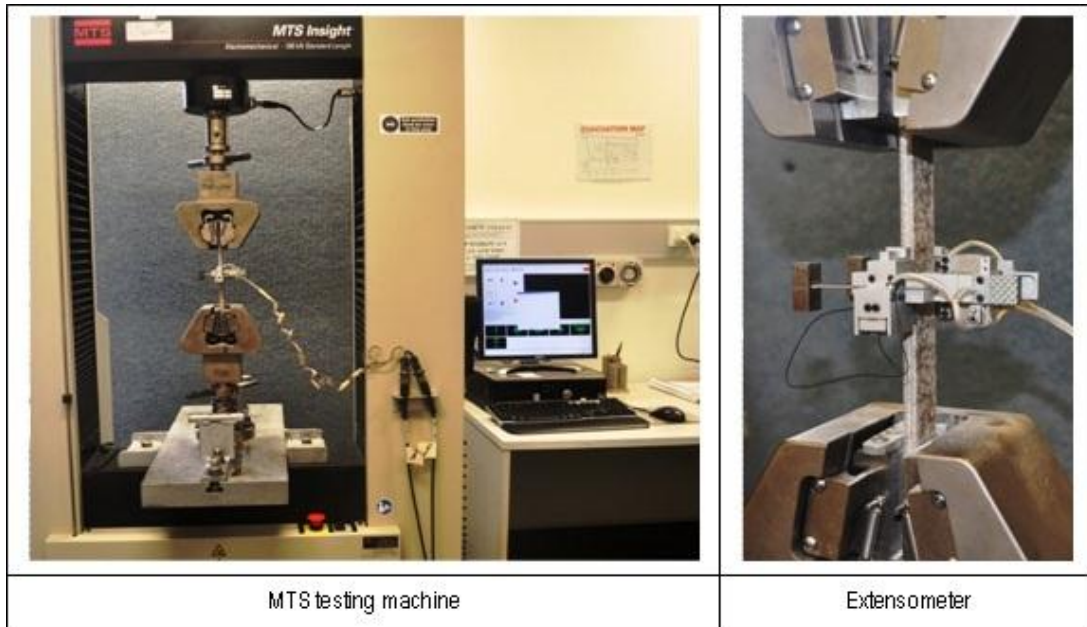


Figure 4.10. Setting-up testing machine for tensile test of NFCs

According to BS EN ISO 527-2:1996, tensile stress is “the tensile force per unit area of the original cross-section within the gauge length, carried by the test specimen at any given moment”. The tensile stress can be obtained using the following equation:

$$\sigma = \frac{F}{A} \dots\dots\dots 4.1$$

Where:

- σ : Tensile stress (MPa)
- F : Measured force (N)

A : Initial cross-sectional area of the specimen (mm)

The nominal tensile strain was calculated as per Equation 4.2.

$$\epsilon_t = \frac{\Delta L}{L} \dots\dots\dots 4.2$$

$$\epsilon_t(\%) = \frac{\Delta L}{L} 100 \dots\dots\dots 4.3$$

Where:

- ϵ_t : Nominal tensile strain
- L : Initial distance between grips (mm)
- ΔL : Increase of the distance between grips (mm)

The modulus of elasticity (in tension) or Young’s modulus was obtained from the following equation:

$$E_t = \frac{\sigma_2 - \sigma_1}{\epsilon_2 - \epsilon_1} \dots\dots\dots 4.4$$

Where:

- E_t : Modulus of elasticity or Young’s modulus (MPa)
- σ_1 : Stress (MPa) measured at the strain value of $\epsilon_1 = 0,0005$
- σ_2 : Stress (MPa) measured at the strain value of $\epsilon_2 = 0,0025$

Poisson’s ratio, which is a ratio of the transverse to the axial strain, was calculated using Equation 4.5.

$$\vartheta = \frac{\epsilon_n}{\epsilon} \dots\dots\dots 4.5$$

Where:

- ϑ : Poisson’s ratio, expressed in a dimensionless ratio with n = b (width) or h (thickness) indicating the normal value chosen
- ϵ : Strain in the longitudinal direction
- ϵ_n : Strain in the normal direction, with n = b (width) or h (thickness)

The results of tensile testing are tabulated in Tables 4.5 to 4.8. The results of tensile test of jute natural fibre composite are presented in Table 4.5 while Table 4.6 shows the tensile properties of sisal fibres. Table 4.7 lists the tensile properties of hemp natural fibre composite and bamboo based composite while Table 4.8 provides the tensile properties of medium density fibre. The table provided some important parameters such as peak load, peak stress, modulus of elasticity and Poisson’s ratio.

Table 4.5. Tensile properties of jute natural fibre composite

Jute natural fibre composite-tensile, thickness (3-4 mm) – (JNC0-TSL)					
Specimen	Area (mm ²)	Peak load (N)	Peak stress (MPa)	Modulus of elasticity (MPa)	Poisson's ratio (mm/mm)
1	111.82	3128	27.97	5641	0.625
2	88.45	3397	38.41	3812	0.284
3	98.46	4197	42.63	4640	0.306
4	111.67	3474	31.11	4025	0.310
5	79.17	3664	46.29	4842	0.278
Mean	97.91	3572	37.28	4592	0.361
Std Dev	14.35	399	7.68	724	0.149
CV	14.65	11.17	20.60	15.77	41.27
Jute natural fibre composite-tensile, thickness (5 mm) – (JNC1-TSL)					
Specimen	Area (mm ²)	Peak load (N)	Peak stress (MPa)	Modulus of elasticity (MPa)	Poisson's ratio (mm/mm)
1	124.00	6669	53.78	4474	0.284
2	128.50	6598	51.34	4498	0.284
3	122.83	6393	52.05	4585	0.286
4	127.33	6955	54.62	4523	0.293
5	125.00	6607	52.86	4705	0.289
Mean	125.53	6644	52.93	4557	0.287
Std Dev	2.35	202	1.31	92	0.004
CV	1.87	3.04	2.47	2.02	1.39

Table 4.6. Tensile properties of sisal natural fibre composite

Sisal (<i>randomly oriented</i>) natural fibre composite-tensile – (SRNC-TSL)					
Specimen	Area (mm ²)	Peak load (N)	Peak stress (MPa)	Modulus of elasticity (MPa)	Poisson's ratio (mm/mm)
1	161.26	3116	19.32	2983	0.386
2	158.95	4087	25.71	3050	0.382
3	165.83	2895	17.46	2997	0.370
4	158.38	4370	27.59	****	****
5	167.50	2300	13.73	4990	0.744
6	167.50	1870	11.16	****	****
Mean	163.24	3107	19.16	3505	0.471
Std Dev	4.22	978	6.49	990	0.183
CV	2.59	31.48	33.87	28.25	38.85
Sisal (<i>unidirectional</i>) natural fibre composite-tensile – (SUNC-TSL)					
Specimen	Area (mm ²)	Peak load (N)	Peak stress (MPa)	Modulus of elasticity (MPa)	Poisson's ratio (mm/mm)
1	91.42	3962	43.34	3550	0.427
2	120.00	4269	35.58	3921	0.443
3	98.33	4303	43.76	3548	0.439
4	88.33	3595	40.70	3858	0.471
5	94.17	3568	37.89	3339	0.429
Mean	98.45	3940	40.25	3643	0.442
Std Dev	12.59	353	3.52	242	0.018
CV	12.79	8.96	8.75	6.64	4.07

Table 4.7. Tensile properties of hemp fibre and bamboo based composite

Hemp natural fibre composite-tensile – (HNC-TSL)					
Specimen	Area (mm ²)	Peak load (N)	Peak stress (MPa)	Modulus of elasticity (MPa)	Poisson's ratio (mm/mm)
1	180.35	5195	28.80	3026	0.409
2	190.51	5717	30.01	2820	0.367
3	166.28	5823	35.02	3356	0.403
4	183.82	6003	32.65	3081	0.383
5	188.08	5708	30.35	2959	0.391
Mean	181.81	5689	31.37	3048	0.391
Std Dev	9.52	301	2.47	198	0.016
CV	5.24	5.29	7.87	6.50	4.09
Bamboo (<i>randomly oriented</i>) composite-tensile – (BRNC-TSL)					
Specimen	Area (mm ²)	Peak load (N)	Peak stress (MPa)	Modulus of elasticity (MPa)	Poisson's ratio (mm/mm)
1	140.19	3535	25.22	3426	0.382
2	142.31	2436	17.12	3068	0.359
3	141.02	2954	20.95	4448	0.429
Mean	141.17	2975	21.10	3647	0.390
Std Dev	1.07	550	4.05	716	0.035
CV	0.76	18.49	19.19	19.63	8.97

Table 4.8. Tensile properties of medium density fibre (MDF)

Medium density fibre (3 mm) – (MDF0-TSL)					
Specimen	Area (mm ²)	Peak load (N)	Peak stress (MPa)	Modulus of elasticity (MPa)	Poisson's ratio (mm/mm)
1	75.00	1296	17.28	2636	0.230
2	75.00	1336	17.82	2617	0.264
3	75.00	1214	16.18	2474	0.264
4	75.00	1279	17.05	2694	0.253
5	75.00	1288	17.18	2595	0.255
Mean	75.00	1283	17.10	2603	0.253
Std Dev	0.00	44	0.59	81	0.014
CV	0.00	3.43	3.45	3.11	5.53
Medium density fibre (6 mm) – (MDF1-TSL)					
Specimen	Area (mm ²)	Peak load (N)	Peak stress (MPa)	Modulus of elasticity (MPa)	Poisson's ratio (mm/mm)
1	151.03	2480	16.42	2695	0.265
2	150.83	2616	17.35	2696	0.245
3	151.03	2387	15.80	2664	0.268
4	151.24	2624	17.35	2603	0.288
5	151.03	2355	15.60	2544	0.253
Mean	151.03	2492	16.50	2641	0.264
Std Dev	0.14	125	0.83	66	0.016
CV	0.09	5.02	5.03	2.50	6.06

As expected a visual examination of data presented in Tables 4.5 to 4.8 shows that the tensile strength of natural fibre composites differ for set of samples. Within each sample set individual test results differ as represented by the standard deviation (StdDev) and coefficient of variation (CV). This noise is usually called experimental error. Montgomery (2009) termed this as a statistical error, meaning that it arises from variation that is uncontrolled and generally unavoidable. The presence of error or noise implies that the tensile strength of the tested specimens is a random variable. This random variable is categorized as a discrete since the set of all possible values is infinite.

Using the average values or means of the data can be misleading when dealing with this typical scattering data. However, most data in scientific publications generally emphasizes their analysis based upon the average values and standard deviation. In order to get more important information from the typical scattering data, the use of graphical method, such as dot-plot diagram, is a better way to quickly see the general location or central tendency of the observation and their spread, as suggested by Montgomery (2009). Therefore, all data presented in the tables have been re-arranged in a dot-plot diagram as shown in the following figures. Figure 4.11 shows the dot-plot diagram of tensile strength of natural fibre composites (NFCs). The x axis represents the type of NFCs tested and the y axis corresponds to the tensile strength of NFCs.

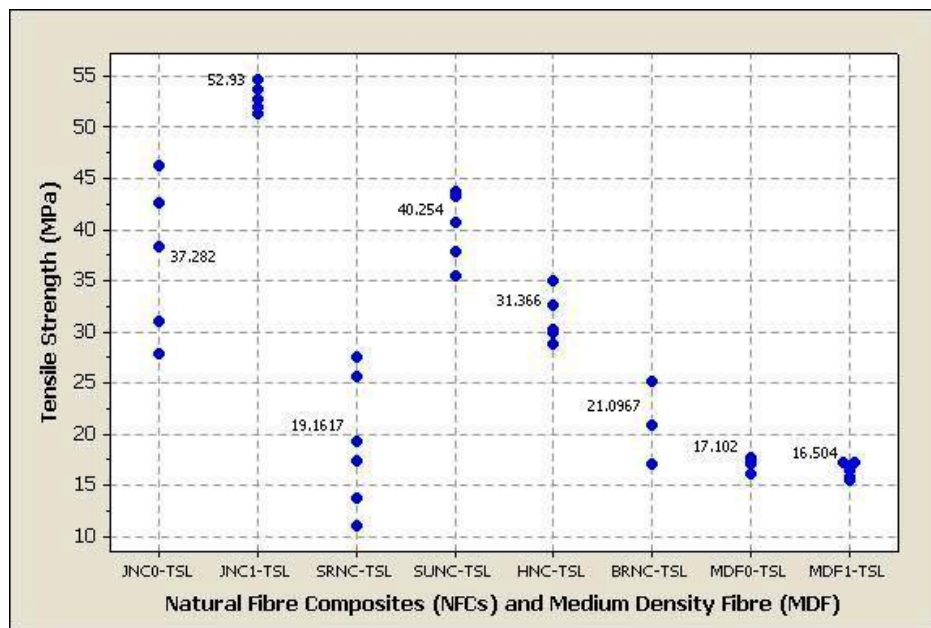


Figure 4.11. The dot-plot diagram of the tensile strength of NFCs and MDF

It can now be easily seen from the above graph that the tensile strength of NFCs have more varied results, except for JNC1-TSL, particularly when they compared to the observation results of medium density fibre (MDF). The average tensile strength of jute fibre composites with 3-4 mm thickness (JNC0-TSL) was 37.282 MPa and 53.93 MPa for samples with the thickness of 5 mm (JNC1-TSL). Although both samples categories were provided from the same fibre, the observed results were greatly differ. While all the thicker specimens shows consistent values of around 51.34 MPa to 54.62 MPa with a standard deviation of only 1.31 MPa, the observed values of thinner specimens labelled as JNC0-TSL fluctuated considerably from 27.97 MPa to 46.29 MPa, with a standard deviation of 7.68 MPa. It was expected that the two average observation values should have similar values. In fact, the difference between them was about 29.56%. However, if a careful attention is given to the distribution of JNC0-TSL specimens, it can be noted that there are three specimens of higher values close to the values of JNC1-TSL specimens. If the average value of JNC0-TSL is calculated based upon these three values, the difference in the average value of the two sample categories can be reduced to 19.81% as the average value of JNC0-TSL has now increased to 42.44 MPa.

Variations in the properties of natural fibre composites have been a tremendous concern of many investigators in this field of research. Those variations on the properties can be affected by many factors such as type of fibre and matrix uses, composition of constituent materials, and also manufacturing process. In this experiment, material type and composition were provided in the same manner; hence the difference in between the tensile strength values of JNC0-TSL and JNC1-TSL are most probably due to the effect of manufacturing process or the process during the preparation of specimens. It was encountered that during the panel preparation the fabrication process of thinner panel was more difficult than the thicker one. As a result, a thinner panel was finally available in the thickness of around 3-4 mm while the required thickness of 5 mm for the thicker panel was achieved almost without any difficulties. In order to provide panel with the required thickness of 3 mm, a modest amount of panel surface was removed from the panel using a sanding machine. Involving this process probably has affected the bonding strength between fibre and matrix that may lead to the reduction of tensile strength of the tested specimens.

The tensile strength distribution of sisal and hemp fibre composites, and bamboo based composites also observed notable varies for each individual run. For the composites reinforced with randomly oriented sisal fibres (SRNC-TSL) the tensile strength values were greatly fluctuated. In this case, a justification or normalization has to be made in order to avoid a misleading analysis. The average values of this specimen group ranges from 11.16 MPa to 27.59 MPa that appear to be concentrated in three clusters. When the first three higher values were taken into consideration, the average value of the tensile strength of SRNC-TSL would be 24.20 MPa. Interestingly, the tensile strength of composites reinforced with unidirectional sisal shows consistent values that range from 35.58 MPa to 43.34 MPa with the average value of 40.25 MPa. The reason is most likely due to the unidirectional sisal fibres providing continuous support for the composites along the longitudinal axis which is the direction of the applied load.

More consistent values of tensile strength have been observed from the hemp natural fibre composites (HNC-TSL) specimens. These values distribute from 28.80 MPa to 35.02 MPa with the standard deviation of 2.47 MPa. It seems that the actual average values can be used without any further justification. In addition, the observation of bamboo based composite had been reduced to only 3 specimens due to the poor quality of panel produced. Originally, five specimens were prepared. However, during the preparation of specimens, it was found that a significant defect appeared at the gauge length of two specimens. The average tensile strength values of composites reinforced with randomly oriented bamboo slices (BRNC) was 21.10 MPa.

Other than showing the tensile strength of NFCs, the figure also shows the result of tensile strength observation of medium density fibre (MDF) which is a competitor material for NFCs that will also be further used in this research for the intermediate layer. Unlike the embedded inconsistency properties of NFCs, the results for each individual run of MDF test were very consistent. The average tensile strength of specimens cut from thinner (3 mm) and thicker (6 mm) panels were only slightly different, 17.1 MPa and 16.50 MPa, respectively. These two values have an almost indistinguishable standard deviation of 0.59 MPa and 0.83 MPa, respectively. The similarity in the observed values of MDF tensile strength indicates the consistency of its

properties. Medium density fibre has been developed for few decades and some concerns related to the manufacturing process have been solved in many ways.

The second concern in this discussion of tensile properties of NFCs and MDF is the distribution of their tensile modulus or Young’s modulus. The distribution of these values is presented in Figure 4.12.

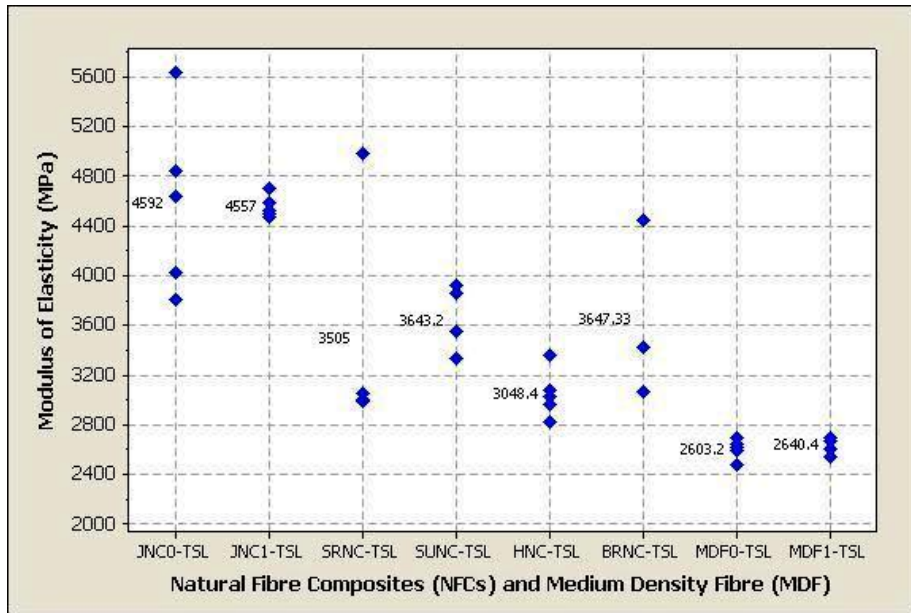


Figure 4.12. The dot-plot diagram of the tensile modulus of NFCs and MDF

Likewise the tensile strength, the distribution of tensile modulus or Young’s modulus of NFCs is also inconsistent, particularly for specimens labelled as JNC0-TSL, SRNC-TSL and BRNC-TSL. More consistent results were noticed for JNC1-TSL, SUNC-TSL and HNC-TSL with the average value of 4557 MPa, 3643.2 MPa and 3048.4 MPa, respectively. It seems that the modulus elasticity of JNC0-TSL specimens has to be justified by considering only three middle values that almost precisely in the same ranges, resulting with a new average value of 4502 MPa. There has a couple of missing values found at the modulus elasticity of SRNC-TSL that can be noticed from Table 4.6, or evidently shown in the dot-plot diagram. The disappearance of the two values was most likely due to the improper attachment of the extensometer onto the specimens during the testing process and subsequently the strains incorrectly recorded. It has also affected the values of Poisson’s ratio of these two specimens. Apart from the unrecorded values, the average value obtained from the other four specimens also failed to represent the actual condition. One of the specimens had a notably high value while

the three specimens had almost identical values. Therefore, the average value was justified to be the average of the three specimens that had identical values which gave the final average value of 3010 MPa. In addition, the actual average value of bamboo based composites was 3647.33 MPa, but using the average value of two close values of 3426 MPa and 3068 MPa, which is 3247 MPa, is considered more acceptable. On the other hand, the modulus elasticity of MDF specimens, both thinner and thicker panels, was notably consistent. The average modulus elasticity values of MDF with 3 and 5 mm thickness were 2603.2 MPa and 2640.4 MPa, respectively.

Another parameter that is also important for any material that includes natural fibre composites is Poisson's ratio. This parameter deals with the way stretching or compressing an object in one direction causes it to compress or stretch in the opposite direction. The ratio measures the extent of this effect in a particular substance which may be vary considerably. The ratio can even be negative, usually in man-made substances. The last column of Table 4.5 to Table 4.8 presents the Poisson's ratio of corresponding NFCs specimens. In order to justify the convenient average value of Poisson's ratio for each specimen category, the content of the last columns of each tables have been re-arranged in the form of dot-plot diagram as presented in Figure 4.15.

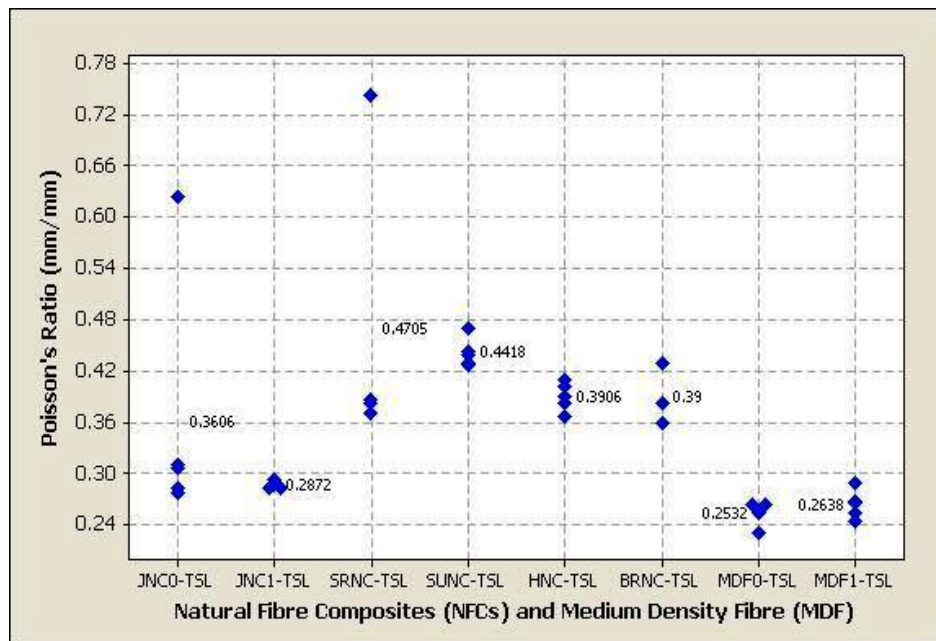


Figure 4.13. The dot-plot diagram of the Poisson's ratio of NFCs and MDF

As clearly shown in the above figure, the distribution of Poisson’s ratio is quite consistent for all groups of specimens tested, both for NFCs and MDF. The exception is for JNC0-TSL and SRNC-TSL that each has one peculiar value. For JNC0-TSL, the Poisson’s ratio ranges from 0.278 to 0.310 and one odd value of 0.625 that resulted with an average value of 0.361. If the outlier value is omitted from the calculation, the new average value will be 0.235. Meanwhile, the SRNC-TSL specimen group will have a new average value of 0.38 when the peculiar value of 0.744 is omitted from the calculation. In addition, all other groups have the average values as shown by the dot-plot diagram in the above figure.

The typical load-extension of MDF specimens are given in the Figure 4.14. The maximum load achieved by the MDF0-TSL specimens were 1283 N in average, and 2492 N for MDF1-TSL specimens producing an almost similar Young’s modulus or modulus elasticity of around 2600 MPa. The typical load-extension graphs of different NFCs tested under the tensile load are demonstrated in Figure 4.15. The graphs clearly show that all NFCs composite specimens exhibit a linear elastic behaviour in tension. For NFCs specimens, the load increased linearly with the extension, with a slight noise caused by the removing of the extensometer during the progress of tensile test. There has actually a slightly decrease in stiffness at some point before the failure which is likely due to the formation of tensile crack in the matrix. In contrast to the behaviour of NFCs, the MDF-TSL group specimens show a slightly non-linear behaviour in which they develop a slight plastic region prior to reaching their ultimate load and fail in an abrupt mode of collapse.

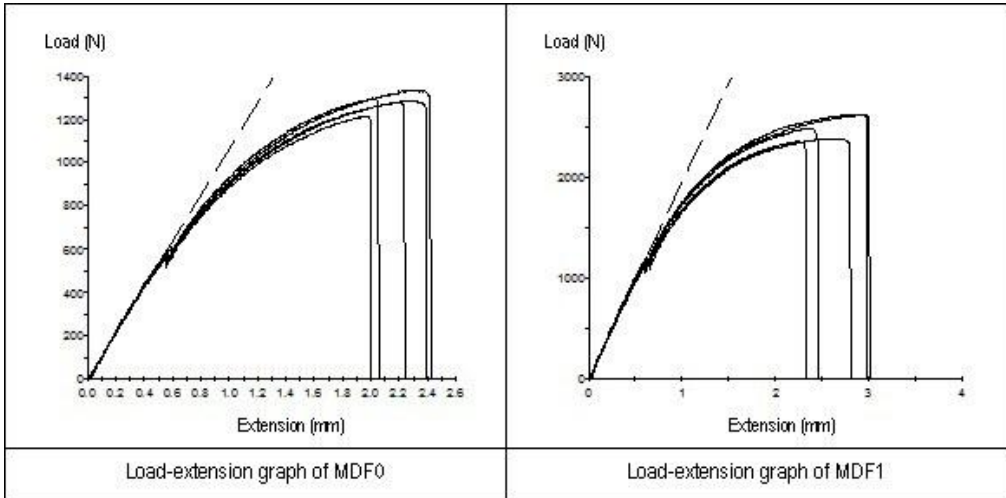


Figure 4.14. Typical load-extension graphs of different MDF

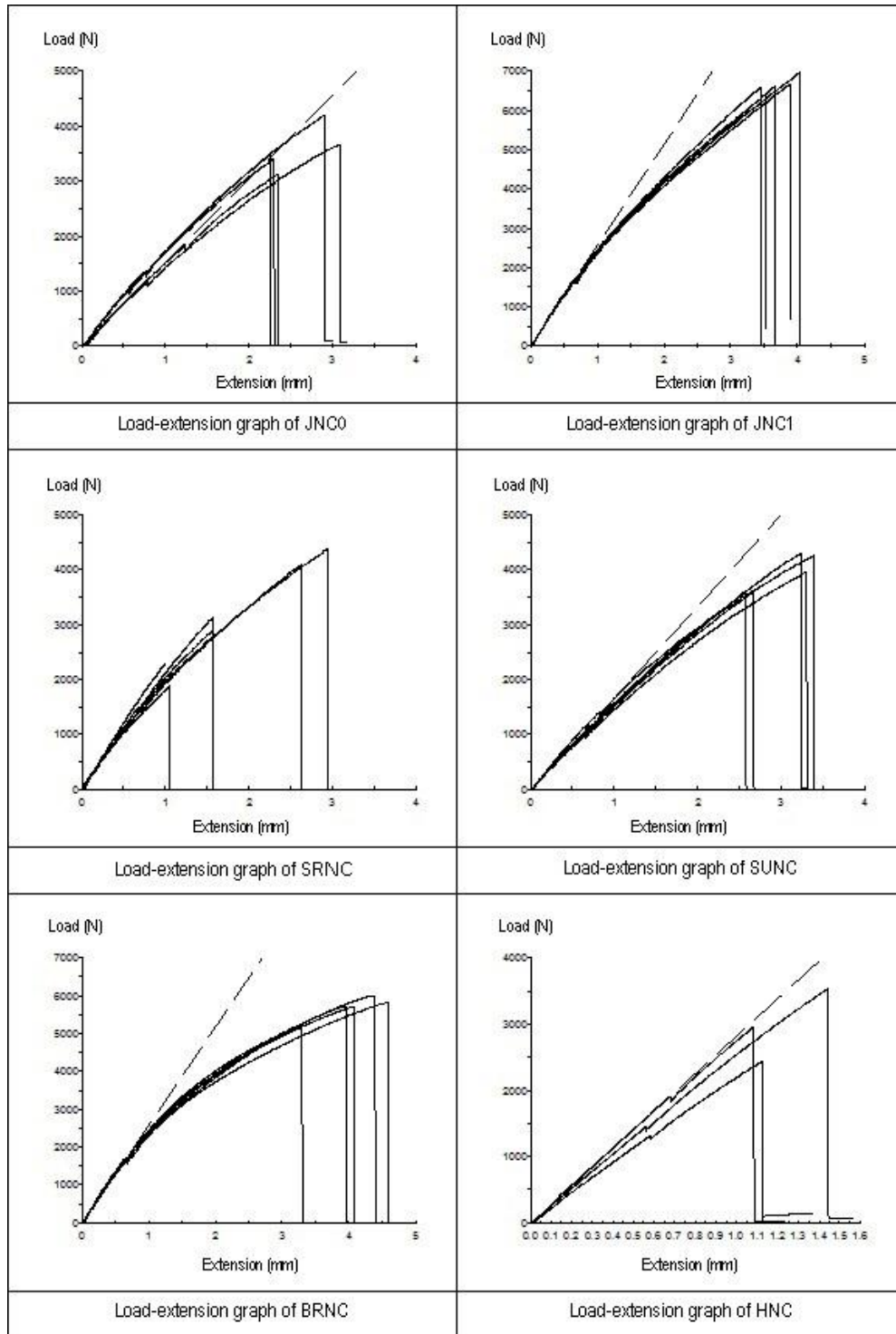


Figure 4.15. Typical load-extension graphs of different NFCs

All the specimens failed due to tensile failure within the gauge length, as shown in Figure 4.16, with no observed failure caused by slippage at the anchorage zone. The tensile failure along the longitudinal was in a brittle manner in which all the specimens suddenly collapsed or cut-off into two pieces.

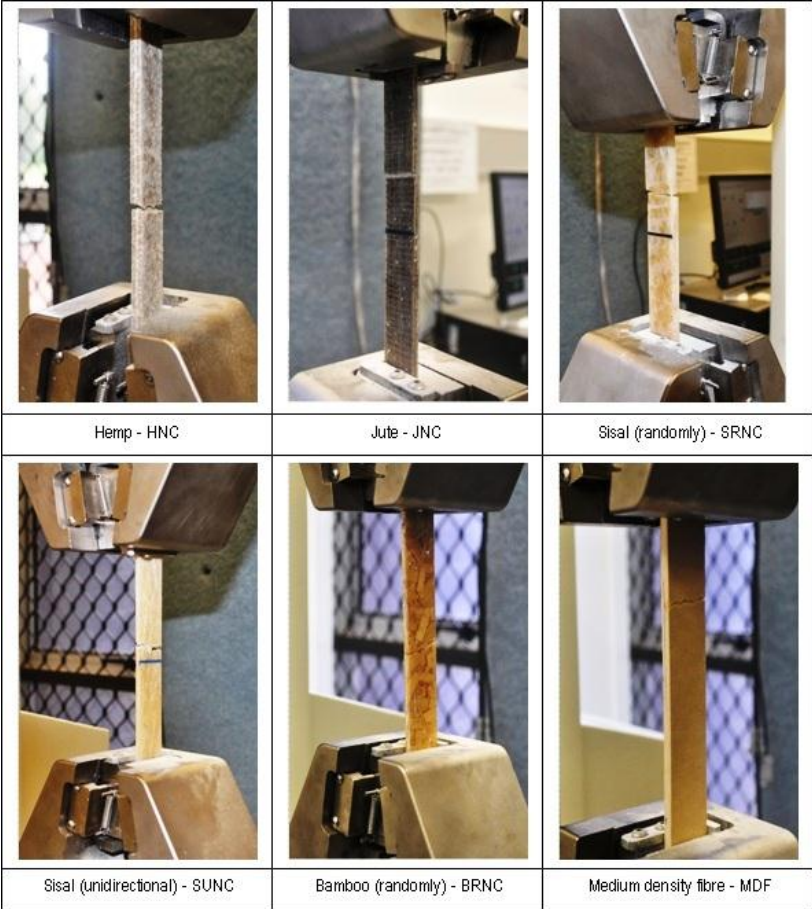


Figure 4.16. Typical tensile failure patterns of different NFCs

In order to provide verification for the data obtained in this research, it is a good practice to compare the properties of current NFCs with existing data published by other researchers. The tensile strength and tensile modulus of different NFCs found in the literature are listed in Table 4.9. A quick visual assessment of data presented in this table implies that the tensile strength of natural fibre composites differ for each reported research work. The reason for this is most probably due to each investigator having employed different types of fibres and material composition, fabricating process or may arise from different testing standards. As can be noted in the table below, the ranges of tensile strength are about 20.40 MPa for coir/polyester composites to 65.5 MPa for sisal/polyester composites. Meanwhile, the tensile strength of NFCs developed in this work lies in between 21.09 MPa for bamboo based composite (BRNC-TSL) to 52.93 MPa for jute/epoxy composite (JNC1-TSL). For the data of tensile modulus, there is a considerable fluctuation on the available published data in which the lowest value was possessed by jute/PVA composites (1300 MPa) and the higher value belonged to the

sisal/polyester (12900 MPa). In fact, there are also some values that are close to the tensile modulus provided in this work that range from 3048.4 MPa to 4592 MPa. They are jute/polyester composite (3700 MPa) and flax/polyester composite (6300 MPa). It can be said that the values provided in this work were reasonably acceptable.

Table 4.9. Tensile strength and tensile modulus of different natural fibre composites from several literatures

No	Fibre	Matrix	Tensile properties		References
			Tensile Strength (MPa)	Tensile Modulus (MPa)	
1	Jute	Polyurethane Chloride	59.3	1300	Khan et al (2011)
2	Jute	Polyester	45.82	3700	Ticoalu et al (2010)
3	Sisal	Polyester	47.10	12900	Mwaikambo (2006)
4	Coir	Polyester	20.40	-	Singh and Gupta (2005); Mohanti et al (2005)
5	Hemp	Polyester	32.90	1421	Rouison et al (2005); Ticoalu et al (2010)
6	Flax	Polyester	61	6300	Rodriguez et al (2005), Ticoalu et al (2010)
7	Sugar palm	Epoxy	30.49	1060	Sastra et al (2006)
8	Banana	Polyester	57	-	Poathan et al (2002)
9	Sisal	Polyester	65.5	1900	Prasad and Rao (2011)

4.4.2. Flexural test

Typically, a flexural test is carried out on simply supported beams. The test specimen is deflected at a constant rate until the specimen fractures or until deformation reached some pre-determined value. During the testing progress, the applied force and the deflection were recorded. Three-point or four-point tests are the two most common methods used for the determination of flexural properties of lamination. In this work, the flexural test was conducted based upon ISO 14125 which is a standard test for the determination of flexural properties of fibre-reinforced plastic composites. The test was carried out using a MTS machine with a maximum load capacity of 10 kN. Five to seven specimens of recommended dimensions were prepared for each panel. A flat rectangular specimen was supported close to the ends and centrally loaded in three-point bending. A typical roller and pin support was used allowing the specimen to rotate in order to minimize membrane stress. The testing speed applied was 2 mm/min. The testing set up for flexural testing of laminate in this work is as shown in Figure 4.17.

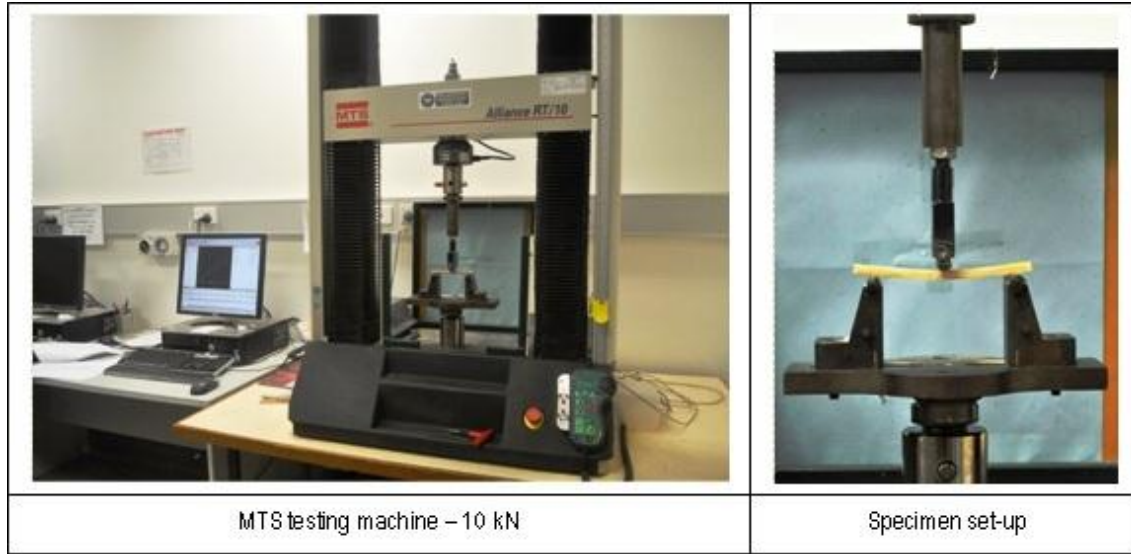


Figure 4.17. Setting-up for flexure test

The calculation and expression of testing results according to the referred standard, EN ISO 14125:1998, are as follows. Flexural stress is the nominal stress in the outer surface of the test specimen at mid span. It is calculated according to the following equation.

$$\sigma_f = \frac{3FL}{2bh^2} \dots\dots\dots 4.6$$

Where:

- σ : Flexural stress (MPa)
- F : Load (N)
- L : Span (mm)
- b Width of specimen (mm)
- h Thickness of specimen (mm)

The second important parameter in flexure test is the flexural modulus. The definition of flexural modulus according to the referred standard is “the modulus of elasticity in flexure which is the ratio of stress difference divided by correspond strain difference”. Flexural modulus is calculated from the following equation.

$$E_f = \frac{L^3}{4bh^3} \left[\frac{\Delta F}{\Delta S} \right] \dots\dots\dots 4.7$$

Where:

- E_f : Flexural modulus of elasticity (MPa)
- ΔS : Difference in deflection between S'' and S'
- ΔL : Difference in load, F at S'' and S'

For the measurement of the flexural modulus, S' and S'' can be calculated from the following equations:

$$S' = \frac{\varepsilon_f'' L^2}{6h} \quad \dots\dots\dots 4.8$$

$$S'' = \frac{\varepsilon_f' L^2}{6h} \quad \dots\dots\dots 4.9$$

Where:

- S' and S'' : Beam mid-point deflections (mm)
 ε_f'' and ε_f' : Flexural strains, corresponds to the given values of flexural strain
 $\varepsilon_f' = 0,0005$ and $\varepsilon_f'' = 0,0025$

The results of flexure testing are tabulated in the Table 4.10 to Table 4.12. The result of the flexure test in regards to jute natural fibre composite is presented in Table 4.10 and Table 4.11 presents the flexure properties of sisal natural fibres. In addition, Table 4.12 shows the flexure properties of the hemp natural fibre composite and the bamboo based composite. The table only shows some important parameters such as peak load, peak flexural stress, deflection at peak and flexural modulus.

Table 4.10. Flexural properties of jute natural fibre composite

Jute natural fibre composite-flexure, thickness (3-4 mm) – (JNC0-FLX)					
Specimen	Peak load (N)	Peak Flexural Stress (MPa)	Deflection at Peak (mm)	Strain at Peak (%)	Flexural Modulus (MPa)
1	162	60.46	4.13	2.46	1186
2	115	41.74	3.44	2.09	1374
3	157	57.26	5.38	3.28	1100
4	141	51.54	3.59	2.16	2770
5	128	50.25	3.29	1.93	1914
6	152	61.66	5.36	3.06	1517
7	144	48.04	4.00	2.52	2434
Mean	143	52.99	4.17	2.50	1756
Std Dev	17	7.18	0.87	0.51	642
CV	11.89	13.55	20.86	20.40	36.56
Jute natural fibre composite-flexure, thickness (5 mm) – (JNC1-FLX)					
Specimen	Peak load (N)	Peak Flexural Stress (MPa)	Deflection at Peak (mm)	Strain at Peak (%)	Flexural Modulus (MPa)
1	231	67.06	5.18	2.53	3784
2	237	66.16	5.09	2.55	3569
3	286	74.05	5.46	2.80	3680
4	214	58.74	4.28	2.14	3267
5	168	47.59	3.67	1.80	2997
Mean	227	62.72	4.74	2.36	3459
Std Dev	43	10.05	0.74	0.39	323
CV	18.94	16.02	15.61	16.53	9.34

Table 4.11. Flexural properties of sisal natural fibre composite

Sisal (<i>randomly oriented</i>) natural fibre composite-flexure – (SRNC-FLX)					
Specimen	Peak load (N)	Peak Flexural Stress (MPa)	Deflection at Peak (mm)	Strain at Peak (%)	Flexural Modulus (MPa)
1	203	47.94	5.42	1.93	2086
2	264	61.82	6.69	2.40	2515
3	227	52.29	5.96	2.15	2960
4	280	65.77	8.46	3.02	2602
5	179	43.93	5.48	1.93	1446
Mean	231	54.35	6.40	2.29	2322
Std Dev	42	9.22	1.26	0.46	580
CV	18.18	16.96	19.69	20.09	24.98
Sisal (<i>unidirectional</i>) natural fibre composite-flexure – (SUNC-FLX)					
Specimen	Peak load (N)	Peak Flexural Stress (MPa)	Deflection at Peak (mm)	Strain at Peak (%)	Flexural Modulus (MPa)
1	174	65.44	4.02	2.39	1961
2	128	53.29	3.24	1.83	3270
3	137	67.16	5.87	3.04	2618
4	114	44.21	3.40	1.99	817
5	120	54.30	3.74	2.03	2642
6	264	88.54	5.86	3.69	1187
Mean	156	62.16	4.35	2.50	2082
Std Dev	57	15.45	1.20	0.73	941
CV	36.54	24.86	27.59	29.20	45.20

Table 4.12. Flexural properties of hemp and bamboo natural fibre composite

Hemp natural fibre composite-flexure – (HNC-FLX)					
Specimen	Peak load (N)	Peak Flexural Stress (MPa)	Deflection at Peak (mm)	Strain at Peak (%)	Flexural Modulus (MPa)
1	167	29.04	6.20	2.28	1881
2	233	54.04	8.29	2.64	2931
3	258	52.27	7.86	2.69	2957
4	263	51.85	7.68	2.65	2532
5	238	48.66	7.01	2.37	2145
Mean	232	47.17	7.41	2.52	2489
Std Dev	38	10.32	0.82	0.19	476
CV	16.38	21.88	11.07	7.54	19.12
Bamboo (<i>randomly oriented</i>) natural fibre composite-flexure – (BRNC-FLX)					
Specimen	Peak load (N)	Peak Flexural Stress (MPa)	Deflection at Peak (mm)	Strain at Peak (%)	Flexural Modulus (MPa)
1	232	62.38	5.99	2.60	1245
2	153	41.71	3.39	1.47	1848
3	165	44.39	4.10	1.79	1347
4	204	56.85	4.87	2.09	1366
5	229	61.35	4.52	1.97	4201
Mean	197	53.34	4.57	1.98	2001
Std Dev	36	9.66	0.97	0.42	1251
CV	18.27	18.11	21.23	21.21	62.52

Likewise to the previous analysis of tensile properties, the data presented in the above tables have been re-arranged in the form of dot-plot diagram in order to obtain understandable and quick information. For flexural properties analysis, only NFCs specimens were observed. For flexural properties analysis, all specimens were labelled as NFCs–FLX. There are two parameter observed in this analysis, that is, flexural strength and flexural modulus. The re-arrangement of flexural strength average values of NFCs is presented in the following figure.

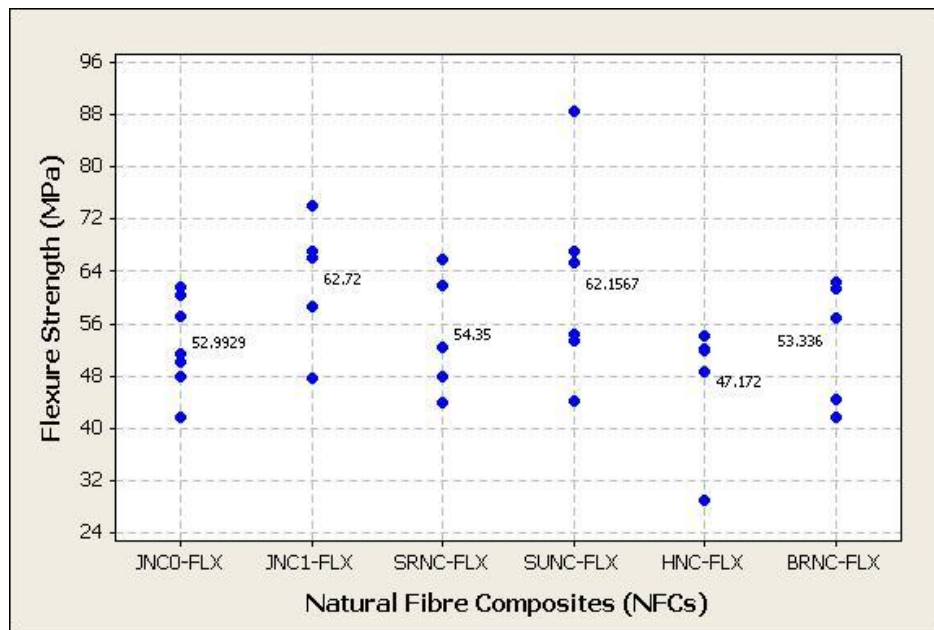


Figure 4.18. The dot-plot diagram of the flexural strength of NFCs

As clearly shown in Figure 4.18, the first impression given by the diagram was that the flexural strength of each observed specimen fluctuated widely. Similarly with the previous analysis, the provided average values for each specimens group cannot immediately be used for the analysis purposes. A careful consideration has to be made to obtain more acceptable average values. For jute fibre composites labelled as JNC0-FLX, the distribution of flexural strength data ranges from 41.74 MPa to 61.66 MPa meaning that they differ for approximately 32.3%. Meanwhile, the actual average value of this sample group was 52.92 MPa. If the two lowest values are neglected from the calculation, a new average value of 56.23 MPa might be obtained. On the other hand, a new average value of 59.88 MPa can be obtained from the specimens JNC1-FLX when the uppermost data is omitted, resulting in an acceptable difference between JNC0-FLX

and JNC1-FLX, which is about 6%. This new gap seems more convenient than the actual difference when all raw data was taken into account, which was about 15.51%.

A scattered impression also appeared within the result of the flexural strength of sisal fibre composites. As can be noticed from Figure 4.18, the distribution of SRNC-FLX data coheres with the average value of 54.35 MPa even though the data actually spreads into two sets of values. However, composite reinforced with unidirectional sisal fibre (SUNC-FLX) has two peculiar observed data, the highest and lowest data of 88.54 MPa and 44.21 MPa, respectively. When these two outlier data are removed, the average value of this sample group changes to 60.04 MPa. A similar situation was observed in HNC-FLX specimens, where an odd value of 29.04 MPa was found among the ranges data of 48.66 MPa to 54.05 MPa. Omitting this odd value might result in a new average value for this data group, which is 51.7 MPa. Likewise to the distribution of SRNC-FLX data, the distribution of flexural strength in the BRNC-FLX group spreads into two clusters with the actual average value of 53.33 MPa. If three highest data are considered, it will give a new average value of 60.13 MPa, or otherwise 43.05 MPa when only two lowest data are considered.

The next concern is the distribution of flexural modulus data for different natural fibre composites investigated in work. As noticeably shown in that figure, there are only two groups of sample spreads quite evenly, that is, JNC1-FLX and HNC-FLX with the average values of 3459.4 MPa and 2489.2 MPa, respectively. Other sample groups need a justification process to obtain more reliable values. The distribution of flexural modulus for different natural fibre composite observed in this work can be observed in the following figure.

Within JNC0-FLX specimens group, two values need to be neglected; the flexural modulus of specimen 4 and specimen 7, resulting in a new average value of 1418.2 MPa. Meanwhile, if the lowest flexural modulus value of 1446 MPa (specimen 5) is excluded from the calculation within SRNC-FLX specimen group, it will change the average value to 2526.25 MPa. In addition, including only three higher values of flexural modulus creates a new average value for SUNC-FLX which is 2843.3 MPa. Lastly, a peculiar value of specimen 5 in BRNC-FLX specimen group can be removed resulting in an average value of 1451.5 MPa.

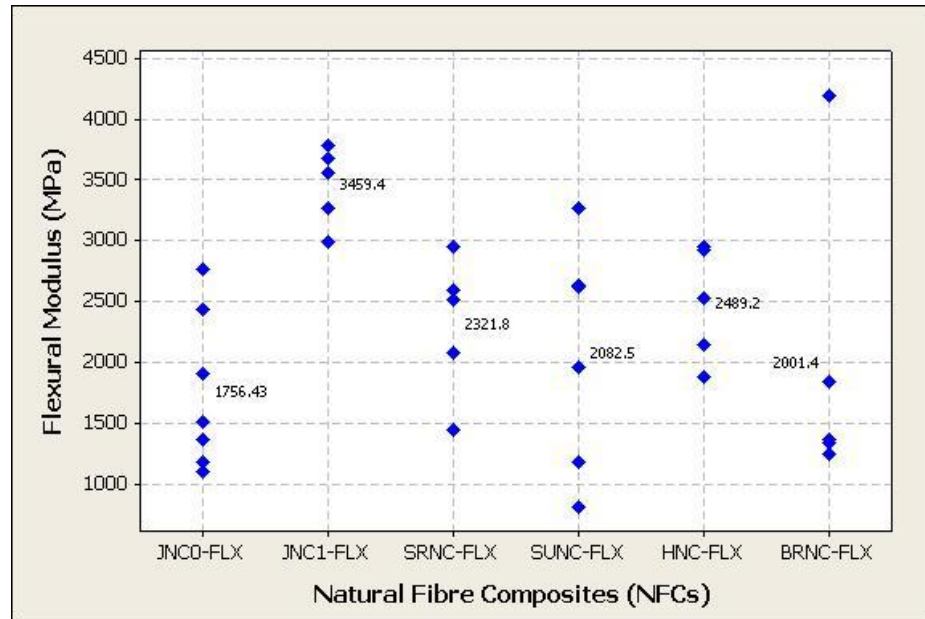


Figure 4.19. The dot-plot diagram of the flexural modulus of NFCs

The typical stress-strain curves of different natural fibre composites tested under flexure are presented in Figure 4.20. As shown by the presented graphs, the stress-strain curves presented a linear elastic behaviour up to a final failure. Some specimens displayed a slight strengthening beyond the point of ultimate load, and then collapsed in a sudden motion. All specimens tested under flexure, regardless of their groups, failed due to fracture at the bottom part which acted a tension region of the specimen under the loading point. This failure is common for specimens tested with a three point bending load. The failure pattern of different natural fibre composites tested under flexure load in this research is shown in Figure 4.21.

The natural fibre composites developed in this work have reasonable flexural properties. As for comparison purposes, a list of published data of flexural properties are presented in Table 4.13. According to the data listed in the table, the flexural strength of natural fibre composites varies from 47.82 MPa to 128.5 MPa while the average values in this work ranges from 47.34 MPa to 62.72 MPa. In addition, the value of flexural modulus obtained in this work ranges from 2001 MPa (2.01 GPa) to 3459 MPa (3.46 GPa) while published literatures give a range of 2.49 GPa to 5.02 GPa. In short, it can be concluded that the values provided in this work were reasonably acceptable.

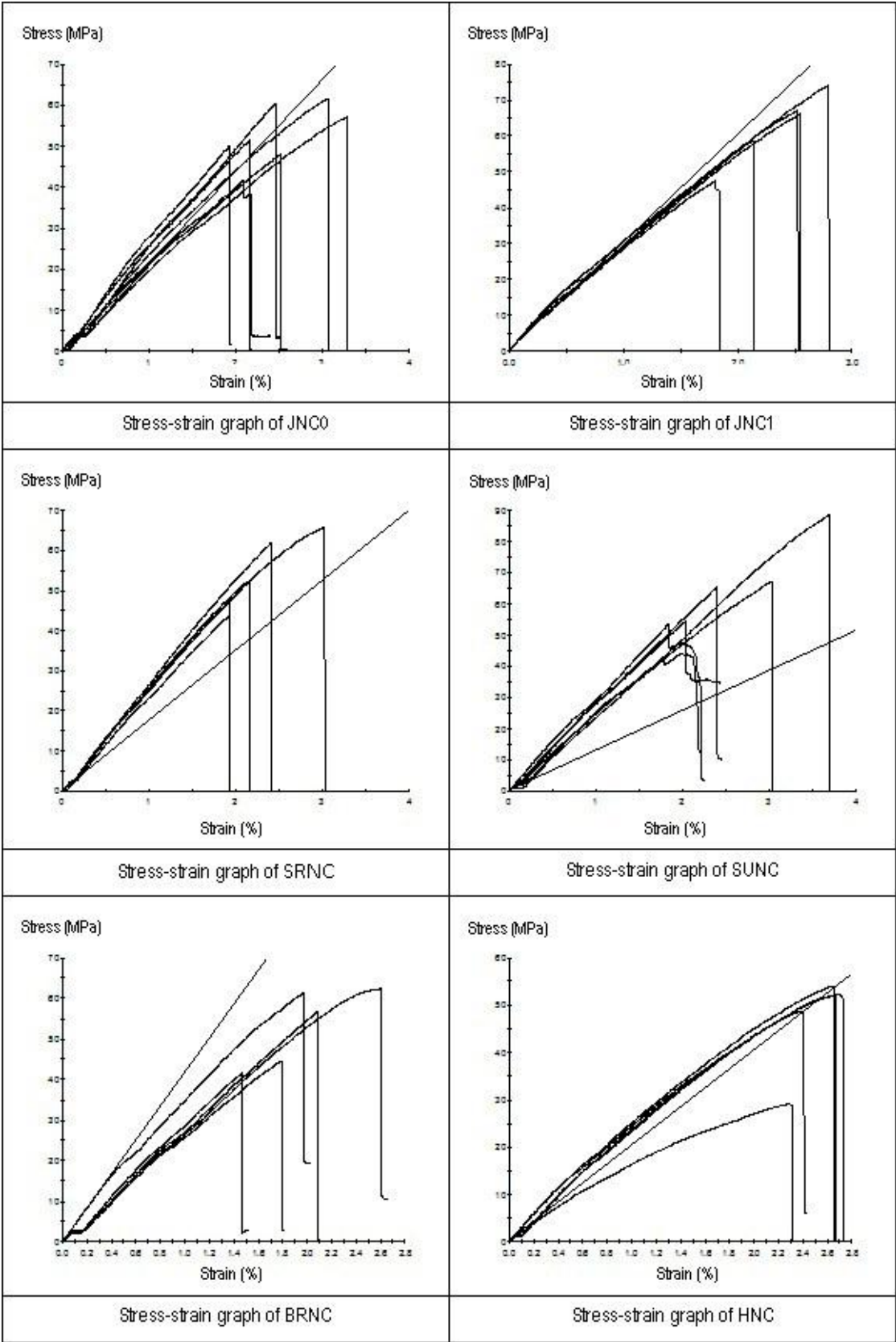


Figure 4.20. Typical stress-strain graphs of different NFCs in flexure

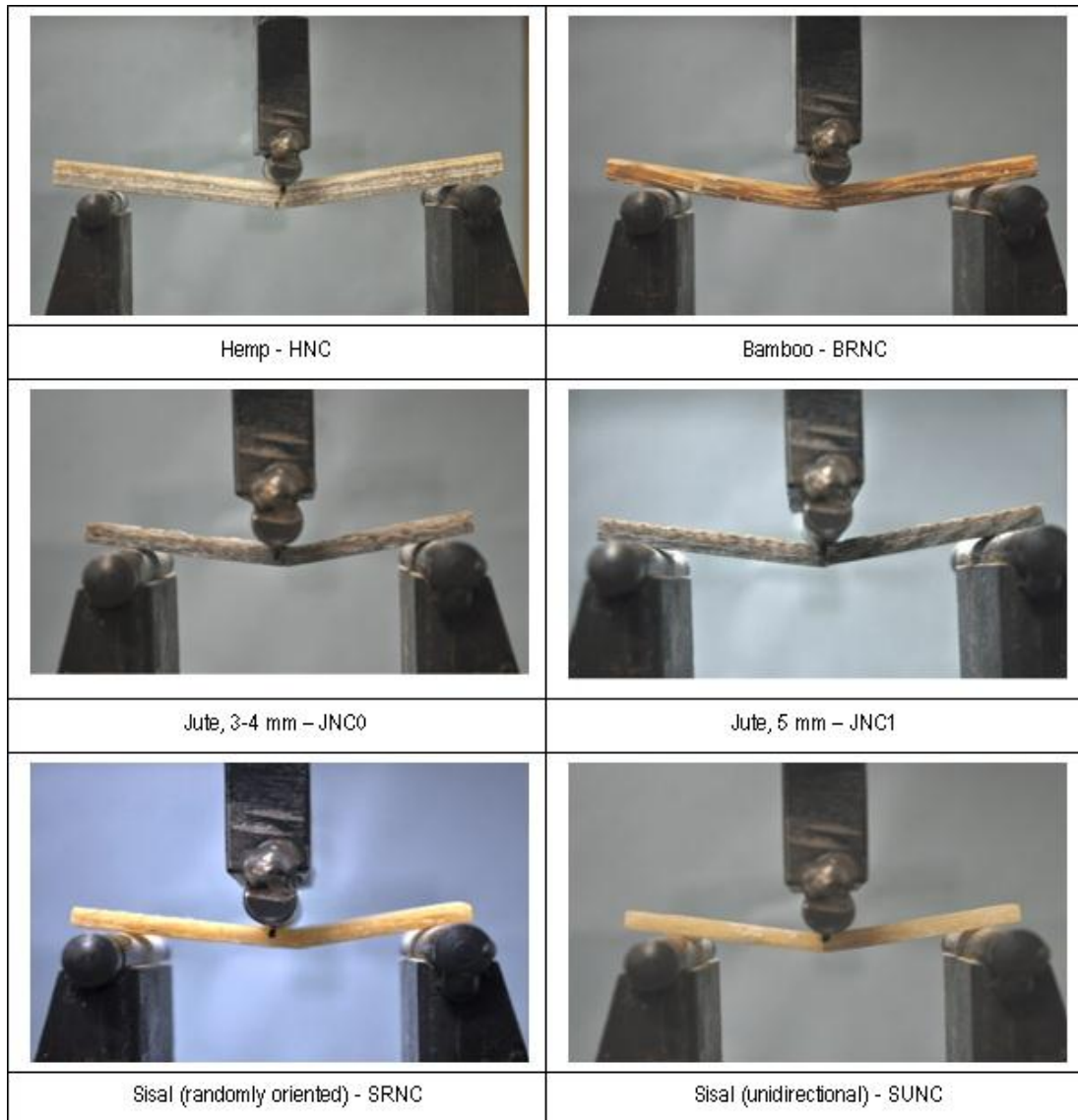


Figure 4.21. Typical flexure failure patterns of different NFCs

Table 4.13. Flexural strength and flexural modulus of different natural fibre composites from several literatures

No	Fibre	Matrix	Flexural properties		References
			Flexural Strength (MPa)	Flexural Modulus (MPa)	
1	Jute	PVC	62.6	3200	Khan et al (2011)
2	Banana	Polyester	65	-	Pothan et al (2002)
3	Gomuti	Epoxy	64.71	3150	Sastra et al (2005, 2006)
4	Gomuti	Polyester	47.82	3400	Ticoalu et al (2010)
6	Jute	Vinylester	128	-	Ray et al (2001)
7	Sisal	Polyester	99.5	2490	Prasad and Rao (2011)
8	Bamboo	Polyester	128.5	3700	Prasad and Rao (2011)
9	Hemp	Polyester	54	5020	Rouison et al (2006); Ticoalu et al (2010)

4.4.3. Compression test

Most research works in this area have been focused only on the tensile and flexural properties of natural fibre composites. Only few works have been related to compression and shear properties analysis. In this research, the analysis of these two mechanical properties focused only on their strength, i.e. compression strength and shear strength. Compression is a fundamental type of test used to characterize materials. Static compression tests apply an escalating compressive load until failure or apply a specific load and hold it for a certain period. In reality, fibre reinforced plastics are particularly valued for their high tensile strength. However, the comparatively low compression strength of some composite reduces their potential application. Therefore, measuring the compression strength of natural fibre composites is of particular interest as well as their tensile strength.

The compression test of NFCs in this research was carried out as per ASTM D 695M standard. This standard is suitable for measuring compressive strength of NFCs as the natural fibre based composites are not very strong. This standard is not suitable for high strength composites due to the low transverse and interlaminar strength of these materials that may lead the specimens to fail by crushing or longitudinally splitting (Mathews, 2000; Hodgkinson, 2000). The test was carried out using a MTS machine with a maximum load capacity of 100 kN. Five specimens with recommended dimensions were prepared for each panel. The testing speed applied was 1.3 mm/min, as recommended by the referred standard. The testing set up for the compression test is shown in the following figure.

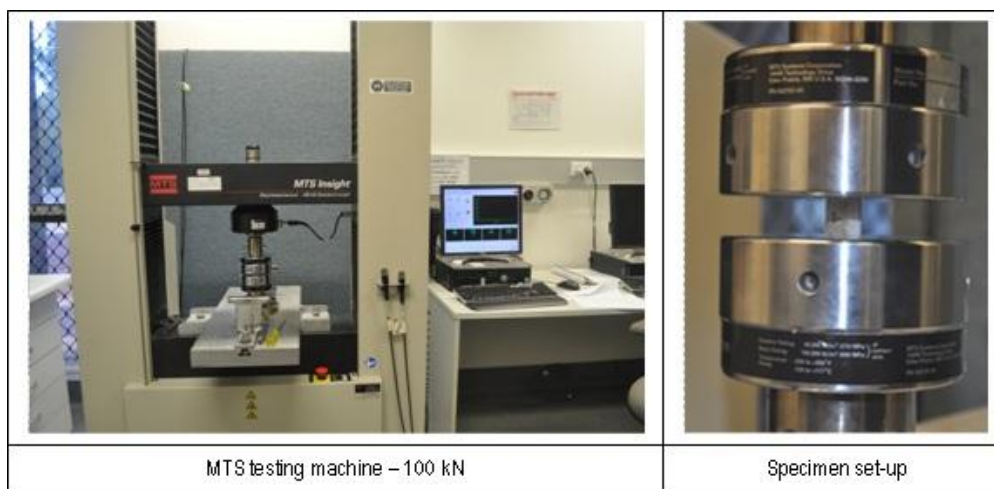


Figure 4.22. Setting-up for compression test of NFCs

According to the ASTM D695M standard, compressive strength can be defined as “the maximum compressive stress carried by a test specimen during a compression test”. It may or may not be the compressive stress carried by the specimen at the moment of rupture. It is expressed in megapascals (MPa). Compressive strength can be obtained using the following equation.

$$\sigma_c = \frac{F_{\max}}{bh} \dots\dots\dots 4.10$$

Where:

- σ_c : Compressive strength (MPa)
- F_{\max} : Maximum load (N)
- b : The width of the specimen (mm)
- h : The thickness of the specimen (mm)

The results of compression testing are tabulated in the Table 4.14 to Table 4.16. Table 4.14 presents the result of the compression testing of jute natural fibre composite while the compression properties of sisal natural fibres are shown in Table 4.15. In addition, Table 4.16 shows the compression properties of a hemp natural fibre composite and bamboo based composite. The table only shows some important parameters such as peak load, peak stress, and compression modulus.

Table 4.14. Compressive properties of jute natural fibre composite

Jute natural fibre composite-flexure, thickness (3-4 mm) – (JNC0-CMP)					
Specimen	Thickness (mm)	Width (mm)	Area (mm ²)	Peak Load (N)	Peak Stress (MPa)
1	4.1	8	32.80	2052	62.56
2	3.9	8.1	31.59	1778	56.28
3	3.8	8	30.40	896	29.47
4	4.2	8	33.60	2386	71.01
5	3.8	8.1	30.78	1206	39.18
Mean	3.96	8.04	31.83	1664	51.70
Std Dev	0.18	0.05	1.35	609	17.05
CV	4.55	0.62	4.24	36.60	32.98
Jute natural fibre composite-flexure, thickness (5 mm) – (JNC1-CMP)					
Specimen	Thickness (mm)	Width (mm)	Area (mm ²)	Peak Load (N)	Peak Stress (MPa)
1	6.6	13.2	87.12	5330	61.18
2	6.6	13.2	87.12	2583	29.65
3	6.4	12.7	81.28	3640	44.78
4	6.7	13.4	89.78	2362	26.31
5	6.5	12.9	83.85	5417	64.60
Mean	6.5	13	85.83	5145	45.30
Std Dev	0.55	13.07	3.30	4080	17.54
CV	8.46	100.54	3.84	79.30	38.72

Table 4.15. Compressive properties of sisal natural fibre composite

Sisal (<i>randomly oriented</i>) natural fibre composite-compressive – (SRNC-CMP)					
Specimen	Thickness (mm)	Width (mm)	Area (mm ²)	Peak Load (N)	Peak Stress (MPa)
1	6.4	12.9	82.56	3689	44.68
2	6.5	13	84.50	4658	55.12
3	6.5	13	84.50	3869	45.79
4	6.5	12.8	83.20	4932	59.28
5	6.6	13.1	86.46	4041	46.74
Mean	6.5	12.96	84.24	4238	50.32
Std Dev	0.07	0.11	1.50	533	6.49
CV	1.08	0.85	1.78	12.58	12.90
Sisal (<i>unidirectional</i>) natural fibre composite-compressive – (SUNC-CMP)					
Specimen	Thickness (mm)	Width (mm)	Area (mm ²)	Peak Load (N)	Peak Stress (MPa)
1	3.9	7.2	28.08	2193	78.10
2	3.5	7.1	24.85	1272	51.19
3	3.6	7.2	25.92	1300	50.15
4	3.6	7.2	25.92	993	38.31
5	3.8	7.7	29.26	2535	86.64
Mean	3.68	7.28	26.81	1659	60.88
Std Dev	0.16	0.24	1.81	666	20.48
CV	4.35	3.30	6.75	40.14	33.64

Table 4.16. Compressive properties of bamboo based and hemp natural fibre composite

Bamboo (<i>randomly oriented</i>) based composite-compressive – (BRNC-CMP)					
Specimen	Thickness (mm)	Width (mm)	Area (mm ²)	Peak Load (N)	Peak Stress (MPa)
1	5.7	11.4	64.98	3499	53.85
2	5.7	11.4	64.98	2646	40.72
3	5.7	11.3	64.41	1095	17.00
4	5.7	11.4	64.98	1354	20.84
5	5.7	11.4	64.98	3023	46.52
Mean	5.7	11.38	64.87	2323	35.79
Std Dev	0	0.04	0.25	1052	16.14
CV	0.00	0.35	0.39	45.29	45.10
Hemp natural fibre composite-compressive – (HNC-CMP)					
Specimen	Thickness (mm)	Width (mm)	Area (mm ²)	Peak Load (N)	Peak Stress (MPa)
1	7.6	15	114.00	4408	38.67
2	7.7	14.8	113.96	4503	39.51
3	7.9	15.1	119.29	3479	29.16
4	7.5	15	112.50	2185	19.42
Mean	7.5	15	114.94	2109	31.69
Std Dev	0.62	14.98	2.98	2781	9.43
CV	8.27	99.87	2.59	131.86	29.76

The data presented in the above tables has been reorganized in the form of dot-plot diagram in order to obtain more comprehensible and immediate information. The dot-plot diagram of compressive strength of NFCs investigated in this research is presented in Figure 4.23.

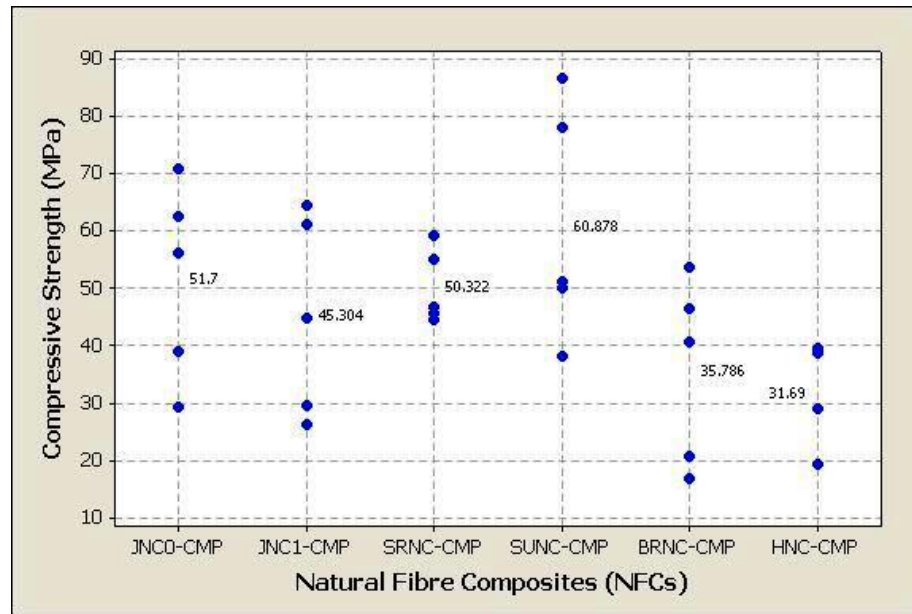


Figure 4.23. The dot-plot diagram of the compressive strength of NFCs

When a glance observation is given to the concentration of data in the above figure, it seems that only two groups of specimens, SRNC-CMP and HNC-CMP, have a consistent compressive strength distribution. The average values of these two specimens group were 50.32 MPa and 31.69 MPa, respectively. The values of remaining four groups need to be normalized in order to obtain more reliable average values. The analysis was focused only on one single parameter, i.e. compressive strength.

Sample JNC0-CMP has an average compressive strength value of 51.70 MPa which ranges from 29.47 MPa to 71.01 MPa. The data of specimen 3 (29.47 MPa) was considered as a peculiar data. Hence, when this data is neglected the average value of JNC0-CMP has now turned to 57.26 MPa. A similar process was applied to the JNC1-CMP samples which have a definite average value of 45.30 MPa. Excluding the data of specimen 2 and specimen 4, results in a new average value of 56.85 MPa. It can be noted here that by doing this normalization process, the difference between the two groups can be significantly reduced, from 11.17% when comparing actual average values to 0.71% after normalization.

The SRNC-CMP specimen group shows less variation in their compressive strength data distribution. The data of this sample group ranges from 44.68 MPa to 59.28 MPa with the average value of 50.32 MPa and a standard deviation of 6.49 MPa. On the other hand, SUNC-CMP sample group has the tendency to distribute into two sets of average value. If the two highest values are considered, the compressive strength of specimen 1 and specimen 5, it gives a new average value of 82.37 MPa. An average value of 46.55 MPa can be obtained when the three lower values of compressive strength are considered. A quick observation into the compressive strength data of BRNC-CMP gives the feeling that the data was not uniformly distributed. The actual average value of this specimens group was 35.79 MPa with the standard deviation of 16.14 MPa. However, the compression strength of BRNC-CMP has the tendency to separate into two levels. When three higher values of the data are considered, the average value increases to 47.03 MPa and only 18.92 MPa when only two lowest data are considered.

The failure pattern of NFCs under compressive load can be observed in Figure 4.24. Unfortunately, only two groups of tested samples are pictured as the specimens were quite small. The typical load-extension curves of different NFCs tested under compressive load in this work are presented in Figure 4.25. As can be observed from the presented graphs, the load-extension curves showed a linear elastic behaviour at the initial stage. After reaching the ultimate load, the curve bends sharply, some becoming flat at the top, indicates a significant reduction in stiffness, and finally descends until the specimens fractured. In other word, the material behaves plastically after the peak load. All specimens tested under compression failed due to fracture at the gauge length.

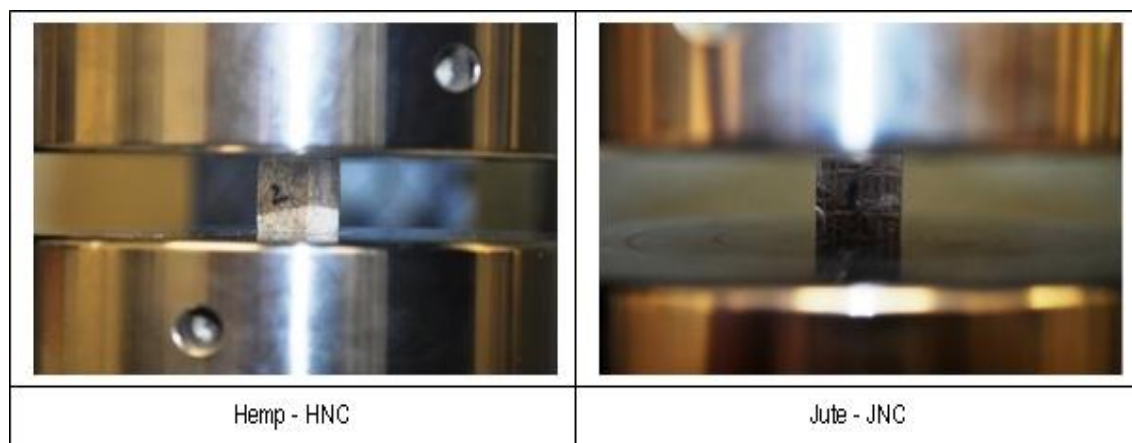


Figure 4.24. Typical compression failure patterns of different NFCs

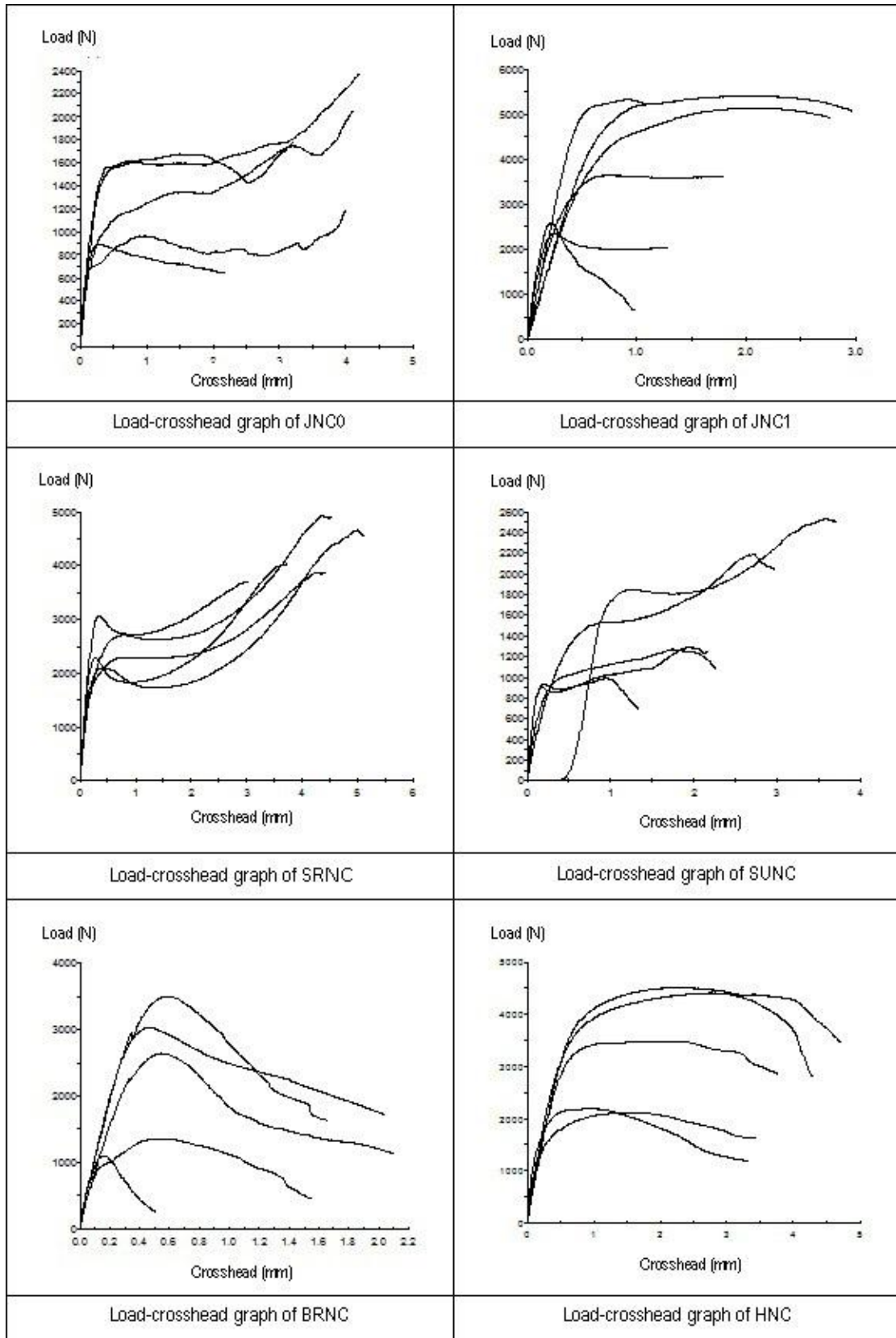


Figure 4.25. Typical load-crosshead graphs of different NFCs in compression

The average values of compressive strength obtained in this work range from 31.69 MPa to 86.64 MPa. While for comparative purposes, the results of previous work dealing with compressive properties analysis are summarized in Table 4.17. As can be seen in this table, the compressive strength of natural fibre composites spreads from 16.75 MPa to 108.07 MPa. This result indicates that the average value of compressive strength obtained in this work were acceptable.

Table 4.17. Compressive strength and compressive modulus of different natural fibre composites from several literatures

No	Fibre	Matrix	Compressive properties		References
			Compressive Strength (MPa)	Compressive Modulus (MPa)	
1	Gomuti	Epoxy	82.08	1930	Ticoalu et al (2011)
2	Gomuti	Vinylester	108.07	2010	Ticoalu et al (2011)
3	Gomuti	Polyester	104.07	2140	Ticoalu et al (2011)
4	Sisal	Polyester	113	-	Naidu et al (2011)
6	Banana	Resin	16.75	-	Samuel et al (2012)
7	Sisal	Resin	42	-	Samuel et al (2012)
8	coconut	Resin	30.35	-	Samuel et al (2012)
9	Hidegardia populifolia	Polyester		114.73	Rajulu et al (2005)

4.4.4. Shear test

Few reported research works point out that shear testing is one of the most complex areas of testing. One of the principal challenges in the development of the measurement of shear properties is the provision of a pure shear stress state in the specimen. In an ideal condition, a shear test method should provide a region of pure shear stress in the specimen throughout the linear or non-linear response regime (Broughton, 2000; Hodgkinson, 2000). Some other reasons that make shear strength determination questionable are; the presence of edges, material coupling, non-pure-shear loading, non-linear behaviour, imperfect stress distribution or the presence of normal shear stress.

Among the available methods for measuring the shear properties of composite laminate, the most commonly used shear test is the Iosipescu shear test. This method is also known as V-notched shear test, described in ASTM standard D5379M. The Iosipescu or V-notched uses a rectangular beam with a symmetrical centrally located v-notched. The beam is loaded by a special fixture applying a shear loading at the v-notch. The specimen is inserted into the fixture with the notch located along the line of

action of loading by means of an alignment that references the fixture. The two halves of the fixture are compressed by a testing machine while monitoring load. In this test, five specimens of tested NFC laminates were prepared. The testing was conducted using a MTS machine with the maximum capacity of 10 kN. The testing machine was set-up to apply the load with the speed of 2 mm/min and the test was set-up as shown in the following figure.

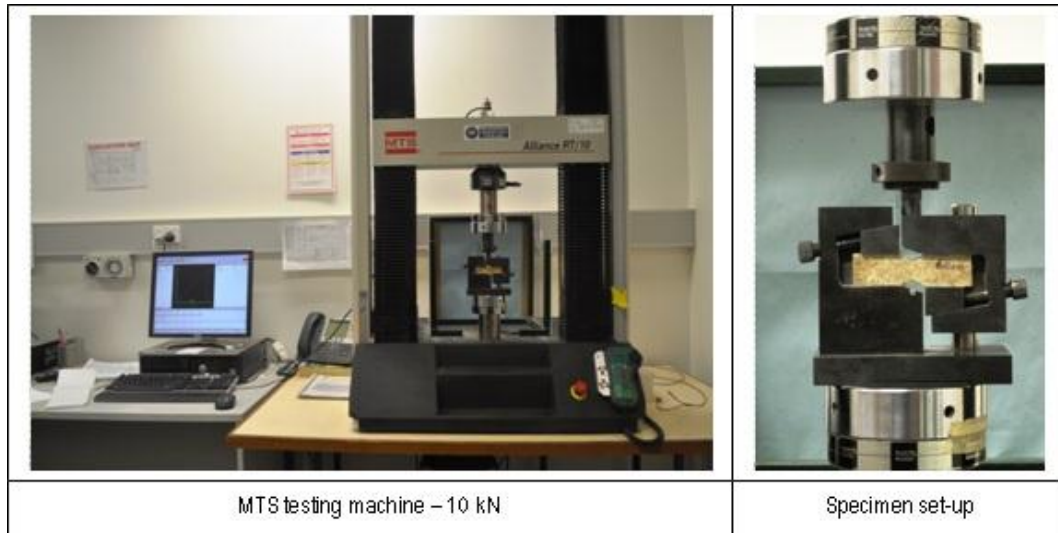


Figure 4.26. Setting-up for shear test of NFCs

The calculation and expression of testing results according to the referred standard, ASTM D 5379M-5, are as follows. The shear strength is the shear stress carried by a material at failure under a pure shear condition. The average shear stress is determined by dividing the applied load by the area of the cross section between the notches. It is calculated according to the following equation.

$$\tau_{ave} = \frac{F}{A} \dots\dots\dots 4.12$$

Where:

- τ_{ave} : Average shear stress (MPa)
- F : Applied load (N)
- A : Area of cross-section between the notches (mm²)

The results of shear testing for different natural fibre composites studied in this work are tabulated in the Table 4.18 to Table 4.20. The shear properties of the jute fibre composite and the sisal natural fibre composite are presented in Table 4.18 and Table 4.19, respectively. Table 4.20 shows the shear properties of bamboo based composites and Table 4.21 shows the shear properties of hemp fibre composite.

Table 4.18. Shear properties of jute natural fibre composite

Jute natural fibre composite-shear, thickness (3-4 mm) – (JNC0-SHR)					
Specimen	Notch Height (mm)	Notch Width (mm)	Deflection at Peak (mm)	Peak Load (N)	Peak Shear Stress (MPa)
1	12.00	3.30	1.71	1181	29.83
2	12.10	3.10	1.64	1084	28.90
3	12.20	3.20	1.99	1159	29.68
4	12.00	3.20	1.31	860	22.39
5	12.00	3.20	1.66	654	17.03
Mean	12.06	3.20	1.66	988	25.57
Std Dev	0.09	0.07	0.24	226	5.68
CV	0.75	2.19	14.46	22.87	22.21

Table 4.19. Shear properties of sisal natural fibre composite

Sisal (<i>randomly oriented</i>) natural fibre composite-shear – (SRNC-SHR)					
Specimen	Notch Height (mm)	Notch Width (mm)	Deflection at Peak (mm)	Peak Load (N)	Peak Shear Stress (MPa)
1	11.90	6.30	1.09	1807	24.10
2	12.00	6.10	1.20	1591	21.74
3	11.90	6.40	0.88	1120	14.71
4	11.70	6.60	1.22	2073	26.84
5	12.00	6.20	1.59	1807	24.29
Mean	11.90	6.32	1.20	1680	22.34
Std Dev	0.12	0.19	0.26	356	4.63
CV	1.01	3.01	21.67	21.19	20.73
Sisal (<i>unidirectional</i>) natural fibre composite-shear – (SUNC-SHR)					
Specimen	Notch Height (mm)	Notch Width (mm)	Deflection at Peak (mm)	Peak Load (N)	Peak Shear Stress (MPa)
1	11.50	4.50	1.64	1213	23.44
2	11.90	4.00	1.96	1078	22.66
3	11.20	3.80	1.28	1039	24.42
4	11.20	3.40	1.40	965	25.35
5	11.00	5.60	1.39	1258	20.42
Mean	11.36	4.26	1.53	1111	23.26
Std Dev	0.35	0.85	0.27	122	1.88
CV	3.08	19.95	17.65	10.98	8.08

Table 4.20. Shear properties of bamboo based composite

Bamboo (<i>randomly oriented</i>) based composite-shear – (BRNC-SHR)					
Specimen	Notch Height (mm)	Notch Width (mm)	Deflection at Peak (mm)	Peak Load (N)	Peak Shear Stress (MPa)
1	11.60	5.60	1.30	1501	23.10
2	12.00	5.60	1.23	1489	22.16
3	11.10	5.60	1.70	1388	22.33
4	12.50	5.60	2.13	1841	26.30
5	11.00	5.60	1.13	1121	18.20
Mean	11.64	5.60	1.50	1468	22.42
Std Dev	0.63	0.00	0.42	259	2.89
CV	5.41	0.00	28.00	17.64	12.89

Table 4.21. Shear properties of hemp natural fibre composite

Specimen	Notch Height (mm)	Notch Width (mm)	Deflection at Peak (mm)	Peak Load (N)	Peak Shear Stress (MPa)
1	12.50	7.50	2.08	2151	22.94
2	12.10	7.70	2.25	2394	25.69
3	12.10	7.60	1.98	2159	23.48
4	11.50	7.70	1.66	1639	18.51
5	12.10	7.20	1.89	1890	21.69
Mean	12.06	7.54	1.97	2047	22.46
Std Dev	0.36	0.21	0.22	289	2.64
CV	2.99	2.79	11.17	14.12	11.75

Following the similar process applied to the previous analysis, the data presented in the above tables have been reorganized in the form of dot-plot diagram in order to obtain more apparent information. The dot-plot diagram of shear strength of NFCs investigated in this research is presented in the following figure.

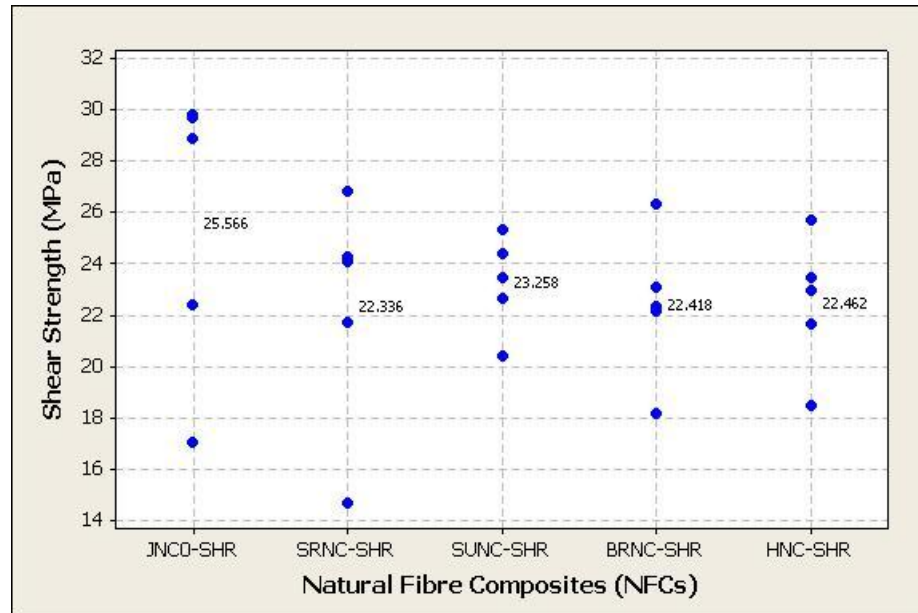


Figure 4.27. The dot-plot diagram of the shear strength of NFCs

It is visually shown in the above figure that the data spread is disproportionate. Likewise to the previous analysis, a normalization process has been made to obtain reliable average values. In this type of mechanical characterization, the specimens for jute fibre composites were cut from thinner panel only with the thickness of 3-4 mm. A quick look at the JNC0-SHR specimens group presented in that graph gives the impression that the variation among their shear strength is considered as a less, except for specimen 5 which has the shear strength of 17.03 MPa. This value has a distinctive

difference of about 42.9% when it is compared to the highest value possessed by specimen 1, which is 29.83 MPa. The average value of this specimens group can be raised to 27.7 MPa when the shear strength of specimen 5 is neglected.

The shear strength distribution of composites reinforced with sisal fibre appears relatively consistent, particularly for specimens under the group of SUNC-SHR. The average value of these specimens can be used without further justification. The shear strength of specimens in this group ranges from 20.42 MPa to 25.35 MPa, with the average values of 23.26 MPa and standard deviation of 1.88 MPa. Meanwhile, the shear strength of specimen 3 in the group of SRNC-SHR has to be ignored as if might increase the average value to 24.24 MPa, which is slightly increased from the actual value of 22.34 MPa.

It is also evidently presented in Figure 4.27 that BRNC-SHR and HNC-SHR specimen groups have one peculiar value, i.e. their lowest value. The average value of BRNC-SHR might be increased to 23.47 MPa if their lowest value of 18.20 MPa, possessed by specimen 5, is neglected. Similarly, HNC-SHR specimen group will have a new average value of 23.45 if the shear strength of specimen 4, which is 18.51 MPa, is ignored. However, the difference between the actual and the new values was only about 4.47% for BRNC-SHR and 4.22% for HNC-SHR. Both values were less than 5%, so using their original average values is also acceptable.

The typical load-crosshead graphs of different natural fibre composites tested under shear in this work are presented in Figure 4.28. As clearly shown in that figure, the stress-strain curves show a linear elastic behaviour at the initial stage. After some point there is a reduction on the stiffness of material until the final failure. The graphs also show that most of the tested specimens failed in a sudden mode of failure. Some specimens, for example in JNC0-SHR group show a non-linear behaviour. The failure of specimens under shear loading was mainly due to the shear failure at the notch of the specimen which is an acceptable mode of failure under the V-notched shear test. As it can be seen in Figure 4.29, all specimens, with the exception for JNC0, failed due to the formation of diagonal cracking at the notch. The representative specimen JNC0 failed due to vertical cracking, also at the notch, which also acceptable for the shear failure of specimen tested using this particular shear test. However, some of the specimens in this group also failed due to the diagonal cracking at their notch.

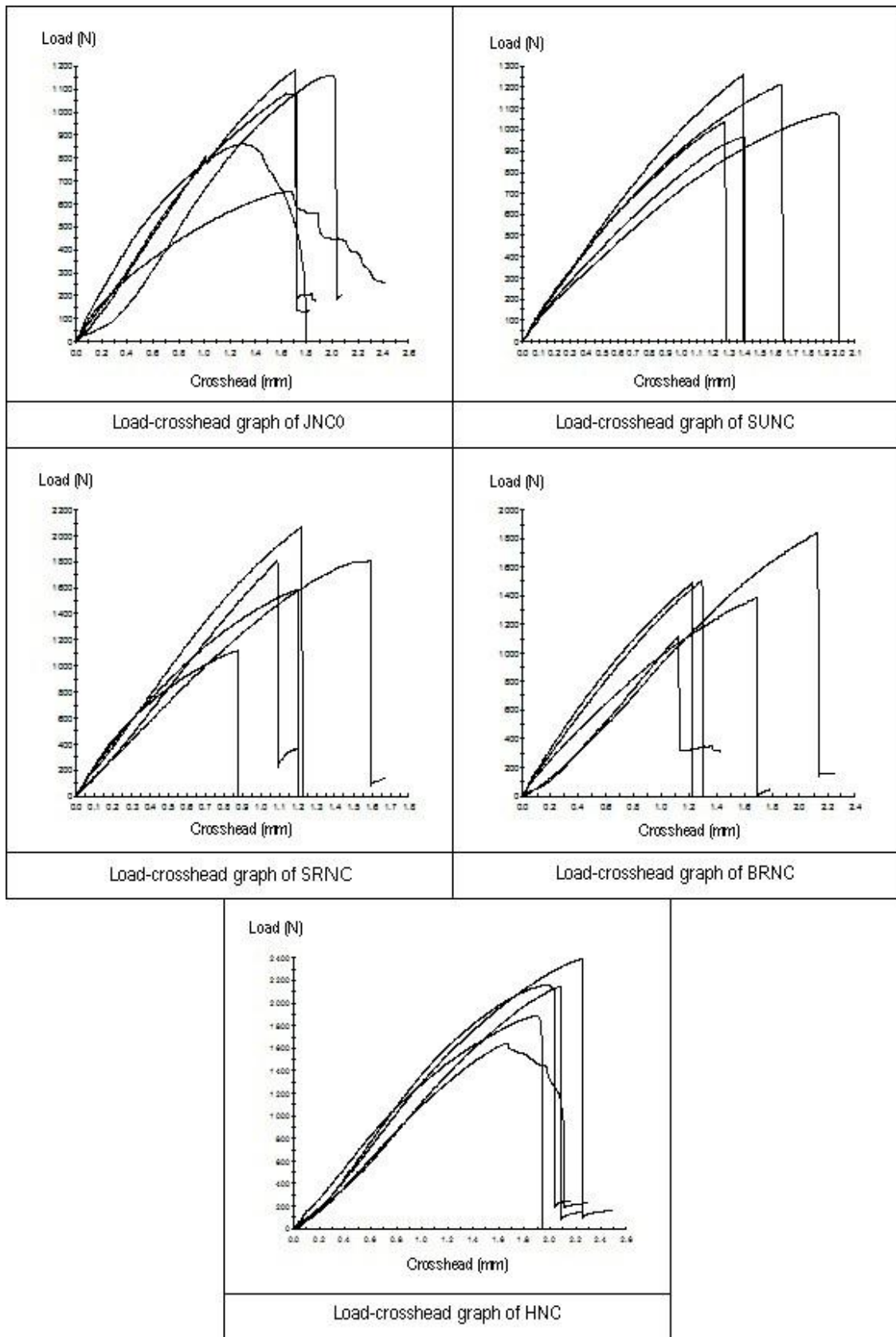


Figure 4.28. Typical load-crosshead graphs of different NFCs in shear

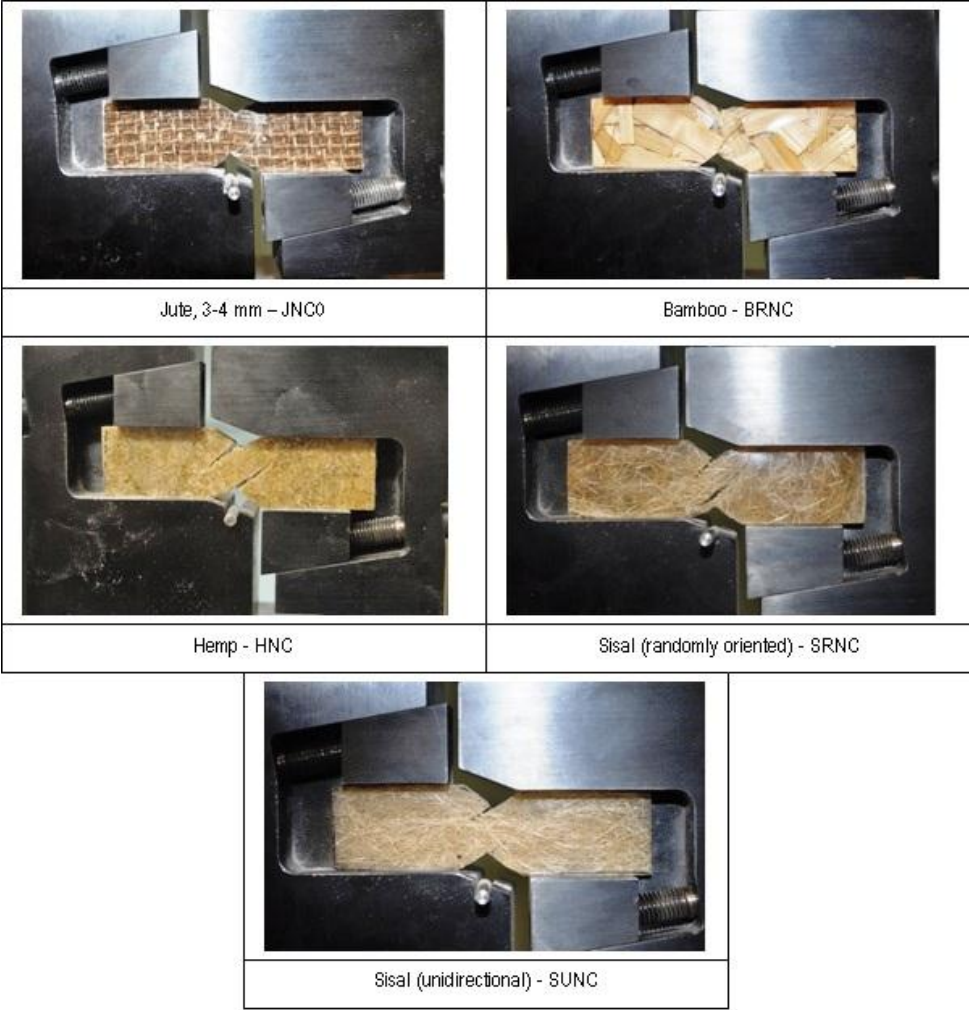


Figure 4.29. Typical shear failure patterns of different NFCs

As previously stated in the early compression analysis part, the most common observed mechanical properties of natural fibre composite are tensile and flexural behaviour. Particularly for shear properties, it is hard to find related literature in this area. Unlike the other properties that were previously discussed, in this case only a single reference can be presented for the comparison purpose. The average values of shear strength provided in this work ranges from 22.42 MPa to 25.57 MPa. These results seem comparable to the work of Franco and Gonzales (2005) in which they found that the shear strength of natural fibre composites made of short henequen fibre reinforced polyethylene (HDPE) matrix ranges from 14 MPa to 19 MPa. It is worthwhile to note here that the work of the above cited references were using a similar method for examining the shear properties of their composites. The tensile and shear properties of HDPE-Henequen fibre composite are as presented in the following figure.

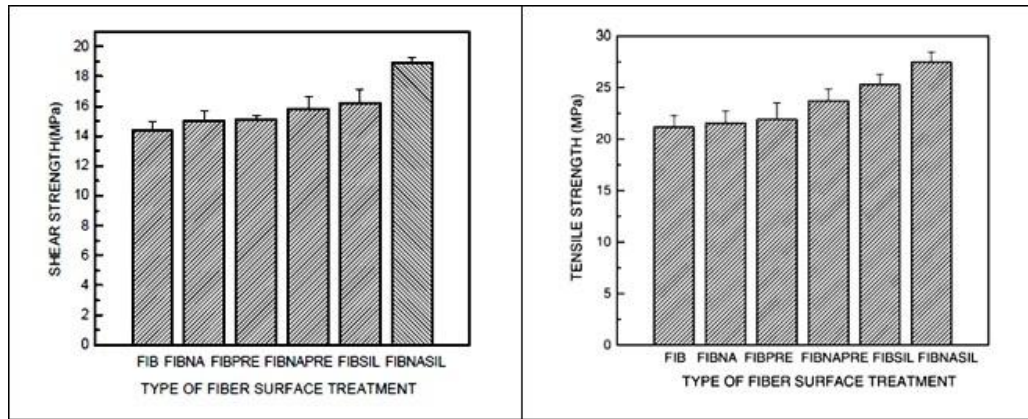


Figure 4.30. Shear and tensile strength of HDPE/Henequen fibre (80/20 v/v) composite (Franco and Gonzales, 2005)

4.5. General Discussions

In this chapter part, a brief discussion about some important findings from the previous analysis, particularly the mechanical properties, has been given. The discussion has focused on the comparison analysis of different natural fibres composites that previously developed in this work. It is important to bear in mind that the analysis has been made based upon the normalized data results. The first subject discussed in this part is the tensile strength of observed material. The comparison of tensile strength among different NFCs and MDF tested in this work is presented in the following figure.

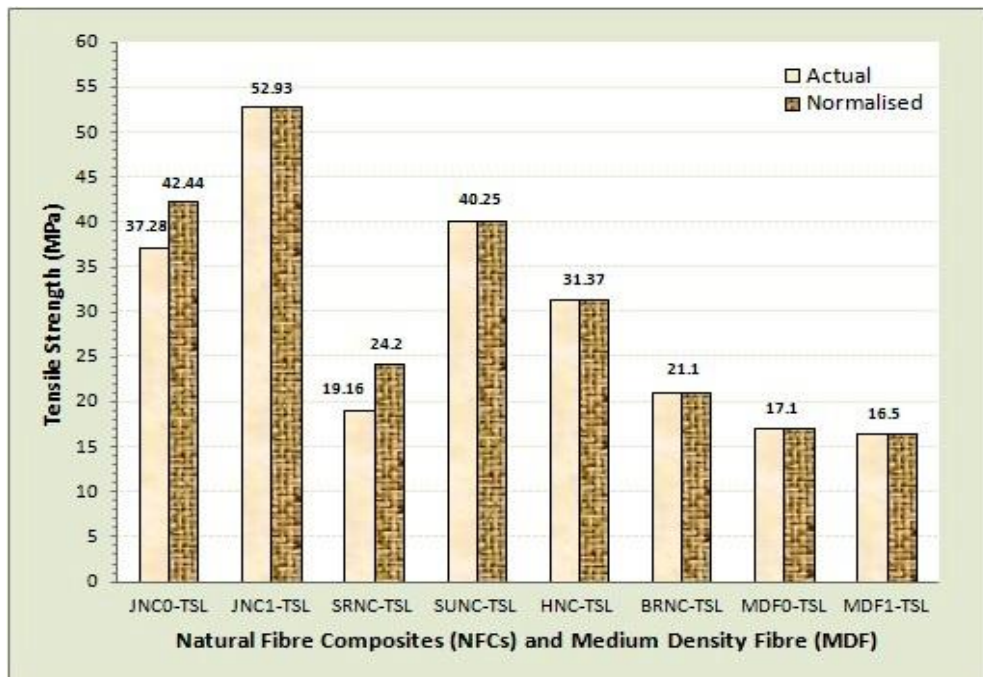


Figure 4.31. The average tensile strength values of different NFCs and MDF

As can be seen from the graph, the jute fibre composite has the highest value of tensile strength. Both specimen groups representing this composite type, JNC0-TSL and JNC1-TSL, have the average value of tensile strength of 42.44 MPa and 52.93 MPa, respectively. These values were followed by SUNC-TSL and HNC-TSL groups with the average tensile strength of 40.25 MPa and 31.37 MPa, respectively. The tensile strength of JNC1-TSL was 23.9% higher than SUNC-TSL and 40.7% than HNC-TSL. It can also be observed from the graph that the three groups have identical actual and normalized values, indicate they have constant tensile strength for all observed specimens. For MDF specimen groups, their average values were at the bottom rank but these values were very consistent.

The second aspect discussed in this part is the tensile modulus of observed materials. Likewise to their tensile strength, jute fibre composites have the highest value of tensile modulus or Young’s modulus, or simply called as Modulus of Elasticity. This value is the most important parameter when considering a material for structural application. The tensile modulus of different NFCs and MDF is presented in the following figure.

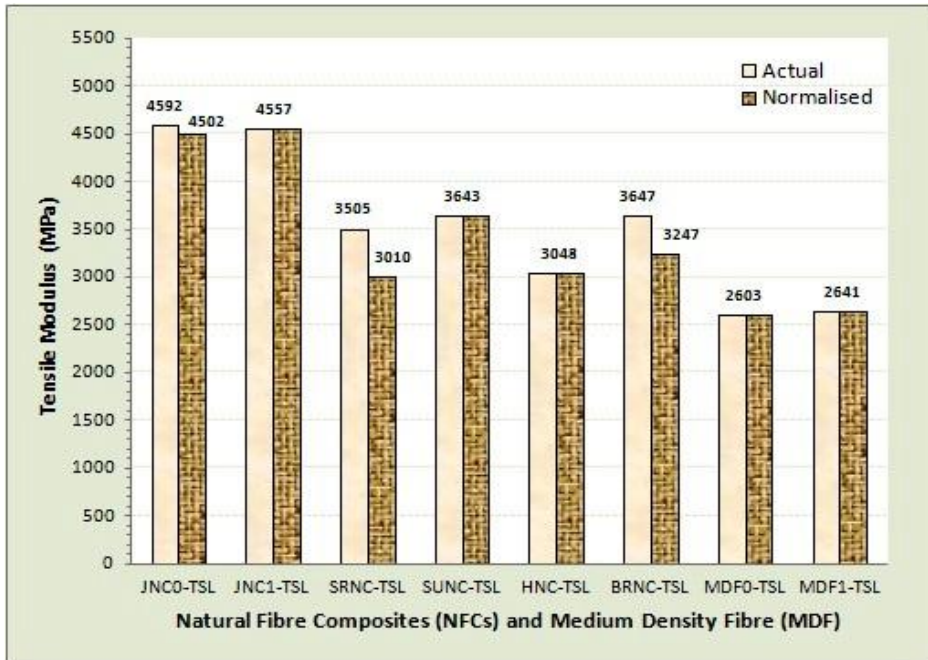


Figure 4.32. The average tensile modulus values of different NFCs and MDF

The average tensile modulus for both sample groups representing jute fibre composites, JNC0-TSL and JNC1-TSL was 4502 MPa and 4557 MPa, respectively.

Again, their values were followed by SUNC-TSL and HNC-TSL in the second and third place with the average values of 3243 MPa and 3048 MPa, respectively. Bamboo based composites, BRNC-TSL, have a higher value than those two groups, but the average value of bamboo is obtained after a normalization process. In parallel with their tensile strength, the tensile moduli of MDF sample group were also consistent at around 2600 MPa. The comparison of tensile modulus of different NFCs and MDF is presented in Figure 4.32.

The last focus of discussion in this part is the Poisson ratio of the observed material. It is important to note that most materials have Poisson's ratio values ranging between 0.0 and 0.5. A perfectly incompressible material deformed elastically at small strains would have a Poisson's ratio of exactly 0.5. The comparison of the Poisson ratio of different NFCs is given in the following figure.

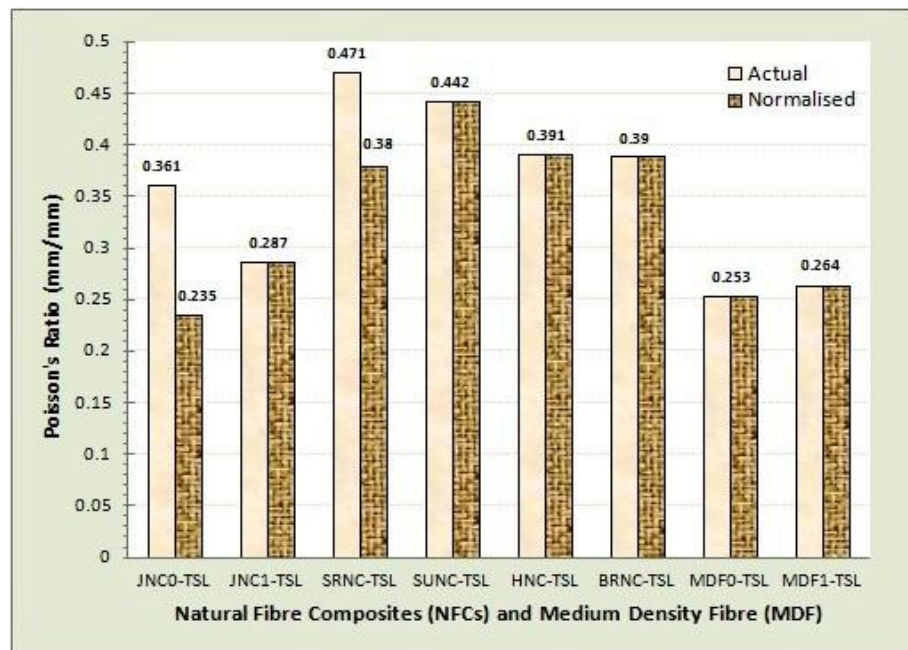


Figure 4.33. The average Poisson's ratio values of different NFCs and MDF

As clearly presented at the above figure, the Poisson ratio of natural fibre composites studied in this work range from the lowest of 0.235 to the highest of 0.442, indicating that the obtained values provided in this work are acceptable. The highest value belongs to the composite reinforced with the unidirectional sisal fibre, SUNC-TSL, which has the Poisson ration of 0.442. In contrast to the previous analysis that always positioned jute fibre composites at the high level, the obtained values of their

Poisson ratio which is 0.235 for JNC0-TSL and 0.287 for JNC1-TSL has located them at the lower category. These values were almost similar to the average Poisson ratio of medium density fibre, MDF0-TSL and MDF1-TSL, which was 0.235 and 0.264, respectively. At the middle level, three specimen groups provided nearly the same value of 0.38, 0.391 and 0.39 that belong to SRNC-TSL, HNC-TSL and BRNC-TSL, respectively.

Considering the further use of materials observed in this work, which is for intermediate layer, it seems that material with lower Poisson’s ratio is most preferred. The reason for this can be explained as follows. As can be seen from the Equation 4.5, Poisson’s ratio is defined as the ratio of normal or lateral strain over the axial or longitudinal strain. The lateral strain might be in the y-axis or z-axis, hence the above equation can be re-written as follows.

$$\vartheta = \frac{\epsilon_y}{\epsilon_x} = \frac{\epsilon_z}{\epsilon_x} \dots\dots\dots 4.13$$

Substituting the value of longitudinal strain as a function of stress and modulus of elasticity material under axial load applied in a direction parallel to the x axis, a new relation can be obtained as follows.

$$\vartheta = \frac{\epsilon_y}{\sigma_x/E} \dots\dots\dots 4.14$$

$$\epsilon_y = \frac{\vartheta\sigma_x}{E} \dots\dots\dots 4.15$$

Where:

- ϑ : Poisson’s ratio, expressed in a dimensionless ratio
- ϵ_x : Strain in the longitudinal direction
- ϵ_y, ϵ_z : Strain in the normal direction
- E : Modulus elasticity of the material (MPa)
- σ_x : Axial stress (MPa)

As can be examined from Equation 4.15, the lateral strain is corresponding to the value of Poisson ratio meaning that the lateral strain is getting higher as the value of Poisson ratio increased. The excessive lateral strain may induce delamination in between the adjacent layer. The actual lateral deformation due to lateral strain may not seem like much, but this tiny or even invisible deformation may significantly affect the bonding strength between the two layers which is provided by the adhesive line. The failure of adhesive to provide sufficient bonding between constituent materials has been

the reason for the delamination failure in sandwich panel. In short, the lower Poisson value of jute fibre composite is actually good for being used as the intermediate layer.

The performance of different natural fibre composites under flexural test, flexural strength and flexural modulus is presented in Tables 4.34 and 4.35. A quick observation at the bar chart presented in Figure 4.34, gives the feeling that all specimen groups have comparable flexural properties. The sample groups of JNC1-TSL and SUNC-TSL possess the highest average value of 59.88 MPa and 60.04 MPa, respectively. Although their values were considered as higher than the other groups, the difference was not really significant. For instance, the difference between JNC1-TSL and SRNC-TSL is only 9.23%, and 13.60% with HNC-TSL.

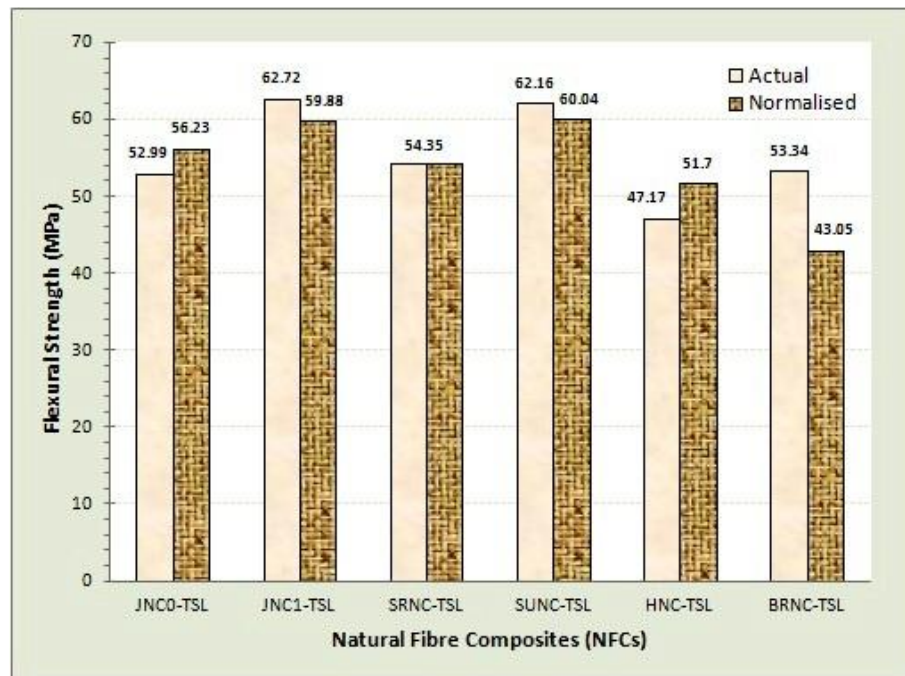


Figure 4.34. The average flexural strength values of different NFCs

The apparent differences among specimen groups can be observed on the graph of flexural modulus, presented in Figure 4.35. Jute natural fibre composite (JNC1-FLX) has the highest average value of flexural modulus. It is worth to note that this value is consistent meaning that the value is not resulted from normalization process. Next is the flexural strength of SUNC-TSL group with the average value of 2843.3 MPa, 17.8% less the average value of JNC1-TSL. This value, however, is a result of a normalization process that indicates an inconsistency of flexural modulus of each observed specimen.

Correspondingly, hemp fibre composite that has an average value of 2489 MPa should be considered in the second grade.

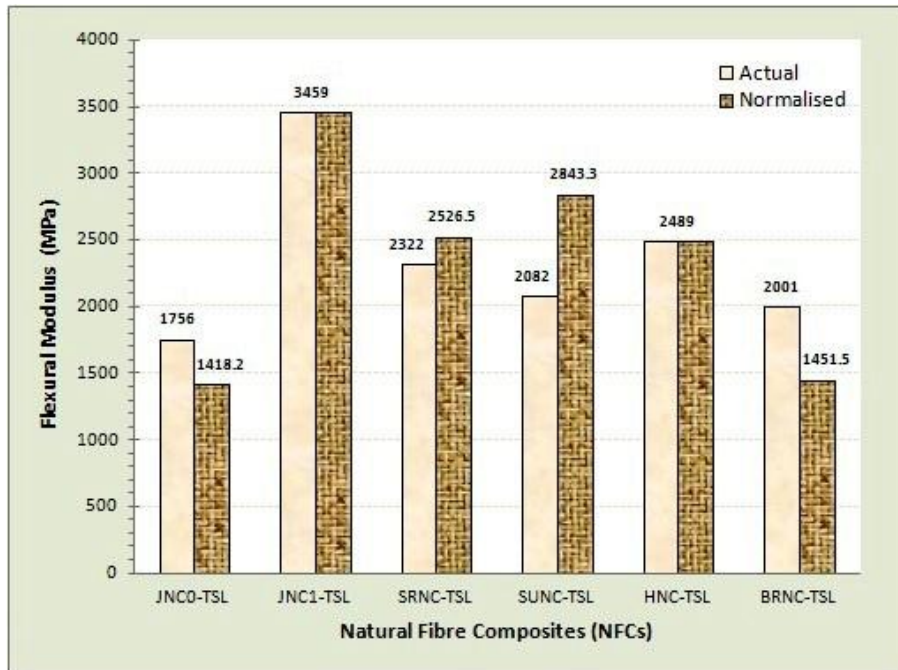


Figure 4.35. The average flexural modulus values of different NFCs

Likewise to the flexural strength analysis, the first impression given by the data of shear strength, shown in Figure 4.36, is that the shear strength of different NFCs investigated in this study was almost comparable. The shear strength of jute fibre composite still occupies the first place with the average value of 27.7 MPa. However, the difference with the rest specimen groups is considered as insignificant. For example, the difference between JNC0-TSL and SRNC-TSL is only 11.9% and 16 % with SUNC-TSL.

Lastly, the average compression strength value of different natural fibre composites is presented in Figure 4.37. The average compression strength of sample groups represented jute fibre composites, JNC0-CMP and JNC1-CMP, were only slightly different of 57.26 MPa and 56.85 MPa. Their values are ranked as the highest among the other NFCs and these values are followed by sisal fibre composites, both SRNC-TSL and SUNC-TSL. The value of these two specimen groups was 50.32 MPa and 46.55 MPa. Nested in the last place is the hemp fibre composite with average value of 31.69 MPa. Bamboo based composite has an average value higher than HNC-TSL and comparable to the average value of SUNC-TSL, which is 47.03 MPa.

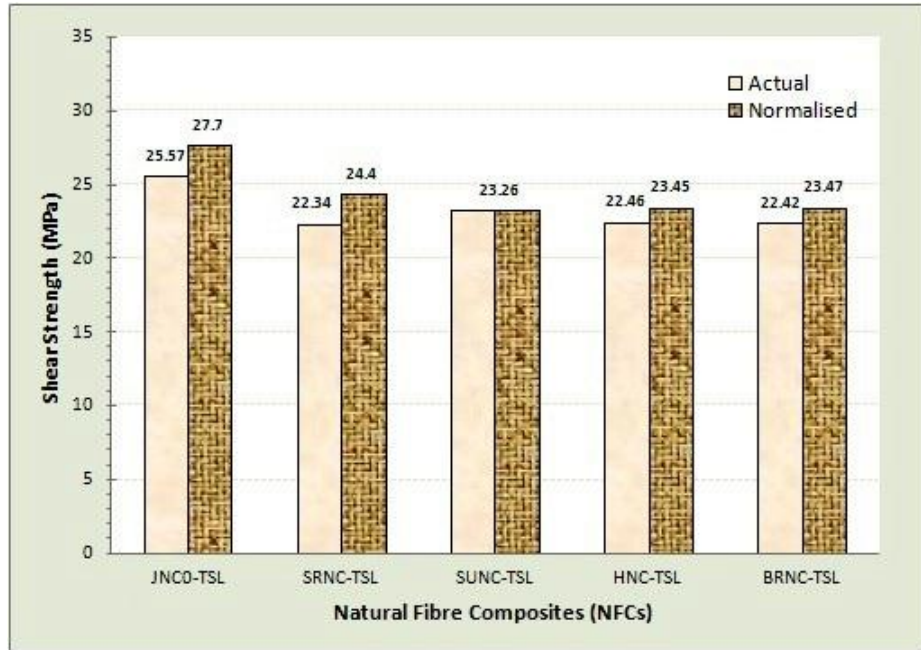


Figure 4.36. The average shear strength values of different NFCs

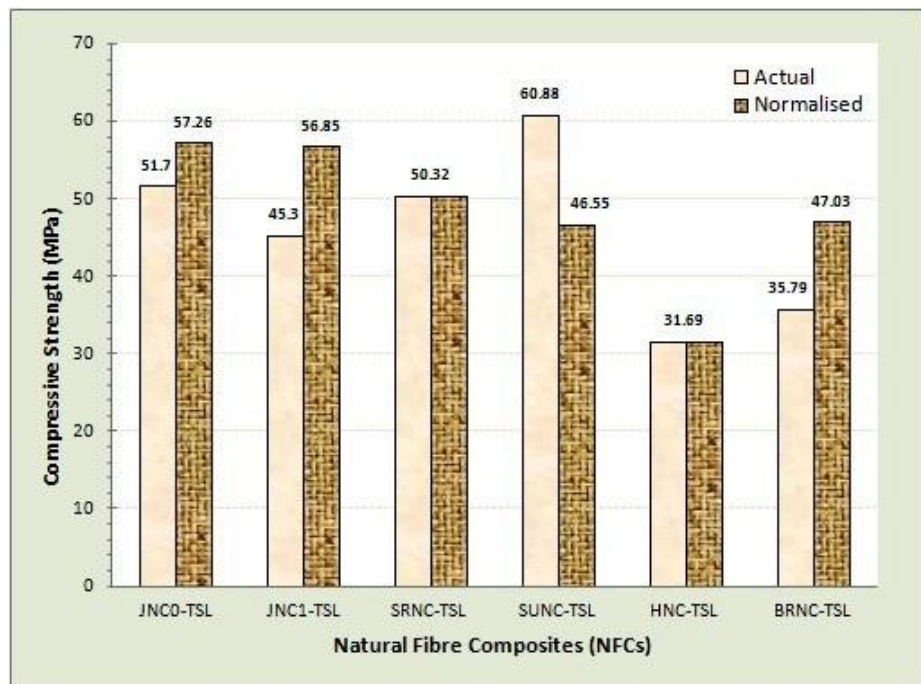


Figure 4.37. The average compression strength values of different NFCs

4.6. Chapter Conclusions

It is important to bear in mind that the main aim of this chapter is actually to develop natural fibre composites that have acceptable mechanical properties to be further incorporated in the hybrid sandwich panel as an intermediate layer. Based on the

previous mechanical properties analysis and general discussions, it seems that jute fibre composites and hemp fibre composites are the best two candidates for the desired application for the following reason.

Jute fibre composites possess the highest average value for almost all the observed mechanical properties in this study while at the same time they also have a lower Poisson ratio. On the other hand, hemp fibre composite has the most consistent properties except for its flexural properties. For all mechanical properties discussed in this work, hemp natural fibre has the same actual and normalized values meaning that its mechanical properties are uniform and consistent. It is also important to note that the availability of jute and hemp fibre, especially the typical fibre used in this research, is much easier than the others. They are available in the form of jute hessian cloth and hemp mat, and most importantly they can be obtained as desired size and volume.

Composite reinforced with unidirectional sisal fibres might also be an excellent choice for their observed mechanical properties. However, the availability concern may prevent the use of this typical form of fibre in a large scale. In addition, the mechanical properties of composite reinforced with unidirectional sisal fibre observed in this study were only based on a small panel that can be easily prepared using unidirectional fibre. When a large panel is required, the problem of obtaining long unidirectional arises. In conclusion, jute and hemp fibre composite are the best candidates for the intermediate layer of a hybrid sandwich panel that will be further investigated in the next experiment.

CHAPTER 5

FLEXURAL BEHAVIOUR OF SUSTAINABLE HYBRID COMPOSITE SANDWICH PANELS

5.1. General

During the last decade, composite sandwich structure with soft rigid expanded polystyrene (EPS) core has been extensively used in building structure. The utilization of such particular structure in building has been considerably increased since the modular panelised system has gained much attention in the housing market. Modular panelised system, which conventionally used in the form of structural insulated panels (SIPs), is rapidly growing trend in construction industry (APA, 1998; Vaidya et al, 2010). However, long time before they found their current growing application in modular system, sandwich panels have been used widely in many building constructions such as for cladding, roofing and other non-structural application.

The typical sandwich panel used in building application commonly consists of metal skins and soft core as reviewed in Chapter 2. Although oriented strand board (OSB) is commonly employed for the skin of sandwich structure in SIPs, the current observed shortcomings of this typical skin such as mould build-up and disintegration in the presence of flood water (Vaidya et al, 2010) has reduced their usage and it was replaced with metal based skins such aluminium or steel. Metal skins are actually preeminent choice for their many advantages, but the price is always a concern when considering them for the skins. Consequently, reducing the thickness of the skin as much as possible is the only way to keep a competitive and reasonable overall cost. On the other hand, using thinner skins may cause the sandwich structure to the early failure such as face wrinkling or inundation. The sustainable hybrid concept offered in this research has been considered as a practical solution for the sandwich panel system, as verified in Chapter 3.

As previously explained, in this research natural fibre composites (NFCs) have been considered as the intermediate layer of the new developed hybrid sandwich panel. The development of natural fibre composites (NFCs) described in Chapter 4 has suggested that the best two candidates for intermediate layer in hybrid sandwich panel are jute fibre composites and hemp fibre composites. This chapter elaborates the flexural behaviour of the newly developed hybrid sandwich panel with natural fibre composites as intermediate layer.

5.2. Flexural Test for Composite Sandwich Structure

Flexural test generally involves bending a material until the material experiences a fracture and determining both the load and deflection required to initiate the break limit which indicates the strength and stiffness of a material. The focal point in a flexural test is the flexural strength, also known as modulus of rupture or fracture strength, which represents the highest stress experienced within a material at its moment of rupture. The flexural behaviour of sandwich structure and its mode of failure have been studied extensively by a number of researchers. An early paper in this area was reported by Kuenzi (1951), which highlighted some of the basic theories of flexure, particularly as applied to sandwich constructions. Having considered various method of applying loads and theoretical analysis, it was found that the measurement of stiffness and strength of sandwich construction could be best obtained by testing the samples under two-point loading, preferably at two quarter-span points. In the centre of Excellence in Engineered Fibre Composites (CEEFC), University of Southern Queensland (USQ), Manalo et al (2009) studied the flexural behaviour of structural fibre composite sandwich beams. The composite sandwich beams were made up of glass fibre reinforced polymer skins and modified phenolic core. The panels were subjected to 4-point static bending test to determine their strength and failure mechanism in flatwise and edge positions. The result of this study showed the potential of this innovative composite sandwich panel for structural laminated beam.

In parallel to this research, Uddin and Kalyankar (2011) reported their study on the manufacturing and structural feasibility of natural fibre reinforced polymer structural insulated panels (NSIPs) for panellised construction. The sandwich panel consists of jute fibre composite skins and EPS core. The jute fibre composite skin was

made up of polypropylene matrix reinforced with treated jute fibre and fabricated using compression moulding method where the fibres and matrices were subjected to pre-define both temperature and pressure. Flexural and impact testings were employed for the structural characterization. The specimens were prepared in the size of 590 x 101 x 25.4 mm with the thickness of laminate skins of 6.25 mm and each category was replicated 4 times. The flexural test was carried out under 3-point bending as per ASTM C-393 standard. It was found that the average failure load of NSIPs was 511.52 N, which was lower than the failure load of sandwich panels with OSB SIPs (978.56 N). However this failure load almost doubled the average value of sandwich panel with glass polypropylene (G/PP SIPs) which was 266.88 N. In term of bending stress, however, NSIPs possessed higher value than the OSB SIPS which was 5.41 MPa and 2.86 MPa, respectively. This value is slightly less than the average flexural stress of G/PP SIPs which was 6.78 MPa. These values indicate that the bending stress of NSIPs was 90% higher than the value of traditional OSB SIPs, and only 20% less than those of G/PP SIPs. Clearly, there is a promising improvement when incorporating natural fibre composites in a sandwich panel structure.

5.3. Sample Preparation

Sandwich panel specimens in this research were prepared at the CEEFC laboratory facilities. Jute and hemp laminates for the intermediate layer were fabricated as per described in Chapter 4. Aluminium skins were purchased from local warehouse in Toowoomba which is aluminium 5005 H34 sheet produced by Austral Wright Metals. Aluminium 5005 is a lean aluminium magnesium alloy, contains nominally 0.8% magnesium, which can be hardened by cold work. It has medium strength, good weldability, and good corrosion resistance. It also has excellent thermal conductivity and low density. It is the most commonly used grade of aluminium in sheet and plate form. An expanded polystyrene (EPS) is used for the core of this hybrid sandwich panel. The commercial name of this EPS core is Isolite[®], purchased from Perth, Australia. Isolite[®] is the brand name of RMAX block moulded flame retardant modified grade of expanded polystyrene. It is a closed cell, resilient, lightweight rigid cellular plastic material which contains no hydro-fluorocarbon (HFC) or hydro-chlorofluorocarbon (HCFC) blowing agents that might cause depletion of ozone in the

upper atmosphere. When used as insulation and cladding EPS provides a reduction in energy use and cost for cooling in summer or heating in winter. The characteristic of Aluminium skin and EPS core used in this research are presented in the following table.

Table 5.1. Properties of aluminium skin and EPS core

Aluminium 5005 H34	
Physical and mechanical properties	
Density (ρ)	2700 kg/m ³
Modulus Elasticity (E)	68.2 GPa
Poisson ratio	0.33
Shear modulus	25.9 GPa
Shear strength	96.5 MPa
Ultimate tensile strength	159 MPa
Yield tensile strength	138 MPa
Isolite[®] EPS	
Physical and mechanical properties	
Grade	VH (Very High)
Density (ρ)	28 kg/m ³
Modulus Elasticity (E)	7250 kPa (7.25 MPa)
Poisson ratio	0.35
Flexural strength	337 kPa
Shear stress	240 kPa

Sandwich panel specimens were manually prepared using a pressing system. All constituent parts were cut into the same length and width and glued together using structural grade adhesive. The NFCs intermediate layers were sanded-up using sanding machine to obtain uniform thickness while aluminium sheet were roughed manually using sandpaper. The EPS core was sliced using hot knife foam cutter to obtain the required thickness. When all constituents ready, they were glued and placed in the pressure system. The system was prepared using wood and the pressure was given by the attached bolts at the end of each lumber. The fresh glued sandwich panel specimens were placed in between two 12 mm hardboards panels and clamped with pieces of wood at the top and bottom side. A torque wrench tool was used when tightens-up all the bolts to ensure uniform pressure were given to the samples. Furthermore, a structural grade adhesive with the commercial name of Kwik Grip Advanced was used for gluing all the sandwich layers together. This adhesive is designed for bonding a variety of materials, both absorbent and non-absorbent, e.g. laminated plastics, MDF, wood, cork, rubber, metals, leather, canvas, fibrous cement sheet and polystyrene foam. As it contains no

organic solvent, it is suitable for bonding materials sensitive to solvent attack, e.g. polystyrene foams. The process of sample preparation is shown in Figure 5.1.



Figure 5.1. Sandwich panel fabrication process

The samples were prepared in two scales, medium and large scale, as presented in Figure 5.2 and 5.3. The medium size specimens were cut and shaped into a span length of 450 mm and the size of 550 x 50 x 22 mm for length, width and thickness, respectively. The large scale specimens were prepared in the size of 1150 x 100 x 52 mm with the span length of 900 mm. Aluminium sheet with the thickness of 0.5 mm was used as the skins for medium size specimens and 1 mm for the large specimens. For the intermediate layer, jute and hemp composite laminates were used with the thickness of 3 mm and 5 mm for the medium and large size specimens, respectively. For the medium size specimens, the thickness of EPS core for control level was 21 mm and 15 mm for the other two levels to maintain a constant overall thickness of 22 mm for the specimen. The large scale specimens were used EPS with the thickness of 50 mm for the control level and 40 mm for both variables to keep the overall thickness of 52 mm. Each level was replicated 5 times; hence the total of samples tested was 15 samples for the medium scale and also 15 samples for the large scale specimens. The arrangements of the flexural test specimens are shown in the following tables.

Table 5.2. Experimental arrangements for flexural testing (*medium scale*)

Samples Code	Skin		Intermediate layer		Core		Number of sample
	Material	Thickness	Material	Thickness	Material	Thickness	
CTR	Aluminium	0.5 mm	None	-	EPS	21 mm	5
JFC	Aluminium	0.5 mm	Jute	3 mm	EPS	15 mm	5
HFC	Aluminium	0.5 mm	Hemp	3 mm	EPS	15 mm	5
Total							15

Table 5.3. Experimental arrangements for flexural testing (*large scale*)

Samples Code	Skin		Intermediate layer		Core		Number of sample
	Material	Thickness	Material	Thickness	Material	Thickness	
CTR	Aluminium	1.0 mm	None	-	EPS	50 mm	5
JFC	Aluminium	1.0 mm	Jute	5 mm	EPS	40 mm	5
MDF	Aluminium	1.0 mm	MDF	5 mm	EPS	40 mm	5
Total							15

The samples were tested using four-point bending load scheme. From technical point of view, the medium scale flexural testing is aimed at selecting the most appropriate NFCs for the intermediate layer. Meanwhile, the large scale sample arrangement was designed to compare the behaviour of hybrid sandwich panel with NFCs intermediate layer and another common available type of building material, medium density fibre (MDF) as the intermediate layer.

5.4. Experimental Program

The static flexural test of hybrid composite sandwich panel was conducted in accordance with the ASTM C 393-00 standard (ASTM, 2000) which is a standard test method for flexural properties of sandwich constructions. This test method covers determination of the properties of flat sandwich constructions subjected to flatwise flexure in such manner that the applied moments produce curvature of the sandwich facing planes. The load was applied at 1/3 and 2/3 of the span length. The schematic illustration and the actual setup of flexural test are given in Figure 5.2 to 5.3.

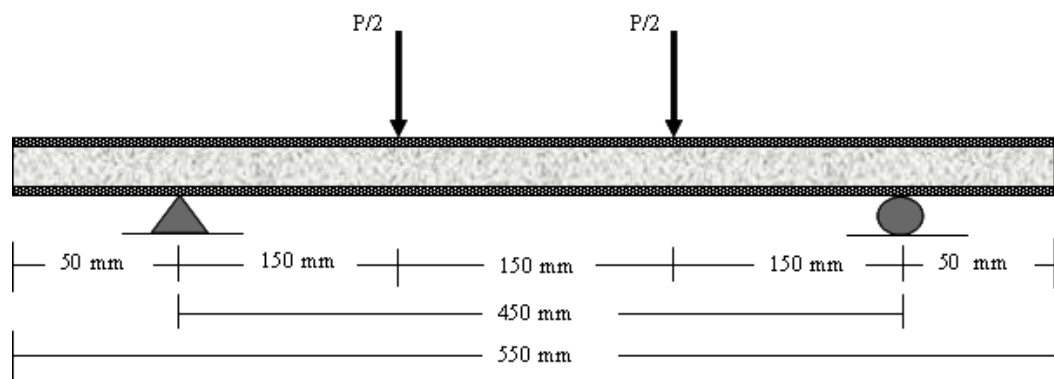


Figure 5.2. The schematic illustration of the flexural test for medium scale specimens

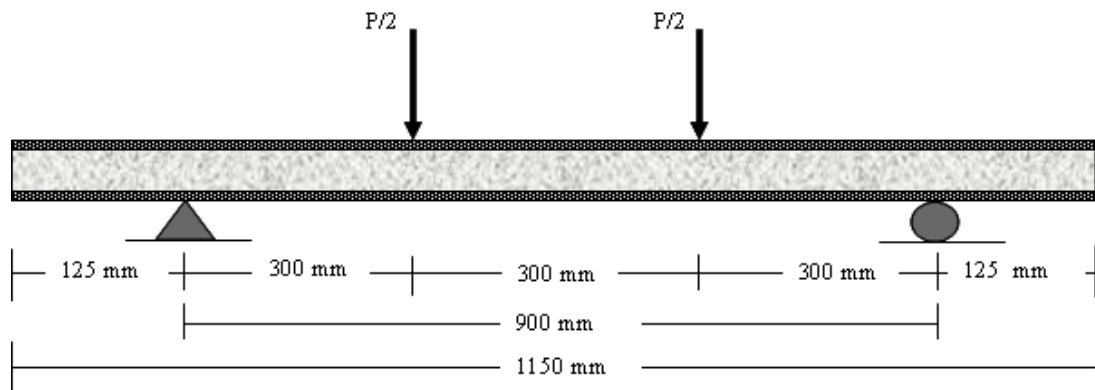


Figure 5.3. The schematic illustration of the flexural test for large scale specimens

The testing was performed using a 100 kN servo-hydraulic machine with a loading rate of 5 mm/min. The loading pins and the supports had a diameter of 20 mm. In order to prevent the existence of early failure, a steel plate was placed between specimen and loading point and also between specimen and support. Strain gauges were attached at the middle top and bottom surface of specimens to record the longitudinal

strain during the progress of testing. The applied load, displacement and strains were obtained using System 5000 data logger. Prior to each run of the testing, the loading pins were setup to nearly touch the top surface of the specimen and the machine then was re-set to the default position. The test was terminated after a visible collapse mechanism encountered or the specimen was undergoing large displacement but could not carry any increased load.



Figure 5.4. The actual set up of flexural test

5.5. Testing Results and Discussions

In this section, some important aspects of flexural testing of hybrid composite sandwich panel will be discussed thoroughly. For a comparison purpose, the behaviour of the hybrid sandwich panels will be compared to the behaviour of conventional sandwich panels that contains no intermediate layer.

5.5.1. Comparison of ultimate load

Figure 5.5 shows the average maximum load carrying capacity and deflection against the type of intermediate layer of the medium scale sandwich panels. It is important to mention here that the presented data in this figure was based upon the result of a normalization process in which one outlier data has been omitted from the calculation. The detail of normalization process is given in Chapter 8. The average ultimate load for sandwich panels with JFC and HFC intermediate layer was 396.55 N and 591.5 N, respectively. On the other hand, the average ultimate load of sandwich panel without intermediate layer was 305.75 N. The results indicated that the load carrying capacity of hybrid sandwich panel with JFC intermediate layer is 29.6% higher than that of conventional sandwich panel, and approximately 93.46 % higher with HFC intermediate layer. The difference in load carrying capacity between the two hybrid sandwich panels is 49.27% in which the load carrying capacity of hybrid sandwich panel with HFC intermediate layer is higher than those with JFC intermediate layer. It can also be observed from this figure that sandwich panel without intermediate layer (CTR) and hybrid sandwich panel with HFC intermediate layer have higher stiffness than the hybrid sandwich panel with JFC intermediate layer. This will be further in next section, on load-deflection behaviour.

The result of flexural testing on large specimens is given in Figure 5.6. The average ultimate load capacity of sandwich panel without intermediate layer was 496.5 N while the average ultimate load capacity for sandwich panels with JFC and MDF intermediate layer was 807.25 N and 1333.5 N, respectively. This means that the load carrying capacity of hybrid sandwich panel with JFC is 62.59 % higher than the load carrying capacity of conventional sandwich panel. More significant improvement in load carrying capacity encountered when MDF is used for the intermediate layer, which is approximately about 168.58% higher. Furthermore, hybrid sandwich panel with MDF intermediate layer sustained 65.19% higher load than the hybrid sandwich panel with JFC intermediate layer. Likewise to the medium size specimens, the stiffness of hybrid sandwich panels with JFC intermediate layer was less than the stiffness of sandwich panels without intermediate layer (CTR) and hybrid sandwich panel with MDF intermediate layer.

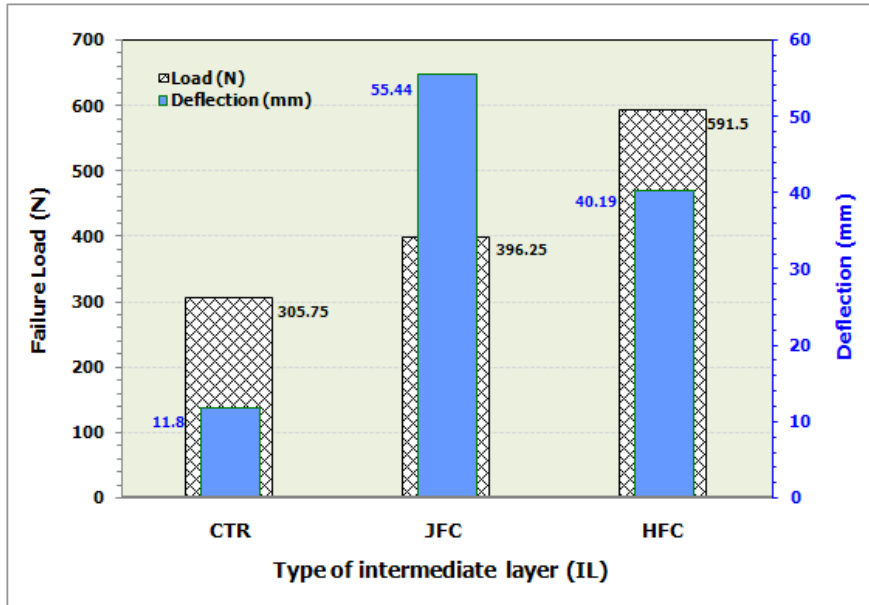


Figure 5.5. The average maximum load carrying capacity and deflection against the type of intermediate layer of medium scale sandwich panels

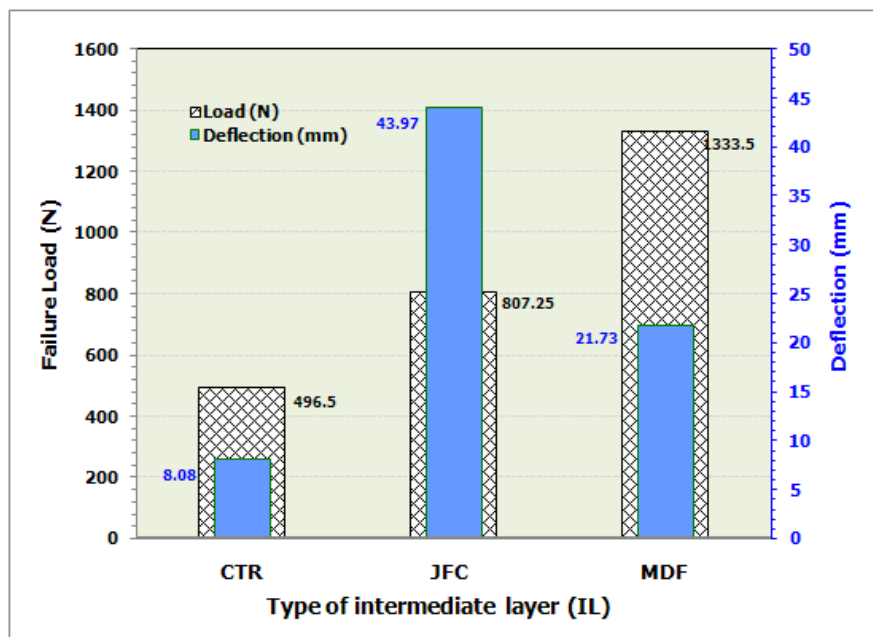


Figure 5.6. The average maximum load carrying capacity and deflection against the type of intermediate layer of large scale sandwich panels

5.5.2. Comparison of load-deflection behaviour

Medium scale specimens

The typical load-deflection graph of sandwich panels with medium size tested in this experiment are presented in Figure 5.7 to 5.9. Figure 5.7 shows the load deflection

graph of conventional sandwich panel (CTR). As indicated in Figure 5.7, all samples behave in similar fashion until reaching their ultimate load. The load-deflection graph shows that the specimens having a typical ductile material. The curves do not show a distinct yield point prior to reach failure, but then decrease sharply at the end of plastic region due to failure initiation in the specimens. It seems that the failure is occurred in a form of sudden cracking of the core due to shear propagation. The graphs consist of an initial linear part followed by a non-linear portion. The linear portion last up to the load of 100 N at the deflection of 2 mm, then the graphs deviate gradually until the ultimate load is reached. Three specimens reached their ultimate load at the deflection of around 12-14 mm, while one specimen failed at the deflection of approximately 10 mm. The configuration of load-deflection curves indicates that the behaviour of such sandwich panel was dominantly governed by the skins, aluminium alloy.

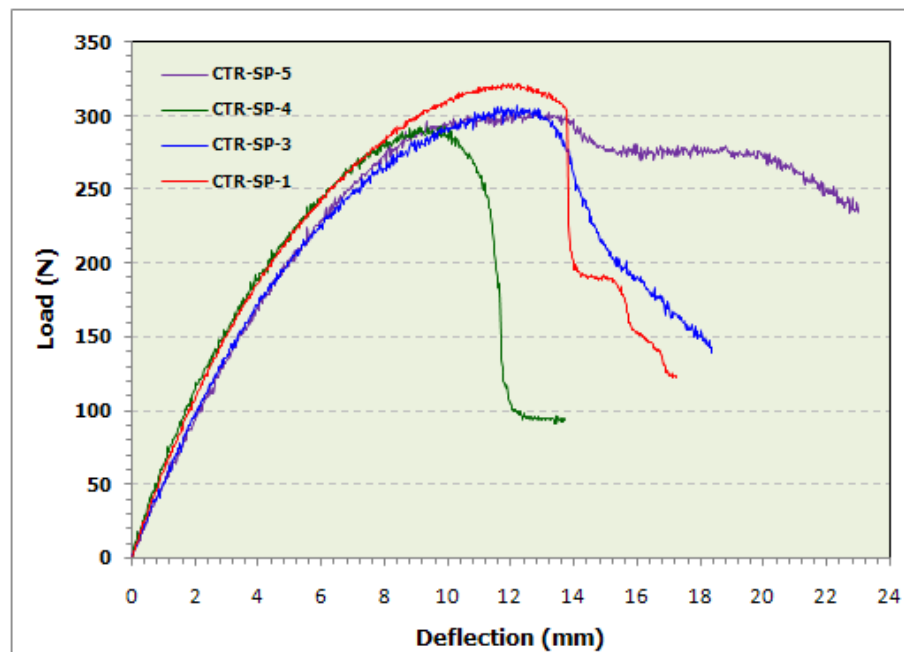


Figure 5.7. Load-deflection graphs of medium scale CTR specimens

The load deflection graph of hybrid sandwich panel with JFC intermediate layer is shown in Figure 5.8. Similar to the configuration of load-deflection curves for CTR specimens, the curves for JFC specimens are also very uniform. The load-deflection behaviour shows a typical ductile behaviour with no sharp drop in the load as occurred at CTR specimens. The graphs have a linear portion up to the load of approximately 150 N and then deviated gradually until reached the ultimate loads. It can also be observed that

the ultimate load of all specimens only differed slightly, but there has a substantial variation of deflection at the point of peak load. For example, although specimens 1 and 5 have identical ultimate load of 414 N, the deflection at the ultimate load was 56 mm and 64 mm, respectively. Similarly, the deflection of specimen 3 and 4 was 45.22 mm and 56.53 mm, respectively when they reached almost a comparable ultimate load of 379 N and 378 N, respectively. After reaching the ultimate value, the load decreases gradually as the deflection increases until the testing was automatically terminated by the testing machine. The failure mode of JFC specimens was a delamination between core and intermediate layer. As it is common encountered in a typical ductile material, the load-deflection curves of JFC specimens do not shows a distinct yield point prior to the ultimate load.

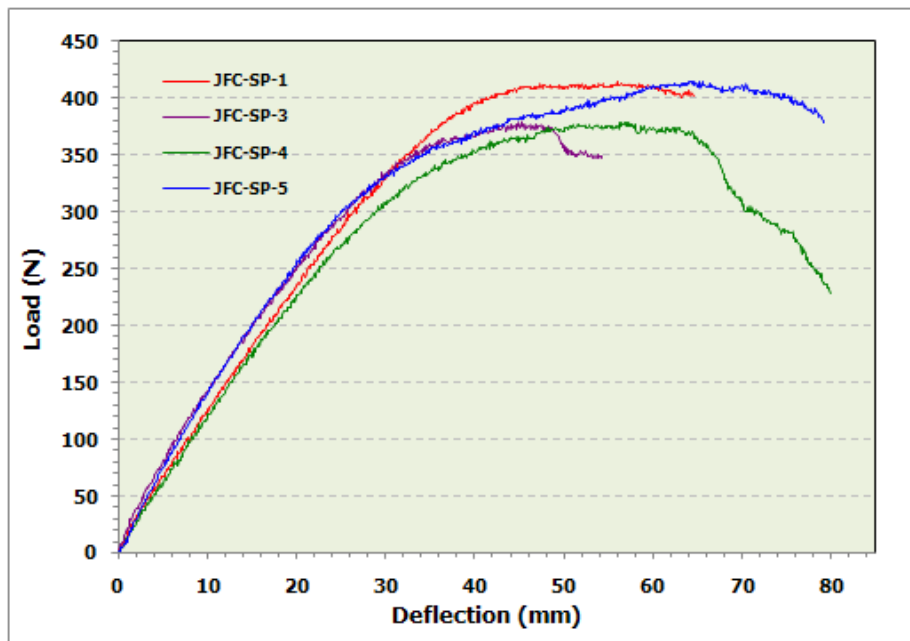


Figure 5.8. Load-deflection graphs of medium scale JFC specimens

The load-deflection graph of hybrid sandwich panel with HFC intermediate layer is shown in Figure 5.9. Unlike the load-deflection curves of CTR and JFC, the curves of the HFC samples showed a substantial variation. The difference started from the initial part and the curve until deviated gradually until reaching the ultimate loads. Although the curves substantially differ, the overall pattern remains the same. It commences with a linear portion then gradually diverges until the ultimate load is reached. There is an abrupt drop in load carrying capacity at the point of ultimate load. The sudden drop was

around 50 N to 100 N. For example, the load dropped from 635 N to 535 N at an identical deflection of 35.09 mm for specimen 4. After this point, the specimen still carried significant load while deflection continuously increased. Generally, the sandwich panel with HFC intermediate layer demonstrated a ductile behaviour up to the ultimate load and then collapsed in a brittle manner. Likewise to the previous two groups, it is also difficult to distinguish a yield point. The graphs deviated steadily until reaching the ultimate load. It was assumed that there had a sudden crack within the core at the initial stage of failure mechanism followed by delamination between the core and intermediate layer.

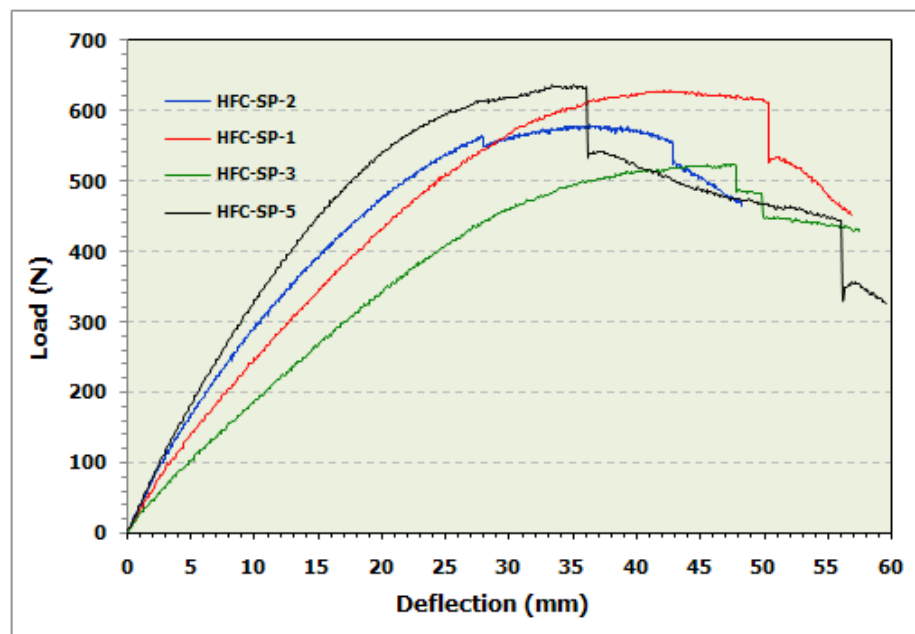


Figure 5.9. Load-deflection graphs of medium scale HFC specimens

For a comparison, one specimen from each category had been selected for a representation of the load-deflection curve. A specimen labelled as CTR-SP-3 was chosen for the depiction of specimens in CTR category while JFC-SP-1 and HFC-SP-1 were selected for JFC and HFC category, respectively. It is very apparent in Figure 5.10 that the introduction of intermediate layer in sandwich panels, which are represented by JFC and HFC curves, has substantially enhanced the load carrying capacity of the sandwich panels. What is also seen in this figure that the introduction of intermediate layer has created more ductile sandwich panels compared to the conventional form of sandwich panels. The two hybrid sandwich panels with NFCs intermediate layer have shown excellent strength and stiffness though there has some concern about the stiffness Sustainable Hybrid Composite Sandwich Panel with Natural Fibre Composites as Intermediate Layer

of the hybrid sandwich panels with JFC intermediate layer. Theoretically the JFC specimens should be stiffer than CTR specimens. However, the existence of debonding mechanism within JFC specimens has reduced the stiffness of the JFC hybrid panels. As indicated earlier, the theoretical concept of sandwich panel is developed based on the assumption that the cross-sections are plane and perpendicular to the longitudinal axis of the unloaded beam remain so when bending takes place. During the initial stage of the test, the CTR and HFC specimens remained plane and failed due to the initiation of shear cracking so that they followed the assumption made for the theoretical framework. Meanwhile the JFC specimens did not follow it as the collapsed mechanism initiated was a debonding mechanism from the beginning so that the cross section did not remain plane during the bending took place. In short, it can be inferred that debonding mechanism is also an important aspect when further develops this new hybrid panel in the future. If the early debonding mechanism within JFC panels can be prevented, it must be stiffer than the panel without intermediate layer. In addition, a sudden drop at ultimate for hybrid sandwich panels with HFC intermediate layer is not desirable for earthquake resistant structure. Based on this outcome, the hybrid sandwich panel with a JFC intermediate layer was selected for the further experiments due to its excellent properties.

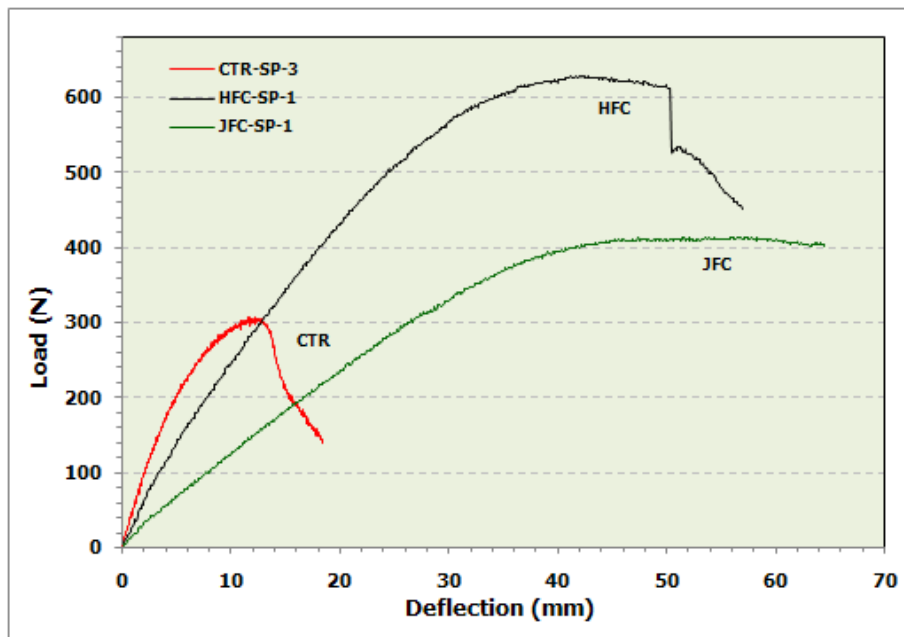


Figure 5.10. Load-deflection graphs of representative specimens for CTR, JFC and HFC in medium scale specimens

Large scale specimens

The load-deflection graphs of sandwich panels with larger scale are presented in Figure 5.11, Figure 5.12 and Figure 5.13. It is worth noting that large scale specimen represents the minimum size of structural insulated panels (SIPs) that are currently available in the market. Figure 5.11 shows the load deflection graph of conventional sandwich panels (CTR). Similar to the curves of CTR specimens in medium scale samples, the graphs consisted of a linear part up to a load of approximately 300 N, followed by a non-linear portion until the ultimate load was reached. The load decreased gradually beyond the ultimate load except for specimen 4. Similar to the case in medium scale experiment, a stiffening behaviour was observed after some drop in load indicating that certain part of sandwich panels sustained more load before the specimen totally collapsed. This is most likely due to the bottom aluminium skin. It is also clearly seen that the ultimate loads for all specimens occurred at a small deflection indicating that the sandwich panels were not very ductile. Beyond the point of linear portion, the load-deflection graphs deviate until they reached their ultimate load. There is no distinct indication of yield point as commonly observed for most ductile material. Overall, the load-deflection behaviour of all CTR specimens in larger scale specimens was similar to those of medium scale specimens.

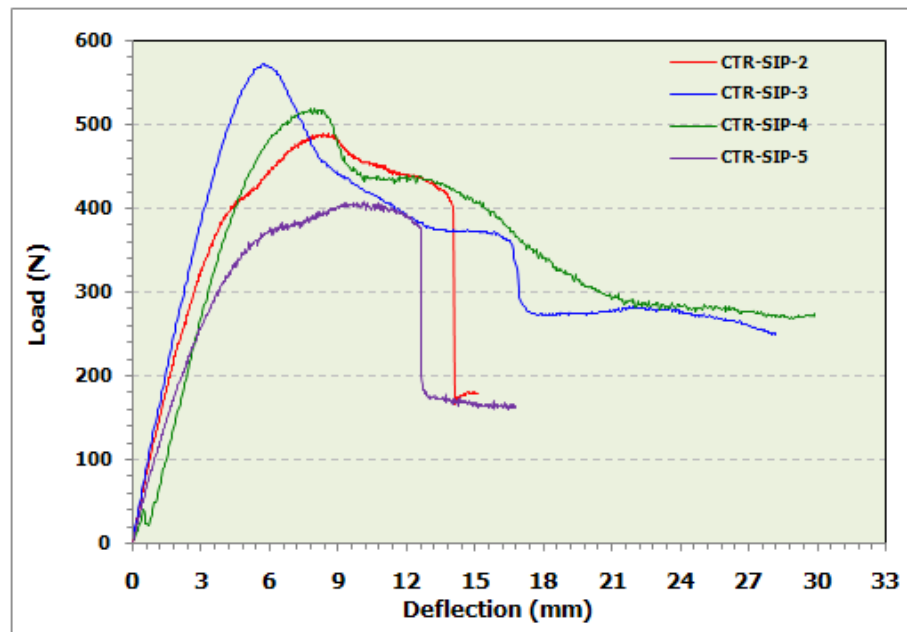


Figure 5.11. Load-deflection graphs of large scale CTR specimens

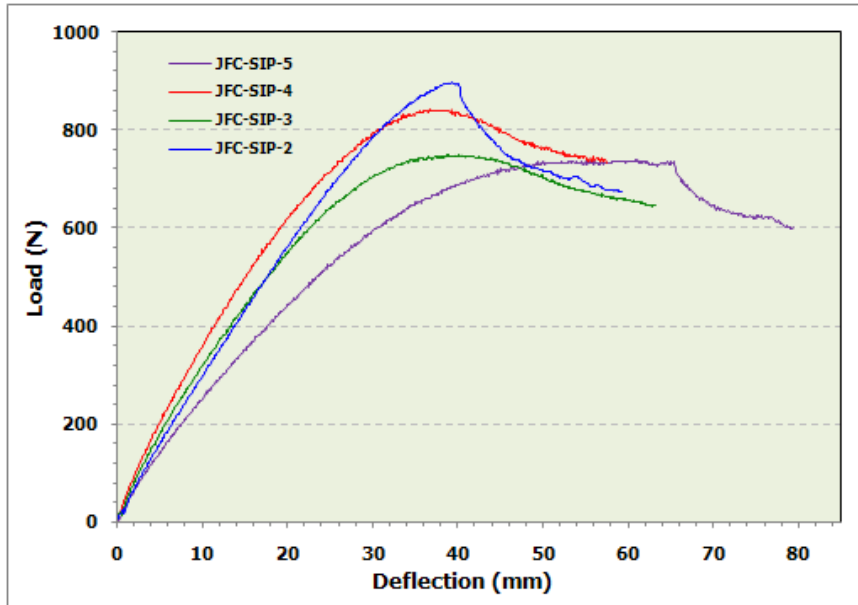


Figure 5.12. Load-deflection graphs of large scale JFC specimens

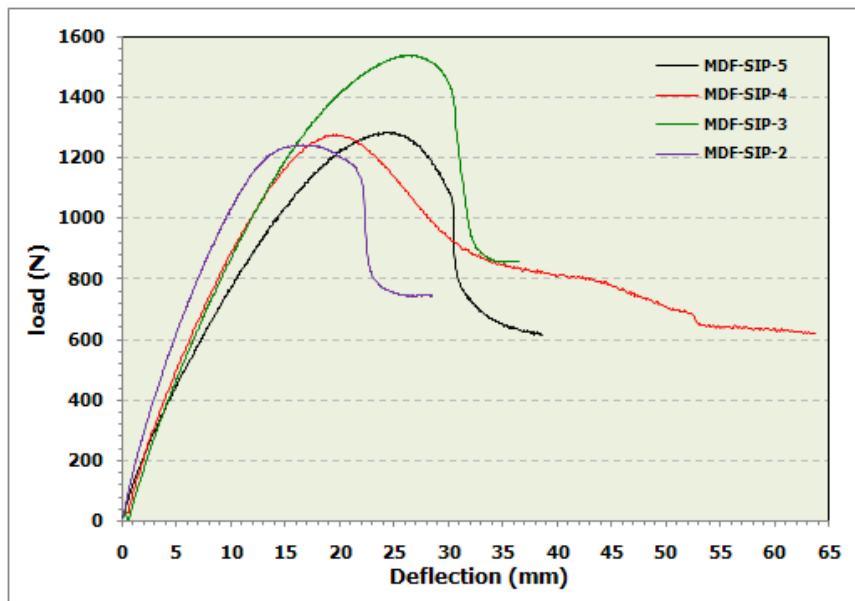


Figure 5.13. Load-deflection graphs of large scale MDF specimens

Figure 5.12 shows the load-deflection graph of hybrid sandwich panel with JFC as an intermediate layer. The graphs initiated with initial straight line up to the load of approximately 200 N, and then deviated gradually forming a plastic region up to the ultimate load. Further, the graphs decreased steadily beyond the ultimate load. As the graph smoothly moved away from the initial linear portion, there had no exact yielding point observed. Three out of four specimens reached their ultimate load at an almost

similar deflection at approximately 40 mm, and the average ultimate load was 807.25 N. The collapse mechanism appears not to be due to shear cracking of the core or cracks initiation in the intermediate layer. It was most likely due to bonding failure between the adjacent constituent materials in the sandwich panels.

The load-deflection curves of the hybrid sandwich panels with MDF intermediate layer are presented in Figure 5.13. As seen in the figure, the sandwich panels behaved in a ductile manner. The curves deviate gradually from the initial linear portion, forming a good plastic region without a clear yielding point. The load decreases sharply beyond the end of plastic region but not in an abrupt manner. It was observed that the failure mechanism was initiated by the loss of bonding strength between sandwich panels' constituent materials. The load-deflection graphs also indicated that hybrid sandwich panels with MDF intermediate layer possessed higher stiffness as the ultimate load was reached at a relatively small deflection, approximately 20-25 mm.

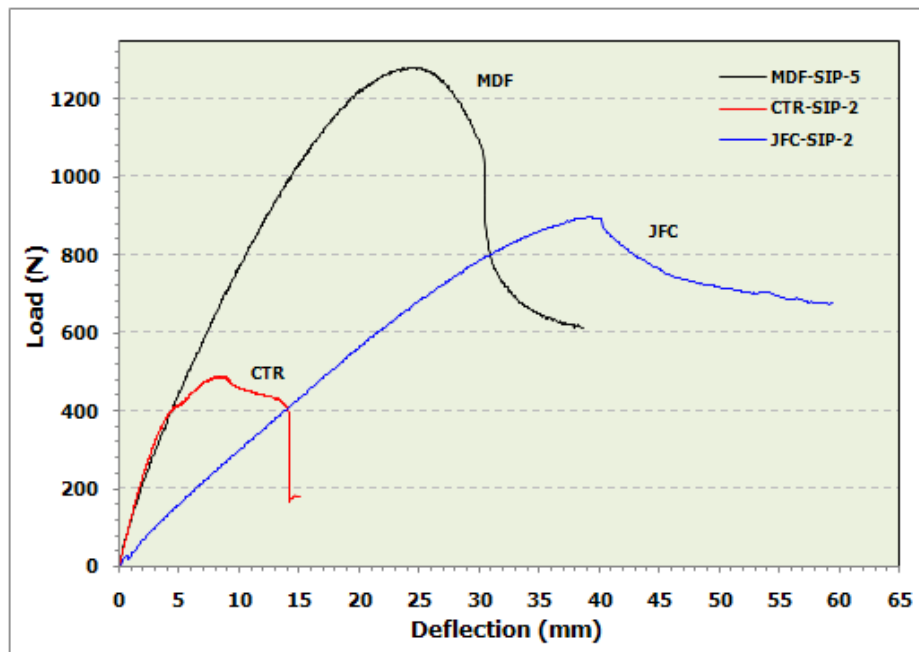


Figure 5.14. Load-deflection graphs of large scale MDF specimens

The comparison of the load-deflection behaviour of sandwich panels in the larger scale specimens is presented in Figure 5.14. It is very clear in the figure that the hybrid sandwich panels with MDF intermediate layer were much stiffer than those with JFC intermediate layer. Sandwich panels with no intermediate layer (CTR) also much stiffer than hybrid sandwich panels with JFC intermediate layer but less than those with MDF

intermediate layer. The CTR specimens reached their ultimate load of approximately 490 N at a deflection of 10 mm while their counterpart of JFC reached the same load at the deflection of approximately 20 mm. Hybrid sandwich panel with MDF intermediate layer reached a similar load at slightly less deflection which was approximately 7.5 mm. In general, although hybrid sandwich panels with JFC intermediate layer were less stiff than those with MDF intermediate layer, the very ductile behaviour of this type of panel has an additional advantage of being much safer when utilised in building.

All the sandwich panels, with or without intermediate layer, behave in a ductile manner. However, there is an obvious advantage when an intermediate layer is incorporated in sandwich panel which is related to the toughness of the material and load carrying capacity. Toughness represents the ability of a material to support loads even after yielding or forming cracks (Somayaji, 1995). The toughness of a material can be measured as the area under the load-deflection curve. The hybrid sandwich panels developed much large area under the load-deflection curve than those of conventional sandwich panels indicating a greater toughness.

It is also worth noting that although hybrid sandwich panels with JFC intermediate layer are less stiff than those with MDF intermediate layer, they are actually tougher as indicated by the larger area under the load-deflection curve. Somayaji (1995) described that an increase in toughness relates to an increase in the amount of energy required to produce a specific damage condition. He also stated that the strength and stiffness of materials might be the most important properties when considering a suitability of a material for use in building. Strength defines the collapse load while stiffness ensures that structure does not deflect too much under load. These two properties are related to the elastic range of load-deflection or stress-strain graph. However, it is also of comparable important to consider the plastic region develops beyond the proportional limit which is related to the ductility of a material. As it was observed, the hybrid sandwich panels withstand large deflections before rupture, which is extremely important when considering them for use in building in which a considerable warning is desired before total collapse. It was observed that more scattered results were obtained for the larger scale test. The reason is most likely due to the size effect, the larger the size the more variability can occur during the preparation and fabrication process of the specimens.

5.5.3. Theoretical and experimental deflections

According to ASTM C 393-00 (ASTM, 2000), the standard test method for flexural properties of sandwich constructions, the total deflection is a sum of deflection due to bending and shear as shown in Equation 5.1.

$$\Delta = \frac{11 PL^3}{768 D} + \frac{PL}{8U} \dots\dots\dots 5.1$$

Where:

- D : The stiffness, N-mm²
- U : Panel shear rigidity, N
- P : Load, N
- L : Span length, mm

However, the above equation is derived for a flexural test under two-point load at one quarter span which is different to the testing program designed for this experiment. The testing program for this experiment is a two-point load with third loading scheme in which the two point loads applied at an equal distance, L/3, of the span length. A general equation for deflection of a beam under four-point loading is as follows (Roylance, 2000):

$$\delta(x) = \frac{P(L-a)}{6LEI} \left[\frac{L}{L-a} (x-a)^3 - x^3 + (L^2 - (L-a)^2)x \right] + \dots 5.2$$

$$\frac{Pa}{6LEI} \left[\frac{L}{a} (x - (L-a))^3 - x^3 + (L^2 - a^2)x \right]$$

For the third load scheme used in this research, a = L/3 and x = L/2. Including these two values in the above equation results in:

$$\delta = \frac{23 PL^3}{1296 EI} \dots\dots\dots 5.3$$

For sandwich panel, this equation can be modified as

$$\delta = \frac{23 PL^3}{1296 (EI)_{eq}} \dots\dots\dots 5.4$$

As mentioned earlier, the contribution of shear deflection should be considered in sandwich panel especially when a low density core is employed. The deformation under four point bending load (third point load) is shown in Figure 5.15.

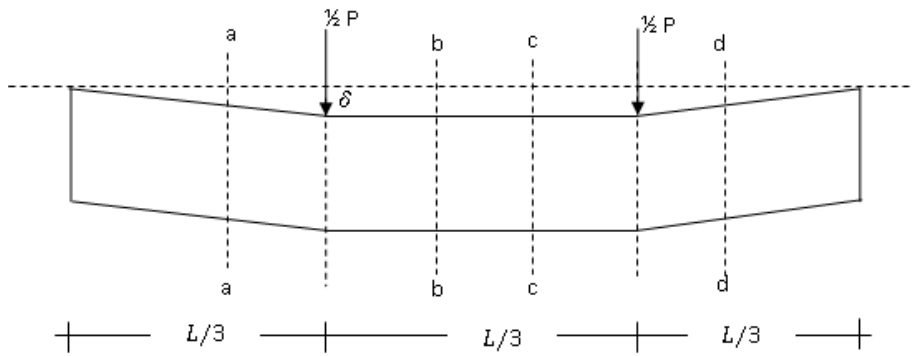


Figure 5.15. Deformation due to core shear under third point loading scheme

The deflection of the loading point due to this deformation mode is given by the following equations:

$$\frac{\delta}{L/3} = \gamma = \frac{Q}{G_c b d} \quad \dots\dots\dots 5.5$$

$$\delta = \frac{Q \cdot L/3}{G_c b d} \quad \dots\dots\dots 5.6$$

Since in third point bending load $Q = P/2$, then

$$\delta = \frac{P/2 \cdot L/3}{G_c b d} \quad \dots\dots\dots 5.7$$

$$\delta = \frac{PL}{6 (G_c b d)} \quad \dots\dots\dots 5.8$$

$$\delta = \frac{PL}{6 (AG)_{eq}} \quad \dots\dots\dots 5.9$$

Hence, the total deflection under 4-point bending load is a linear superposition of the deflection due to bending and shear, which gives:

$$\delta = \frac{23 PL^3}{1296 (EI)_{eq}} + \frac{PL}{6 (AG)_{eq}} \quad \dots\dots\dots 5.10$$

The above equation confirms the equation derived by Manalo et al (2009) for sandwich panel beam in flatwise position:

$$\Delta = \frac{23 PL^3}{1296 D} + \frac{PL}{6 AG} \quad \dots\dots\dots 5.11$$

The shear modulus of core material (G_c) can be obtained by using the following relationship:

$$G_c = \frac{E}{2(1 + \nu)} \dots\dots\dots 5.12$$

Somayaji (1995) stated that determining shear modulus experimentally is difficult, and using the above relationship provides a convenient procedure to establish such value. Initially, the theoretical bending stiffness of each sandwich panel was calculated based upon Equation 3.8 for conventional sandwich panels and Equation 3.51 for hybrid sandwich panels. For analysis proposes those two equations are rewritten as follows:

$$(EI)_{eq} = E_f \frac{bt^3}{6} + E_f \frac{btd^2}{2} + E_c \frac{bc^3}{12} \dots\dots\dots 5.13$$

$$(EI)_{eq} = E_f \left[\frac{bt_f^3}{6} + \frac{bt_f d_1^2}{2} \right] + E_i \left[\frac{bt_i^3}{6} + \frac{bt_i d_2^2}{2} \right] + E_c \frac{bt_c^3}{12} \dots\dots\dots 5.14$$

The theoretical values of deflection were estimated as per Equation 5.10 with the corresponding equivalent bending stiffness $(EI)_{eq}$ for conventional and hybrid sandwich panels. The results are tabulated in Table 5.4 and Table 5.5. An example calculation of the theoretical deflection is included in Appendix-A.

Table 5.4 presents the theoretical and experimental deflection values of medium scale sandwich panels in the linear elastic region. Two loads have been chosen in the elastic region of the load-deflection curve, which are 50 N and 100 N for the comparison purposes. In general, the experimental values were in reasonable agreement with the theoretical values. The differences range from 3.9% to 35.4%. Most of the sandwich panels showed experimental values lower than the theoretical values, which according to Teles et al (2012) can be considered as highly desirable in the design.

Table 5.4. Theoretical and experimental deflection values of medium scale sandwich panels for 50 and 100 N load.

Samples	Geometric		$(EI)_{eq}$	P	δ_b	δ_s	δ_{theo}	δ_{exp}	$\frac{\delta_{theo}}{\delta_{exp}}$	%	
	b	t_c									
CTR	1	51.57	22.8	478993062	50	0.17	1.18	1.35	1	1.35	35.4
		51.57	22.8	478993062	100	0.34	2.37	2.71	2	1.35	35.4
	3	51.3	22.2	451118121	50	0.18	1.23	1.41	1.2	1.17	17.1
		51.3	22.2	451118121	100	0.36	2.45	2.81	2.3	1.22	22.2
JFC	3	50.3	15.03	509155453	50	0.16	1.85	2.01	2.1	0.96	-4.5
		50.3	15.03	509155453	100	0.32	3.69	4.01	6	0.67	-33.1
	5	50	15.05	507097313	50	0.16	1.86	2.02	2.1	0.96	-4.0
		50	15.05	507097313	100	0.32	3.71	4.03	6	0.67	-32.8
HFC	1	50.5	16.55	546612658	50	0.15	1.67	1.82	1.9	0.96	-4.3
		50.5	16.55	546612658	100	0.30	3.34	3.64	3.5	1.04	3.9
	5	52.5	17.2	601680685	50	0.13	1.55	1.68	1.4	1.20	20.1
		52.5	17.22	601680685	100	0.27	3.09	3.36	3	1.12	12.1

Table 5.5. Theoretical and experimental deflection values of large scale sandwich panels for 50 and 100 N load.

Samples	Geometric		$(EI)_{eq}$	P	δ_b	δ_s	δ_{theo}	δ_{exp}	$\frac{\delta_{theo}}{\delta_{exp}}$	%	
	b	t_c									
CTR	2	101.2	51.9	9666786849	50	0.07	0.53	0.60	0.55	1.09	8.9
		101.2	51.9	9666786849	100	0.13	1.06	1.20	0.95	1.26	26.0
	4	99.5	51.17	9243807464	50	0.07	0.55	0.62	0.55	1.12	12.5
		99.5	51.17	9243807464	100	0.14	1.10	1.24	1.1	1.12	12.5
JFC	3	100.7	40.23	11370452155	50	0.06	0.69	0.75	0.8	0.93	-6.7
		100.7	40.23	11370452155	100	0.11	1.38	1.49	2	0.75	-25.3
	4	100.3	40.17	11298051840	50	0.06	0.69	0.75	0.8	0.94	-6.2
		100.3	40.17	11298051840	100	0.11	1.39	1.50	2	0.75	-24.9
MDF	3	99.63	39.33	9908906154	50	0.07	0.71	0.78	0.7	1.11	11.2
		99.63	39.33	9908906154	100	0.13	1.43	1.56	1.5	1.04	3.7
	5	100.7	39.2	9962759772	50	0.06	0.71	0.77	0.7	1.10	10.4
		100.7	39.2	9962759772	100	0.13	1.42	1.55	1.5	1.03	3.0

It can be seen that for the control group (CTR) the difference between theoretical and experimental values ranges from 17.1% to 35.4%. For sandwich panel with JFC intermediate layer, the theoretical framework tended to underestimate the experimental deflection values. The theoretical estimation were approximately 4%-33.1% lower than the experimental values. Meanwhile, the theoretical deflection values for sandwich panel with HFC intermediate layer were higher than the experimental values, except for specimen 1 under 50 N load. The difference for this specimen group ranges from 3.9% to 20.1%. Table 5.4 also shows the geometrics of specimens and equivalent bending stiffness of both conventional and hybrid sandwich panels. It is clearly shown that the hybrid sandwich panels provide reasonably higher equivalent bending stiffness. The result is certainly not surprising since the hybrid sandwich panels embedded an intermediate layer which was considered when estimating the equivalent bending stiffness. Theoretically, when bending stiffness increased the deflection should be decreased. However, it is not always the case in sandwich panels as shown in Table 5.4. Under the same load, the deflection of hybrid sandwich panel even higher than those of conventional sandwich panels.

For example, the sandwich panels with JFC and HFC intermediate layer have the theoretical deflection values of 2.02 mm and 1.82 mm, respectively. While conventional sandwich panel without intermediate layer (CTR) has a theoretical deflection value of 1.35 mm. The reason for this can be clearly obtained by checking the contribution of bending and shear deformation of the core to the overall deflection. As seen in Table 5.4, bending only contributes around 8% to 13% to the total deflection. For instance, the

deflection due to bending for specimen 3 under 100 N load was 0.36 mm, which was only 12.81% of the overall deflection of 2.81 mm. On the other hand, the shear deformation of the core, which has very low shear modulus ($G_c=2.69$ MPa), was the main contributor for the overall theoretical deflection, approximately 87% to 92%. The result confirms the finding reported by Sharaf et al (2010) which stated that the shear deformation is the significant contributor for the overall deflection of sandwich panels with soft core. They reported that the contribution of shear deformation to the overall deflection is about 75% for sandwich panel with soft core and approximately 50% for hard core.

It seems that for deflection due to shear deformation of the core, as per Equation 5.8, the contribution of specimens geometric, the width and the thickness of the core, is crucial. As seen in Table 5.4, the thicknesses of CTR specimens' core (t_c) were substantially higher than those of hybrid sandwich panel with JFC and HFC intermediate layer that resulting in smaller deflection. The thicknesses of the core for CTR group in medium scale samples showed in the table were around 22.2-22.8 mm. While the core thicknesses of hybrid sandwich panels were measured around 15.3 to 17.2 mm.

Table 5.5 presents the theoretical and experimental deflection values of the larger scale sandwich panels. Similar to the values for medium scale specimens, there is reasonably agreement between the theoretical and experimental findings that range from 3.7% to 26% within the elastic region of load-deflection curves. It was also observed that the experimental values were mostly lower than the theoretical values. The theoretical deflection values for sandwich panels with JFC intermediate layer are, however, lower than the experimental values. For the control group, the difference was approximately 8.9% to 26%. Within JFC group, the values differ by 6.2% to 25.3% while for MDF group the difference ranges from 3% to 11.2%. The contribution of shear deformation of the core to the total deflection of large scale specimens is also significant which ranges from 88% to 92% meaning that the contribution of bending was only about 8% to 12%. Overall, the deflection of hybrid sandwich panel was slightly larger than those of conventional sandwich panel although they have higher equivalent bending stiffness. The introduction of intermediate layer does not contribute much to reduce the deflection of sandwich panel as the main contributor for the total deflection was the shear

deformation of the core that mostly determined by the geometric of the samples and the thickness of the core.

5.5.4. Comparison of load-strain behaviour

Medium scale specimen

The typical load-strain relationship of medium scale sandwich panels tested in this research is shown in Figure 5.16. The strain gauges were attached in the middle of the top and bottom surface of the sandwich panel beams to measure the longitudinal strain. It is clearly demonstrated in the figure that the load-strain measurement of hybrid sandwich panels with JFC and HFC intermediate layer are higher than the conventional sandwich panels (CTR). The representative curve for each specimen category suggests that the longitudinal strains at the top (compression) and the bottom (tension) surfaces increased linearly with the load only at the very early region at the load of about 50 N to 100 N. Beyond this particular point, the curves started to deviate steadily until they reached their ultimate loads. The curves for hybrid sandwich panels showed better ductile behaviour in which no distinct yield point observed prior to the point of ultimate load.

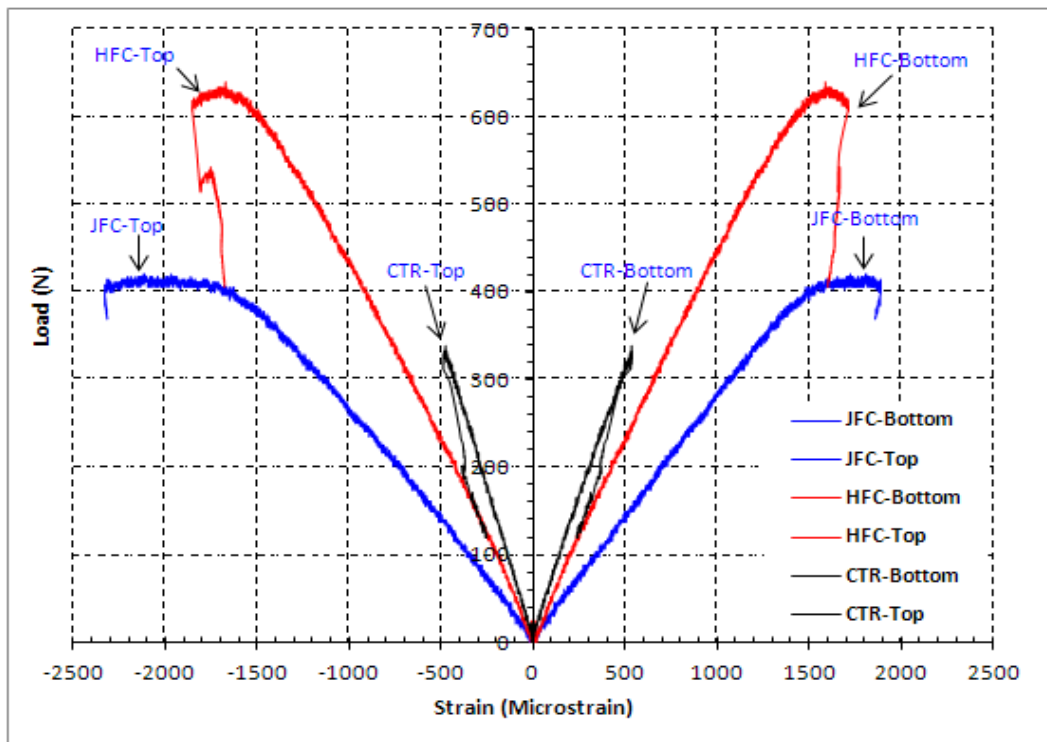


Figure 5.16. Load-strain relationship for medium scale sandwich panels

The representative curve for CTR category showed a linear elastic behaviour up to the load of approximately 80 N and started to initiate plastic region beyond this point. The strain at this point was comparable for both compression and tension sides, which was approximately 100 microstrains. The specimen failed at a load of around 330 N corresponding to a compression strain of 480 microstrains and 540 microstrains for the tension side. This means that the skin behaved slightly stiffer in compression than in tension. The representative curve for JFC group failed at a load of around 420 N that corresponds to 1900 microstrains at the tension side and 2350 microstrains at the compression side which means that the skin behaved reasonably stiffer in tension side than in compression. The curve for JFC specimen was linear at the initial portion up to the load of about 100 N and started to move away forming a non-linearity beyond this point. The strain at this point was 300 microstrains for tension and 350 microstrains for the compression side.

Unlike the two previous sample categories, the representative curve for HFC group failed at almost comparable strain for both compression and tension, which was 1750 microstrains for bottom surface (tension), and 1850 microstrains for top surface (compression) side. These strains correspond to the load of approximately 640 N. The curve also showed an initial linear portion up to the load of 100 N at which the curve started to deviate forming a plastic region.

The higher values of ultimate load of hybrid sandwich panels is attributed to the presence of intermediate layer which prevented the compression buckling of the aluminium skins, thereby delaying its failure. As discussed earlier, the CTR specimen failed at only 480 microstrains in compression side. This value is only about 20% of the compression strain of JFC specimen (2350 microstrains) and 26% of strain at HFC specimen (1850 microstrains). This also indicates that, for conventional sandwich panel (CTR), the aluminium skin was not optimally utilised due to prematurely failed of sandwich panel under shear or skin buckling.

There is also evidence that the strain at the skin of CTR specimen reached a significant amount after reaching the peak load. For example, the medium scale CTR specimen failed at 335 N with the corresponding strain values of 480 microstrains at the top surface and 540 microstrains at the bottom surface. After reaching its peak load, the strain decreased to 260 microstrains for compression side and 240 microstrains for

tension side. Considering the typical failure for the conventional sandwich panel which was a shear failure of the core, the behaviour can be explained that once the failure occurred within the specimen, the aluminium skins tried to return to its original length as the deformation was still in the range of its elastic region. The strains, however, never returned to zero meaning that there has already a slightly permanent set inside the aluminium skin. This occurrence also existed to HFC specimen although it was not as much as what had happened inside the CTR skin specimen, but never existed for JFC specimen. The reason is that the aluminium skin for JFC specimen had already stretched beyond its linear elastic capacity and a permanent set already established.

Large scale specimen

Figure 5.17 shows the comparison of load-strain curve for the three different sample categories of tested sandwich panels in large scale specimen. As expected, the large scale specimen behaved much stiffer than the medium scale specimens. The maximum ultimate load almost doubled the values for medium scale while both compression and tension strains only half of the medium scale specimens.

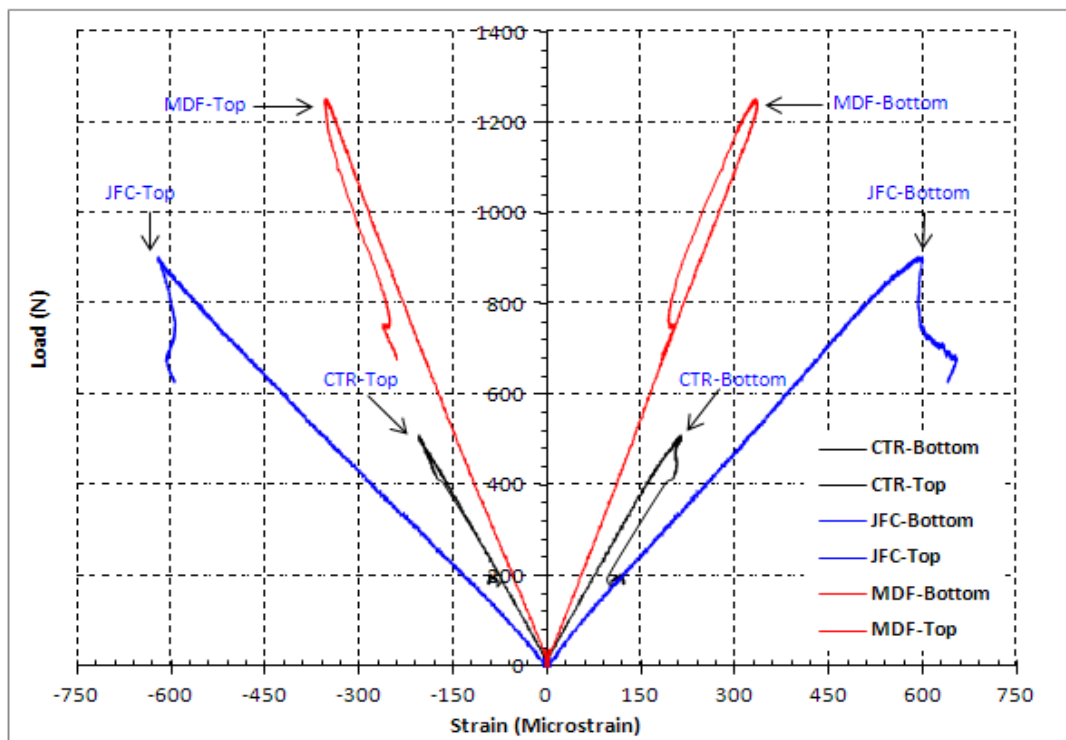


Figure 5.17. Load-strain relationship for large scale sandwich panels

It can be observed from the figure that the top and bottom surface strains for all specimen categories (CTR, JFC and MDF) have similar strain values. For example, the representative curves for CTR group have a similar strain values for both compression and tension sides, at 210 microstrains. A slightly different strain values was found for MDF specimen; 330 microstrains in tension and 360 microstrains in compression side. Comparable strains were also observed for JFC specimen; the strain for compression and tension sides was 620 microstrains and 600 microstrains, respectively. It is also worth noting that the CTR specimen failed at 210 microstrains which was only 58% of strain at MDF specimens and 35% of compression strain of JFC specimen. Overall, the introduction of intermediate layer helps the sandwich panels to sustain larger compression strain prior to reach their ultimate loads that has prevented them to prematurely fail under compression buckling.

5.5.5. Comparison of mode of failure

Medium scale specimen

Failure mechanism analysis is divided into two parts based upon the scale of specimens and within the same scale the analysis is focused separately for different sample categories. Figure 5.18 shows the typical failure modes of the medium scale conventional panels. There are two types of failure mechanism that were observed for medium scale CTR specimen. The first is a shear failure of the core that began as a debonding at the interface of skin and core near the loading point towards the edge. At the point where the bond strength of skin-core was higher than the shear strength of the core, the core shear failure started as an individual cracks tilted of about 45° to the neutral axis. More dispersed cracks diagonally appeared towards the bottom part as the loading increased. With the continued loading, the cracks propagated continuously along the bottom part and terminated at the roller (CTR-M-1, CTR-M-4, CTR-M-5 and CTR-M-6). Such failure mechanisms were also reported by Harte et al (2000).

The second is an indentation failure of the specimen around the loading point, as shown in CTR-M-2 and CTR-M-3. Two rectangular plates were placed between the loading point and the top surface of specimens to avoid early indentation failure. However, it was difficult to reach a perfectly balanced position of the loading roller at the plate resulting in unbalance loading transferred from the plate to the specimen. This

observed fact triggered an indentation failure at the top surface of the specimen at the edge of the plate. Indentation began with the deformation of the skin followed the plate's edge profile. This typical failure mechanism was also reported by Harte et al (2000) for sandwich panel tested under static flexural test. It seems that the use of relatively thin aluminium skin with the thickness of only 0.5 mm has triggered this type of failure mechanism.

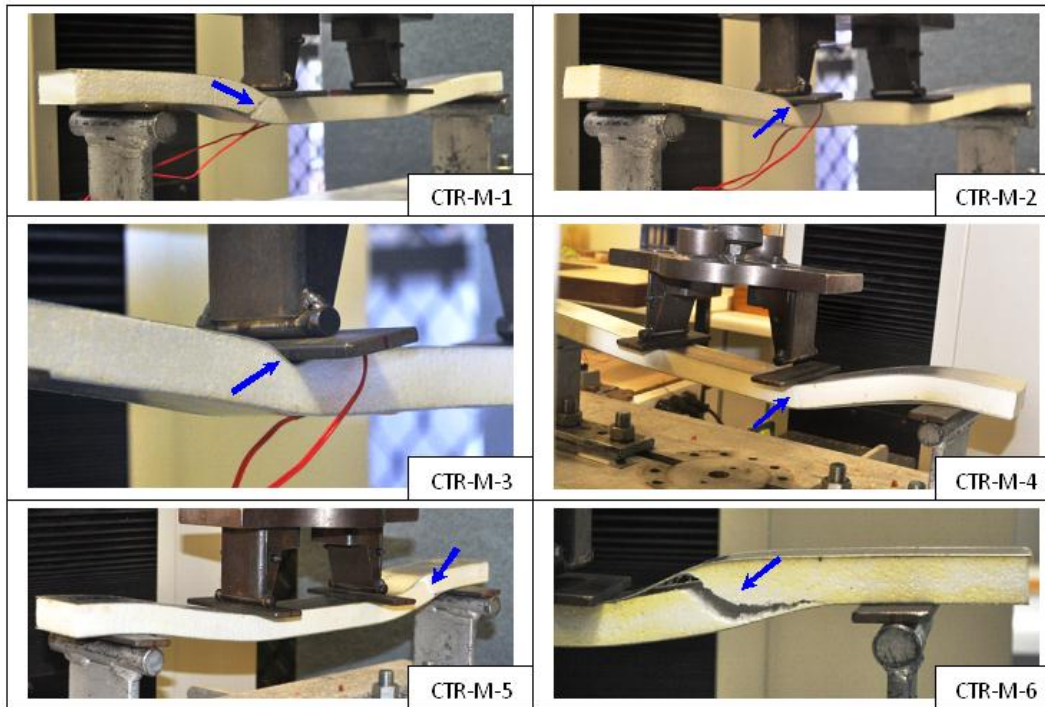


Figure 5.18. Failure mechanisms of medium scale CTR specimen

Figure 5.19 presents the failure mechanism for medium scale hybrid sandwich panels with JFC intermediate layer. It can be observed that the debonding at the interface of intermediate layer-core was the only observed failure mode for this sample category and accordingly the load-deflection curves for this sample category were similar. The failure mechanism might be explained as follows. As the flexural loads applied and increased continuously, the bottom part of the specimen stretched and conversely the upper part compressed. Accordingly, the foam core behaved in the same manner as the deflection increased gradually. It is most likely that the debonding mechanism began when the compression stress at the upper intermediate layer and core interface exceeded its bond strength. The figure also clearly shows that there was no

trace of EPS foam on the debonded interface indicating poor bond strength between the core and the intermediate layer (JFC-M-6).

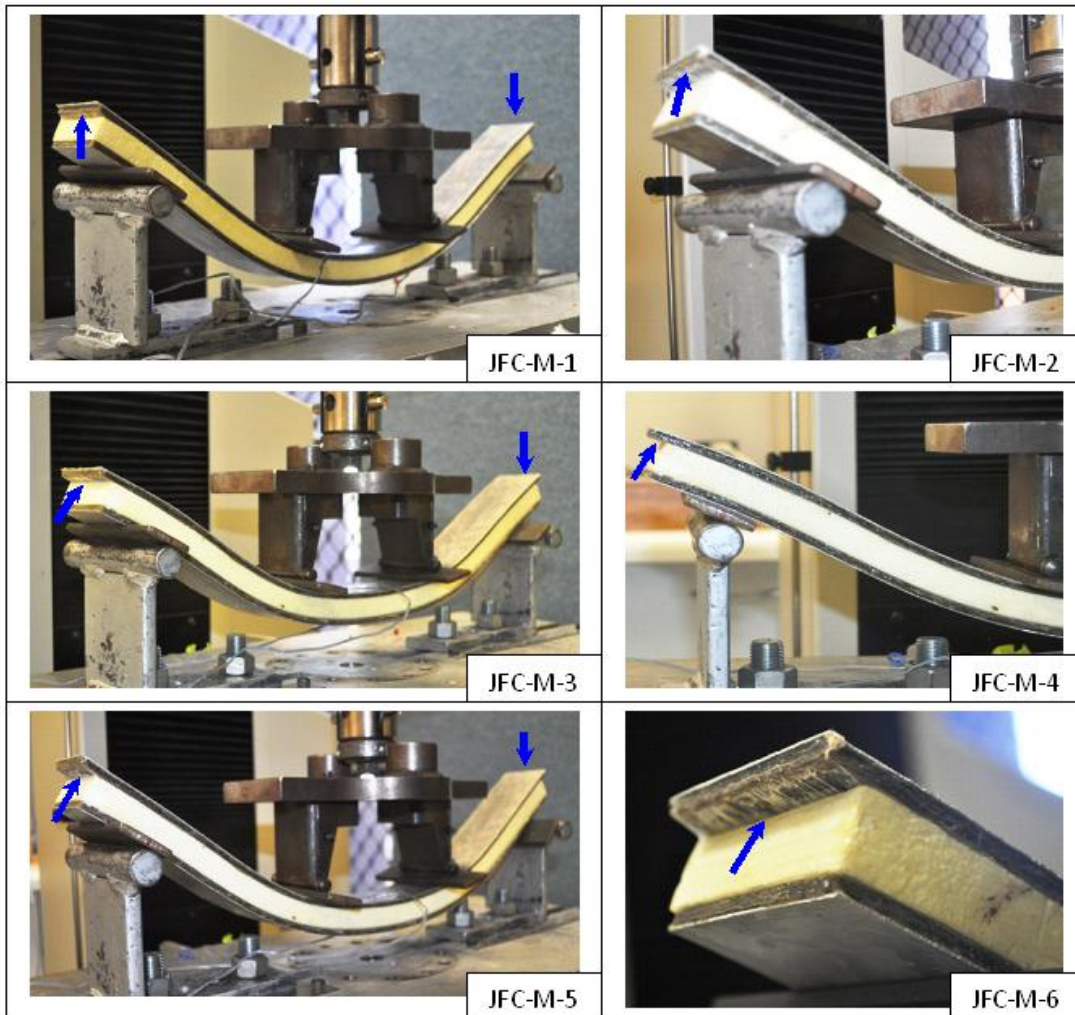


Figure 5.19. Failure mechanisms of medium scale JFC specimen

There are two different types of failure mechanism for hybrid sandwich panels with HFC intermediate layer; debonding of the core-intermediate layer and shear failure of the core. Similar to the shear failure of conventional sandwich panels, the failure mechanism began with a minor crack near the edge of plate under the loading point. The cracks then propagated towards the bottom intermediate layer at an angle of approximately 45° to the longitudinal axis. As the load increased, the bottom end of the diagonal cracks became larger triggering a delamination between core and intermediate layer. No failure was observed within the intermediate layer. It seems that the core shear failure would take place if the bond at the interface of core-intermediate layer had an adequate strength to sustain more loads or the debonding or delamination mechanism is Sustainable Hybrid Composite Sandwich Panel with Natural Fibre Composites as Intermediate Layer

established if the bond strength was reasonably lower. As a result of different failure mechanisms, the shape of load-deflection curves for this sample category was quite different to each other even though the pattern remained the same, as shown in Figure 5.9. The failure modes for hybrid sandwich panels with HFC intermediate layer is shown in Figure 5.20.

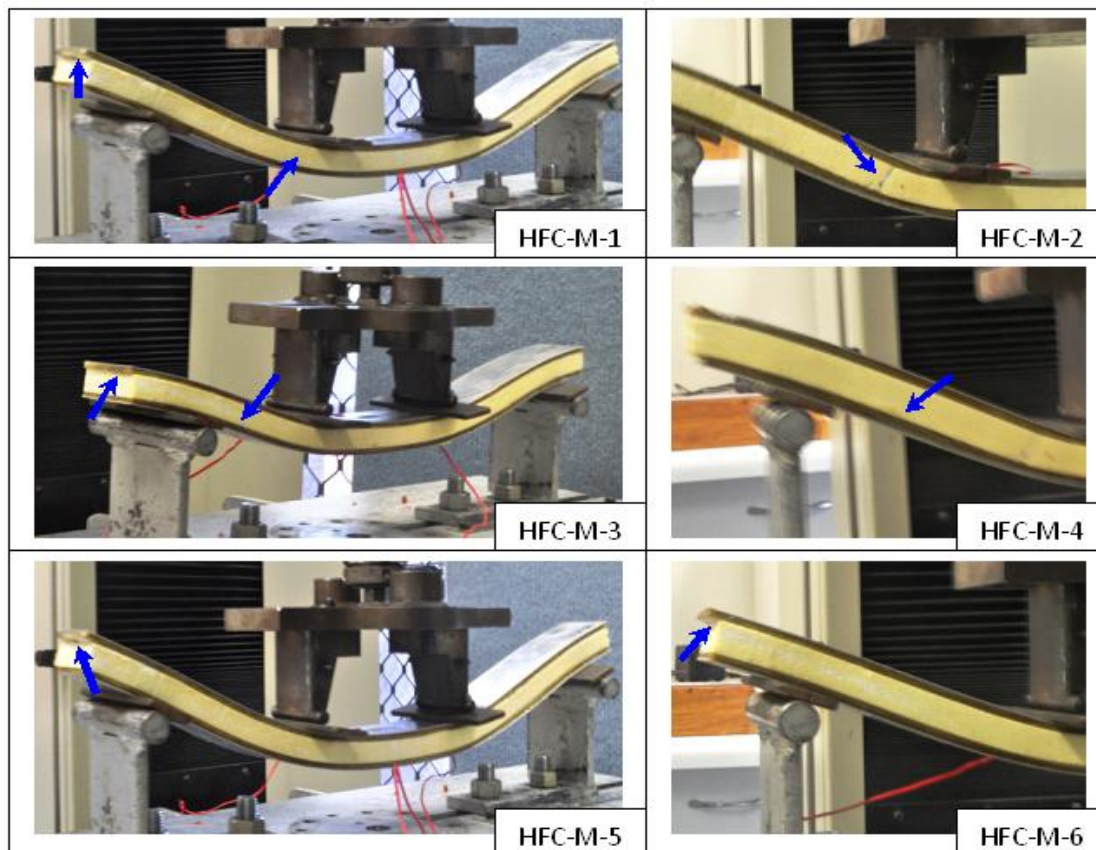


Figure 5.20. Failure mechanisms of medium scale HFC specimen

Large scale specimen

Figure 5.21 shows the type of failure mechanisms for large scale CTR specimen which was diagonal shear crack, vertical shear crack and debonding of the core-skin. The diagonal shear core failure mechanism was similar to that of medium scale specimen (CTR-L-1 and CTR-L-5). The second mode of shear failure initiated as an individual crack at the bottom part under the loading point. The crack then propagated toward the inner roller point at the top forming a vertical crack pattern with an angle of almost 90° . As loading continued, the bottom crack grew triggering a delamination between core and skin, as seen in CTR-L-3 and CTR-L-4. According to Mirzapour et al (2005), this particular failure mechanism was governed by the foam core and is called a Sustainable Hybrid Composite Sandwich Panel with Natural Fibre Composites as Intermediate Layer

foam core stretching phenomenon. The foam core cell stretched at the tension side of the specimen as the load increased initiating multiple cracks at the lower part just below the inner roller.

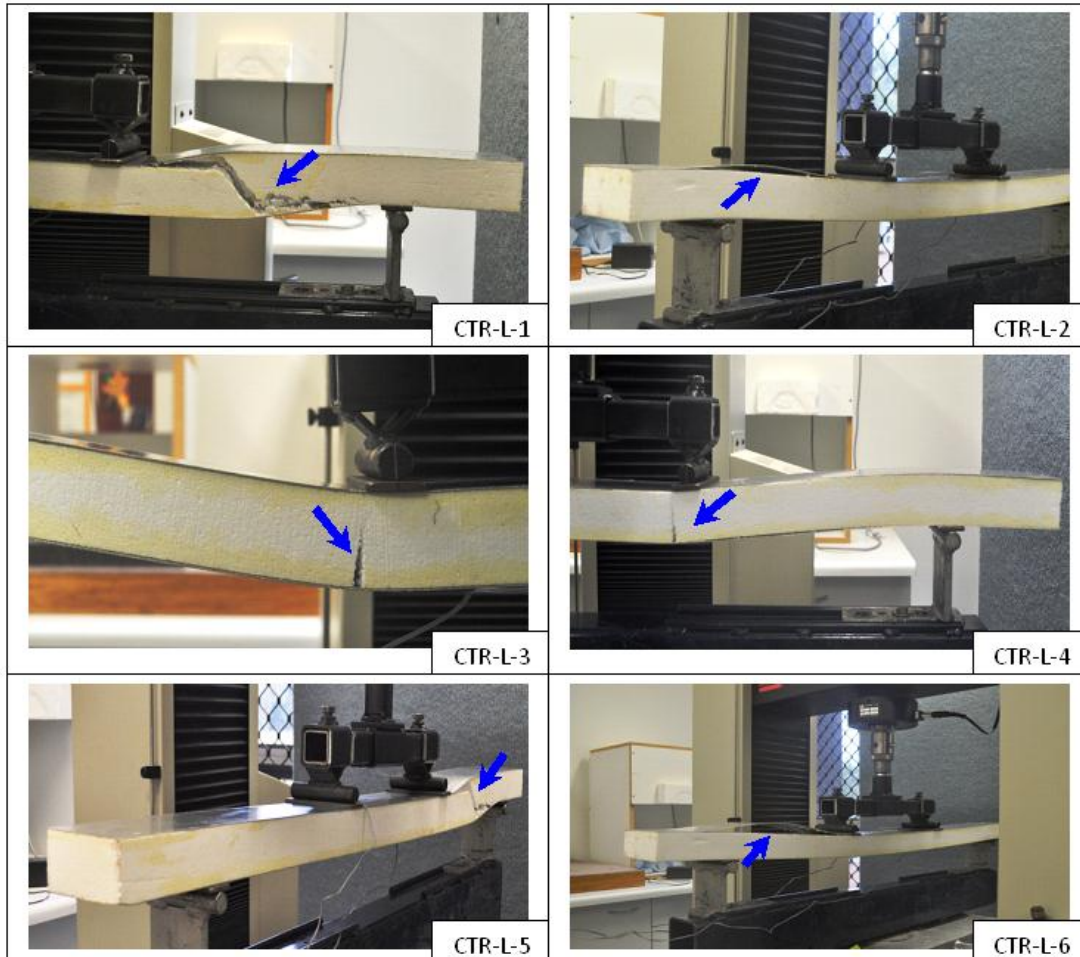


Figure 5.21. Failure mechanisms of large scale CTR specimen

Another type of failure mechanism observed for large scale specimen was the debonding at the interface of the core and skin at the upper part, as shown in CTR-L-2 and CTR-L-6. The debonding started near the loading point and quickly propagated along the interface toward the edge of the specimen. Such failure mode was also a common failure mechanism for sandwich panel beam tested under flexural load (Mahfuz et al, 2004; Mirzapour et al, 2005). It seems that the primary reason for this particular failure mechanism was the weak bond strength at the interface of the skin and core. It is clearly shown in the figure there was no trace of EPS foam core on the

debonded interface meaning that the bond strength was significantly lower than the shear strength of the core.

Figure 5.22 shows the failure modes of large scale hybrid sandwich panels with JFC intermediate layer. Unlike the failure mechanism at its medium scale that only failed under debonding mechanism, the large scale panels collapsed under two types of failure modes; delamination of the core-intermediate layer and shear failure of the core.

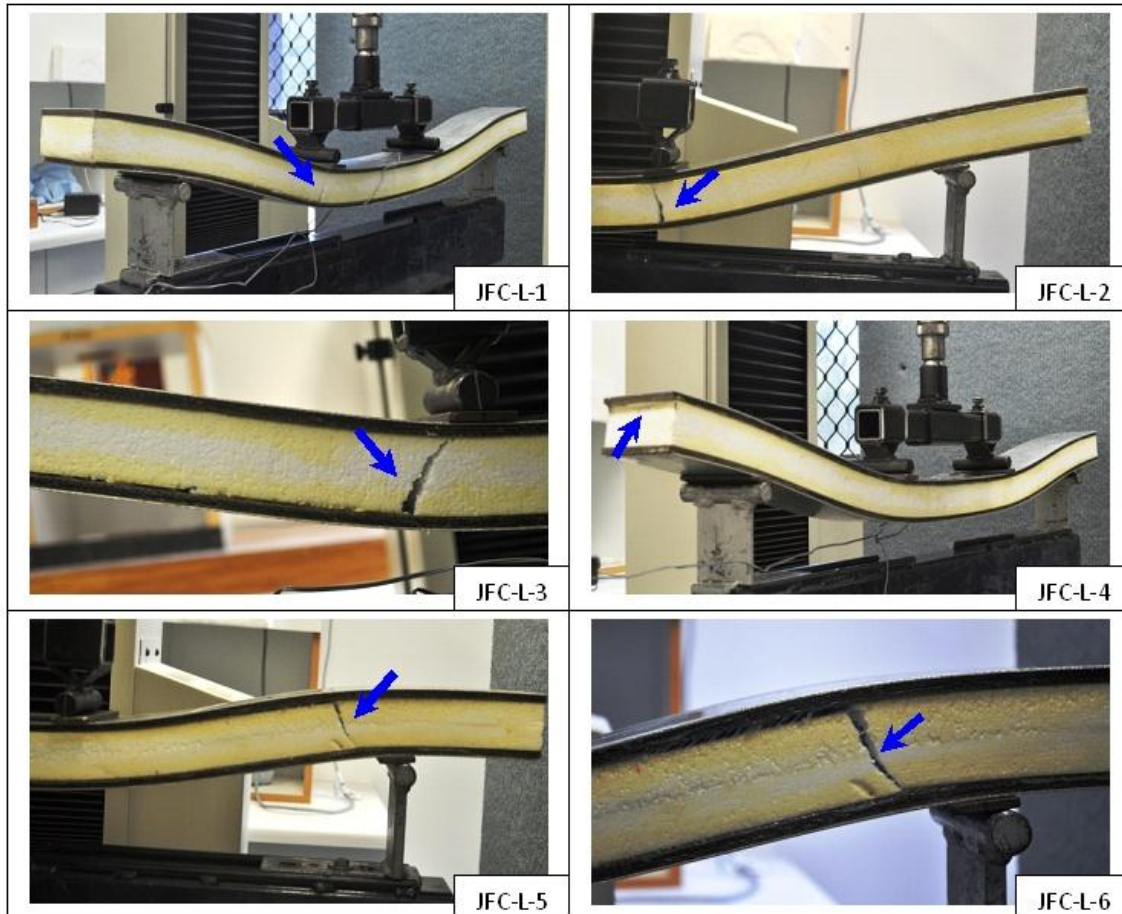


Figure 5.22. Failure mechanisms of large scale JFC specimen

The load-deflection failure curves of this specimen group clearly showed the distinction of the two failure mechanisms. The specimens failed due to delamination mechanism obtained a smooth curve without any sudden changes in the load-deflection relationship, as observed for all curves of JFC at medium scale. On the other hand, sudden change beyond the peak load point was a common configuration of load-deflection curve for specimen failed due to shear failure of the core. As seen in Figure 5.22, the shear failure of the core was frequently accompanied by the debonding

mechanism at the interface of the core and intermediate layer. In parallel to the shear failure of the core at other specimen groups, the failure mechanism began with an individual crack that initiated either near the loading point or the support roller, both within the shear span of the specimens. The cracks then propagated as the loading was increased and finally terminated at a point near the support roller.

The failure mechanism of hybrid sandwich panels with MDF intermediate layer is depicted in Figure 5.23. As seen in the figure, the principle failure mode of this sample category was shear failure of the core with or without debonding at the interface of core and intermediate layer (MDF-L-1 to MDF-L-5).

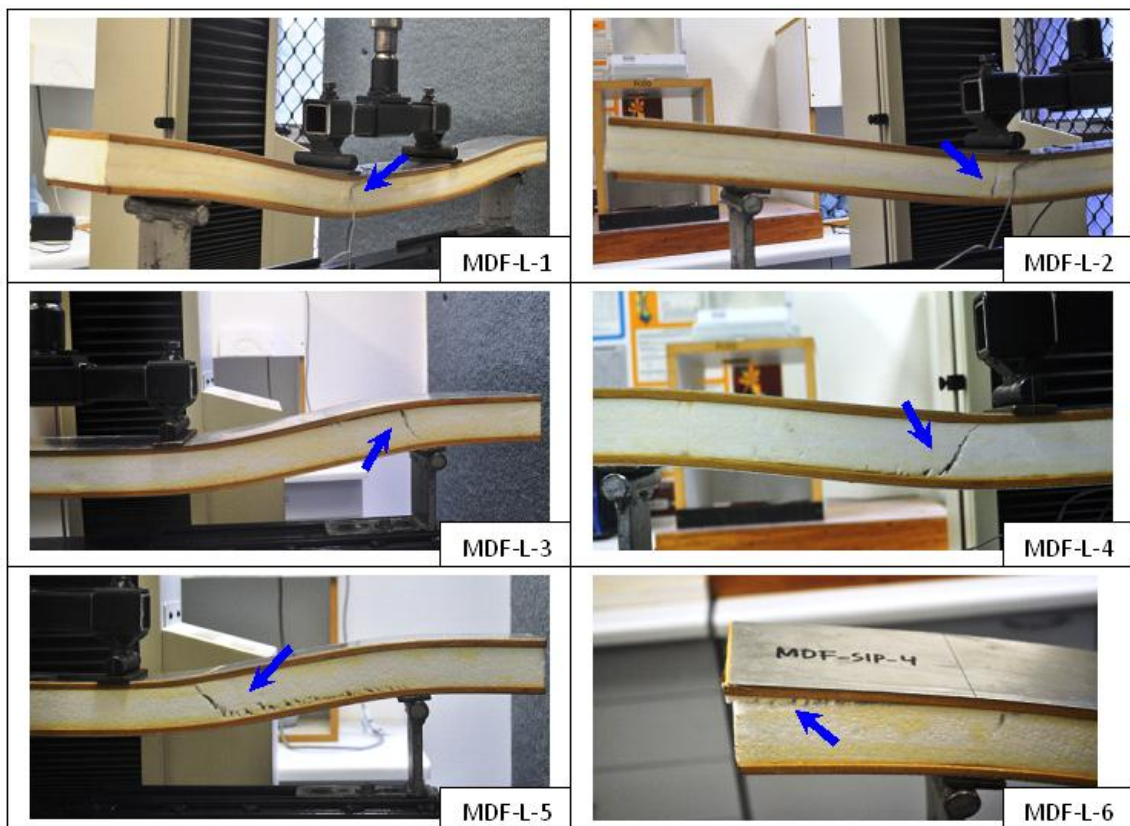


Figure 5.23. Failure mechanisms of large scale MDF specimen

In contrast to the debonding mechanism in the JFC hybrid sandwich panels caused by the weak bond strength throughout the length of the specimen, such mechanism in this sample category occurred only within the shear region as shown in MDF-L-3 and MDF-L-4. The other failure mechanism was a longitudinal shear failure of the core initiated at the edge of the specimen as shown in MDF-L-6. As noticeably shown in this figure, a significant amount of EPS core was left with the intermediate layer at the

debonded interface. This suggests that the bond strength at the interface of the core-intermediate layer exceeded the compression strength of the core resulting in higher load bearing capacity of the specimens.

In summary, the introduction of intermediate layer provided a reasonable support for the thin aluminium skin to carry the bending loads and has prevented the occurrence of premature failure mechanisms such as indentation or delamination of skin and core as observed in the conventional sandwich panels. It is also important to note that there has no observed failure at both intermediate layer and skin of hybrid sandwich panels, or at the interface between them. This indicates that the flexural loads had been transferred to the core of the sandwich panel resulting in core shear failure that triggered debonding at the interface of core and intermediate layer.

5.6. Chapter Conclusions

The experimental investigation of hybrid sandwich panels with intermediate layer has been carried out under 4-point static bending loads. The flexural behaviour and failure mechanisms of the hybrid sandwich panels have been compared to the conventional sandwich panels without an intermediate layer. The experimental work was designed as a single factor experiment at both medium and large scale specimens. This chapter provides an overall analysis of the total load-strain behaviour of the various composite evaluated. The relative behaviour of the panels using serviceability criteria such as deflection/span limits will follow the same pattern. The results show that the hybrid sandwich panel performs better than the conventional sandwich panels. More specific findings are outlined as follows.

- 1) The load carrying capacity of medium scale hybrid sandwich panel with JFC intermediate layer was 29.60% higher than conventional sandwich panel, and correspondingly 93.46% higher for sandwich panel with HFC intermediate layer. For large scale panels, the load carrying capacity of hybrid sandwich panel with JFC and MDF was approximately 62.59 % and 168.58 % higher than the load carrying capacity of conventional sandwich panel, respectively.
- 2) Both types of sandwich panels, with or without intermediate layer, behave in a ductile manner. However, there has an obvious change in load-deflection curve when intermediate layer was incorporated in sandwich panels which were related

to the toughness of the material. Hybrid sandwich panels developed much large area under the load-deflection curve than those of conventional sandwich panels.

- 3) The deflection of hybrid sandwich panel was slightly larger than those of conventional sandwich panel although they have higher equivalent bending stiffness. The introduction of intermediate layer does not contribute much to the reduction of the deflection of hybrid sandwich panel as the main contributor for the total deflection was shear deformation of the core that mostly determined by the shear modulus and the thickness of the core.
- 4) The proposed model for predicting the deflection of hybrid sandwich panels provided fairly agreement results with the experimental values. The differences range from 3.9% to 35.4%. Most of the sandwich panels showed experimental values lower than the theoretical values that can be considered as highly desirable in the design.
- 5) The introduction of intermediate layer helps the sandwich panels to sustain larger compression strain prior to reach their ultimate loads that has prevented them to prematurely fail under buckling or indentation.
- 6) The intermediate layer prevented the occurrence of premature failure mechanisms such as indentation or delamination of skin and core due to buckling resulting in higher flexural ultimate load carrying capacity.

CHAPTER 6

DEVELOPMENT OF A TESTING RIG FOR THE DIAGONAL IN-PLANE SHEAR TEST OF SANDWICH PANELS

6.1. General

Shear testing is commonly performed to measure the in-plane shear properties of a composite material, including in-plane shear strength, in-plane shear modulus, or both properties. Shear testing has proven to be one of the most difficult areas of mechanical property testing. While shear modulus measurements are considered accurate, there is difficulty in measuring shear strength. The presence of edges, material coupling, non-pure shear loading, non-linear behaviour, or the presence of normal stresses makes shear strength determination questionable (www.netcomposites.com). Ideally, for quantitative shear measurements, the shear stress must be uniform in the test section of the specimen throughout the linear and non linear response regimes. This region should be located in one of the maximum shear stress areas relative to all other regions of the specimens. In addition, a unique relationship should exist between the applied load and the magnitude of the shear stress in the test section. This chapter reports the development of a testing rig for diagonal in-plane shear test of sandwich panels.

6.2. Shear Test for Composite Sandwich Panels

As the number and diversity of applications for fibre reinforced composite materials continues, the need for new and improved test methods also increases. One area of continuing development of testing methods is that of shear testing to measure the shear strengths and shear moduli of fibre reinforced composites. Depending on the composite material to be tested and what material properties are to be measured, one particular shear test method may be preferred over others. Although several test methods have been developed to address these needs, there has no single shear test

universally accepted to date as the preferred method for obtaining the in-plane shear properties of composite materials. The primary prerequisite for the test assembly should be truly representative of approved practice and should include details likely to occur that may affect the performance of the desired product (Reardon, 1980).

The in-plane shear performance of sandwich structures has been evaluated by many researchers employing various methods. Much information and data has been accumulated. Some of those tests are; the direct shear test, tie-rods test, picture-frame shear test or diagonal shear test and the racking test. The racking test is the most frequently employed method when investigating in-plane shear of the panel (Tissel, 1993). Generally, racking tests have followed a standard method such as ASTM E 72 (ASTM, 1997). According to this standard, racking tests that apply an incremental load to the top of a test wall specimen approximately 2400 x 2400 mm in size can be considered as a full scale test as it represents the practical dimensions of a wall structure. Although the racking test is considered as a more reliable method to deliver a similar result to real application, its application has been limited due to the requirements of testing space, time, manpower and cost. Bi and Coffin (2006) explained that a full scale wall racking test is expensive and time consuming to run, except for the purpose of qualifying a board. For product development, there is a need for a more convenient and less expensive test method that could be used to evaluate the in-plane shear characteristic of a panel.

In the early stage of sandwich structure development in the 1960's, a diagonal in-plane shear test method was used for determining in-plane shear modulus and strength. This shear test is now being re-considered by some researchers for both cost and resources reasons. The diagonal deformable square sample has the advantage of being able to be tested on standard test machines, using relatively basic test rigs. The panel size required for the testing is in between 350 to 850 mm, significantly reducing the cost and also allows duplication of samples to be tested. The following section will focus on the diagonal in-plane shear test, particularly the testing method using a diagonal tension load.

6.2.1. Type of diagonal shear test

There are several terms given by researchers to this test such as picture-frame shear test (Lee and Munro, 1986), deformable square test (Castenie et al, 2004),

diagonal shear test (Mosalam et al, 2008) and even small-scale racking test (Bi and Coffin, 2006). Based on the way the load is transmitted to the specimen, the diagonal in-plane shear test can be divided into two categories; diagonal tension and diagonal compression test.

The diagonal tension shear test is performed using deformable square panels. The principle consists of applying a tension load along the square vertical diagonal, as shown in Figure 6.1. The frame transfers the tension load vertically to the specimen and at the same time the compression load along the horizontal axis produces a pure state of shear within the specimen. Usually, the loads are transmitted from the frame to the specimen by bolting (Castenie et al, 2004). Such methods are widely used in the aeronautical fields and also for testing naval structures. An appropriate design of the testing frame is very important to ensure that a uniform stress develops in the sample. A poorly made frame will cause excessive stress in the corners and premature local failures.

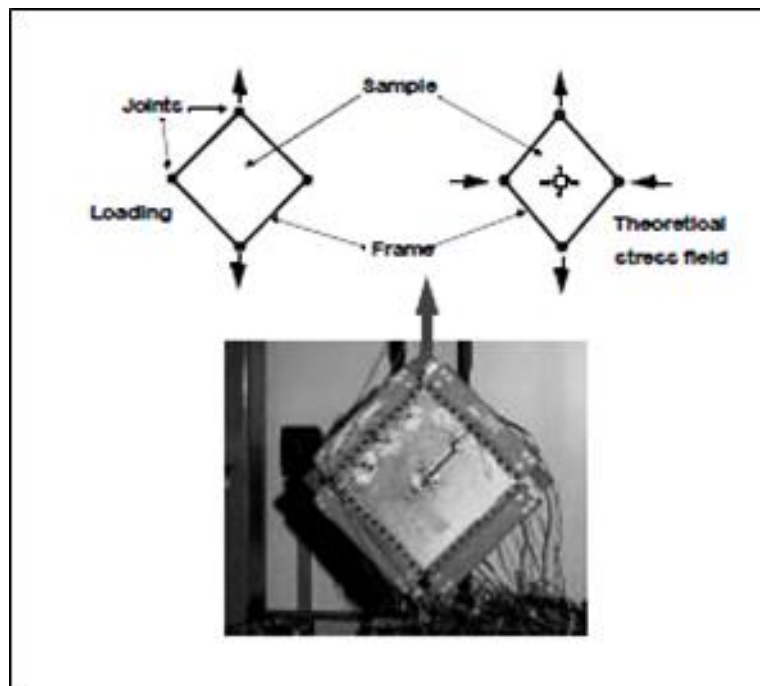


Figure 6.1. Diagonal tension test using deformable square panel (Castenie et al, 2004)

As the name implies, the diagonal compression test involves applying a vertical load in a compression direction which creates a horizontal tension load distribution within the specimen. The concept is, however, similar to that of the diagonal tension

test with the exception for the direction of the applied load. For a sandwich structure however, the best way to investigate the in-plane shear under diagonal test scheme may be to use tension apparatus as suggested by Kuenzi et al (1962). They noted that in the early sandwich work, a compression type of loading apparatus was commonly used to induce shear. However, it was found later that the compression arrangement was unsatisfactory because it tended to amplify initial eccentricities and, for that reason, produced a low result. They also mentioned that a tension type of apparatus would develop the same quality of shear and would also produce greater buckling loads than would apparatus of the compression type.

While the diagonal in-plane shear test on sandwich structures is mostly conducted with a tension load arrangement, the diagonal compression test remains important to investigate the in-plane shear of masonry structure. Santa-Maria et al (2004) used such a test method to study the in-plane shear behaviour of masonry panels externally strengthened with CRFP laminates and fabric. Marcari and Fabbrocino (2007) employed the test method to develop design criteria for FRP strengthened tuff walls. More recently, Ismail et al (2010) employed the test to explore the diagonal shear behaviour of unreinforced masonry wallettes strengthened using twisted steel bars. The arrangement of testing rig and the sample set are shown in Figure 6.2. In the following sections, this testing method will not be further discussed as it is not suitable for sandwich structure..

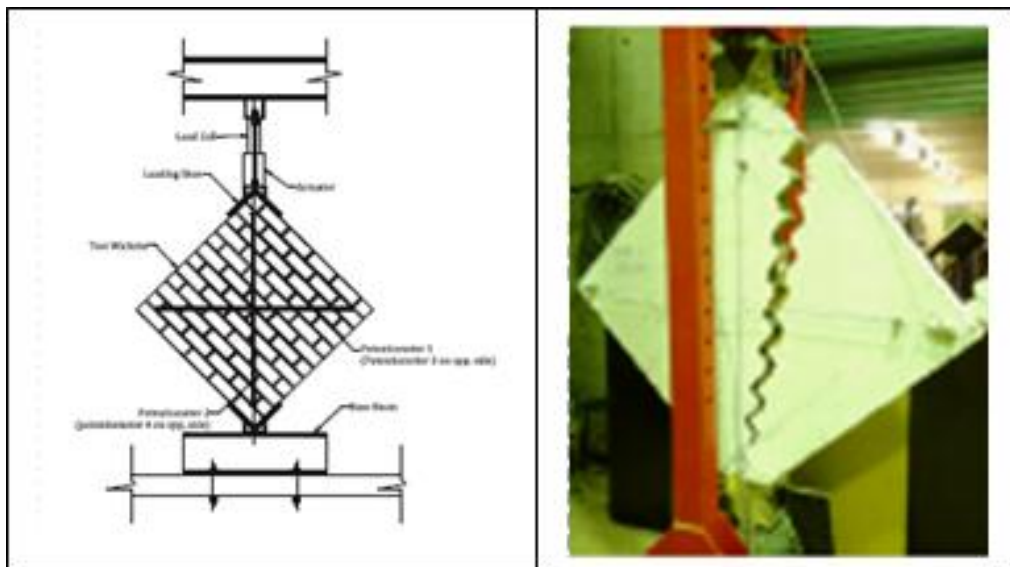


Figure 6.2. *Left:* Diagonal compressions shear testing arrangement.
Right: actual testing (Ismail et al, 2010)

6.2.2. Diagonal tension shear test of sandwich panels

In this section, a number of studies reported in the literature dealing with diagonal tension test of sandwich panels are reviewed. The review aims to gain an understanding of the way in which the testing has been carried out including the applied boundary conditions, the loading frame, the constituent materials as well as the dimensions of the panel tested. Brief comments about the failure modes are also included.

Kuenzi et al (1962) reported their work on the assessment of shear stability of flat sandwich panels. The objective of their work was to obtain information concerning the elastic stability of flat panels of sandwich construction subjected to edgewise shear and to develop a possible rational design method of such panels. The experimental set-up of this work is shown in Figure 6.3. The panels were tested in a hydraulic machine. Pins placed near the ends of loading rails were loaded through links attached to a central loading pin at each end of the vertical diagonal of the specimen. Plywood loading rails were bonded to both facings at all four edges of the panels. The corners of the panel were cut so that there was approximately 3.2 mm (1/8 inch) clearance between the nearest corners of the adjacent edge rails. Cut out corners were curved to minimize stress concentrations. As it can be seen in the figure, a tension type of loading apparatus was used to induce shear in the panel.

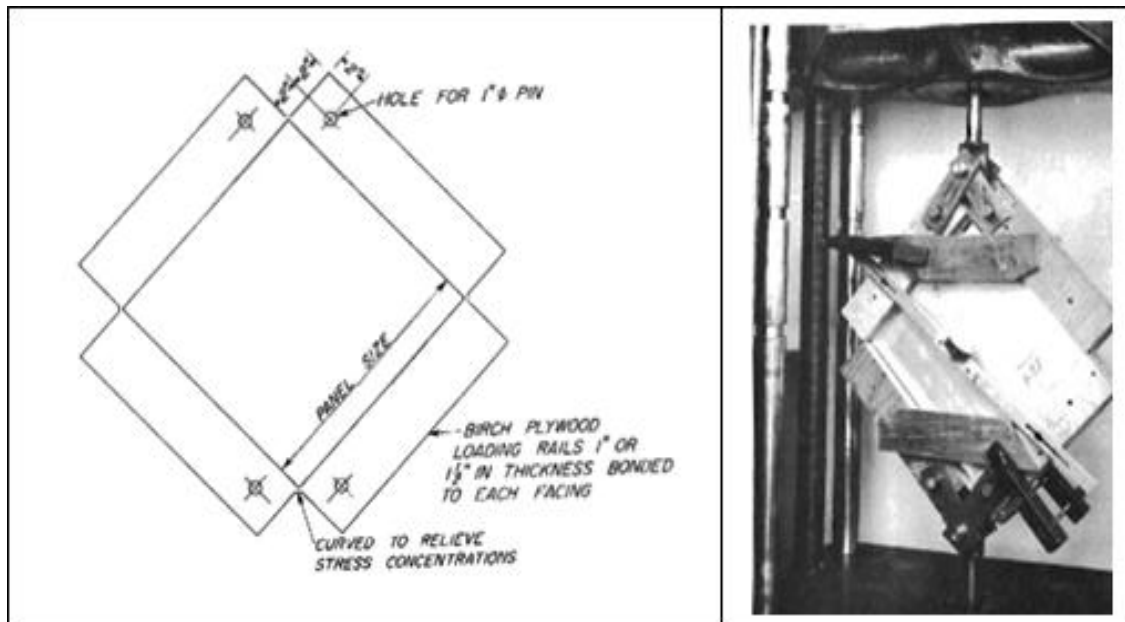


Figure 6.3. *Left:* Testing arrangement. *Right:* actual testing set-up (Kuenzi et al, 1962)

All samples consisted of a similar skin; clad aluminium alloy 24S-T3 with a thickness of either 0.3 mm (0.012 inch), 0.5 mm (0.02 inch) or 0.8 mm (0.032 inch). Three types of core were used; end grain balsa, hard sponge rubber and corkboard sheet. The sizes of panels ranged from 355.6 x 355.6 mm (14 x 14 inch) to 863.6 x 863.6 mm (34 x 34 inch). Final failure of the panels occurred at or slightly above the buckling load. The failure occurred suddenly and was usually of the crimping type caused by sudden failure of the core due to high stress induced by buckling.

Morgenthaler et al (2005) conducted a comparison analysis of two in-plane shear test for sandwich structure. The work was aimed at finding out a suitable experimental set-up to evaluate the in-plane shear properties of sandwich plate. The first setup was a rail shear test based on ASTM D4255 with increased size to allow analysis of the shear buckling and face wrinkling of sandwich structure. The second test was a diagonal tension test using a square sample with incorporated aluminium bars on every side. The density, type and thickness of core were varied as well as the face thickness. The two types of experimental setup are shown in Figure 6.4.

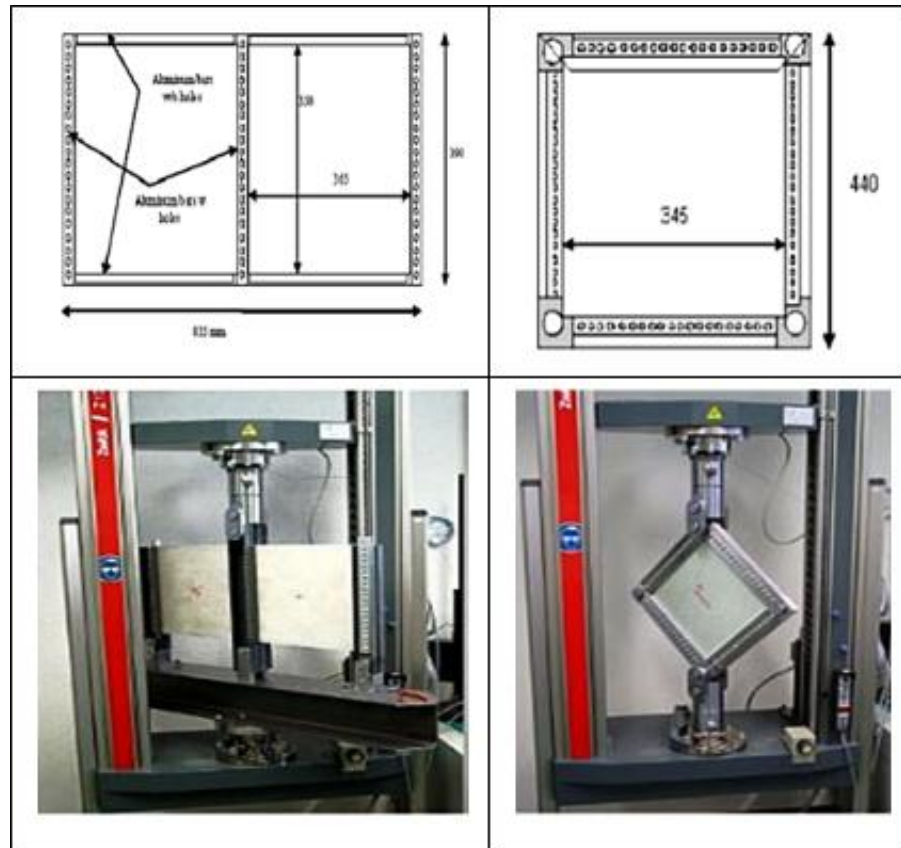


Figure 6.4. *Above:* Testing arrangement. *Bottom:* actual testing (Morgenthaler et al, 2005)

The geometry of samples tested under first experimental scheme was 390 x 835 including aluminium bar frames and 440 x 440 mm for the second test setup. The thickness of samples varied from 6.42 mm to 17.58 mm. The typical observed failure modes were skin shear failure, shear buckling of the panel and skin wrinkling. The primary conclusion drawn from this work was that using a square sample mounted on each side to a steel frame (the second setup) was more appropriate to create a shear field in the sample. The other setup failed as the sample was able to be bent, thus disturbing the shear field in the sample.

In a symposium on shear and torsion testing held by ASTM, Youngquist and Kuenzi (1961) presented their work at the U.S. Forest Products laboratory on shear and torsion testing of wood, plywood and sandwich construction. This paper briefly described the test method, traced the history of some of the methods, and presented a discussion of their advantages, disadvantages and suitability. Figure 6.5 shows the method of panel shear test of plywood using compressive loading (left) and tensile loading (right). For the tensile loading method, the specimens were glued to a hardwood loading blocks. Strain measurements taken at various points on the panel showed that within the elastic range a nearly uniform strain distribution was possible. They also suggested that a great care must be given in the alignment of the holes for the loading pins and in the proper location of the text fixtures.

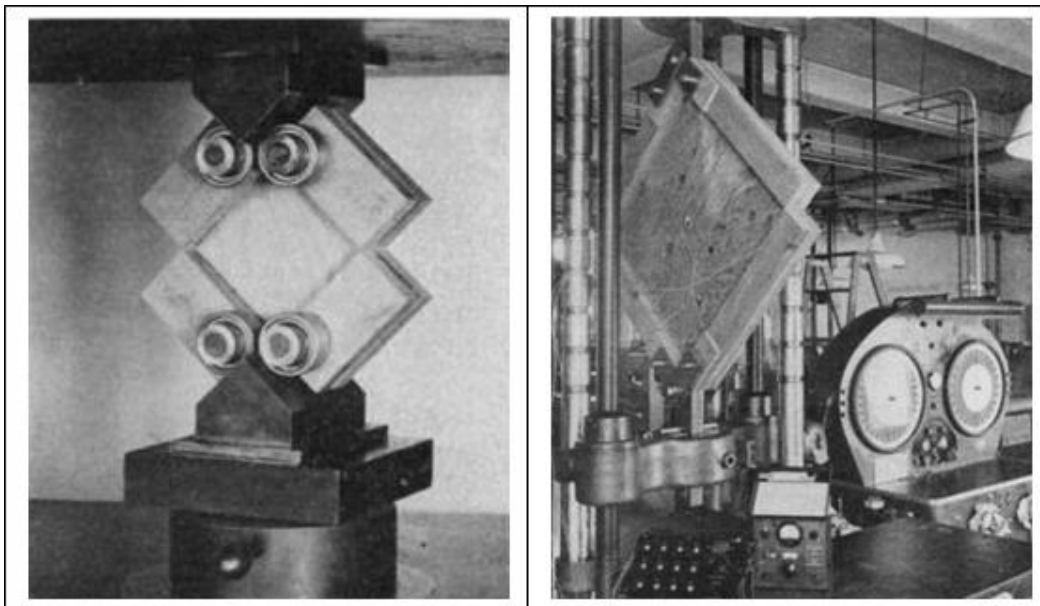


Figure 6.5. *Left:* Panel shear test of plywood using compressive loading.
Right: using tensile loading (Youngquist and Kuenzi, 1961)

Bryan (1961) carried out a photoelastic investigation of the stress distribution in the panel and found that the stress distribution deviated substantially from pure shear; accordingly the method was not appropriate for measuring the in-plane shear modulus. However, they showed that at the critical region (which along the edge) the stress state was essentially uniform pure shear and thus recommended that this test should be an accurate method for determining the in-plane shear strength. The set-up of this experiment, which was a picture frame panel, is shown in Figure 6.6.

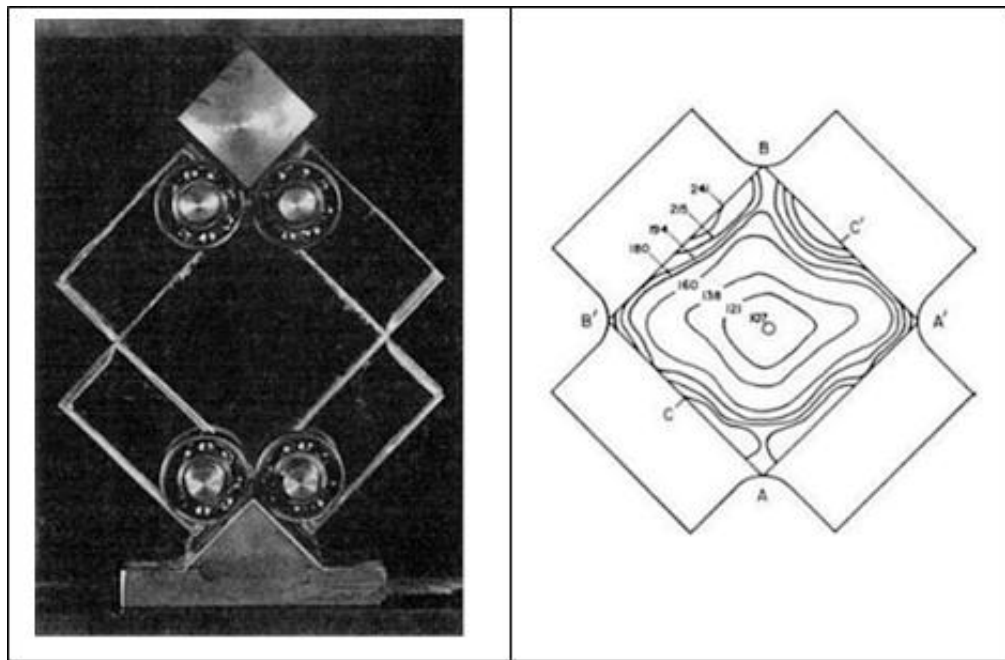


Figure 6.6. *Left:* Photoelastic model in position for loading. *Right:* isochromatic pattern for model showing the constant maximum stress for each fringe (Bryan, 1961)

De-Iorio et al (2002) noted that the shear test can be carried out on a rectangular or square thin panel where the panel edges were joined along to form a mechanism by four rigid rods which are mutually hinged at their ends. If the material is orthotropic, with two principal directions parallel to the panel edges, or if it is isotropic, it is possible to impose the displacements that correspond to a uniform shear stress distribution in the panel. The shear test fixture of this work is shown in Figure 6.7. Bi and Coffin (2006) applied a tension load scheme to the specimen panels in order to investigate their racking performance. They called the test as a small-scale racking test developed to evaluate paperboard-based sheathing materials used in framed wall-construction. Two simplified small-scale racking testers (406 x 406 mm and 813 x 813 mm) were

designed, built and evaluated. The results provided practical insight into the racking response of framed and sheathed walls. The load-deformation responses of framed and sheathing boards were measured, and initial racking stiffness and racking strength were proposed as parameters for characterizing the board. The test results showed that the initial paperboard racking stiffness correlated to the elastic modulus, but that the response was insensitive to the orientation and dimension of the specimen. The testing arrangement for this study is shown in Figure 6.8.

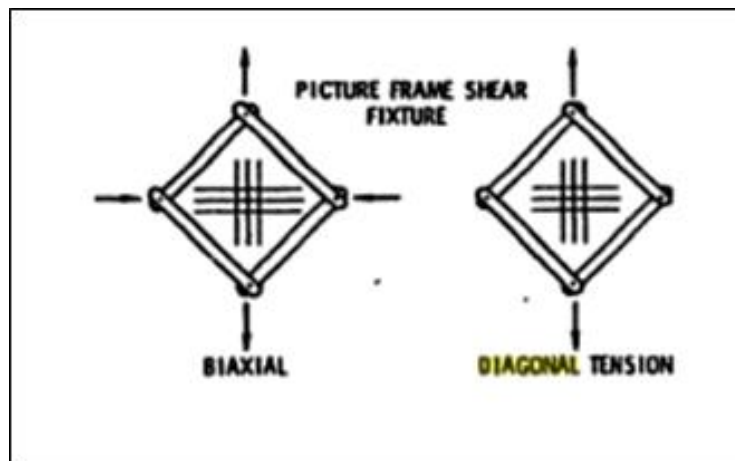


Figure 6.7. Shear test fixture described by De-Iorio et al (2002)

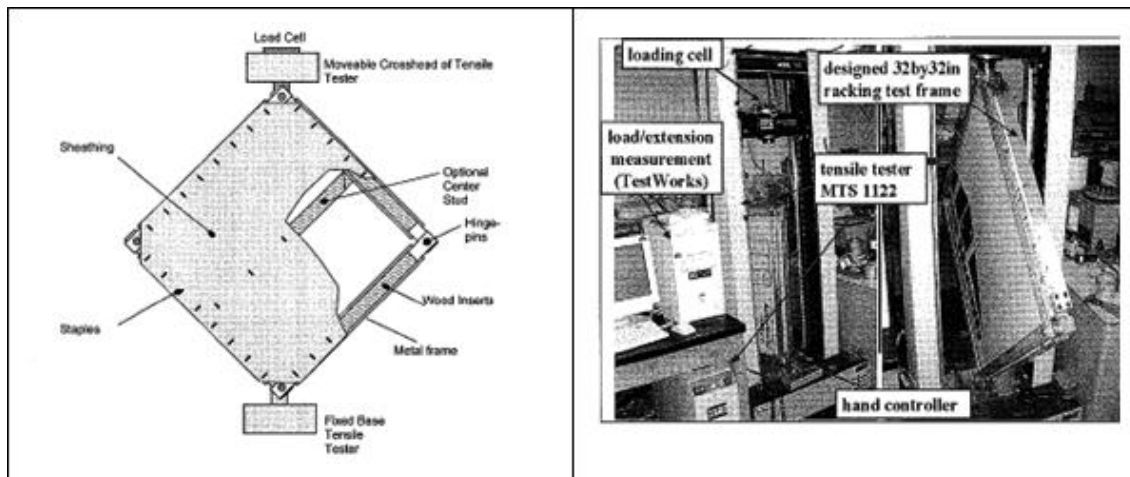


Figure 6.8. *Left*: Testing arrangement. *Right*: actual testing (Bi and Coffin, 2006)

The diagonal tension test is also used in other structural components such as concrete panels. Hossain and Wright (1998) developed a profiled concrete shear panels that may be used as core walls in framed construction. The typical panel was actually a sandwich structure that consisted of two profiled steel sheeting as the skin with concrete

as the core. It was assumed that the composite walls would resist shear loading in three ways; shear resistance of the profile steel sheeting as a skin, concrete core and the shear resistance that existed in between the sheet and the concrete core. A reduced scale model test of approximately 1/6 scale of actual panel had been tested to investigate the behaviour of the profiled concrete shear panels. A shear rig capable of applying load between 25 and 250 kN to the panel was used. The test panels were clamped between pairs of frame members using a sufficient number of bolts providing adequate clamping force for shear forces to be transferred from shear frame to the panels by friction. The shear panels were tested by applying tensile forces across a diagonal of the test frame. The profiled models had a clear internal dimension of 500 x 500 mm between frames boundaries. The overall dimensions were 620 x 620 mm providing an effective dimension of 560 x 560 mm. The testing details are shown in Figure 6.9.

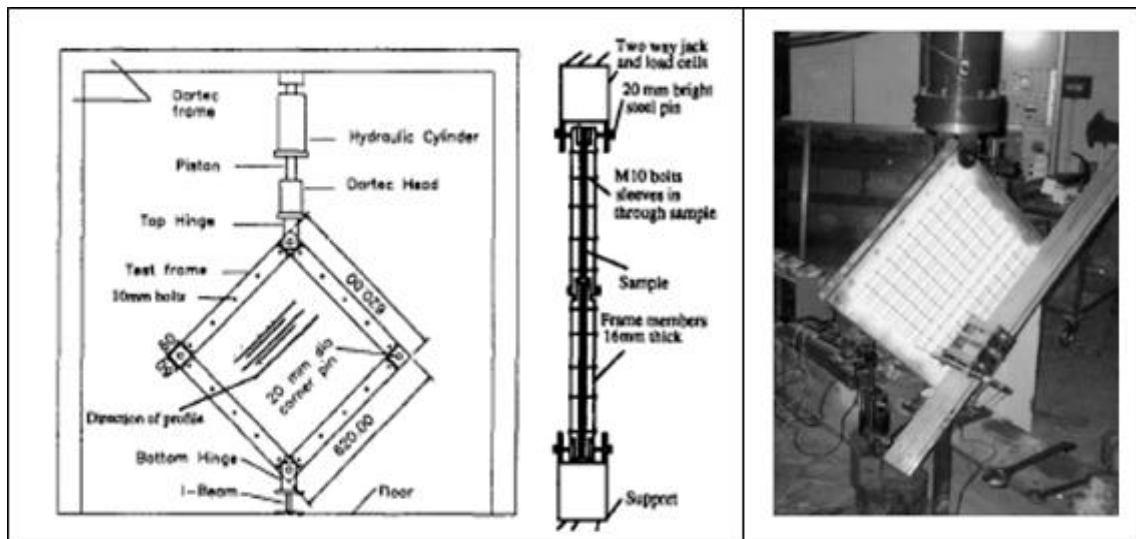


Figure 6.9. *Left*: Testing arrangement. *Right*: actual testing (Hossain and Wright, 1998)

Kim et al (2006) investigated the shear capacity of infill panels using a diagonal tension test. The study suggested that the shear capacity of infill panels can be increased by using a unique strain hardening ECC reinforced with short random fibres of polyvinyl alcohol. The ECC panel was composed of a common mortar matrix and polymer fibres. The geometry of the panels was 600 x 600 square mm with the thickness of 100 mm adopted from ASTM E 519. The testing was conducted on a 1000 kN capacity testing machine. Two LVDTs were attached to measure the displacement in vertical and horizontal directions. The loading surface between the specimen and the

loading shoe was a gypsum capping to achieve a uniformly distributed load on the specimen. The load was applied at a uniform rate of 0.6 mm/min so that the maximum load could be reached in between 1 to 2 minutes. The observed failure mode for the concrete specimen was a brittle matrix failure while ECC shear wall system failed after a high ductility performance at a higher peak load. A large localised crack formed in the concrete near the loading shoes as the loading approached the peak value, and a diagonal tension line developed rapidly throughout the entire specimen as the load reached its peak. The testing details are shown in Figure 6.10.

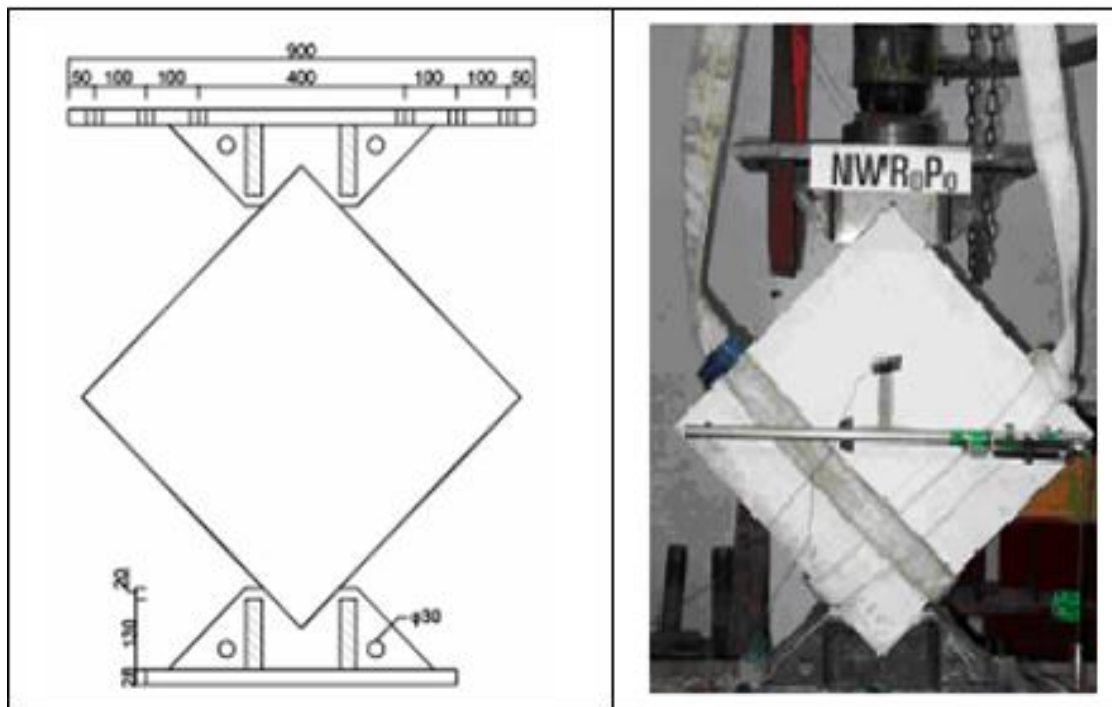


Figure 6.10. *Left: Testing arrangement. Right: actual testing* (Kim et al, 2006)

Mosalam et al (2008) reported their work on the seismic evaluation of structural insulated panels (SIPs) using diagonal tension test and racking test. The SIPs were made of two 11 mm fibre cement mortar facings with EPS core of 94 mm thick, for an overall thickness of 116 mm. The EPS core had a nominal density of 16 kg/m^3 and the panels were rated with an R-value of 25 for walls. The dimension of test panels was $609.6 \times 609.6 \text{ mm}$ ($2' \times 2'$ feet) and they were loaded monotonically with an average target rate of 8.89 kN/sec (2 kips/sec) according to ASTM E519 (1988). It was found that the fibre cement mortar facings as well as the polyurethane adhesive failed in a brittle fashion. The basics of this experimental test are shown in Figure 6.11.

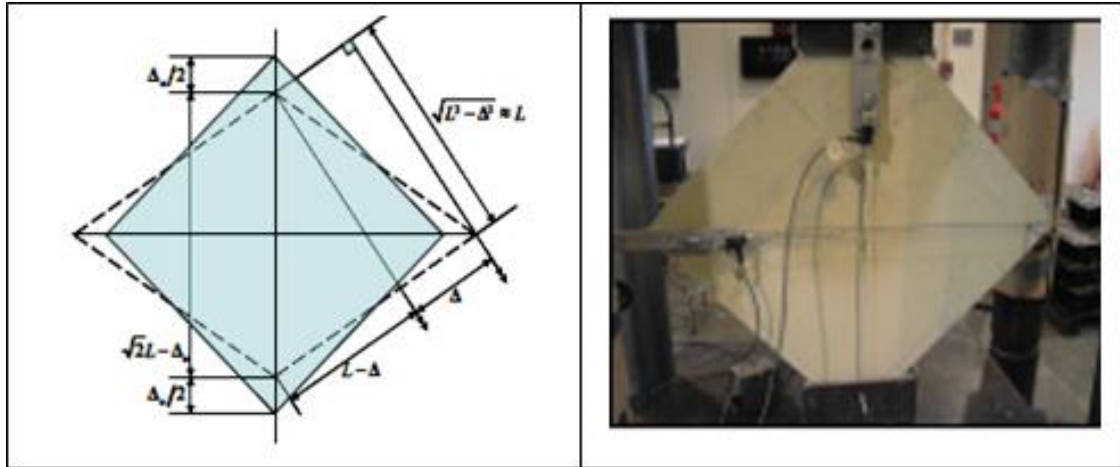


Figure 6.11. *Left: Basic assumption. Right: Actual testing (Mosalam et al, 2008)*

After reviewing a number of studies dealing with in-plane shear test of sandwich panels available in the literatures, some findings can be summarized as follows. First, there are two types of diagonal in-plane shear test based on the way the load is applied to the specimen; diagonal tension and diagonal compression test. The diagonal compression test is more frequently used in the testing of concrete and masonry structure. While diagonal tension is often used for wood based panels or sandwich panels that naturally weak in compression.

Second, there are two boundary conditions related to the jointing system of the testing rig. The first type has four pin jointed corners (Morgenthaller et al, 2005; Bi and Coffin, 2006; Hossain et al, 1998) and the second type employs 2 pin jointed corners at the location where the load is applied (Castenie et al, 2004; Kuenzi et al, 1962; Youngquest and Kuenzi, 1961; Bryan, 1961). The first type was designed based on the assumption that in the real industry application of wall panel, all the edges are clamped using a rigid border. However, during the panel test the specimen may experience lower stress since part of load was transferred directly to the other load pin without passes through the specimen. The second type was designed to overcome this shortcoming.

Third, the typical panel test specimens for the diagonal shear test are in the range of 300-850 mm in size which is significantly smaller than the typical size of a racking wall test. Lastly, the typical failure modes of diagonal tension test are typically crimping, sudden failure of the core, skin shear failure shear buckling of the panel and skin wrinkling. The outcomes from the review are considered in the design and development of testing rigs by the authors.

6.3. Investigation on Various Shear Testing Rig Designs

6.3.1. Hardwood testing rig

Initially, it was decided to use a hardwood loading rail or testing rig as previously used by Youngquest and Kuenzi (1961) and Kuenzi et al (1962). In that work, the specimens were glued to the hardwood loading rail using epoxy glue. The panel was tested in a hydraulic testing machine, Avery Testing Machine, with the maximum load capacity of 100 kN. The load was applied through links attached to a central loading at each end of the vertical diagonal of the specimen (Figure 6.13). Two strain gauges were placed at the centre of the specimen to measure vertical and horizontal strain at the front and back side of the specimen using a strain data logger (System 5000). Unfortunately, it was observed that the panel premature failed at a very low load of approximately 3500 N. The result of the test is shown in Figure 6.12, while the testing set-up with the first proposed testing rig is presented in Figure 6.13.

The failure initiated at the glue line between the panel and the testing rig. The epoxy interface between the edge of specimen and loading rail was the weakest point of the testing arrangement. It was also found that preparing samples that perfectly fitted inside the loading frame was nearly impossible, while on the other hand a perfect match between specimen and loading rail is a prerequisite for a good bonding between them. Based on this preliminary test, it was decided to design a more appropriate testing rig and that the newly developed testing rig should be pre-tested prior to use in the real test.

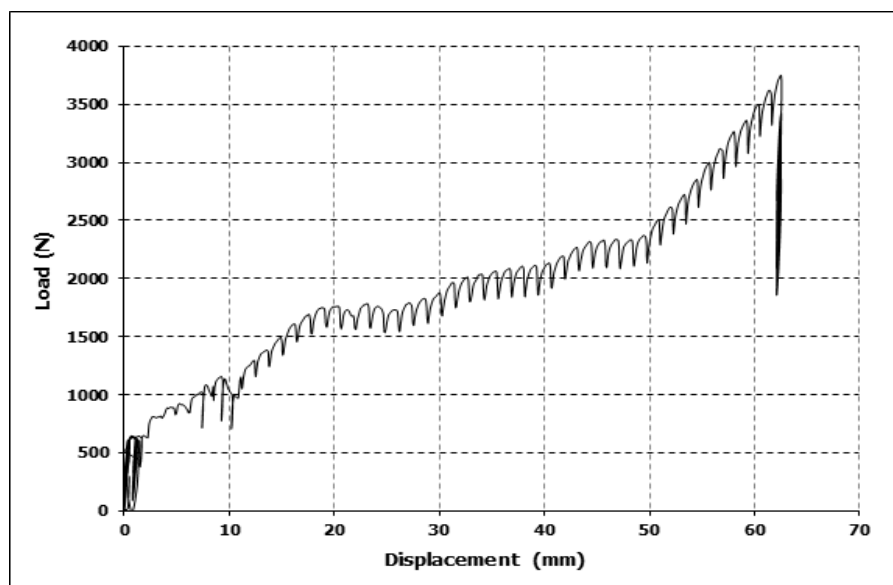


Figure 6.12. Test results of the test using hardwood testing rig

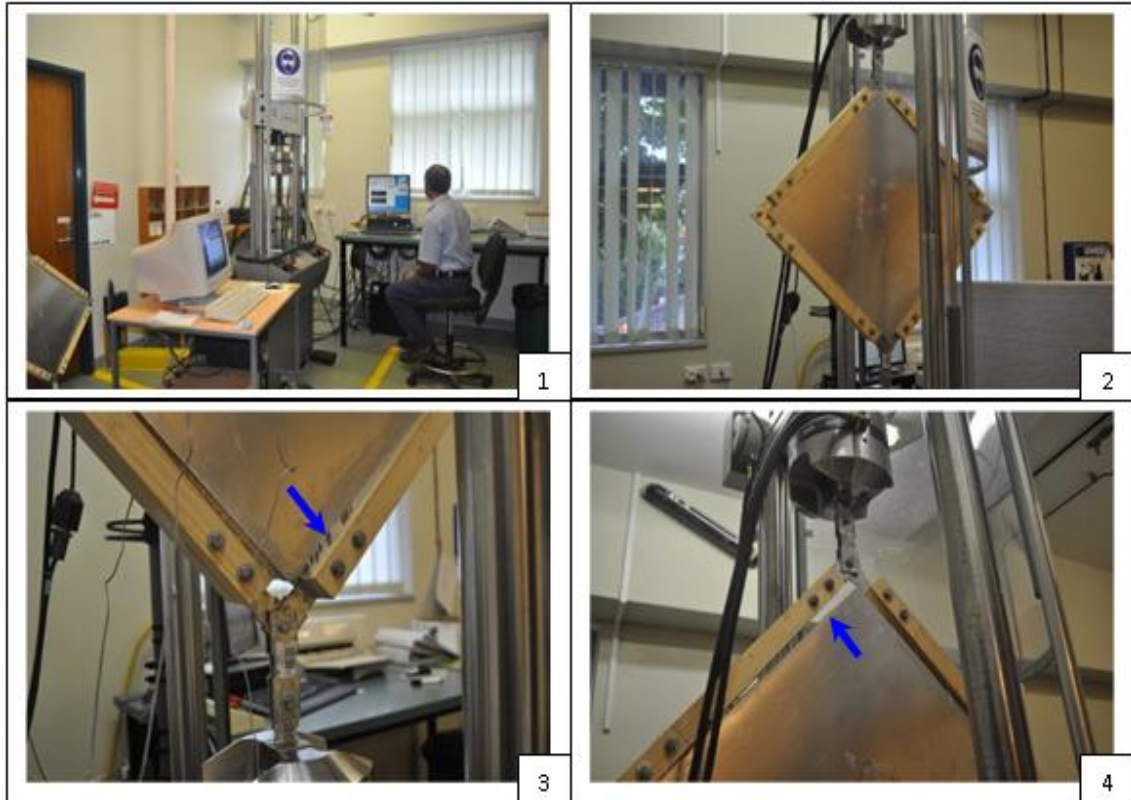


Figure 6.13. Testing set-up and failure mechanisms of the test with hardwood testing rig

6.3.2. Assessment of different types of testing rig using small-scale prototypes

Based on the preliminary prototype rig which was discussed in Section 6.3.1, five further different configurations of testing rigs were developed and assessed. The specimens used in the testing were prepared from a polyethylene sheet. The reason of using this specimen material was to observe the likely pattern of deformation during the progress of the testing. The basic idea of this evaluation was based on the work of Cao et al (2008), Sun and Pan (2005), Zhu et al (2007) and Mohammed et al (2000), where the in-plane shear deformation of woven fabric composite was assessed. The configuration of the test rig itself was based on the work of other researchers who were investigating the in-plane shear test of sandwich panel as presented in Table 6.1.

The frames were prepared using Balsa wood with the size of 220 x 220 mm. The specimens were attached to the loading rail using either glue or small bolts. The specimens were tested in a Hounsfield Testing Machine, with a maximum load capacity of 10 kN, which was adequate for the testing arrangement. The front and side views of each prototype of testing rig are shown in Figure 6.14.

Table 6.1. The configuration of small-scale testing rig prototypes

Frame types	Description	References
Frame A	Single discontinuous frame with pin at upper and bottom corners only. No pin was placed at side corners. Panel was placed inside and glued within the frame. Light wood stiffeners were glued around the edge to perfectly fit the panel inside the frame.	Kuenzi et al, 1962; Youngquest and Kuenzi,1961; Bryan, 1961.
Frame B	Double continuous frame with pin at all four corners. Panel was placed in between the upper and bottom frame and connected with bolts.	Morgenthaler et al, 2005; Hossain and Wright, 1998
Frame C	Single continuous frame with pin at all four corners. Panel was sitting on the frame and connected with bolts with upper unconnected frame.	Bi and Coffin, 2006
Frame D	Single continuous frame with pin at all four corners. Panel was placed inside the frame by gluing it to the frame.	Modification to the work of Kuenzi et al, 1962
Frame E	Single discontinuous frame with pins at upper and bottom corners only. Panel was placed inside by gluing it side by side with the frame. Similar to Frame A, but the frame members were shorter to avoid stress concentration at the side corner and also without light edge stiffeners.	Modification to the work of Kuenzi et al, 1962

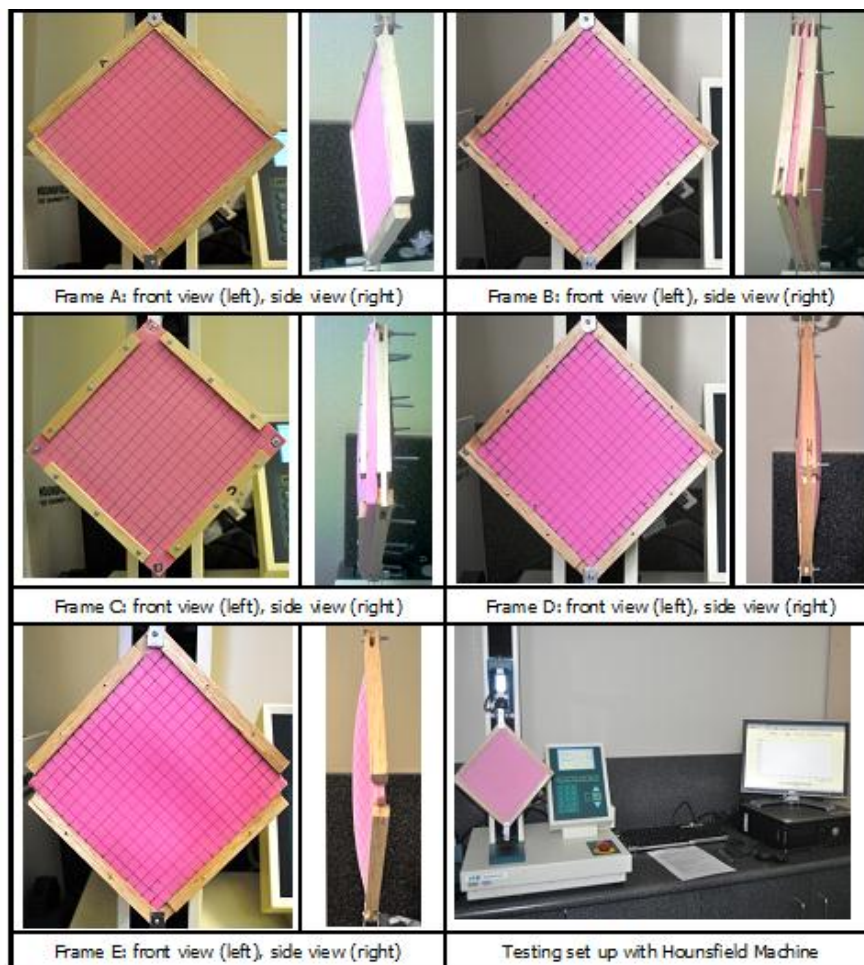


Figure 6.14. Front and side view of each prototype of testing rig

Figure 6.15 shows the bar-chart of the testing results while Figure 6.16 presents the load-deformation curves. Some important findings from the testing are summarised as follows: Frames A and E demonstrated similar performance for both load and extension as their configuration were almost identical. Frames C and D achieved a similar failure load but the extension was different. Frame B obtained the lowest failure load among all testing specimens while the extension was higher than Frame D but lower than the rest specimens. Although Frame B provided the lowest load transferred to the polyethylene sheet material, the fact that the frames did not fail during the testing process suggested that it might be producing a uniform shear distribution within the specimen.

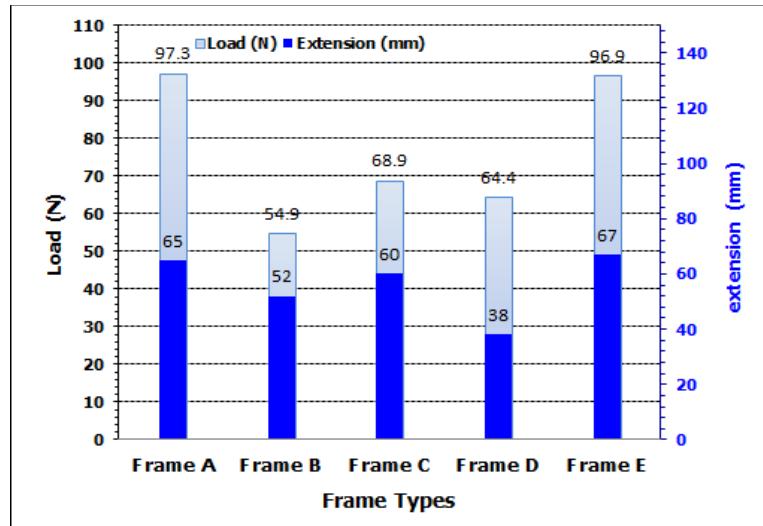


Figure 6.15. The bar-chart of the testing results for each frame prototype

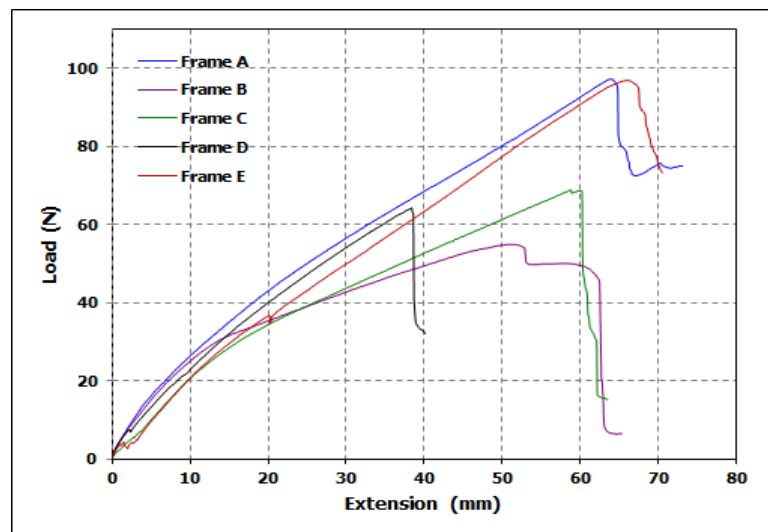


Figure 6.16. Load-extension graph of the testing results for each frame prototype

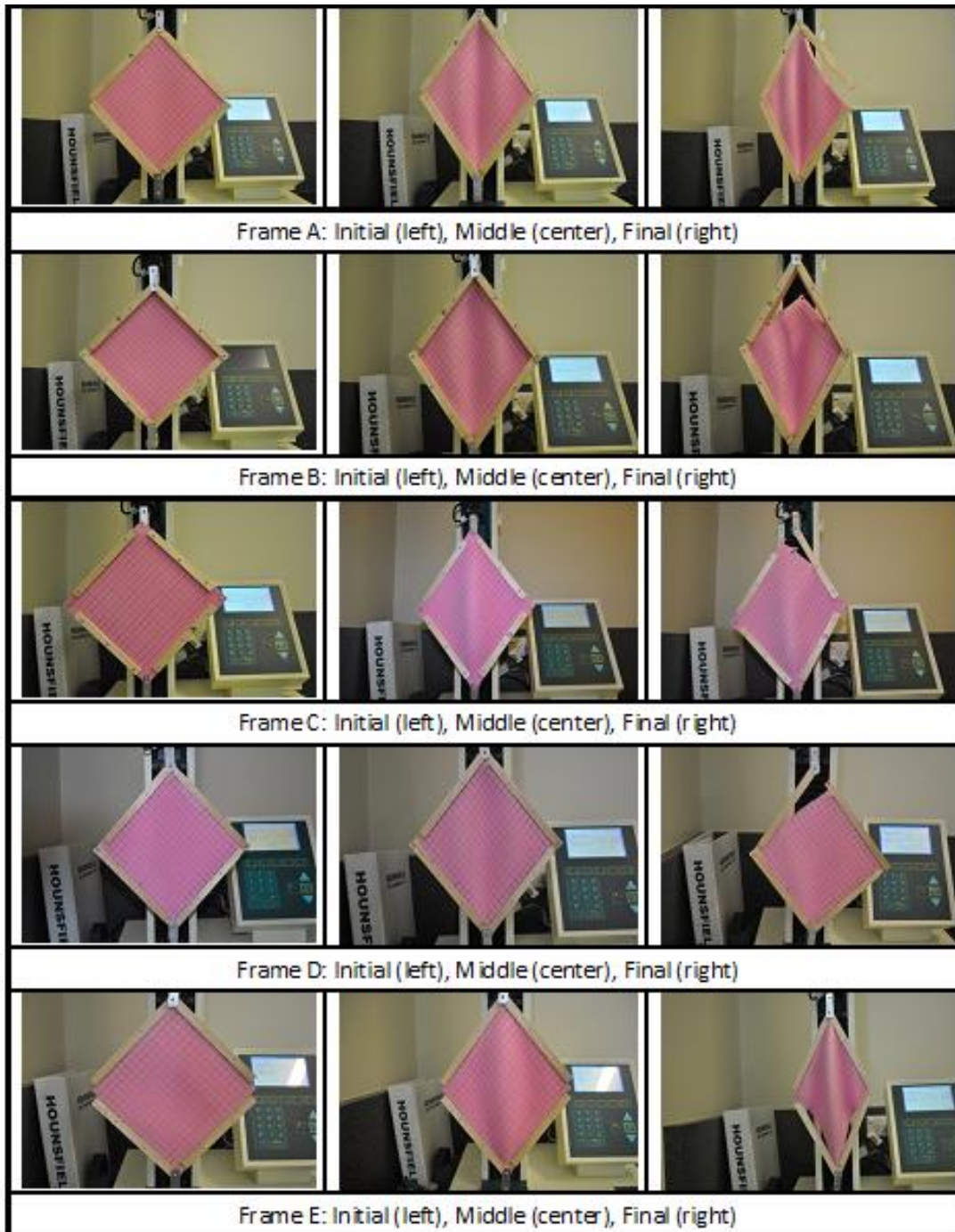


Figure 6.17. Failure mechanism for each frame prototype

As it can be seen from the failure mechanism showed in Figure 6.17, all four frames (A,C,D and E) failed suddenly which indicated that those attained higher loads might also be contributed by the frame, which is not preferred in this type of test. Following this testing result, the prototype Frame B was selected for further investigation for the in-plane shear testing of the sandwich panel.

6.4. Design of the Steel Testing Rig

6.4.1. Testing rig preparation

Figure 6.18 shows the testing rig developed for the in-plane shear testing of the sandwich panel. The frame was prepared using steel plate as higher loads were expected for the actual testing of sandwich panel. The overall size of the frame was approximately 580 x 580 mm, providing a 500 x 500 mm clear size within the frame for the specimens. All four corners were pin-jointed using bolts to obtain free-movement to vertical and horizontal direction. The panel specimen was then placed in the frame by connecting upper and bottom frame using 8 mm bolts, 6 for each side. The frame was connected to the MTS testing machine using extension plates linked with another single plate to match the space between the machine's loading points.

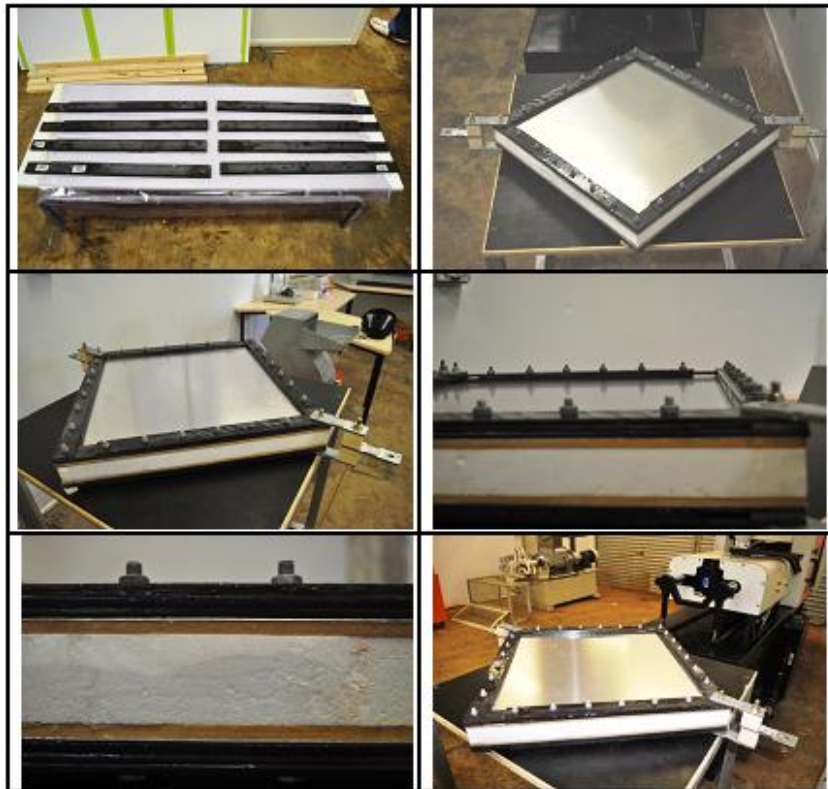


Figure 6.18. Proposed steel testing rig with the specimen inside

6.4.2. Trial testing with MDF board specimen

A number of trial tests with MDF board specimens were conducted prior to carrying out the actual testing to ensure that the rig was capable fulfilling its purpose. Most importantly was to make sure that the testing rig was able to transfer a shear load

along the edge of the panel. A second reason was to observe the effect of cutting the corner of the specimen as suggested by Kuenzi et al (1962) to reduce the stress concentration around the corner of the panel and the frame. The MDF board was cut to the required size into two shapes; one as a whole panel specimen and the other one was a specimen with the corners cut. The setting up and the final condition of the panels after the completion of the test is presented in Figure 6.19.

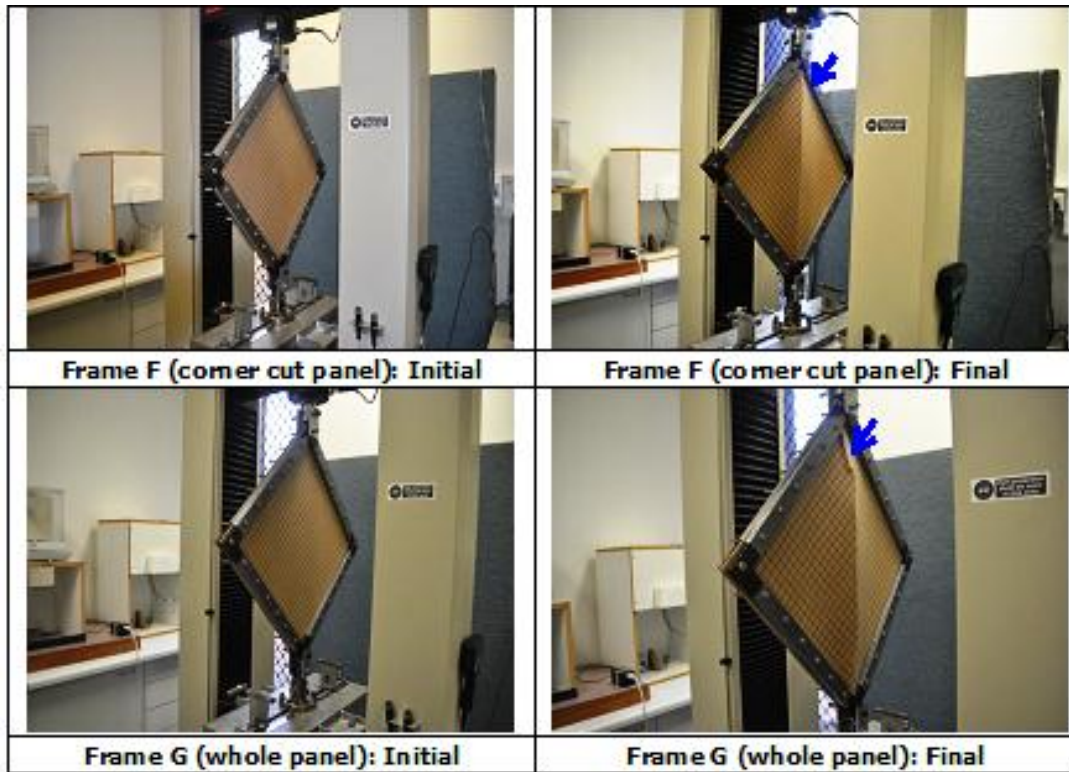


Figure 6.19. The setting-up of the trial test with MDF board specimens

The results of the trial tests are presented in Figure 6.20 and Figure 6.21. It can be observed from the bar-chart, Figure 6.20, that the whole panel showed a slightly higher load carrying capacity, which was 27616 N. This value was only about 8.39 % higher compared to the load carrying capacity of the corner cut panel. However, if a carefully attention is given to the curves provided by both specimens, as shown in Figure 6.21, it can be noticed that an early failure was occurred inside the whole panel at much lower load of approximately 19800 N compared to the first sign of failure existed in the corner cut panel specimen which was approximately 24400 N. The early failure occurred at the whole panel specimen was most likely due to the stress concentration at the corner of the testing rig as also indicated by the post-test condition as shown in Figure 6.19.

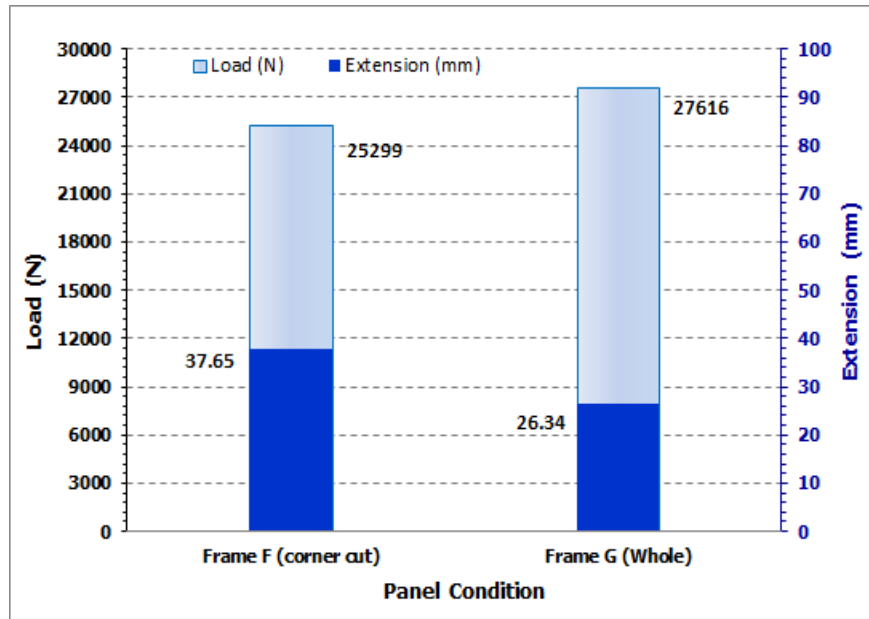


Figure 6.20. The bar-chart of the trial test results with MDF panels

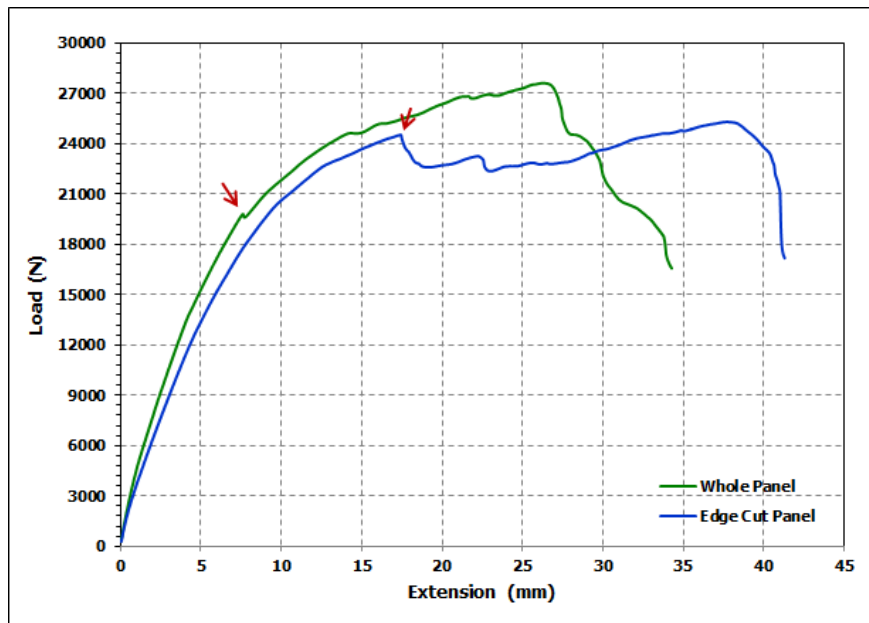


Figure 6.21. The load-deflection curves of the trial test results with MDF panels

6.4.3. Failure patterns

After removing the panels from the testing rig, a thorough examination was carried out of the failure pattern of the panels. The observation was based on the cracking path as it progressed during the test and for this purposes the cracking patterns were carefully marked to obtain a clear failure maps. The results of this work are presented in Figures 6.22 and 6.23.

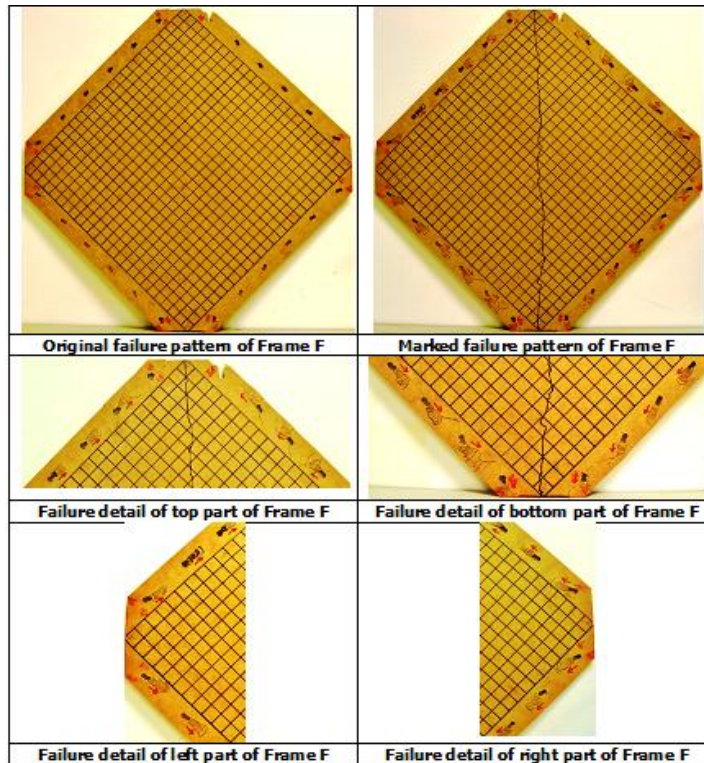


Figure 6.22. Post-test failure patterns of corner-cut MDF panels

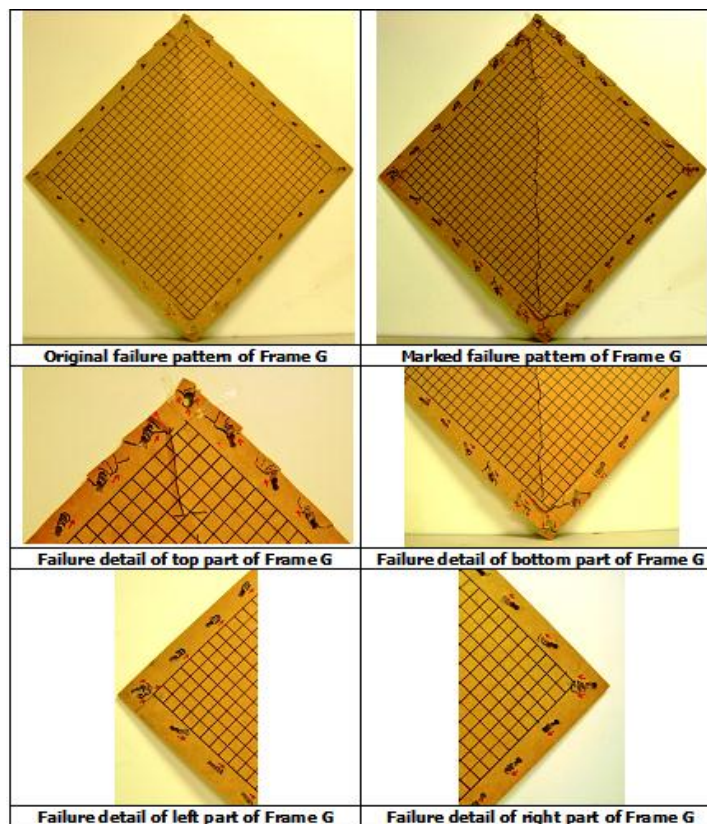


Figure 6.23. Post-test failure patterns of whole MDF panels

It is clearly seen in Figures 6.22 and 6.23 that the frame has successfully transferred the shear load along the edge of the panel as indicated by the failure patterns. The trial test using MDF board confirmed that the frame was able to transfer the shear load along the side of the panel producing pure shear inside the panel. It is also important to note that cutting the corners of the panel specimen has reduced the stress concentration at the corners, preventing the occurrence of early failure inside the tested specimen.

6.4.4. Trial testing with sandwich panel specimen

Having successfully employed the testing rig to induce the shear failure within the MDF panels, there remained a need to ensure that the loading frame was able to perform such a failure mechanism for the sandwich panels. Hence, some trial tests were conducted prior to the real in-plane shear test of the sandwich panels. The results of the trial test with sandwich panel specimen are presented in Figures 6.24 and 6.25. As it can be seen from the figures, the maximum load reached at the first trial was only 19269 N. The second and third trials obtained quite comparable maximum load, which was 66992 N and 57780 N, respectively. The last trial obtained a maximum load of 90301 N before the test was terminated.

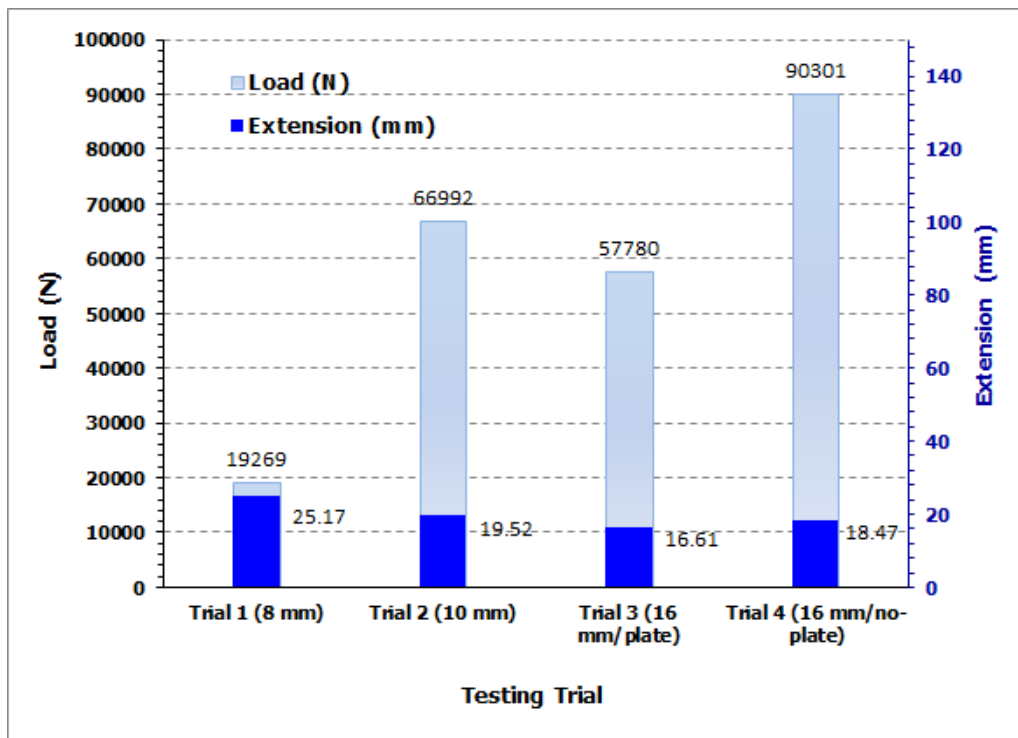


Figure 6.24. Bar-chart of trial tests with different conditions

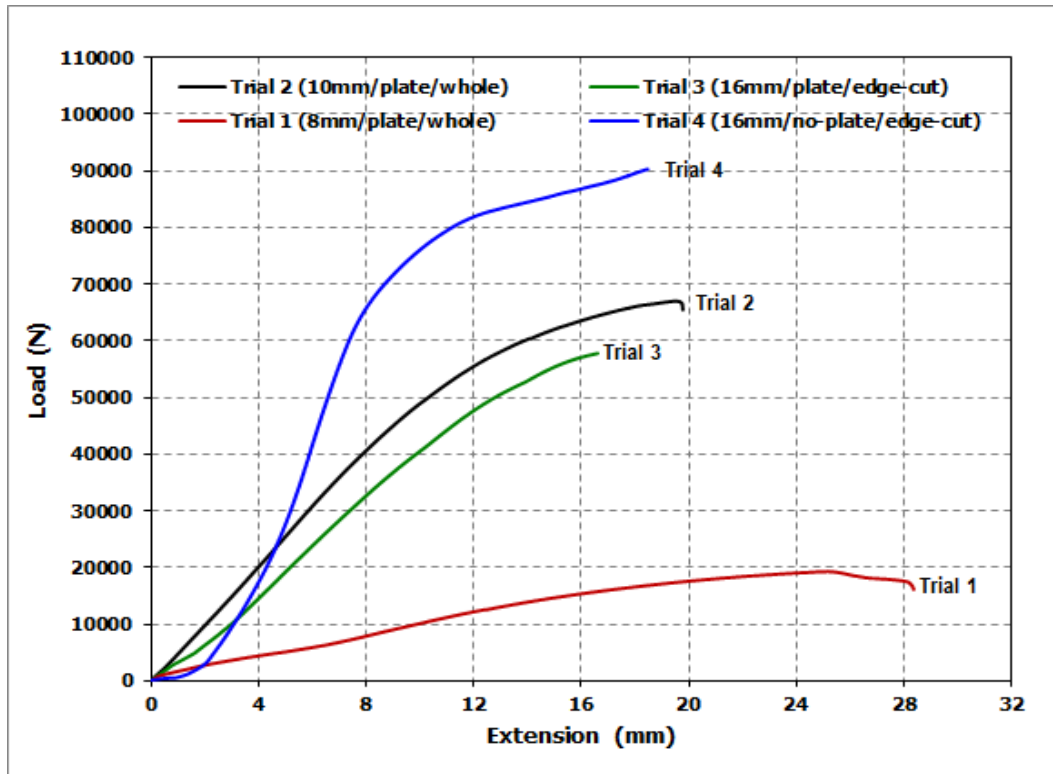


Figure 6.25. Load-extension graphs of trial tests with different conditions

The first trial was carried out using connection bolts of 8 mm diameter. Four strain gauges were placed at the front and back side, 2 on each side and a data logger System 5000 was connected to the machine for recording the strain. The testing was prematurely terminated as the top and bottom connecting bolts failed at the load of 19269 N. It was decided to modify the connection bolt to a bigger and stronger size. In the second trial, the connecting bolt at the loading point was changed to 16 mm diameter in size while the connecting bolt inside the panel was a 10 mm in size. Again the failure was occurred at the connecting bolt, which was at the connecting bolt within the panel at the maximum load of approximately 66992 N. The failure mechanisms for those two trials are presented in Figure 6.26. Based on the unsuccessfully results, it was decided to replace the connecting bolt within the panel with larger bolts with a diameter of 16 mm. Thus, both connecting bolt were 16 mm in size. The failure mechanism for the subsequent trials is presented in Figure 6.27. It can be observed from the figure that again the connecting bolt was the vulnerable point for the initiation of failure mechanism. The connecting bolt at the load transfer point was bent and the test was deliberately terminated at the load of 57780 N.

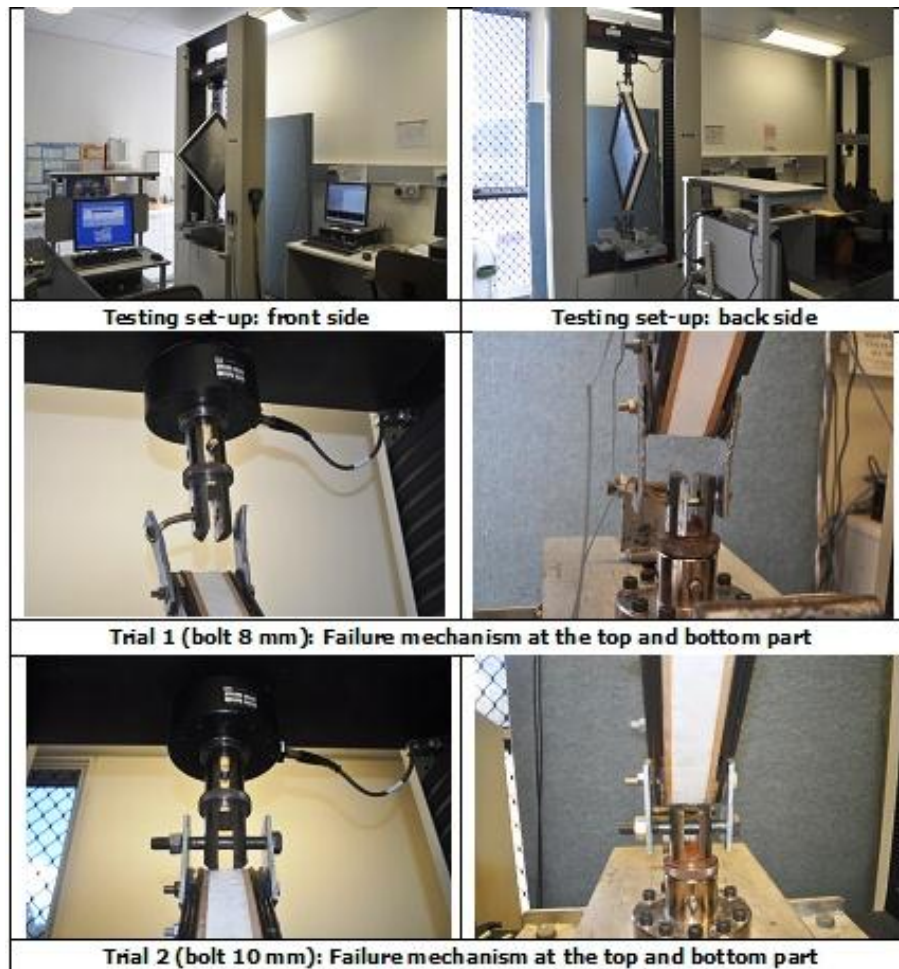


Figure 6.26. Failure mechanisms at the first and second trial of the test

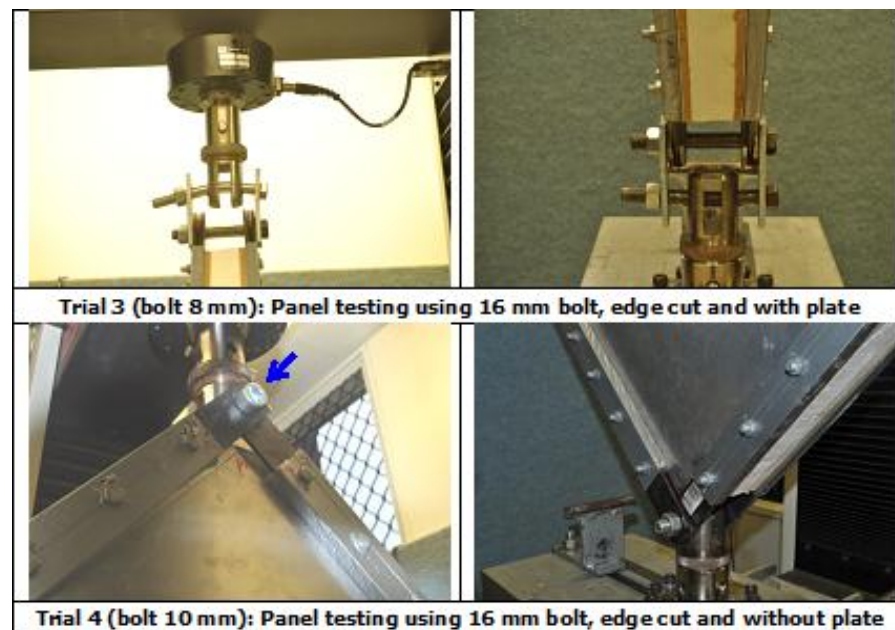


Figure 6.27. Failure mechanisms at the third and fourth trial of the test

Having carefully observed the typical failure pattern, it was decided to omit the connection plate between panel and load transfer point of the machine. The machine was then connected to the frame without an extension plate which meant that there was only a single connecting bolt between the testing rig and the testing machine. The testing results indicated that the new approach was successful. The maximum achieved failure load was 90301 N without any noticeable damage of the connecting bolts. The testing was deliberately stopped at this load as the maximum capacity of the MTS machine is only 100 KN. It is worth noting that the panel was still able to carry some further load beyond this point. The final developed steel testing rig was able to successfully allow examination of the in-plane shear behaviour of sandwich panel. The final plan would be to reduce the panel size to allow testing to failure using the available MTS testing machine.

6.5. Chapter Conclusions

The main conclusion drawn from this chapter was that the steel testing rig designed has been able to investigate the in-plane shear behaviour of sandwich panel. Some important findings are outlined as follows.

- 1) The diagonal tension shear test has been re-considered by some researchers for both cost and resources reasons to investigate the in-plane shear behaviour of wall panels, especially at the initial development of a product. Such a test only requires a smaller size specimen than the standard racking test which may reduce the cost. It also has the advantage of being used on standard test machines.
- 2) The final testing rig developed has all four corners pin-jointed using bolts to obtain free-movement to vertical and horizontal directions. This works better than those with only two pin-jointed corner at the top and bottom corners. In addition, cutting the corners of specimen has prevented the presence of early failure mechanism due to stress concentration.
- 3) Connecting the testing rig to the load transfer point of the machine without any extension plate has prevented the stress concentration at such particular point resulting in a good transformation of load and successfully inducing shear stress within the panel.

CHAPTER 7

THE IN-PLANE SHEAR BEHAVIOUR OF SUSTAINABLE HYBRID COMPOSITE SANDWICH PANELS

7.1. General

The sustainable hybrid sandwich panel developed through this research has shown excellent performance under flexural loading as discussed in Chapter 5. However, the flexural behaviour examined in the previous chapter was in the form of a beam structure. It is also of equal importance to examine the behaviour of newly developed hybrid sandwich as a panel structure, such as for a wall panel. Shear behaviour, or in-plane shear behaviour, is a critical behaviour that needs to be carefully understood when using sandwich panels for a wall. This is of special significance when the wall is considered as being structural. It was expected that introducing an intermediate layer could enhance the in-plane shear behaviour of sandwich panels. This chapter discusses the in-plane shear behaviour of the new developed hybrid sandwich panel based on the diagonal tension test developed by the author as described earlier in Chapter 6.

7.2. Theoretical concept of diagonal tension shear test

A number of theoretical backgrounds have been proposed to study the in-plane shear behaviour of composite materials under diagonal tension test. Some of the relevant available literature is discussed. Mohammed et al (2000) used diagonal tension shear testing to investigate the shear deformation and micro mechanics of woven fabrics composites. Although the study was not related to a sandwich structure, it provides good basic theory of diagonal tension shear testing. The geometry of the testing set-up is illustrated in Figure 7.1. The testing machine measured the tensile force, F_x , and the extension, $2\Delta l$. The shear load was obtained by translating the tensile load, F_x , into shear components, F_s , using Equation 7.1.

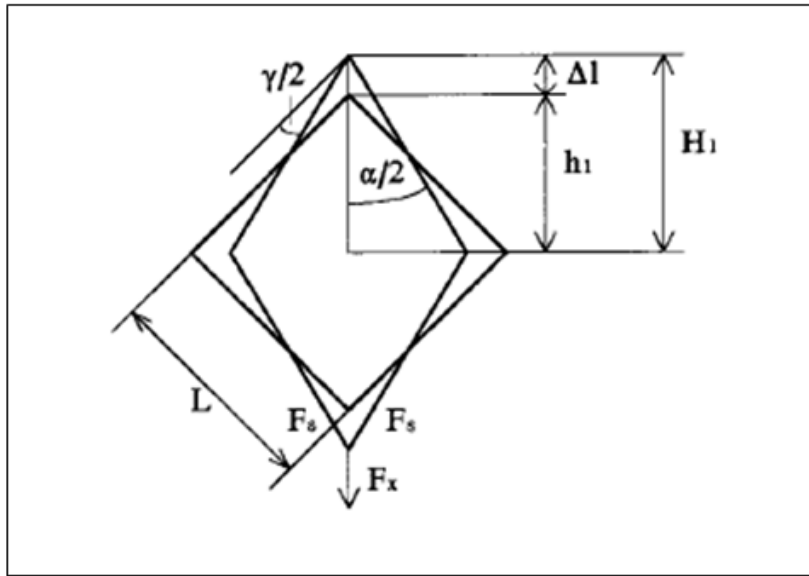


Figure 7.1. Geometrical analysis of the picture frame (Mohammed et al, 2000)

The tensile force can be translated into shear components, F_s by the following relation:

$$F_s = \frac{F_x}{2 \cos(\alpha/2)} \quad \dots\dots\dots 7.1$$

If the thickness (H) of the fabric does not change during shear before wrinkling occurs and the shear stress is homogeneous, then the shear stress can be obtained using the following equation.

$$\tau_s = \frac{F_s}{LH} \quad \dots\dots\dots 7.2$$

In the discussions of the shear test results, Mohammed et al (2000) plotted the applied load from the Instron machine against the shear angle. Shear angle is an important parameter in the investigation of shear behaviour of composite structure. Based on the geometry as seen in Figure 7.1, it follows:

$$H_1 = h_1 + \Delta L \quad \dots\dots\dots 7.3$$

$$\cos(\alpha/2) = \frac{L \cos(\pi/4) + \Delta L}{L} \quad \dots\dots\dots 7.4$$

The shear angle is then expressed as:

$$\gamma = \frac{\pi}{2} - \alpha \quad \dots\dots\dots 7.5$$

A similar equation was employed by Cao et al (2008) when they studied the mechanical behaviour of woven fabric composites. The geometry of the testing set up of this work is shown in Figure 7.2. In the research, the shear force (F_s) was calculated based upon the measured tensile force and the frame configuration as:

$$F_s = \frac{F}{2 \cos \alpha} = \frac{F'' - F'}{2 \cos \alpha} \dots\dots\dots 7.6$$

Where F is the net load obtained by subtracting an offset value of F' from the machine and recorded value of F'' when fabric is being deformed in the picture frame. The shear angle in this work was obtained by using Equation 7.7. In this work, Cao et al (2008) plotted the shear force versus shear angle when they discussed the shear test results.

$$\gamma = 90^\circ - 2\theta \dots\dots\dots 7.7$$

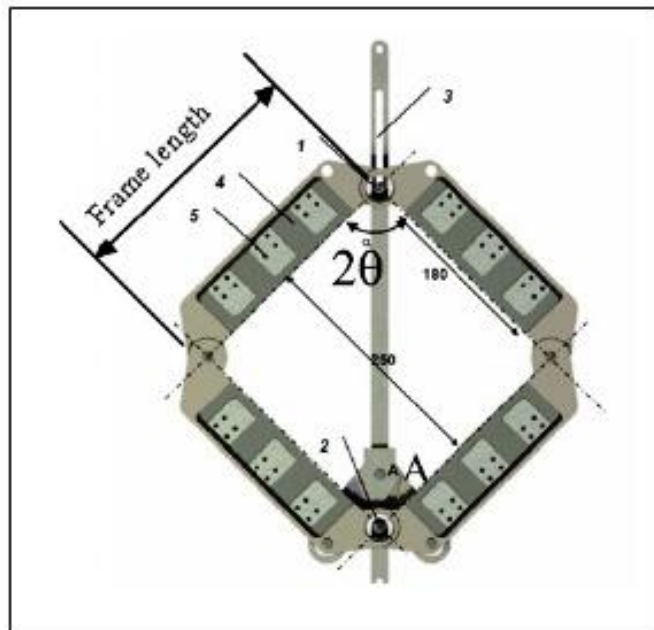


Figure 7.2. Schematic of the picture frame (Cao et al, 2008)

Another study that also employed the diagonal tension shear test was conducted by Hossain and Wright (1998). The study was aimed at investigating the behaviour of profiled concrete shear panels that may be used as core wall framed construction. The geometrical configuration of the test is shown in Figure 7.3. It was assumed that when the diagonal force is applied through the top hinge, the test panel $abcd$ undergoes shear deformation resulting in a deformed shape of $ab'c'd'$. When the deformed shape is

rotated clockwise in which ab' coincides with ab , the shear force (V) and shear displacement (δ) can be obtained using the following equations:

$$V = 1/2 P \cos \phi_d \quad \dots\dots\dots 7.8$$

$$\delta = \frac{\Delta}{\cos \phi_d} \quad \dots\dots\dots 7.9$$

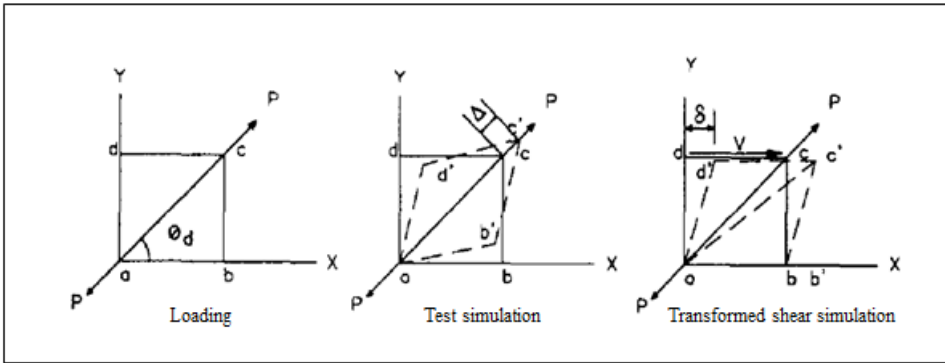


Figure 7.3. Schematic of the diagonal tension test (Hossain and Wright, 1998)

The above concept of obtaining shear displacement is similar to the method described in ASTM E 564 (ASTM, 1997). According to this standard, which is a standard practice for static load tests for panels of building construction, the horizontal shear displacement is calculated on the basis of the diagonal elongation. The schematic of the testing set up is shown in Figure 7.4.

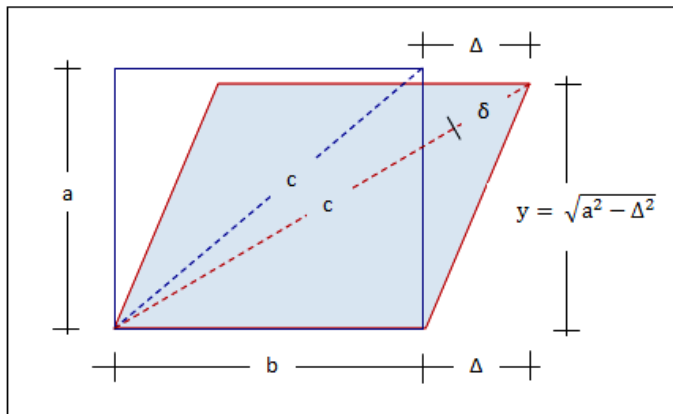


Figure 7.4. Schematic of testing set up as per ASTM 564 (ASTM, 1997)

As it can be seen in the figure, the diagonal of the original and deformed shape are expressed as follows:

$$c^2 = a^2 + b^2 \quad \dots\dots\dots 7.10$$

$$(c + \delta)^2 = (b + \Delta)^2 + y^2 \quad \dots\dots\dots 7.11$$

Substituting Equation 7.10 into Equation 7.11 gives:

$$a^2 - \Delta^2 + \delta^2 + 2c\delta - 2b\Delta = y^2 \quad \dots\dots\dots 7.12$$

If the value of:

$$\delta^2 + 2c\delta - 2b\Delta = 0 \quad \dots\dots\dots 7.13$$

Then,

$$y = \sqrt{a^2 - \Delta^2} \quad \dots\dots\dots 7.14$$

The horizontal shear displacement (Δ) can be obtained by solving Equation 7.13, which gives:

$$\Delta = \frac{\delta^2 + 2c\delta}{2b} \quad \dots\dots\dots 7.15$$

In the shear test result discussions, they plotted the diagonal load against the diagonal deformation. The paper focussed on the discussion of the strain analysis within the panels. Another important theoretical concept for diagonal tension shear test was proposed by Kunzi et al (1962) for a sandwich structure. The theoretical framework of this work was developed based upon the assumption that sandwich panels failed due to shear buckling load. The stresses for the tension diagonal in-plane shear test were calculated using Equation 7.16.

$$q_f = \frac{P}{2f\sqrt{a^2 + b^2}} \quad \dots\dots\dots 7.16$$

Where a and b are the width and length of the panel, $\sqrt{a^2 + b^2}$ is the diagonal length of the panel and f is the thickness of the face. As the panels tested in the experiment had an equal length and width, the above equation can be simplified as:

$$q_f = \frac{P}{2\sqrt{2}af} \quad \dots\dots\dots 7.17$$

For this research, the interpretation of the experiment results was based upon the framework developed by the above researchers (Mohammed et al, 2000 and Kuenzi et al, 1962)

7.3. Sample preparation

The sandwich panel specimens for in-plane shear testing were prepared in the same manner as outlined for the samples for flexural testing. Jute and MDF laminates

were selected for the intermediate layer. The properties of Aluminium skin and EPS core as presented in Table 5.1 in Chapter 5 were used for the theoretical analysis. The procedures for sample preparation were as discussed in Chapter 4. The sandwich panel specimens were prepared using a manual pressing system in which all constituent parts were cut into the same length and width and glued together using Kwik Grip Advanced adhesive. It was slightly more difficult to prepare the required EPS core with hot knife foam cutter as previously used for beam specimens. A special tool, as presented in Figure 7.5, was then prepared to slice the EPS core to obtain the required thickness. The experiment which was designed as a single factor experiment only allowed one parameter to be varied. Hence when the material for the intermediate layer was selected as the single factor to be varied during the experiment, all other parameters include the thickness of the specimens were maintained constant.

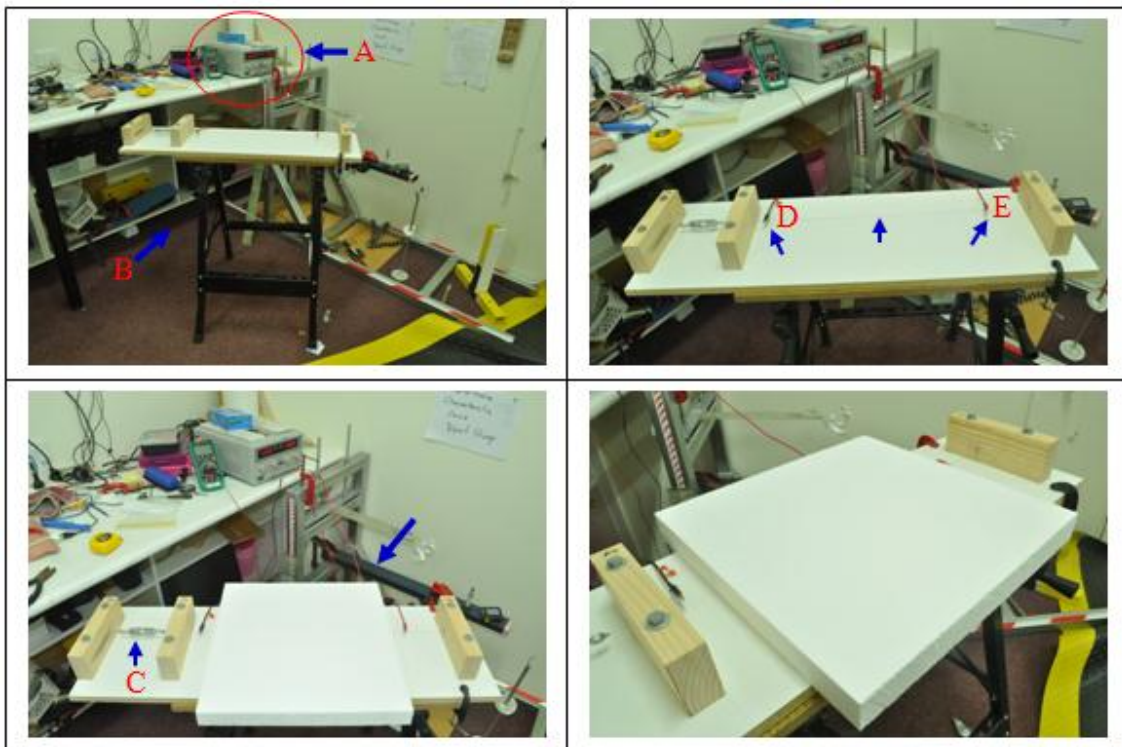


Figure 7.5. Special equipment and process of cutting EPS core for shear panel. (A) Volt-ampere, (B) Supporting frame, (C) Eye bolts, (D) and (E) Hot wire.

The specimens had overall dimensions of 380 x 380 mm providing a clear internal dimension of 300 x 300 mm between frame boundaries. The width of the steel frame was 40 mm each that makes up the total width of 80 mm. The overall thickness was maintained at 26 mm for all specimens. The aluminium sheet with the thickness of 0.5

mm was used as the skins while Jute and medium density fibre (MDF) with a thickness of 3 mm were employed as the intermediate layer. Control sandwich panels without intermediate layer were also prepared for comparison purposes. The thickness of EPS core for the control specimens was 25 mm and 19 mm for the specimens with intermediate layer. Each specimen group was replicated 5 times with a total of 15 samples tested. The sample arrangement for the in-plane shear specimens is shown in Table 7.1. The process of preparing the sandwich panel specimens for such testing is shown in Figure 7.6.

Table 7.1. Sample arrangements for in-plane shear testing

Samples Code	Skin		Intermediate layer		Core		Number of samples
	Material	Thickness	Material	Thickness	Material	Thickness	
CTR	Aluminium	0.5 mm	None	-	EPS	25 mm	5
JFC	Aluminium	0.5 mm	Jute	3 mm	EPS	19 mm	5
MDF	Aluminium	0.5 mm	Hemp	3 mm	EPS	19 mm	5
Total							15

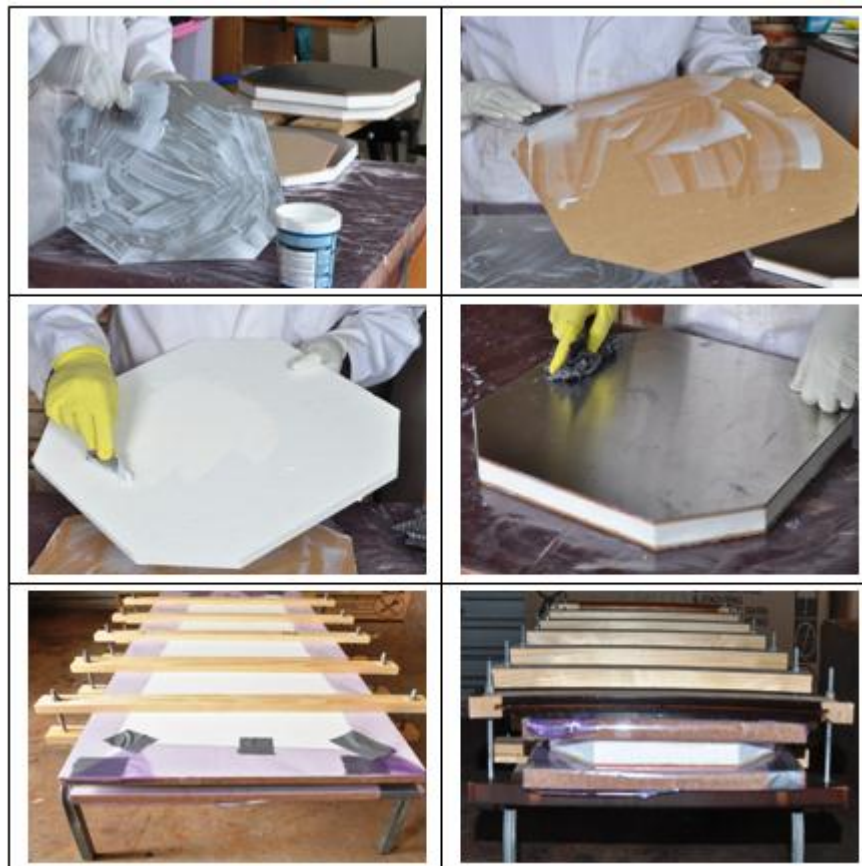


Figure 7.6. Fabrication process for shear panel specimens

7.4. The Experimental Program

As previously described in Chapter 6, the panels were tested by applying a tensile force along the diagonal of the test frame simulating pure shear. The diagonal force applied to the top hinge was transferred to the shear frame through a connector plate between the load cell and the testing rig. The load was then further transferred via a corner bolt with a diameter of 16 mm and frame members to the panel and finally transmitted to the bottom hinge. The test panels were clamped between pairs of steel frame members using 6 bolts with a diameter of 8 mm. This provided adequate clamping force for shear forces transfer from the shear frame to the test panels by friction. The testing rig enables to freely rotate by placing a pin bolt with the diameter of 16 mm at each corner. This ensured that the frame did not contribute to the load carrying capacity of the system. The corners of the panel were cut so that there was approximately 5.6 mm clearance in order to enable the connector plate to go through to the frame while minimizing stress concentration at the corners. The general schematic details of the shear testing rig assembly are shown in Figure 7.7, while Figure 7.8 presents the actual set up of the testing.



Figure 7.7. Schematic illustration of diagonal tension shear test

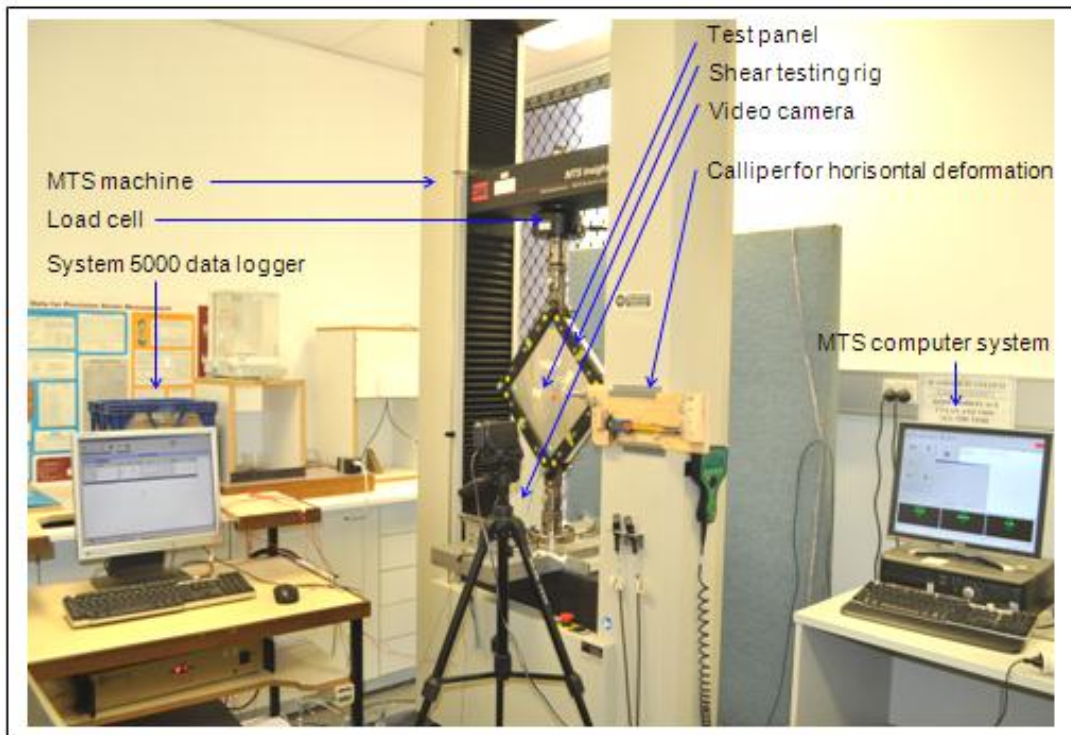


Figure 7.8. Actual test set-up for sandwich panel under diagonal tension shear test

The load was applied through a 100 kN MTS servo-hydraulic universal testing machine using a load rate of 5 mm/min. Strain gauges were placed on the test panels to evaluate the strain evolution during the course of the test. The strain gauges were produced by Tokyo Sokki Kenkyujo Co Ltd with the gauge length of 60 mm and gauge factor of $2.11 \pm 1\%$. The strain gauges were attached directly to the surface of sandwich panels using cyanoacrylate adhesive, which also produced by Tokyo Sokki Kenkyujo Co Ltd. The strain gauges placed at the front side were labelled as A_1, A_2, \dots, A_6 and the corresponds strain gauges at the back side were labelled as B_1, B_2, \dots, B_6 . The first four gauges, A_1 to A_4 , were placed at the edges of the panels near the frame to evaluate the strain evolution along the edges of the panels. The strain gauge A_5 was placed along the vertical diagonal while strain gauge A_6 was located as to measure the strain at the horizontal diagonal of the panel. The same strain gauges placement configuration was used at the back side of the panels. A computer-aided data system, System 5000 data logger, was employed to monitor the load-deformation response and strains during testing. The load was applied incrementally until the failure of the test panels to determine the shear failure and also the mode of failure. The configuration of strain gauges placement is provided in Figure 7.9.

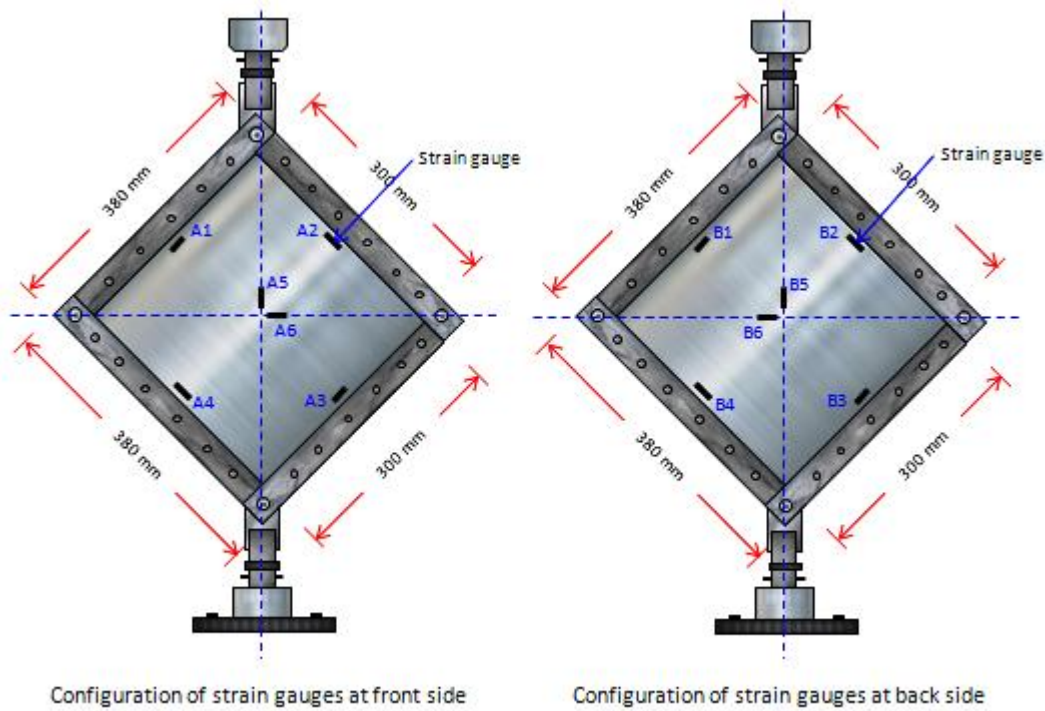


Figure 7.9. The configuration of strain gauges placement throughout the panels

7.5. Testing Results and Discussions

Several important aspects of the in-plane shear testing of the developed sandwich panel will be discussed in detail here. For comparative purposes, the behaviour of the hybrid sandwich panels will be compared to that of conventional sandwich panels as a control group.

7.5.1. Comparison of ultimate load, in-plane shear load and shear stress

The results of the in-plane shear test are presented in Table 7.2. Data presented in column 3 and 4 were obtained from the experimental testing. The shear loads in column 5 were obtained using Equation 7.1 while the shear stresses in column 6 were obtained using Equation 7.2. The thickness H in Equation 7.2 referred as the whole thickness of the composite laminate as it was only a single layer laminate. In this experiment, H is the effective thickness of the specimen which was equal to the total thickness of the skins for CTR specimens. For hybrid sandwich panels, the effective thickness was calculated by introducing modular ratio (n) to transform the intermediate layer into an equivalent aluminium skin. The shear angles shown in column 7 were calculated as per

Equation 7.5. The shear displacements in column 8 were calculated based upon the general relationship of a shear angle and shear displacement which defined that the shear angle is equal to the shear displacement (Δ) divided by the width of a specimen (a) as shown in Figure 7.4.

Table 7.2. Diagonal tension shear test results

Specimen Group	Specimen	Diagonal Load (F_s) (N)	Extension (δ) (mm)	Shear Load (F_s) (N) Eq. 7.3	Shear Stress (τ_s) (MPa) Eq. 7.4	Shear Angle (γ) ($^\circ$) Eq. 7.7	Shear Displ. (Δ) (mm) Calculated
1	2	3	4	5	6	7	8
CTR	CTR-1	9228	7.73	6409.37	21.36	2.09	10.95
	CTR-2	10043	14.48	6868.10	22.89	3.96	20.78
	CTR-3	13575	22.75	9111.76	30.37	6.30	33.14
	CTR-4	9051	13.17	6208.24	20.69	3.60	18.86
	CTR-5	9367	12.05	6441.49	21.47	3.28	17.22
Average		10252	14.04	7007.79	23.36	3.85	20.19
Stdev		1894.74	5.49	1200.45	4.00	1.54	8.12
CV		18.48	39.11	17.13	17.13	40.03	40.24
JFC	JFC-1	49006	15.52	33434.46	79.61	4.25	22.32
	JFC-2	47921	19.73	32384.16	77.11	5.44	28.59
	JFC-3	53834	26.98	35795.47	85.23	7.52	39.61
	JFC-4	51127	14.72	34945.09	83.20	4.03	21.14
	JFC-5	47192	14.42	32277.60	76.85	3.95	20.69
Average		49816	18.27	33767.36	80.40	5.04	26.47
Stdev		2692.38	5.31	1560.75	3.72	1.51	8.00
CV		5.40	29.09	4.62	4.62	30.00	30.23
MDF	MDF-1	21809	23.38	14617.95	39.94	6.48	34.10
	MDF-2	22324	25.97	14877.05	40.65	7.23	38.06
	MDF-3	22442	29.38	14843.25	40.56	8.22	43.34
	MDF-4	22366	23.73	14979.57	40.93	6.58	34.63
	MDF-5	22908	29.92	15133.44	41.35	8.38	44.18
Average		22369.8	26.48	14890.25	40.68	7.38	38.86
Stdev		390.99	3.07	189.51	0.52	0.89	4.73
CV		1.75	11.59	1.27	1.27	12.08	12.18

The above experimental results of diagonal in-plane shear testing were plotted as the average of ultimate diagonal load, vertical deformation, in-plane shear load, shear displacement, shear stress and shear angle against the type of intermediate layer. As expected the experimental data for the MDF was the most consistent with a CV of only 1.75% (for F_s). The JFC data was also very good with a CV of 5.4% while the CV for CTR was surprisingly high at 18.48%, but it remained within acceptable levels. Figure 7.10 presents the average of ultimate diagonal load and vertical deformation against the type of intermediate layer of sandwich panel. As it can be observed from the figure, the average ultimate diagonal load for hybrid sandwich panels with JFC and MDF

intermediate layer was 49816 N and 22369 N, respectively. These values were significantly higher than the load carrying capacity of the sandwich panel without intermediate layer, which was only 10252.8 N.

In more general terms, it can be said that the introduction of JFC and MDF intermediate layer has increased the diagonal load carrying capacity of sandwich panels by 385.9% and 118.2%, respectively. These values were obtained by comparing the load carrying capacity of hybrid sandwich panels (JFC and MDF) to the control specimen group (CTR). The comparison between the two hybrid sandwich panels shows that the panels with JFC intermediate layer were stronger than the panels with the MDF intermediate layer by 122.7%. This indicates that the material employed for the intermediate layer can provide significant contribution to the overall performance of the hybrid sandwich panels. It also seen in the figure that the hybrid sandwich panels with the JFC intermediate layer were stiffer than the sandwich panels with MDF intermediate layer and the panels without an intermediate layer. The sandwich panels with JFC intermediate layer reached their ultimate loads with less deformation compared to the other two sandwich panels.

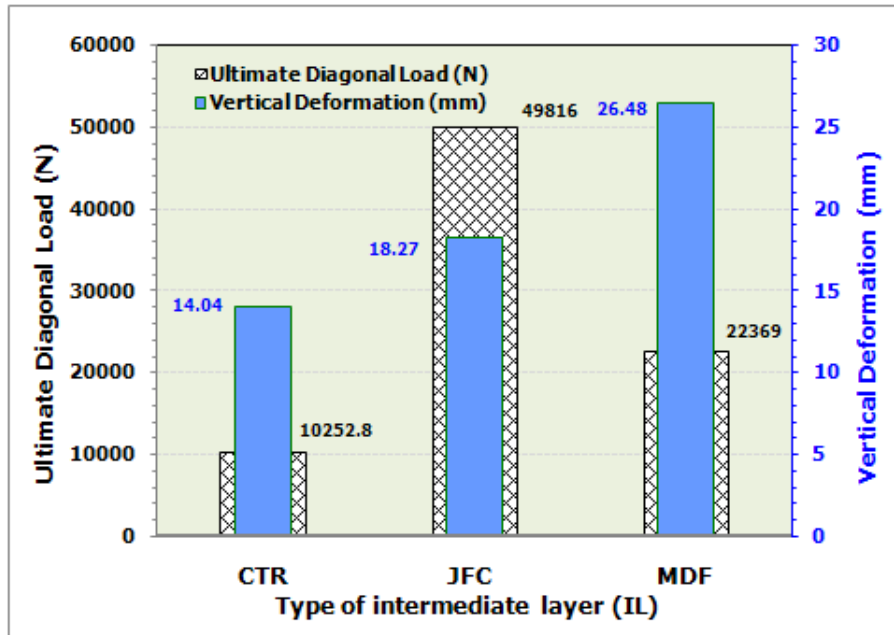


Figure 7.10. The average ultimate diagonal load and vertical deformation against the type of intermediate layer of sandwich panel

Figure 7.11 presents the average of in-plane shear load and shear displacement against the type of intermediate layer of sandwich panel, while Figure 7.12 shows the

ultimate shear stress and shear angle against the type of intermediate layer. In general, the two figures show a similar trend (Figure 7.10). The average in-plane shear load of sandwich panels with JFC and MDF intermediate layer was about 381.9% and 112.5% higher than the sandwich panels without an intermediate layer. The difference between the two hybrid sandwich panels was approximately 126.8% where the hybrid panels with a JFC intermediate layer carried a higher load than the panels with a MDF intermediate layer.

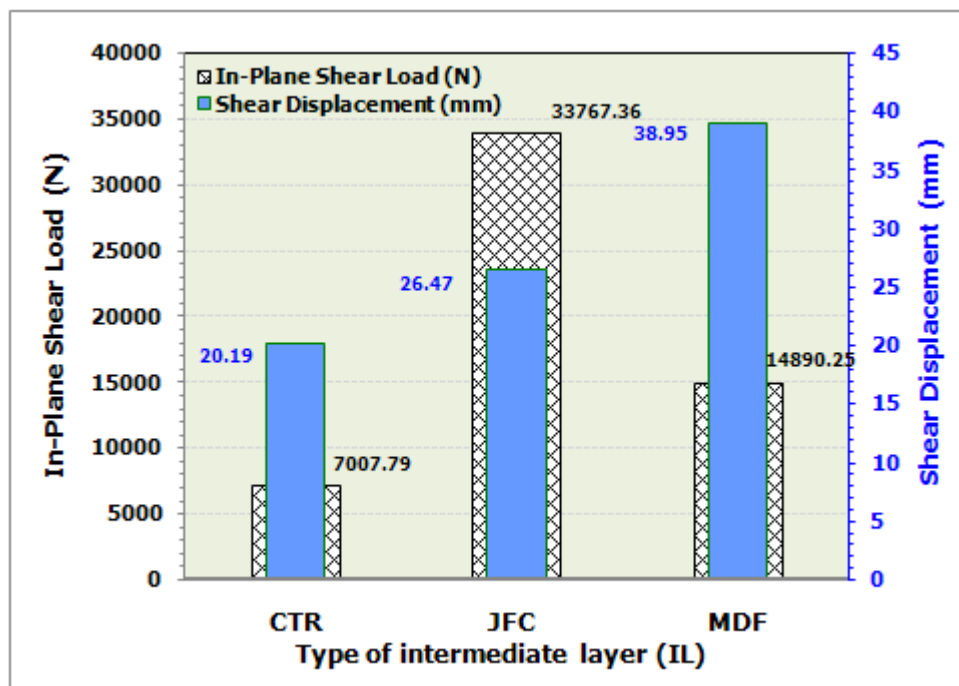


Figure 7.11. The average ultimate in-plane shear load and shear displacement against the type of intermediate layer of sandwich panel

Similarly, the comparison of percentage values show in Figure 7.12 was very close to the values configuration obtained in Figure 7.10. The average in-plane shear stress of sandwich panels was around 83.9 MPa for panels with the JFC intermediate layer and approximately 43.2 MPa for panels with MDF intermediate layer. The average shear stress of conventional panels without intermediate layer was only around 24.2 MPa. This means that the improvement of shear stress provided by the introduction of an intermediate layer was about 384.9% for the JFC and 118.3% for the MDF. The shear stress of panels with the JFC intermediate layer was superior to the panels with a MDF intermediate layer by 122.2%.

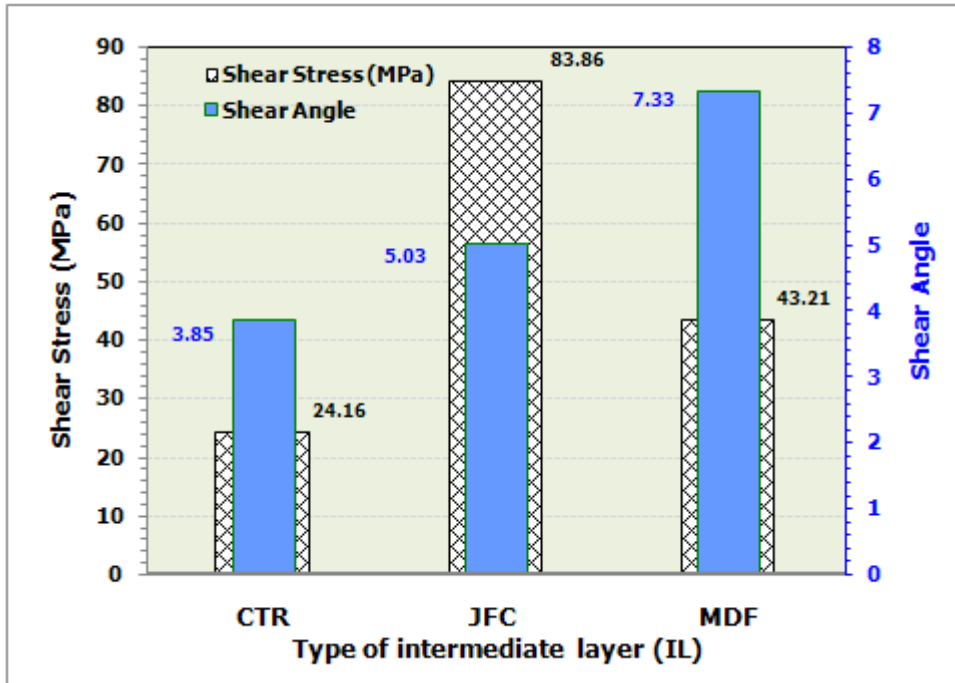


Figure 7.12. The average shear stress and shear angle against the type of intermediate layer of sandwich panel

7.5.2. Comparison of load-deflection behaviour

The graphs showing the relation between the ultimate diagonal load and the vertical extension for all the three specimen groups are presented in Figures 7.13 to 7.15. Prior to undertaking a comprehensive analysis, it is worth to describe how the specimens were labelled, as the labels are shown in a different way to the previous analysis. For example, in the current and further analysis the first specimen of control group (CTR) was labelled as CTR-1-12 (previously, CTR-1). The label had the meaning of being as the first out of five CTR specimens with 12 strain gauges attached, 6 at the front side and 6 at the back side, as previously shown in Figure 7.9.

Figure 7.13 presents the load-extension graph of conventional sandwich panels without any intermediate layer as the control (CTR) specimens. A quick inspection of the graph gives an impression that the specimens behaved differently. However, if a carefully attention is paid to the pattern of the graphs, they have a similar trend in that they start with some noise in the early part and then move up linearly until reaching an ultimate load of approximately 9000 N at an extension of around 6 mm. Beyond this point, there was a quick increase in the extension without any significant increase in load, indicating that the buckling load had been reached. The extension increased

continuously until about 13 mm and then the load dropped slightly until the test was automatically terminated by the testing machine.

Three out of five specimens behaved in almost identical pattern, which were CTR-1-12, CTR-4-4 and CTR-5-0. Specimen CTR-3-6 behaved differently compared to the others but the overall trend remained the same. It started with a noise at the early stage in which the extension increased quickly without any significant increase in load up to an extension of 2.5 mm. This phenomenon is called “slack deformation” (Bi and Coffin, 2006), which is a particular deformation caused by the slack connection of the designed shear tester frame to the MTS testing machine. They stated that it is difficult to completely zero out the weight of the frame and sample. Similar behaviour occurred at the first three of the tested specimens which were JFC-3-6, MDF-3-6 and CTR-3-6. It seems that at the first three specimens, the machine was not fully zeroed resulting in slack deformation.

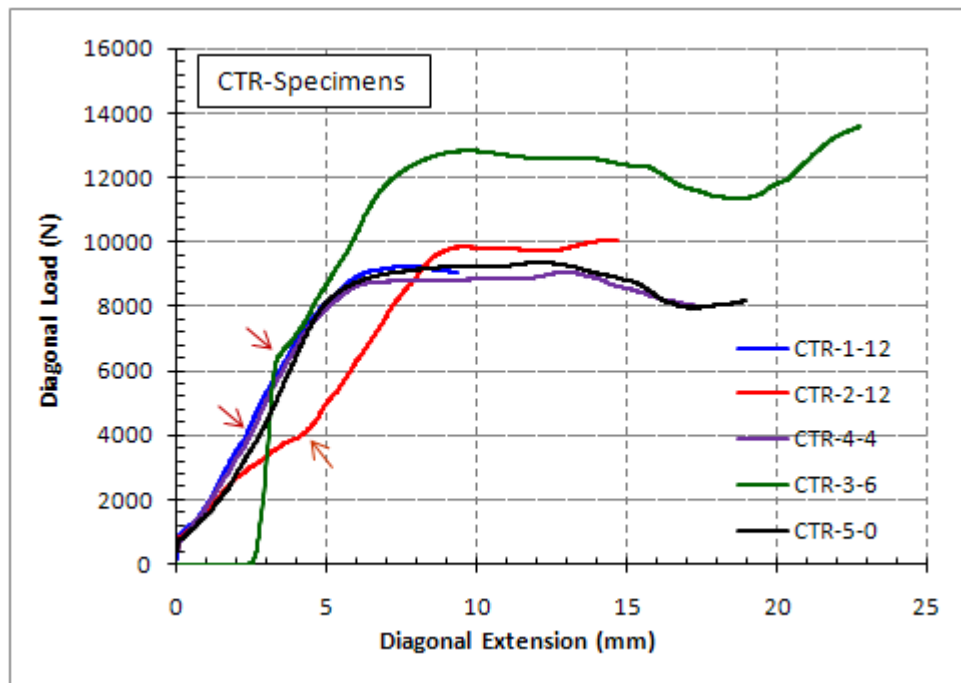


Figure 7.13. Diagonal load-vertival extension of CTR specimens

Specimen CTR-2-12 also appeared slightly different to the others. However, apart from that this might be a sign of early cracking of the core at the load of approximately 4000 N, the general pattern of load-extension graph of the specimen remained the same. The graph increased continuously until around 9800 N and then started to form a plastic region beyond the point of ultimate load. In short, it can be said that at the early stages

the CTR specimens behaved as an integral sandwich structure (indicated by the linear part of the graph), then as the stress induced by the buckle formation increased constantly, the panels then disintegrated. After this point only the skins carried the further load, as indicated by the plateau of the graph which represents a ductile behaviour of the aluminium skin until final failure was reached. The failure mechanism may take the form of skin buckle followed by a separation of skin and core due to the loss of the adhesive bond or a shear crimping of the skin. The diagonal load-extension graph of the hybrid sandwich panels with the JFC intermediate layer is presented in Figure 7.14. The general trend of the plots is similar.

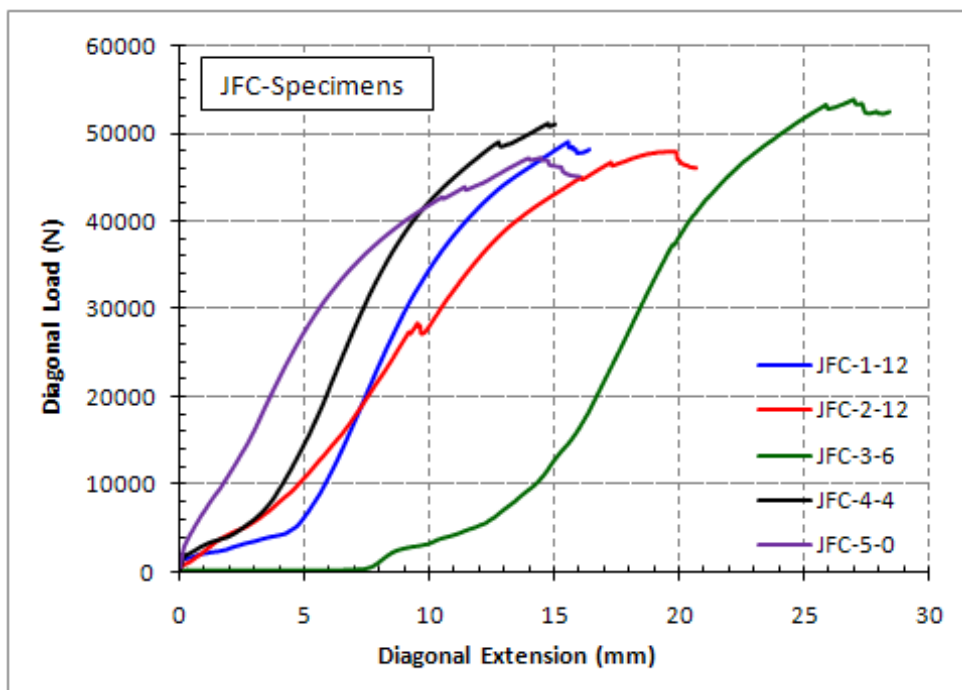


Figure 7.14. Diagonal load-vertical extension of JFC specimens

Three out of five specimens behaved were similar, which were JFC-3-6, JFC-4-4 and JFC-1-12. They started with a quick increase in the extension at the early load up to approximately 5000 N then increased linearly with the increase in the load. Since the stress concentration continuously increased due to the compression load from off-diagonal side, the graphs started to deviate gradually at loads of approximately 41000 N to 42500 N, where the shear buckling load might have been reached. The final failure of the specimens occurred at slightly above the buckling loads. These failure mechanisms occurred suddenly as shear failure of the core due to the high stress concentration induced by the buckle mechanism. The only difference in the plots was that in JFC-1-12

there was a noticeable change in the graph at a load of around 28000 N that most likely a sign of cracking initiation within the core.

The experimental results for the diagonal tension test on hybrid sandwich panel with MDF intermediate layer are depicted on Figure 7.15, where the diagonal load-vertical extension is represented. As it shown in the figure, all graphs have a similar pattern with the exception for specimen MDF-5-0. Two of the specimens had a slack deformation at the initial stage, which were MDF-4-4 and MDF-3-6.

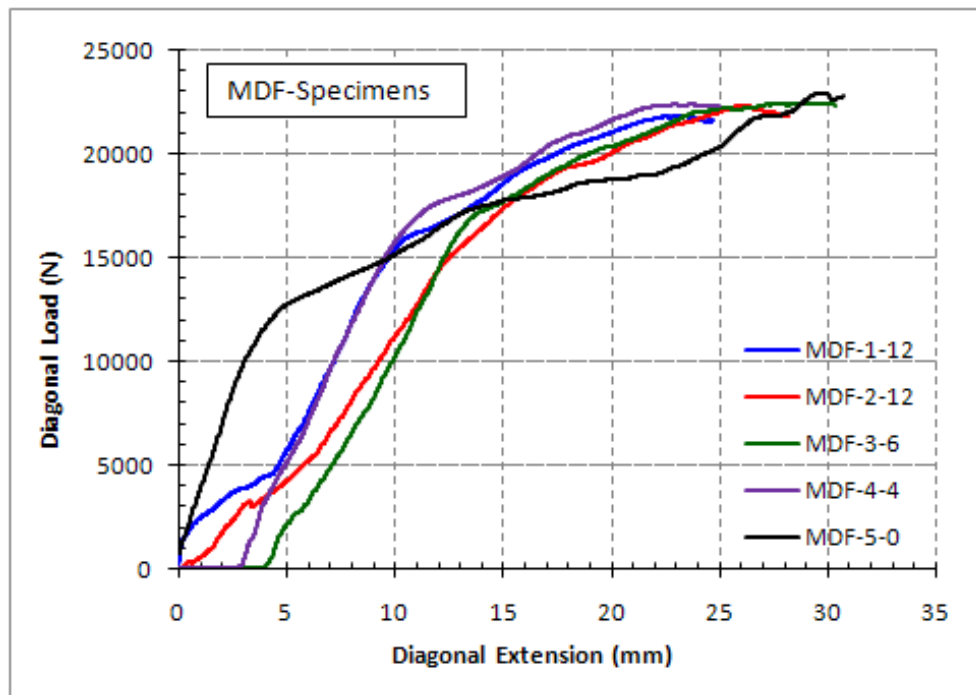


Figure 7.15. Diagonal load-vertical extension of MDF specimens

Unlike the load-extension graphs for hybrid sandwich panels with the JFC intermediate layer that collapsed suddenly, there was no sudden change in the load for all the MDF specimens. The extension continuously increased without any significant changes in the load carrying capacity until the test was automatically terminated by the machine. It seems that the collapse mechanisms had finalised when the specimens reached the buckling load in the form of delamination between the intermediate layer and core. Beyond this point all the remaining load was carried by the aluminium skin and MDF intermediate layer.

As the final stage of this load-extension comparison analysis, a specimen from each sample category was selected for comparison as presented in Figure 7.16. Specimens CTR-2-12, JFC-1-12 and MDF-1-12 were selected as being representative for Sustainable Hybrid Composite Sandwich Panel with Natural Fibre Composites as Intermediate Layer

each sample category. The hybrid sandwich panels with JFC intermediate layer show excellent strength and stiffness, while the one with MDF intermediate layer behaved somewhat more ductile but less stiff than the panels with JFC intermediate layer. Overall, the introduction of intermediate layer, especially the JFC, has shown a significant contribution to the enhancement of the load carrying capacity of the sandwich panels.

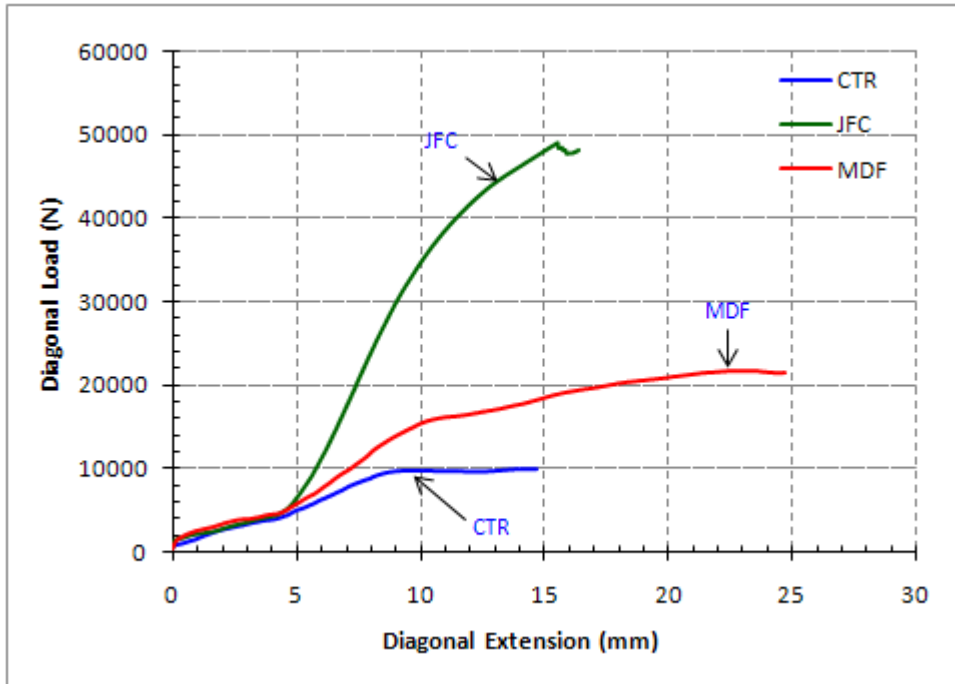


Figure 7.16. Diagonal load-vertical extension of representative specimens for CTR, JFC and MDF sandwich panel

7.5.3. Comparison of failure modes

The failure modes of the sandwich panels evaluated using diagonal tension shear test are provided in Figures 7.17 to 7.20. The failure modes were observed both during the course of the testing as well as after the specimens had been removed from the testing rig to more closely examine any particular form of failure mechanism. The failure modes during the progress of the test are demonstrated in the top part of the figure, and the pictures in the bottom part of the figure represent the identified failure mechanism after failure.

The failure modes observed for CTR specimens are presented in Figure 7.17. As can be seen in the figure, there were at least two failure mechanisms identified. First, a face wrinkling due to large stress concentration along the diagonal axis of the specimen,

as shown in picture CTR-1 and CTR-3. A careful assessment of the removal specimen after the test, as shown in picture CTR-4, has clearly shown the sign of face wrinkling at the vertical diagonal axis of the specimen. The buckling had caused adhesive bond failure between the skin and the core as shown in Figure 7.18 (A). The second mode was shear crimping of the face within the CTR specimen during the course of the testing. The best way how to explain this failure mechanism is by looking at the typical failure mechanism under compression load shown in Figure 7.18 (B and C).

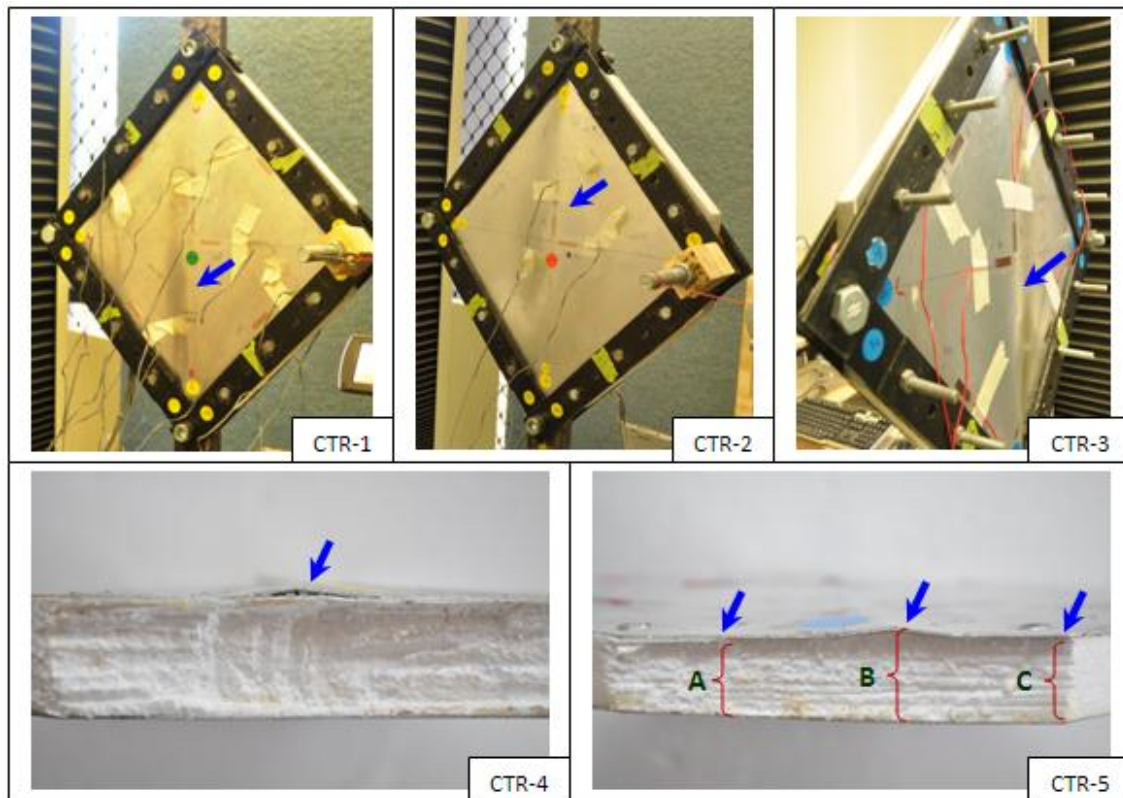


Figure 7.17. Shear failure mechanism of CTR specimens

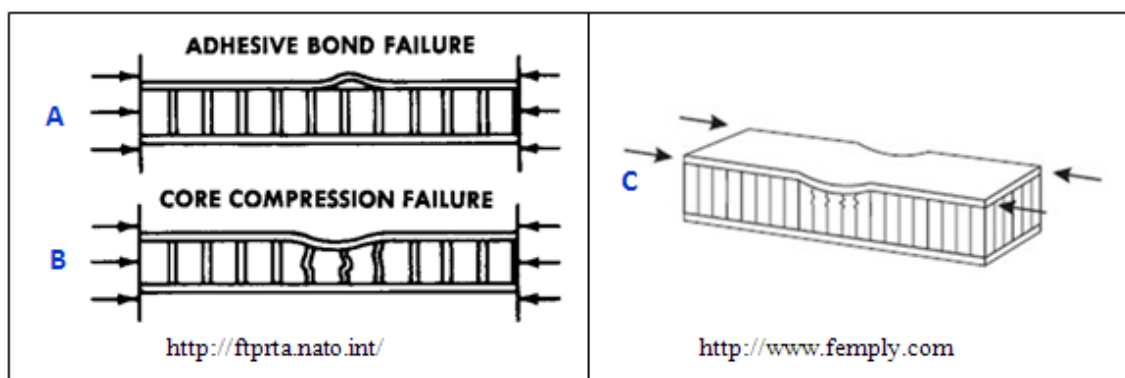


Figure 7.18. Failure mechanism of sandwich panel under compression buckling load

The crimping mechanism is actually triggered by a downward pressure from the skin. When the core fails to provide sufficient support, it may cause the shear crimping that damage the core. As seen in Figure 7.17, the aluminium face at the diagonal axis buckled quite significantly creating a downward pressure to the adjacent part (CTR-2). The effect of such mechanism is shown in the picture of CTR-5 in Figure 7.17, which shows a change in the thickness of the specimen at particular parts, showing the buckle and the reduced section of the specimen as a result of shear crimping.

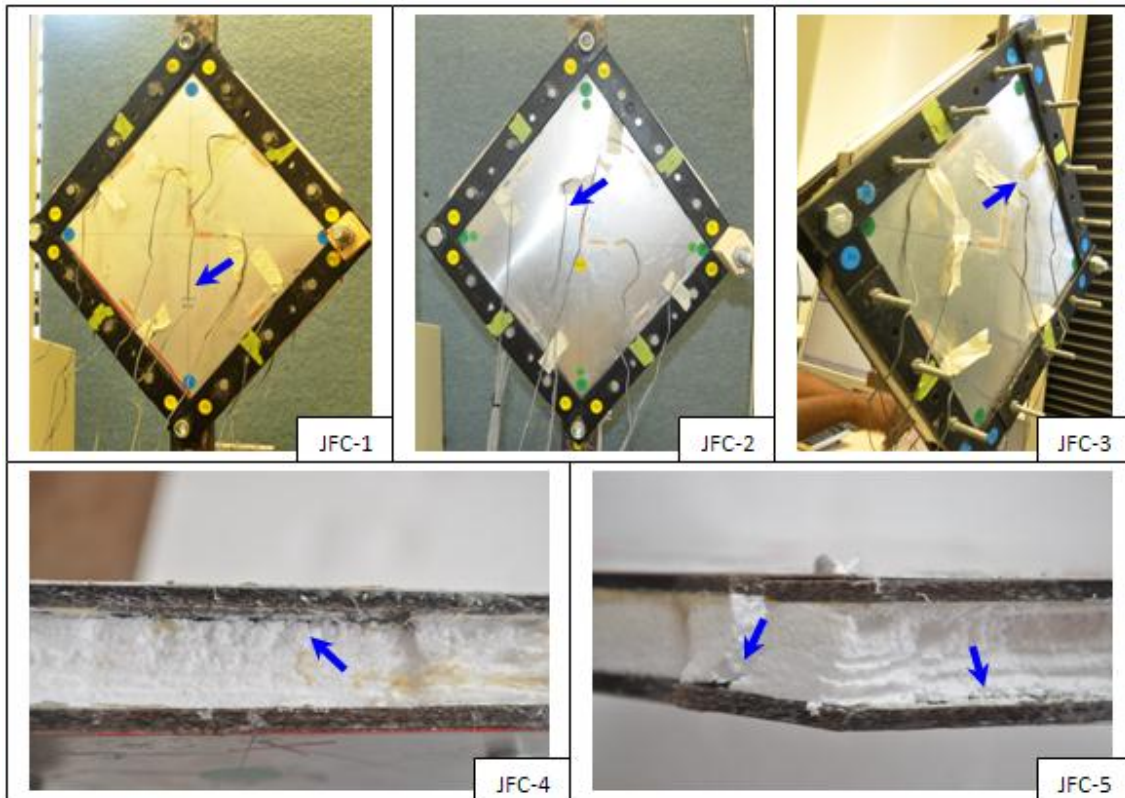


Figure 7.19. Shear failure mechanism of JFC specimens

The failure modes for the hybrid sandwich panels with the JFC intermediate layer is shown in Figure 7.19. A visual inspection of the typical failure modes observed for this type of panels reveal that the panels failed due to shear cracking of the core. The panels buckled as a whole in which all the constituents of the sandwich panels behaved as an integrated part and carried the loads together until final failure. As previously discussed in load-extension section, the failure mechanism was abrupt failure of the core, as seen in picture JFC-4 and JFC-5 in Figure 7.19. As seen in the figure (JFC-1, JFC-2 and JFC-3), there was no partial disintegration of the specimen. It also can be observed in the figure that the cracking process occurred in the core, as confirmed by a

significant amount of EPS residual along the failed core near the intermediate layer. The skin, intermediate layer and core were acting together to carry the in-plane shear load until final failure. Overall, the hybrid sandwich panels with JFC intermediate layer behaved as a single integrated panel resulting in higher load carrying capacity.

The failure modes of hybrid sandwich panels with MDF intermediate layer are shown in Figure 7.20. Unlike the behaviour of hybrid panels with JFC intermediate layer, the failure mechanism of sandwich panels with MDF intermediate layer seems very close to that of the CTR specimens. As it can be seen in Figure 7.20 (MDF-1, MDF-2 and MDF-3), there is an indication of face disintegration at the surface of the specimens, particularly seen in picture MDF-3 and MDF-3. What might have been occurred in MDF-2 and MDF-3 was that a wrinkling of the aluminium face occurred as shown in picture MDF-5. The face wrinkling mechanism in the MDF was slightly different to that of the CTR specimens as there was no observed damage to the core. As seen in picture MDF-5, the thickness of the core remained the same after failure, suggesting that the existence of intermediate layer has stabilised the core to keep its role so that the skin has carried the load until the final failure was occurred.

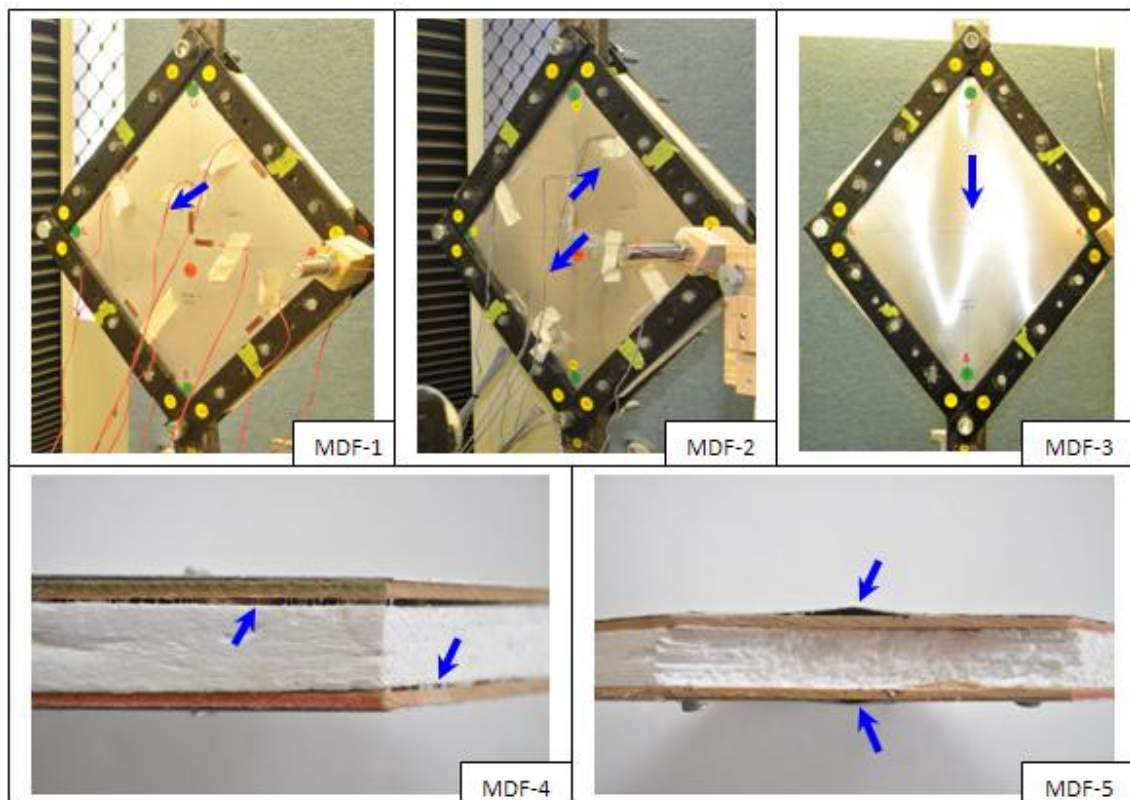


Figure 7.20. Shear failure mechanism of MDF specimens

The other mechanism was in the form of delamination of the core with the intermediate layer. As the stress increased due to the shear buckling, it caused rupture between the intermediate layer and the core. It can also be observed that there was no trace of EPS foam failure at the interface between the intermediate layer and the core, indicating poor bond strength. After delamination the load was carried by the undisturbed skin and intermediate layer until final failure.

7.5.4. Comparison of load-strain behaviour

The relationship between load and strain development for the CTR-2-12 panel is shown in Figure 7.21 for the strains at the front side and Figure 7.22 for the back side. Figure 7.23 shows the load-deflection of the selected specimen as well as its failure modes. As it can be seen in the figures, the tensile strains in the loaded diagonal (A₅ and B₅) confirmed the development of diagonal tension in the panel. The compression strains in the off-loaded diagonal also confirmed the diagonal compression state. The compression strain at the back side (B6) changed from a compression to tension state at a load of approximately 3500 N. This could be related to the formation of an early failure mechanism that may have changed the principal stress trajectory within the panel. This is shown in the load-extension graph of the specimen in Figure 7.23 (left).

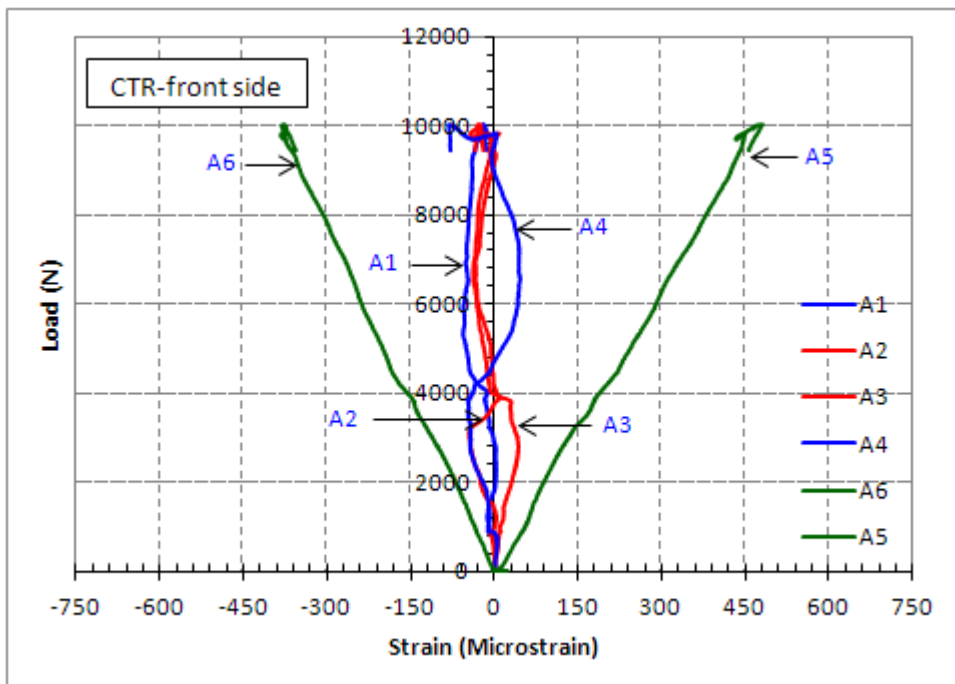


Figure 7.21. Load-strain (front side) relationship of representative of CTR specimens

The evolution of strains parallel to the edges of specimens near the loading rail at front side (A_1 , A_2 , A_3 and A_4) also verified the development of diagonal tension state within the panel. Based upon the geometrical arrangement, strain A_1 and A_4 should be opposite each other that also should be for strain A_2 and A_3 . As it can be seen in Figure 7.21, these strain gauges performed as expected. The direction of strains changed at a load of approximately 4000 N. This change could be related to the formation of early failure mechanism within the panel. The strains parallel to the edges of specimen at the back side (B_1 , B_2 , B_3 and B_4) showed irregularly strains. At the initial stage up to the load of approximately 3500 N, the strains showed the deformation as expected in which B_1 and B_4 should be opposite each other, and similarly for the strain B_2 and B_3 . However, beyond this load all strains indicated a compression state. The irregular strains at the back side might be indication that a failure mechanism had developed at the back side, as seen in picture CTR-3 in Figure 7.17. The appearance of long bolts in this picture verified that it was a back side capture, to distinguish from the other two pictures (CTR-1 and CTR-2) in the same figure.

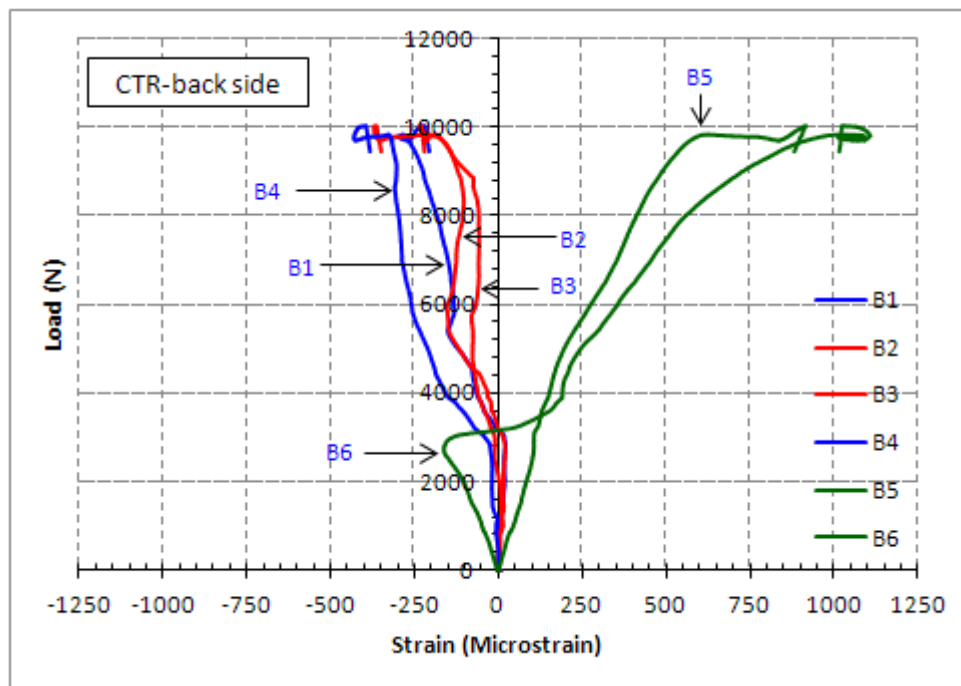


Figure 7.22. Load-strain (back side) relationship of representative of CTR specimens

The mode of failure shown in Figure 7.23 (right) verified that the failure mechanism occurred on one side. As it can be seen in the figure, the bottom part (front side) of the specimen remained intact while the top surface (back side) deformed

significantly. Overall, the recorded strains confirmed the development of tension-compression state along the diagonal side of the tested specimen.

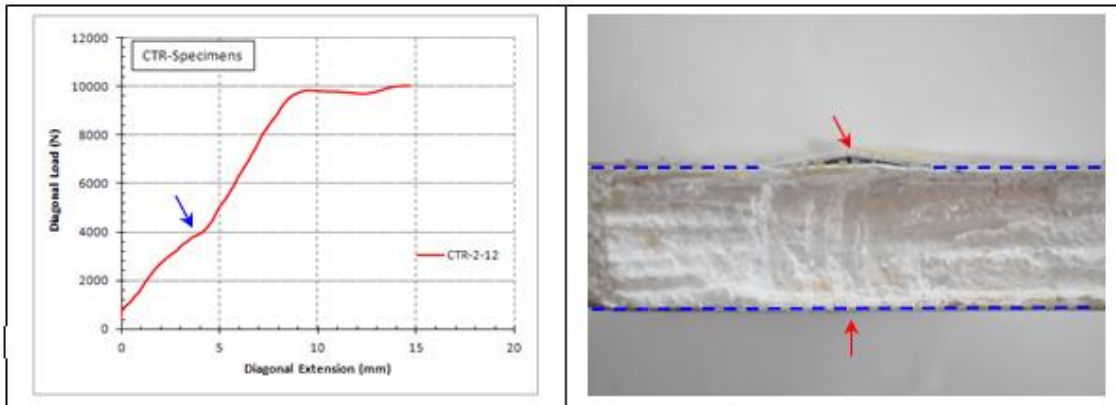


Figure 7.23. Load-extension graph of specimen CTR-2-12 and its mode of failure

The load-strain relationships of JFC-1-12 specimen group are presented in Figures 7.24 and 7.25 for the front and the back side, respectively. The development of tension-compression state along the diagonals was confirmed from the plotting of diagonal strains in both figures. As shown in both figures, the tension-compression state followed the direction of applied load along the diagonals. The tension strains (A_5 and B_5) occurred at the loaded diagonal, while the compression strains (A_6 and B_6) took place at the off-loaded diagonal.

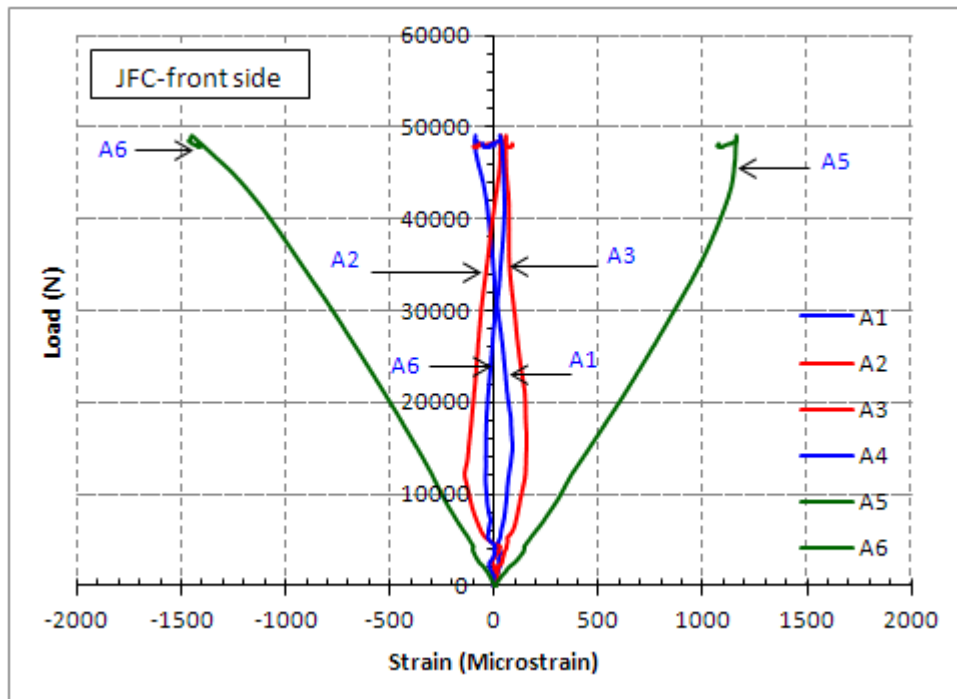


Figure 7.24. Load-strain (front side) relationship of representative of JFC specimens

Strain development on both sides followed the theoretical expected direction until a sudden failure occurred at a load of approximately 49000 N. The strains along the edges of the specimens at the front side showed ideal strain conditions for the tensile diagonal test arrangement. Strain A_1 and A_4 showed comparable values but in opposite sign. The same strain condition was also observed for the strains at A_2 and A_3 . The strains at the back side (B_1 , B_2 , B_3 and B_4) showed a little noise in the initial stage at the load of approximately 5000 N. At this point strain direction changed significantly indicating the formation of initial failure within the panel most likely in the form of initial cracking inside the core.

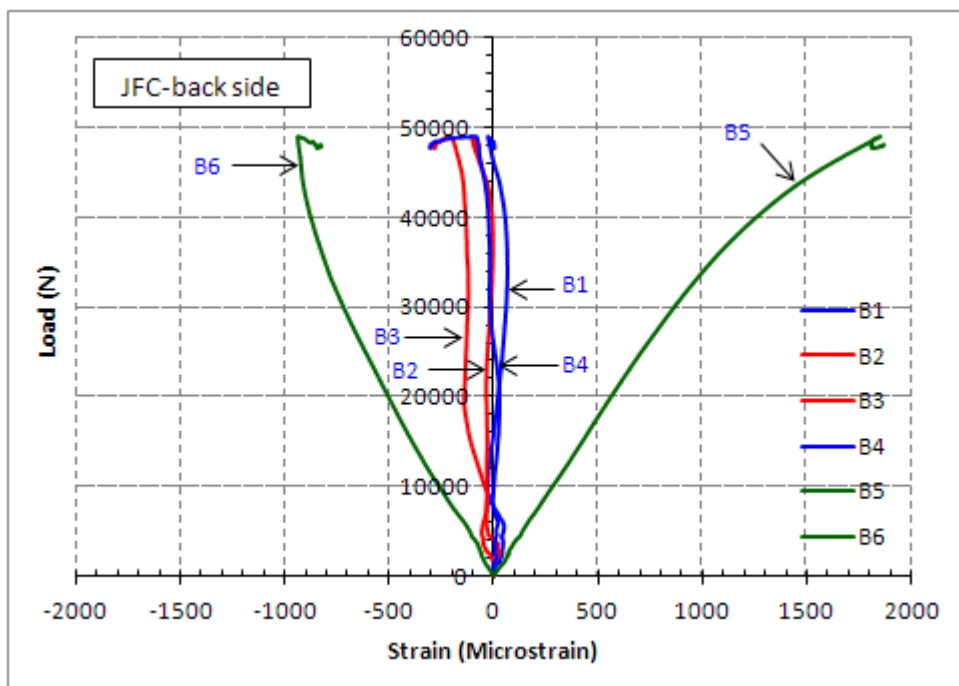


Figure 7.25. Load-strain (back side) relationship of representative of JFC specimens

The load-extension graph of the representative specimen (JFC-1-12), shown in Figure 7.26, verified the load-strain curve. It can be seen that extension increased much higher than load up to 5000 N and an extension of about 5 mm. Beyond that point the graph behaved linearly until then deviated steadily until the ultimate load. At the final stage around the load of 42000 N, all the edge-parallel strains changed their directions into a compression state. The mode of failure shown in Figure 7.26 also validated that small deformation or disintegration occurred at the face and that the principal failure mechanism was due to the cracking of the core. As it can be seen in the figure, both the top and bottom surfaces of the specimen remained undisturbed.

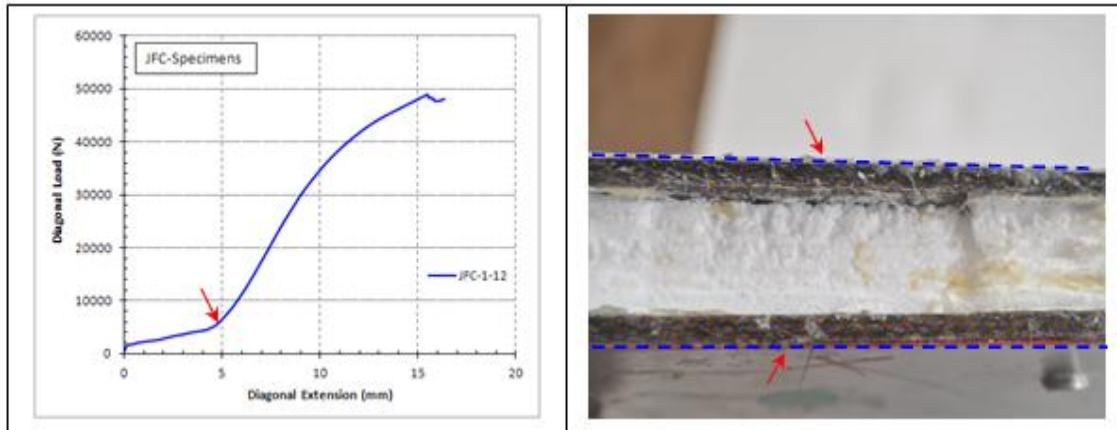


Figure 7.26. Load-extension graph of specimen JFC-1-12 and its mode of failure

Figures 7.27 and 7.28 present the relationship between load and strain development of specimen MDF-1-12 as the representative sample for MDF specimens group. The tension-compression state followed the direction of the applied load along the diagonals. Strain A_5 and B_5 were in tension, while strains A_6 and B_6 in a compression state. The evolution of tension and compression strain at the front side (A_5 and A_6) was initially linear with a slight change around 17000 N, which might be caused by the formation of failure mechanism. This was confirmed by a substantial change in the slope of load-extension graph presented in Figure 7.29 (left).

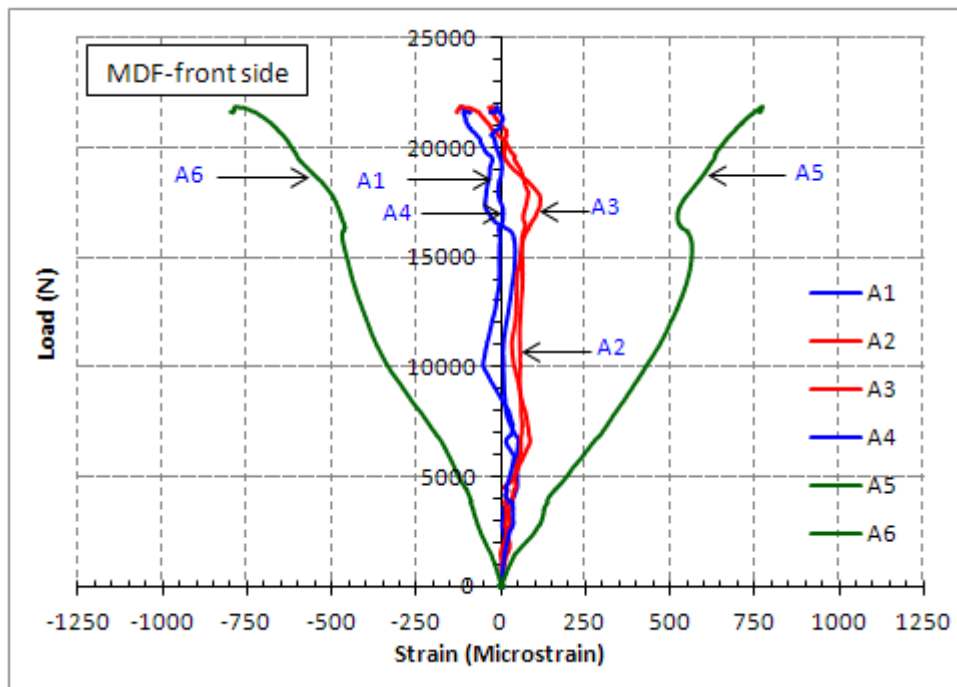


Figure 7.27. Load-strain (front side) relationship of representative of MDF specimens

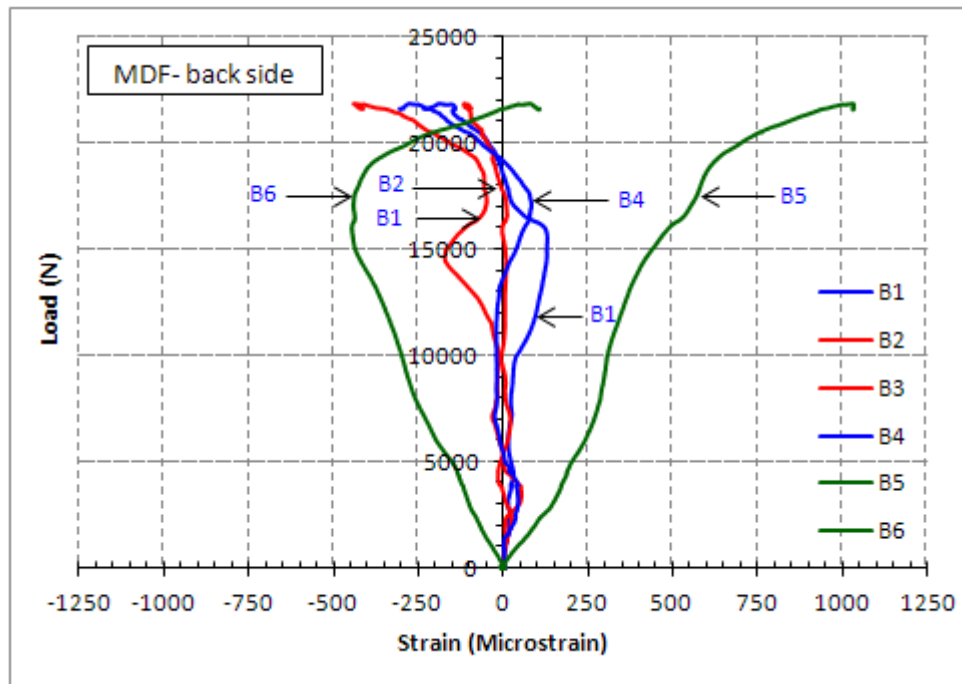


Figure 7.28. Load-strain (back side) relationship of representative of MDF specimens

The strains at the back side showed the development of a failure mechanism within the panel. As seen in Figure 7.28, the off-diagonal strain (B_6) that should be in compression suddenly changed to a tension strain. It seems that the MDF intermediate layer stabilised the core to support the skin so that premature failure mechanisms such as early face wrinkling or face shear crimping, as found in the CTR specimen, were delayed. The specimen finally collapsed under a significant higher load than the CTR specimen.

As it is shown in Figure 7.29 (right), the failure mechanism of specimen MDF-1-12 was a wrinkling of the face due to the bond failure between the face and intermediate layer under high strength concentration triggered by a buckling mechanism. The formation of buckling mechanism is seen in the load-extension graph of the specimen MDF-1-12 in the same figure. The failure mechanism in Figure 7.29 (right) verified what had been observed in the evolution of tension-compression strain at the front and the back side of the specimen. Tension and compression strain at the front side (A_5 and A_6) remained consistent. The top surface (back side) of damaged specimen was wrinkled and that condition was well represented by a considerable change of the compression strain (B_6) at around 17500 N (Figure 7.28).

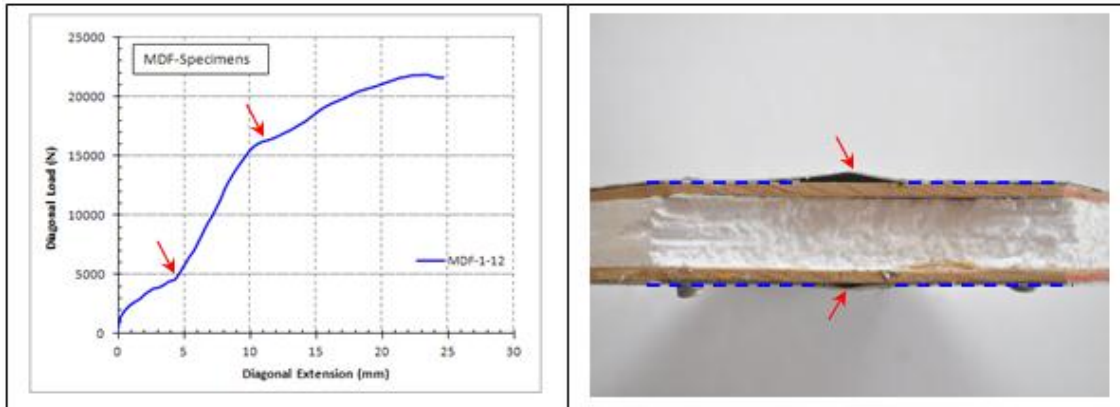


Figure 7.29. Load-extension graph of specimen MDF-1-12 and its mode of failure

A comparison of tension-compression strains for all the representative specimens was considered as a useful way to demonstrate how the introduction of intermediate layer substantially enhanced the in-plane shear behaviour of the sandwich panels. A comparison graph is presented in Figure 7.30, which is the comparison of strains measured at the front side of the specimen.

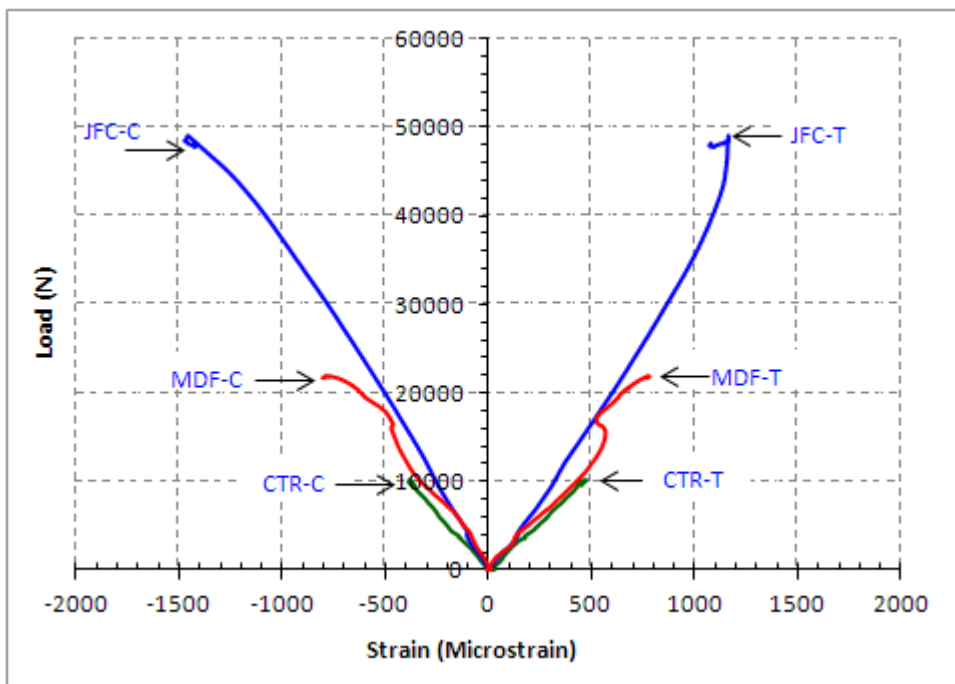


Figure 7.30. Load-strain relationship of different sandwich panels category

It is clearly seen in the figure that the deformation capability of hybrid sandwich panels is notably higher than the conventional sandwich panels without any intermediate layer. The curve for the CTR specimen shows a linear elastic behaviour up to the

ultimate load is reached. The maximum tension strain was around 500 microstrains, and only about 380 microstrains for the compression strain at the load of about 10000 N. The maximum tension compression strains of MDF specimen were quite similar of approximately 800 microstrain for both tension and compression strain. The strain increased linearly with the load up to around 18500 N. Beyond this point, there was a significant change in the shape of the graph until the ultimate load was reached. Similarly, the load-strain behaviour of JFC specimen also shows a linear elastic behaviour up the load of approximately 45000 N, then slightly deviates prior to the ultimate load of about 48000 N. The maximum tension and compression strain was approximately 1200 and 1450, respectively. Figure 7.30 demonstrates the overall performance of the JFC panel where both superior stiffness and strength are seen. As measured by the area under the load/strain plot the JFC panel also shows much higher toughness. When considered in an actual building the JFC panel exhibits the potential to provide both good serviceability related to deflection and strength related to the ultimate capacity.

7.5.5. The interpretation of diagonal shear test results

As indicated earlier in Section 7.2, the data from diagonal in-plane shear testing can be interpreted in different ways. The results of the experiment in this research were interpreted and presented in Table 7.2 mainly based upon the theoretical framework proposed by Mohammed et al (2000). However, the testing results may also be interpreted as per Kuenzi et al (1962). In this method, the sandwich panel was assumed to fail under buckling shear loads. The experimental facing stresses of a conventional sandwich panel can then be obtained by Equation 7.16 or Equation 7.17. While the experimental facing stress of hybrid sandwich panel may be obtained by using the two equations and slightly modifying the effective thickness (f) by introducing modular ratio (n) to transform the intermediate layer into an equivalent aluminium skin, as shown in the following equation:

$$q_f = \frac{P}{2f_{eq}\sqrt{a^2 + b^2}} \dots\dots\dots 7.18$$

Where a and b are the width and length of the panel, and f_{eq} is the equivalent thickness which can be obtained with the following expression.

$$f_{eq} = f + \frac{E_i}{E_f}i = f + ni \quad \dots\dots\dots 7.19$$

As the panels tested in this experiment have the same length and width, the above equation can be simplified as:

$$q_f = \frac{P}{2\sqrt{2} f_{eq}a} \quad \dots\dots\dots 7.20$$

The interpretation of experimental data provided from the in-plane shear testing for CTR specimens are presented in Table 7.3. The table presents both ultimate diagonal load and shear buckling load. Kuenzi et al (1962) stated that sudden increased in deflection or strain indicated that the buckling load had been reached. For the CTR specimen, the loads at early identified failure mechanism were also included for further analysis.

Table 7.3. Experimental results interpretation for CTR specimens

Load descriptions	Specimen	Load (N)	Facing thickness (mm)	Panel width (mm)	Experimental facing stress (MPa)
Ultimate diagonal load	CTR-1	9228	0.5	300	21.75
	CTR-2	10043	0.5	300	23.67
	CTR-3	13575	0.5	300	31.99
	CTR-4	9051	0.5	300	21.33
	CTR-5	9367	0.5	300	22.08
Average					24.17
Buckling load	CTR-1	9000	0.5	300	21.21
	CTR-2	9500	0.5	300	22.39
	CTR-3	10000	0.5	300	23.57
	CTR-4	8750	0.5	300	20.62
	CTR-5	9000	0.5	300	21.21
Average					21.80
Load at early identified failure mechanism	CTR-1	4000	0.5	300	9.43
	CTR-2	4000	0.5	300	9.43
	CTR-3	6000	0.5	300	14.14
	CTR-4	-	0.5	300	-
	CTR-5	-	0.5	300	-
Average					10.99

The interpretation of experimental data provided from the in-plane shear testing for sandwich panels with JFC and MDF intermediate layer are presented in Tables 7.4 and Table 7.5, respectively. Likewise to the previous table, the loads were divided into two categories; ultimate diagonal loads and buckling loads. The average of interpretation results obtained as per Kuenzi et al (1962) was then compared to the average results of the experiments that earlier obtained as per Mohammed et al (2000)

which was presented in Table 7.2. The results of such comparison are presented in Table 7.6. A quick visual examination of data presented in the table gives the impression that the two different methods provide comparable results. The difference between the average results was only about 3.46% for CTR specimens, 4.61% for JFC specimens and 5.45% for MDF specimens.

Table 7.4. Experimental results interpretation for JFC specimens

Load descriptions	Specimen	Load (N)	Facing thickness (mm)	Equivalent thickness (mm)	Panel width (mm)	Experimental facing stress (MPa)
Ultimate diagonal load	JFC-1	49006	0.5	0.70	300	82.74
	JFC-2	47921	0.5	0.70	300	80.91
	JFC-3	53834	0.5	0.70	300	90.89
	JFC-4	51127	0.5	0.70	300	86.32
	JFC-5	47192	0.5	0.70	300	79.68
Average						84.11
Buckling load	JFC-1	42000	0.5	0.70	300	70.91
	JFC-2	41500	0.5	0.70	300	70.07
	JFC-3	42500	0.5	0.70	300	71.75
	JFC-4	42000	0.5	0.70	300	70.91
	JFC-5	41000	0.5	0.70	300	69.22
Average						70.57

Table 7.5. Experimental results interpretation for MDF specimens

Load descriptions	Specimen	Load (N)	Facing thickness (mm)	Equivalent thickness (mm)	Panel width (mm)	Experimental facing stress (MPa)
Ultimate diagonal load	MDF-1	21809	0.5	0.61	300	41.83
	MDF-2	22324	0.5	0.61	300	42.81
	MDF-3	22442	0.5	0.61	300	43.04
	MDF-4	22366	0.5	0.61	300	42.89
	MDF-5	22908	0.5	0.61	300	43.93
Average						42.90
Buckling load	MDF-1	21000	0.5	0.61	300	40.27
	MDF-2	21500	0.5	0.61	300	41.23
	MDF-3	22000	0.5	0.61	300	42.19
	MDF-4	22000	0.5	0.61	300	42.19
	MDF-5	22000	0.5	0.61	300	42.19
Average						41.62

Table 7.6. Comparison of the average results for different specimen groups

Specimens Group	Mohammed et al (2010)	Kuenzi et al (1962)	Percentage difference
CTR	23.36	24.17	3.46
JFC	80.40	84.11	4.61
MDF	40.68	42.90	5.45

7.5.6. Theoretical evaluation of shear strength of sandwich panels

Existing models for diagonal in-plane shear stress

As indicated earlier, the failure of a sandwich structure is a very complicated phenomenon due to the numerous possible failure mechanisms in one or more of the constituent materials that make up the structure. These failure mechanisms have been analysed and tested by many researchers with several possible failure mechanisms for described. Mamalis et al (2008) mentioned some such as face micro-buckling, face wrinkling, core shear, and indentation. For sandwich panels tested under in-plane shear, there are three possible failure mechanisms; general shear buckling, skin shear failure and skin wrinkling (Morgenthaler et al, 2005). Two existing models for sandwich panels under in-plane shear that are related to this work are described below.

Kuenzi et al (1962)

The early work on using diagonal tension shear test for assessing the in-plane shear of sandwich panels was carried out by Kuenzi et al (1962). The work dealt with the shear stability analysis of flat panels of sandwich construction. They proposed the formula 7.23 for the facing stress at which the panel buckles is:

$$q_f = \frac{N_{cr}}{f_1 + f_2} \dots\dots\dots 7.21$$

The buckling shear load was obtained with the following equation:

$$N_{cr} = \frac{\pi^2 D}{a^2} L_{cr} \dots\dots\dots 7.22$$

Hence,

$$q_f = \frac{\pi^2 D}{a^2 (f_1 + f_2)} L_{cr} \dots\dots\dots 7.23$$

With the value of D expressed as follows:

$$D = \frac{E_f}{\lambda_f} \frac{f_1 f_2 h^2}{(f_1 + f_2)} \dots\dots\dots 7.24$$

The complete expression for shear buckling is given by:

$$q_f = \frac{\pi^2 E_f f_1 f_2 h^2}{a^2 \lambda_f (f_1 + f_2)^2} L_{cr} \dots\dots\dots 7.25$$

Where:

- q_f : Shear buckling stress (MPa)
- N_{cr} : Buckling load (N)

- f_1, f_2 : Facings thickness (mm)
- E_f : Facing modulus of elasticity (MPa)
- λ_f : Poisson's ratio of facings
- a, b : Width and length of the panel (mm)
- L_{cr} : Buckling load factor
- c : Core thickness
- h : The effective depth

For clamped panels, the buckling load factor (L_{cr}) can be obtained by the following equations:

$$L_{cr} = 1 + \left[L_0 - \frac{4}{3} \left(1 + \frac{a^2}{b^2} \right) S \right] \quad , \text{ when } S < \frac{3/4}{1 + \frac{a^2}{b^2}} \quad \dots\dots\dots 7.26$$

$$L_{cr} = \frac{1}{S} \quad , \text{ when } S \geq \frac{3/4}{1 + \frac{a^2}{b^2}} \quad \dots\dots\dots 7.27$$

The core shear parameters(S) can be obtained by the following relation:

$$S = \frac{\pi^2 f_1 f_2 c E_f}{a^2 \lambda_f \mu_c (f_1 + f_2)} \quad \dots\dots\dots 7.28$$

Where μ_c is the shear modulus of the core. They also noted that whenever L_{cr} is equal to $1/S$ as defined in Equation 7.32, then the buckling stress can be estimated by the following equation.

$$q_f = \frac{h^2 \mu_c}{c(f_1 + f_2)} \approx \frac{h \mu_c}{(f_1 + f_2)} \quad \dots\dots\dots 7.29$$

Hoff and Mautner (1945) and Mamalis et al (2005)

The other work was carried by Morgenthaler et al (2005) who performed two different experimental set-ups to find a suitable experimental set-up for in-plane shear properties of sandwich panels. In their analysis, the equation derived from wrinkling face mode of failure as discussed by Zenkert (1995) was employed, which is:

$$\sigma = a^3 \sqrt{E_f E_c G_c} \quad \dots\dots\dots 7.30$$

The above equation was obtained earlier by Hoff and Mautner (1945) as explained by Kollar and Springer (2003), with the constant value (a) of 0.91, but for practical use they recommended the value of 0.5, which gives:

$$\sigma = 0.5^3 \sqrt{E_f E_c G_c} \quad \dots\dots\dots 7.31$$

Mamalis et al (2008) also used this equation when they proposed their model for predicting the load carrying capacity of hybrid sandwich panel with intermediate layer under flexural bending load that failed due to a wrinkling of the skins. Considering a typical failure mechanism observed in this in-plane shear test which was a shear buckling that resulted in a wrinkling of the skins, this approach may still relevant to be discussed although such work was not dealing with in-plane shear load. The proposed model of Mamalis et al (2008) is presented as follows:

$$\frac{P}{b} = \frac{2t_f t_c}{L} \sqrt[3]{E_f E_i G_i} \dots\dots\dots 7.32$$

The wrinkling stress can be obtained by re-writing this equation as:

$$\sigma = \frac{P}{b2t_f} = \frac{t_c}{L} \sqrt[3]{E_f E_i G_i} \dots\dots\dots 7.33$$

Classical Euler shear equation as per Alinea and Dastfan (2006), and Johns (1971)

Understanding classical analysis of plates under shear is also important when dealing with buckling of panels subjected to shear load. Alinia and Dastfan (2006) stated that the critical shear stress of flat rectangular plates that is widely accepted is given by the following equation:

$$\tau_{cr} = \frac{k_s \pi^2 E}{12(1 - \nu^2)} \left(\frac{t}{b}\right)^2 \dots\dots\dots 7.34$$

Where:

- E : Young modulus (MPa)
- ν : Poisson’s ratio
- t : Plate’s thickness (mm)
- b : Plate’s breadth (mm)
- k_s : Shear buckling coefficient

At earlier time, Johns (1971) expressed this equation as:

$$\tau_{cr} = \frac{K_s \pi^2 D}{db^2} \dots\dots\dots 7.35$$

$$D = \frac{Ed^3}{12(1 - \nu^2)} \dots\dots\dots 7.36$$

Where:

- d : Plate thickness (mm)
- D : Plate rigidity (Nmm)

Proposed models

Modified Kuenzi Model

An empirical equation based on the properties of constituent materials as developed by Kuenzi et al (1962) was proposed to analyse the buckling shear of the hybrid sandwich panels with an intermediate layer. The model was actually an extended form of the Kuenzi’s model to take into account the contribution of an intermediate layer. Two simple approaches were introduced. The first approach was by calculating the buckling shear stress due to the contribution of skin and intermediate layer separately and then summing up the results. The second approach was by introducing a particular term of equivalent bending stiffness (D_{eq}), instead of D , which was an equivalent bending stiffness due to the contribution of skin and intermediate layer. Hence the first approach can be written as follows:

$$q_f = \frac{N_{cr}}{f_1 + f_2} + \frac{N_{cr}}{i_1 + i_2} \dots\dots\dots 7.37$$

$$q_f = \frac{\pi^2 D_f}{a^2 (f_1 + f_2)} L_{cr} + \frac{\pi^2 D_i}{a^2 (i_1 + i_2)} L_{cr} \dots\dots\dots 7.38$$

$$q_f = \frac{\pi^2 E_f f_1 f_2 h_1^2}{a^2 \lambda_f (f_1 + f_2)^2} L_{cr} + \frac{\pi^2 E_i i_1 i_2 h_2^2}{a^2 \lambda_i (i_1 + i_2)^2} L_{cr} \dots\dots\dots 7.39$$

The second approach is expressed as follows:

$$D_{eq} = D_i + D_f \dots\dots\dots 7.40$$

$$D_{eq} = \frac{E_f}{\lambda_f} \frac{f_1 f_2 h_1^2}{(f_1 + f_2)} + \frac{E_i}{\lambda_i} \frac{i_1 i_2 h_2^2}{(i_1 + i_2)} \dots\dots\dots 7.41$$

$$q_f = \frac{\pi^2 D_{eq}}{a^2 (f_1 + f_2)} L_{cr} \dots\dots\dots 7.42$$

Modified Hoff-Mautner Model

The basic equation obtained by Hoff and Mautner (1945) was modified by taking into account the contribution of intermediate layer with the following equation:

$$\sigma = 0.5^3 \sqrt{E_f E_c G_c} + 0.5^3 \sqrt{E_i E_c G_c} \dots\dots\dots 7.43$$

Modified Mamalis Model

When a sandwich panel is subjected to an in-plane shear load, the direct bending stresses (axial σ_{xy} , σ_{yy} and τ_{zy}) are distributed relative to the stiffness of the constituent

materials. A very good explanation about this phenomenon can be found in an Aerospace engineering blog (<http://aerospaceengineering.com/sandwichpanel>). A spring analogy was used; when two springs are aligned in parallel and fixed on one end are displaced by the same extension (x), the load carried by one of the spring will be twice as high as that by the other spring if the stiffness of the spring is equal to twice of the second spring. This means that, when an intermediate layer has been introduced into sandwich panel, the core is then no longer holds a significant in-plane load. The Mamalis model can then be modified by replacing the thickness of core (t_c) to the thickness of intermediate layer (t_i) to obtain the constant value, which leads to a slightly change of the equation to:

$$\sigma = \frac{t_i}{L} \sqrt[3]{E_f E_i G_i} \dots\dots\dots 7.44$$

7.5.7. Comparison analysis between theoretical model and experiment results

Modified Kuenzi Model vs Experimental results

The predicted results using Modified Kuenzi Model are presented in Table 7.7 for Approach-1 and in Table 7.8 for Approach-2, as per Equations 7.39 and 7.42, respectively. As seen in Table 7.8 (column 6), the model obtained the average buckling shear stress of 69.85 MPa for CTR specimens, and a similar value of 78.3 MPa for both JFC and MDF specimens. When these values were compared to the experimental results, it can be said that the model has failed to accurately predict the shear strength of CTR and MDF specimens. The difference between the value obtained by the model and the experiment was around 189% and 82.6% for the CTR and MDF specimens, respectively. These shear strength values were obtained when comparing the value obtained by the model to the shear stress values induced by the ultimate diagonal load. The difference even become higher when the model’s value was compared to the shear induced by the buckling shear load, which was about 220.3% and 88.2% for CTR and MDF, respectively. These difference values were definitely considered as unacceptable.

However, the proposed model has successfully predicted the shear buckling of JFC specimens. The shear strength obtained by the proposed model was about 78.3 MPa, which was only 7.4% less than the actual ultimate experimental value of 84.1 MPa. An opposite situation was encountered when compared the model’s stress value to the shear stress induced by the buckling shear load. The model provided higher value by

10.9% than the actual experiment value meaning that the difference between the model and the experimental value was approximately in the range of 10%, which considered as an acceptable value. Interestingly, the Approach-2 of modified Kuenzi model has obtained a very good agreement result between the theoretical and experimental value. The model obtained a stress value of 69.245 MPa while the average stress induced by the identified buckling load was approximately 70.572 MPa, that lead them differ by only 1.92%.

Table 7.7. Predicted results using Modified-Kuenzi Model (Approach-1)

Specimens Group	D_f	D_i	S_f	L_{cr}	σ_{f-mdl}	$\sigma_{f-exp-ult}$	$\sigma_{f-exp-buc}$
1	2	3	4	5	6	7	8
CTR	12441659	-	19.516	0.051	69.842	24.166	21.802
JFC	12441659	3459503.06	19.516	0.180	78.318	84.106	70.572
MDF	12441659	2019013.00	19.516	0.309	78.318	42.902	41.617

Table 7.8. Predicted results using Modified-Kuenzi Model (Approach-2)

Specimens Group	D_{eq}	S_{eq}	L_{cr}	σ_{f-mdl}	$\sigma_{f-exp-ult}$	$\sigma_{f-exp-buc}$
CTR	12441659.06	19.516	0.051	68.842	24.166	21.802
JFC	15901162.19	25.157	0.040	69.245	84.106	70.572
MDF	14460672.19	22.750	0.044	69.634	42.902	41.617

The reason why the proposed models has unsuccessfully predicted the strength of CTR and MDF specimens was most probably due to the existence of different failure mechanism developed within the specimen groups. As already mentioned previously, the failure mechanism of sandwich structure can be triggered by various mechanisms. The Kuenzi model was developed with the assumption that the panel would fail under shear buckling load, as was observed as the main failure mechanism of the JFC panels. The other two specimen groups, CTR and MDF, might not fail under that particular failure mechanism so that the shear stress induced within the panel could not be predicted accurately with the Modified Kuenzi Model. A complete calculation analysis using this modified model is included in Appendix-B.

Modified Hoff-Mautner Model vs Experimental results

This model was originally developed for the case of skin wrinkling of sandwich plates. The predicted results by the proposed modified model, as per Equation 7.43, are presented in Table 7.9. Likewise to the Modified Kuenzi Model, the current proposed model has also unsuccessfully predicted the strength of CTR and MDF specimens. The results differ by 127.4% and 71.2% for CTR and MDF specimens, respectively. The

model has, however, obtained an approximately 9% in difference between the theoretical and ultimate experimental stress values of JFC specimens, which is approximately similar to the results provided by the Modified Kuenzi Model. A complete calculation analysis using this modified model is included in Appendix-B.

Table 7.9. Predicted results using Modified-Hoff-Mautner Model

Specimens Group	a	E_i	E_c	G_c	σ_{f-mdl}	$\sigma_{f-exp-ult}$	$\sigma_{f-exp-buc}$
CTR	0.5	-	7.25	2.685	54.953	24.166	21.802
JFC	0.5	4502	7.25	2.685	77.162	84.106	70.572
MDF	0.5	2603	7.25	2.685	73.455	42.902	41.617

Modified Mamalis Model vs Experimental results

The predicted results provided by the model as per Equation 7.44, are shown in Table 7.10. Unlike the two previous models that had failed to accurately predicted the strength of MDF specimens, the current proposed model obtained a reasonable agreement between the theoretical and experimental stress values of the MDF specimens. The obtained theoretical shear strength of MDF was 40.27 MPa, while the average of experimental shear stress induced by the ultimate diagonal load was 42.90 MPa and 41.61 MPa due to the buckling load. It means that they only differ by 6.5% for ultimate load and 3.3% for buckling load. The results suggested that the hybrid sandwich panels with MDF intermediate layer would most likely fail due to the wrinkling of the aluminium face. This modified model was unable to accurately predict the strength of CTR and JFC specimens. A complete calculation analysis using this modified model is included in Appendix-B.

Table 7.10. Predicted results using Modified-Mamalis Model

Specimens Group	a	E_i	E_c	G_c	σ_{f-mdl}	$\sigma_{f-exp-ult}$	$\sigma_{f-exp-buc}$
CTR	0.0589	-	7.25	2.685	6.48	24.166	21.802
JFC	0.0070	4502	7.25	2.685	58.30	84.106	70.572
MDF	0.0070	2603	7.25	2.685	40.27	42.902	41.617

While the three proposed models were unsatisfactorily predicting the strength of the CTR specimens, the use of classical Euler shear equation, as per Equation 7.34, might obtain a reasonable answer for such case. The predicted shear stresses of sandwich panels based upon this model are presented in Table 7.11. The shear buckling coefficient (K_s) for this model was determined as per Pollock (1993). As can be seen in the table, the classic Euler shear equation provided a theoretical value of only 10.481

MPa, which was approximately half of the ultimate experimental stress value. However, when a carefully attention was given to the load-extension graphs of CTR specimens, there had actually a strong indication that 3 out of 5 of the CTR specimens already failed at early loads prior to reached their ultimate loads. These identified early failure loads have been included in the Table 7.3. The average shear stress induced by these early failure loads was about 10.99 MPa, which was pretty similar to the value obtained by the model, 10.461 MPa. This indicated that the CTR specimens were not fail under the two previous circumstances, global buckling or skin wrinkling, in which the JFC and MDF sandwich panels were most likely collapsed.

Table 7.11. Predicted results using Classical Euler shear stress model

Specimens Group	E_f	E_i	ν_i	K_s	$\sigma_{f\text{-mdl}}$	$\sigma_{f\text{-exp-ult}}$	$\sigma_{f\text{-exp-buc}}$
CTR	68200	-	-	15	10.481	24.166	21.802
JFC	68200	4502	0.235	15	33.972	84.106	70.572
MDF	68200	2603	0.253	15	24.190	42.902	41.617

Overall, the use of Modified Kuenzi Model and Modified Hoff-Mautner Model have been reasonably predicted the strength of hybrid sandwich panels with JFC intermediate layer, while the Modified Mamalis Model has predicted the strength of hybrid sandwich panels with a MDF intermediate layer. The strength of sandwich panels without intermediate layer (CTR) was reasonably predicted by the Classical Euler shear equation.

7.6. Chapter Conclusions

The in-plane shear behaviour of hybrid sandwich panels with an intermediate layer had been examined under a tension diagonal shear test. The in-plane shear behaviour and failure mechanisms of the hybrid sandwich panels have been compared to the conventional sandwich panels. The results of experimental investigation showed that incorporating intermediate layer within a sandwich structure significantly enhanced the in-plane shear behaviour of the hybrid sandwich panels developed in this thesis. More specific findings are outlined as follows.

- 1) The incorporation of JFC and MDF intermediate layer within sandwich panel has increased the diagonal load carrying capacity of sandwich panels by 385.9% and 118.2%, respectively. The average in-plane shear load of sandwich panels with JFC and MDF intermediate layer was about 381.9% and 112.5% higher

than such value of the sandwich panels without intermediate layer. While the improvement of shear stress given by the introduction of intermediate layer was about 384.9% for JFC and 118.3% for the MDF.

- 2) Hybrid sandwich panels with the JFC intermediate layer show excellent strength and stiffness. The panels with MDF intermediate layer behaved less stiff than the panels with JFC intermediate layer. The introduction of the intermediate layer, especially the one that made of JFC, has shown a significant contribution to the enhancement of the load carrying capacity of the sandwich panels.
- 3) Hybrid sandwich panel with either MDF or JFC intermediate layer has a better deformation capability than the conventional sandwich panels. Based upon the tension strains measurement, the deformation capability of hybrid sandwich panels with MDF intermediate layer is 1.6 times higher than the conventional sandwich panels, and 2.4 times for the panels with JFC intermediate layer. The enhancement is even more significant when the analysis uses the compression strain. The deformation capability of hybrid sandwich panels with MDF intermediate layer is 2.1 times higher than the conventional sandwich panels, and 3.8 times for the panels with JFC intermediate layer. If the comparison is made under a same load, the hybrid sandwich panels with JFC and MDF intermediate layers deform less than the conventional sandwich panel providing better deflection serviceability.
- 4) The results of the experiments were analysed as per Mohammed et al (2000) and Kuenzi et al (1962). The two methods provided comparable results. The difference between the average results was only about 3.5% for the CTR specimens, 4.6% for the JFC specimens and 5.5% for MDF specimens
- 5) Modified Kuenzi Model and Modified Hoff-Mautner Model have reasonably predicted the strength of hybrid sandwich panels with the JFC intermediate layer that collapsed under a buckling mechanism. The Modified Mamalis Model has successfully predicted the strength of hybrid sandwich panels with MDF intermediate layer that failed due to face wrinkling or delamination between intermediate layer and core. The strength of sandwich panels without an intermediate layer (CTR) has reasonably predicted with the Classical Euler shear equation.

CHAPTER 8

SIGNIFICANCE ANALYSIS OF THE FLEXURAL AND IN-PLANE SHEAR BEHAVIOUR OF HYBRID SANDWICH PANELS

8.1. General

Statistical significance is a mathematical tool that is commonly used to determine whether the outcome of an experiment is the result of a relationship between specific factors or merely the result of chance (Gunsch, 2013). Commonly, such a concept is used in the fields in which research is conducted through experimentation. It is frequent to summarize statistical comparisons by declarations of statistical significance or non-significance (Gelman and Stern, 2006). The statistical analysis of the data will produce a number that is statistically significant if it falls below a certain percentage called the confidence level or level of significance. Further, Gunsch (2013) explained that statistical significance is used to reject or accept what is called the null hypothesis, which usually states that there is no relationship between two variables. In a simple expression, statistical significance means that there is a good a relationship exists between two variables (*www.csulb.edu*).

This chapter focuses on the significance analysis of the experimental results obtained from the laboratory testing program for evaluating flexural and in-plane shear behaviour of sandwich panels. Statistical significance does not always mean that the finding is important or that it has any decision-making utility (*www.statpac.com*), so the researcher must always examine both the statistical and the practical significance of any research finding (*www.csulb.edu*).

8.2. Significance and statistical analysis in composite research

Although significance or statistical analysis is rarely found as a primary approach in composite sandwich panel research, it has been extensively used in the broad field of

composite material research. Some case studies are provided as follow. A study on the significance effect of microwave curing on tensile strength of carbon fibre composites was reported by Balzer and McNabb (2008). The statistical analysis employed was a two-way analysis of variance (Anova) using a statistical software SPSS 14.0. The results showed that the curing time and microwave process had a significant effect on the tensile strength of the carbon fibre composites. Jun et al (2008) reported their work on the optimization of processing variables in wood-rubber composite panels manufacturing process. The results of experiments were statistically analysed using a response surface method (RSM). The Design-Expert statistical software was employed to determine the significant factors that affected the properties of the composite panels. It was concluded that the density and the interaction of different variables were the significant factors affecting the final properties of the boards.

Shahdin et al (2009) used a design of experiments (DoE) approach to study the significance of low energy impact on modal parameters for composite beams. The experiment was a 5 x 2 full factorial design. The results showed that damping ratio was more sensitive parameter for the damage detection than the natural frequency. A Taguchi method used by Satapathy and Patnaik (2008) to analysis the dry sliding wear behaviour of red mud filled polyester composites. It was found that significant control factors and their interactions primarily influenced the results. Venkateshwaran and ElayaPerumal (2012) reported their work on the mechanical and absorption properties of woven jute/banana hybrid composites. Statistical analysis using one-way Anova was employed to analyse the results of the experiments. The results suggested that the layering pattern had significant effect on the mechanical properties of the composites.

A two-level full factorial design of experiment was used by Dwivedi et al (2007) to study the abrasive wear behaviour of bamboo powder filled polyester composites. The results indicated that the powder loading had significantly affected the wear behaviour. Aktas (2007) reported his research work on the statistical analysis of bearing strength of glass fibre composites materials. The bearing strength of woven glass fibre composites were analysed using Weibull distribution. The results suggested that approximately 99% reliability values of each bearing strength configuration was equivalent to the 0.7 average values of the bearing strength. A response surface methodology (RSM), which is a statistical design of experiment method, was employed

by Mathivanan et al (2010) to analysis the factors influencing deflection in sandwich panels subjected to low-velocity impact. The results revealed that the deflection of increased with the increasing of height of fall of the mass of the impactor.

8.3. Significance Analysis for Flexural Behaviour of Hybrid Sandwich Panels

8.3.1. Experiment results

The failure loads and deflections of medium scale specimen tested under flexural testing scheme are listed in Table 8.1, while those of large scale specimen are presented in Table 8.2. For a simplicity reason, the significance analysis in this chapter is only made for the data of load. As seen in the above tables that the coefficient variation (CV) of the actual data ranges from 9.39 to 16.05 for medium size specimens and 18.13 to 42.51 for large size specimens. The CV value for medium scale specimens are considered as fairly acceptable. The coefficient variation of large scale samples is, however, apparently unacceptable. The ratio of mean to standard deviation or CV should be of the order of 3 or more, but the value of 33% has often been stated as the permissible upper limit of CV (Johnson and Welch, 1939; Patel et al, 2001).

Table 8.1. Failure loads of medium scale samples under flexural test

Samples number	Treatments based upon intermediate layer used					
	CTR		JFC		HFC	
	P (N)	δ (mm)	P (N)	δ (mm)	P (N)	δ (mm)
1	321	11.92	414	56	628	42.24
2	415	15.4	473	62.18	579	36.37
3	307	12.18	379	45.22	524	47.04
4	293	9.89	378	56.53	481	37.86
5	302	13.2	414	64	635	35.09
Average	327.60	12.52	411.60	56.79	569.40	39.72
Stdev	49.90	2.01	38.64	7.34	66.53	4.90
CV	15.23	16.05	9.39	12.93	11.68	12.34

Table 8.2. Failure loads of large scale samples under flexural test

Samples number	Treatment (based upon intermediate layer used)					
	CTR		JFC		MDF	
	P (N)	δ (mm)	P (N)	δ (mm)	P (N)	δ (mm)
1	1060	14.16	1178	36.8	734	22.82
2	489	8.58	898	39.36	1241	16.53
3	572	5.7	751	38.72	1537	26.4
4	518	7.84	842	36.69	1275	19.41
5	407	10.18	738	61.11	1281	24.58
Average	609.20	9.29	881.40	42.54	1213.60	21.95
Stdev	258.97	3.16	178.44	10.45	293.12	3.98
CV	42.51	34.03	20.25	24.56	24.15	18.13

The CV values shown in the tables, especially in Table 8.2, indicated that the data was scatter. The fluctuation in the distribution of experimental data can be easily observed in Figure 8.1 and Figure 8.2. It is clearly shown in these figures that each level of samples in both medium and large scale specimen has at least one outlier data.

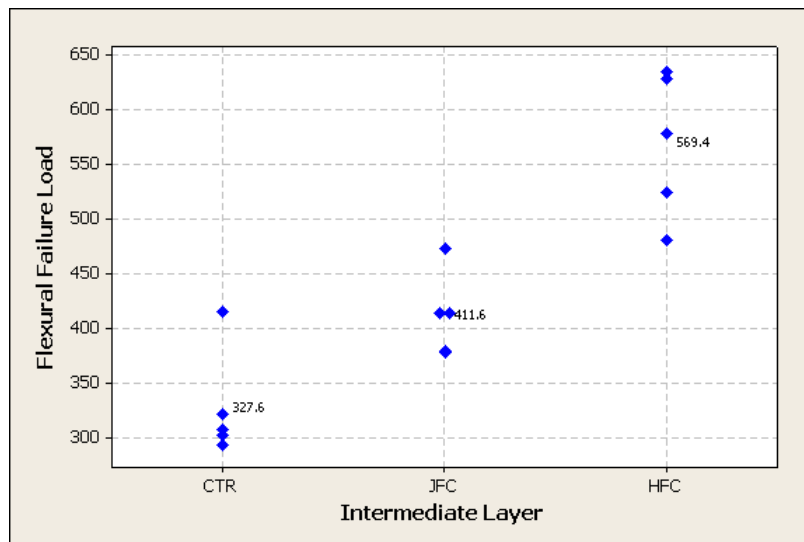


Figure 8.1. Dot-plot diagram for medium scale samples under flexural test

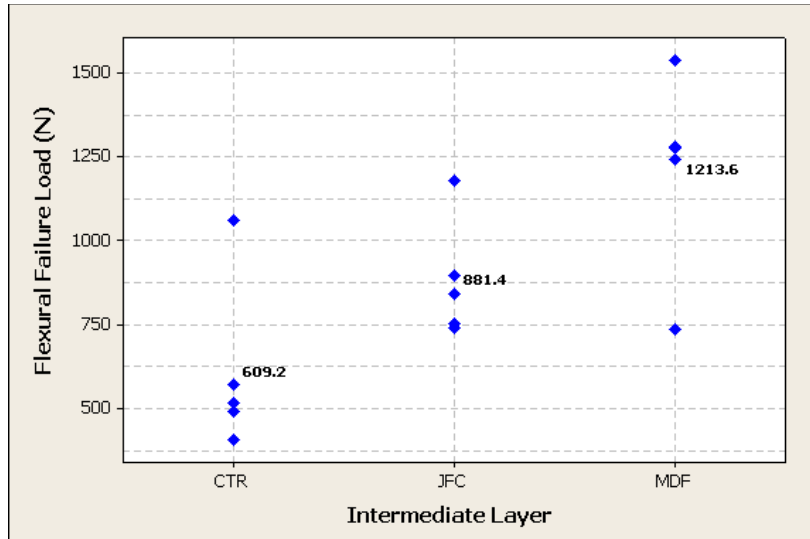


Figure 8.2. Dot-plot diagram for large scale samples under flexural test

Removing these values, by conducting normalization process, will produce more consistent or less fluctuated data. Montgomery (2009) stated that a very common defect of data is the presence of one or more outliers that can seriously distort the analysis of variance, so when a potential outlier is located, careful investigation is called for.

Frequently, the cause of the outlier is a mistake in calculations or data coding or copying errors. For medium scale specimen, the failure load of specimen 2 in CTR and JFC, and specimen 4 for HFC are considered as an outlier, with the value of 415 N, 473 N and 481 N, respectively (Table 8.1). The value of specimen 1 for all sample levels in large scale specimen is considered as an outlier. These values, as shown in Table 8.2, are 1060 N, 1178 N and 734 N for CTR, JFC and MDF, respectively.

The experimental data resulting from the normalization process are presented in Table 8.3 and Table 8.4. As it can be seen in Table 8.3, the coefficient variation of CTR, JFC and HFC for load has now reduced to 3.83%, 5.17% and 8.7%, respectively. The previous CV values for each level prior to the normalization process, as shown in Table 8.1, was 15.23%, 9.39% and 11.68% for CTR, JFC and HFC, respectively. Similarly, a considerable reduction in the CV value is also encountered for the experimental data of large scale experiment. The actual CV value of each level for large specimen, as shown in Table 8.2, was 42.51%, 20.25% and 24.15 for CTR, JFC and MDF factor level. After the normalization process, these values (as presented in Table 8.4) were reduced to 13.87%, 9.43% and 10.26% for the corresponding factor level. The significance analysis, which is discussed in the following section, was using data provided from the normalization process as presented in Tables 8.3 and 8.4.

Table 8.3. The results of normalization process for medium scale samples

Samples number	Treatments based upon intermediate layer used					
	CTR		JFC		HFC	
	P (N)	δ (mm)	P (N)	δ (mm)	P (N)	δ (mm)
1	321	11.92	414	56	628	42.24
2	307	12.18	379	45.22	579	36.37
3	293	9.89	378	56.53	524	47.04
4	302	13.2	414	64	635	35.09
Average	305.75	11.80	396.25	55.44	591.50	40.19
Stdev	11.70	1.39	20.50	7.73	51.44	5.53
CV	3.83	11.75	5.17	13.94	8.70	13.76

Table 8.4. The results of normalization process for large scale samples

Samples number	Treatment (based upon intermediate layer used)					
	CTR		JFC		HFC	
	P (N)	δ (mm)	P (N)	δ (mm)	P (N)	δ (mm)
1	489	8.58	898	39.36	1241	16.53
2	572	5.7	751	38.72	1537	26.4
3	518	7.84	842	36.69	1275	19.41
4	407	10.18	738	61.11	1281	24.58
Average	496.50	8.08	807.25	43.97	1333.50	21.73
Stdev	68.87	1.86	76.16	11.48	136.81	4.56
CV	13.87	23.04	9.43	26.12	10.26	20.98

8.3.2. Analysis and discussions

The significance analysis in this research is carried out using analysis of variance as described in Chapter 3. The experiments were arranged as a single factor experiment in which 3 levels of a factor had been examined. The factor refers to the type of intermediate layer used in the sandwich panel and such factor was levelled as 0, 1 and 2 as required by Minitab 15 software. For medium scale specimen, level 0 was the conventional sandwich panel without intermediate layer or control level (CTR) while level 1 and 2 refer to as jute fibre composite (JFC) and hemp fibre composite (HFC), respectively. In large scale scheme, level 1 and 2 refer to as Jute fibre composite (JFC) and medium density fibre (MDF) while level 0 was a control level (CTR) which is sandwich panel without intermediate layer. For the analysis purpose, as recommended by Montgomery (2009), the data for Anova are tabulated as follows.

Table 8.5. Tabulated data for analysis of variance (Anova)

Medium Scale						
Factor levels	Observations				Totals	Averages
	1	2	3	4		
Level 0 (CTR)	321	307	293	302	1223	305.75
Level 1 (JFC)	414	379	378	414	1584	396.25
Level 2 (HFC)	628	579	524	635	2366	591.50
Large Scale						
Factor levels	Observations				Totals	Averages
	1	2	3	4		
Level 0 (CTR)	489	572	518	407	1986	496.50
Level 1 (JFC)	898	751	842	738	3229	807.25
Level 2 (MDF)	1241	1537	1275	1281	5334	1333.50

From the above tables, some important parameters for theoretical calculations can be determined such as replications ($n = 5$), total number of samples ($N = 12$), and number of levels or treatments ($a = 3$). The significance analysis for medium and large scale specimens are discussed separately in the following sections.

Medium scale samples

Initially, the theoretical total corrected sum squares (SS_T) and treatment sum square ($SS_{\text{treatments}}$) were calculated as per Equation 3.73 and 3.74, respectively. The sum of square of difference (SS_E) was then calculated based upon the results of the above two equations as defined by Equation 3.75. The subsequent steps were determining the mean square for treatment ($MS_{\text{treatments}}$) and the error mean square (MS_E) using Equation 3.77

and 3.78, respectively. Finally, the value of F_0 can be obtained as per Equation 3.79. The results of the theoretical calculations were then presented in a particular table as recommended by Montgomery (2009). The table, as shown as Table 8.6, contains all important parameter for further use to make a significance judgment.

Table 8.6. Analysis of variance table for single-factor experimental design

Source of variations	Sum of square	Degrees of freedom	Mean square	F_0
Between treatments	$SS_{\text{treatments}} = \frac{1}{n} \sum_{i=1}^a y_i^2 - \frac{y^2}{N}$	$a - 1$	$MS_{\text{treatments}}$	$F_0 = \frac{MS_{\text{treatments}}}{MS_E}$
Error (within treatments)	$SS_E = SS_T - SS_{\text{treatments}}$	$N - a$	MS_E	
Total	$SS_T = \sum_{i=1}^a \sum_{j=1}^n (y_{ij} - \bar{y}_{...})^2$	$N - 1$		

The theoretical results of the analysis of variance for medium scale sandwich panels are summarized in Table 8.6, while the detailed theoretical calculation is included in Appendix C. The results of analysis obtained by statistical software Minitab 15 is presented in Table 8.7.

Table 8.6. The theoretical results of Anova for medium scale sandwich panels

Source of variations	Sum of square	Degrees of freedom	Mean square	F_0
Intermediate layer	170621.20	2	85310.58	79.91
Error	9608.50	9	1067.61	
Total	180229.70	11		

Table 8.7. Analysis of variance results for medium scale sandwich panel obtained by statistical software Minitab 15

One-way ANOVA: Flexural Load versus Intermediate Layer					
Source	DF	SS	MS	F	P
Intermediate Layer	2	170621	85311	79.91	0.000
Error	9	9609	1068		
Total	11	180230			

S = 32.67 R-Sq = 94.67% R-Sq(adj) = 93.48%

Individual 95% CIs For Mean Based on Pooled StDev

Level	N	Mean	StDev
0	4	305.75	11.70
1	4	396.25	20.50
2	4	591.50	51.44

Pooled StDev = 32.67

As presented in Table 8.6 and Table 8.7, the theoretical calculations were in good agreement with the Anova results obtained by statistical software Minitab 15. It can be noted here that the mean square between treatments (85311) was few times larger than the mean square within the treatments or error mean square which was only 1068. This indicates that the treatments differ. The other way to make a significance decision is by using the F value (F_0). The value of F_0 for medium scale sandwich panels, as seen in Table 8.6 and Table 8.7, was 79.91. Instead, the F value obtained from the F-distribution table for $F_{(0.05;2,9)}$ was 4.26. This value, which is called as F table, was obtained by using the significance level of 95% ($\alpha = 0.05$), 3 levels ($a = 3$) and 12 samples ($N = 12$). Since the value of F_0 (79.91) was much higher than the value of F table (4.26), the null hypothesis (H_0) should be rejected, as stated in Equation 3.81, meaning that there are a significant difference in the treatments means.

For this experiment, the null hypothesis was actually trying to state that the load carrying capacity of all types of tested sandwich panels (CTR, JFC and HFC) were equal. However, the statistical significance analysis showed that the average values of the three types of sandwich panels were significantly different. Since the average values or means of the JFC and HFC was higher than CTR, it can be concluded that the load carrying capacity of hybrid sandwich panels is significantly higher than the conventional sandwich panels. In addition, as the confidence level used in the Minitab analysis was 95%, it means that the finding has a 95% chance of being true. Alternatively, the finding has a 5% of not being true as it was analysed with the assumption of the probability error (α) of 0.05. A value of P, or frequently called as P-value, could also be used for drawing a conclusion. The rule is that if the P-value is less than α (0.05) which is an error tolerance level, it can be concluded that there has factor levels or treatments that have different means. It is clearly presented in Table 8.7 that the P-value of medium scale specimen was very small, which is approximately 0.000.

A pairwise comparison between all factor levels might be conducted to support the decisions drawn from Anova results. There are several possible test methods for this purpose such as Dunnet's test, Tukey's test and Fisher's test to mention a few. The three pairwise tests were also conducted using Minitab 15 software and the results are discussed separately as follows.

all confidence intervals include only a positive numbers. Another way of drawing a decision is by looking at the critical value of each level. As it can be seen in Table 8.9, the critical value of reference level was 2.61. This value is much lower than the critical value of level 1 and level 2 which was 90.50 and 285.75, respectively. Overall, it can be concluded that the load carrying capacity of level 1 (JFC) and level 2 (HFC) is much higher than level 0 (CTR).

Table 8.9. The results of Dunnett’s test for medium scale sandwich panels obtained by statistical software Minitab 15

Dunnett's comparisons with a control

Family error rate = 0.05
 Individual error rate = 0.0281
 Critical value = 2.61

Control = level (0) of Intermediate Layer
 Intervals for treatment mean minus control mean

Level	Lower	Centre	Upper	
1	30.10	90.50	150.90	(-----*-----)
2	225.35	285.75	346.15	(-----*-----)

-----+-----+-----+-----+-----
 80 160 240 320

The third pairwise method is a Fisher’s test which is pretty similar to the Tukey’s test. The result of Fisher test for medium scale sandwich panels is presented in Table 8.10. As seen in the table, none of the confident intervals contains zero number meaning that all levels differ. It is also noticeable in the table that the critical values or the centre confident levels were comparable to the critical values obtained on Tukey’s test. The difference is only for their lower and upper values.

Table 8.10. The results of Fisher’s test for medium scale sandwich panels obtained by statistical software Minitab 15

Fisher 95% Individual Confidence Intervals
All Pairwise Comparisons among Levels of Intermediate Layer

Simultaneous confidence level = 88.66%
 Intermediate Layer = 0 subtracted from:

Intermediate Layer	Lower	Centre	Upper	
1	38.23	90.50	142.77	(--*--)
2	233.48	285.75	338.02	(--*)

-----+-----+-----+-----+-----
 -150 0 150 300

Intermediate Layer = 1 subtracted from:

Intermediate Layer	Lower	Centre	Upper	
2	142.98	195.25	247.52	(--*--)

-----+-----+-----+-----+-----
 -150 0 150 300

Table 8.13. The results of Tukey’s test for large scale sandwich panels obtained by statistical software Minitab 15

Tukey 95% Simultaneous Confidence Intervals
All Pairwise Comparisons among Levels of Intermediate Layer

Individual confidence level = 97.91%
Intermediate Layer = 0 subtracted from:

Intermediate Layer	Lower	Centre	Upper	
1	115.7	310.8	505.8	-----+-----+-----+-----+-----
2	642.0	837.0	1032.0	(---*---) (---*---)
				-----+-----+-----+-----+-----
				-500 0 500 1000

Intermediate Layer = 1 subtracted from:

Intermediate Layer	Lower	Centre	Upper	
2	331.2	526.3	721.3	-----+-----+-----+-----+-----
				(---*---)
				-----+-----+-----+-----+-----
				-500 0 500 1000

Table 8.14. The results of Dunnett’s test for large scale sandwich panels obtained by statistical software Minitab 15

Dunnett's comparisons with a control

Family error rate = 0.05
Individual error rate = 0.0281
Critical value = 2.61
Control = level (0) of Intermediate Layer
Intervals for treatment mean minus control mean

Level	Lower	Centre	Upper	
1	128.2	310.8	493.3	-----+-----+-----+-----+-----
2	654.5	837.0	1019.5	(-----*-----) (-----*-----)
				-----+-----+-----+-----+-----
				250 500 750 1000

Table 8.15. The results of Fisher’s test for large scale sandwich panels obtained by statistical software Minitab 15

Fisher 95% Individual Confidence Intervals
All Pairwise Comparisons among Levels of Intermediate Layer

Simultaneous confidence level = 88.66%
Intermediate Layer = 0 subtracted from:

Intermediate Layer	Lower	Centre	Upper	
1	152.78	310.75	468.72	-----+-----+-----+-----+-----
2	679.03	837.00	994.97	(--*--) (--*--)
				-----+-----+-----+-----+-----
				-500 0 500 1000

Intermediate Layer = 1 subtracted from:

Intermediate Layer	Lower	Centre	Upper	
2	368.28	526.25	684.22	-----+-----+-----+-----+-----
				(---*---)
				-----+-----+-----+-----+-----
				-500 0 500 1000

It can be observed from the presented tables that all the confidence intervals have a positive number. For Tukey's test, as shown in Table 8.13, the comparison of level 0 to level 1 and level 2 has the value of 115.7 and 642 for the lower values and 505.8 and 1032 for the upper values with the critical values of 310.8 and 837 for level 1 and level 2, respectively. This indicates that the load carrying capacity of hybrid sandwich panels with JFC and HFC intermediate layer is significantly higher than the conventional sandwich panels (CTR). For Dunnett's test, it is clearly shown in Table 8.14 that all confidence intervals include only a positive numbers and the critical value of control level as the reference was 2.61. The obtained value is much lower than the critical value of level 1 and level 2 which was 310.8 and 837, respectively. Overall, it can be concluded that the load carrying capacity of level 1 and level 2 is much higher than reference level. In addition, the Tukey's test also showed positive values of confident intervals as presented in Table 8.15.

8.4. Significance Analysis for In-Plane Shear of Hybrid Sandwich Panels

8.4.1. Experiment results

The failure loads and deformations of specimens tested under in-plane shear testing are listed in Table 8.16. It can be observed from the table that the coefficient variation (CV) of the in-plane shear load test results was 18.48 for CTR, 5.40 for JFC and 1.75 for MDF. These CV values are considered as highly acceptable especially for JFC and MDF panels. The excellent consistency in the distribution of experimental data can be easily observed in Figure 8.3.

Table 8.16. Failure loads of specimens tested under in-plane shear loading scheme

Samples number	Treatments based upon intermediate layer used					
	CTR		JFC		MDF	
	P (N)	δ (mm)	P (N)	δ (mm)	P (N)	δ (mm)
1	9228	7.73	49006	15.52	21809	23.38
2	10043	14.48	47921	19.73	22324	25.97
3	13575	22.75	53834	26.98	22442	29.38
4	9051	13.17	51127	14.72	22366	23.73
5	9367	12.05	47192	14.42	22908	29.92
Average	10252.80	14.04	49816.00	18.27	22369.80	26.48
Stdev	1894.74	5.49	2692.38	5.31	390.99	3.07
CV	18.48	39.12	5.40	29.08	1.75	11.59

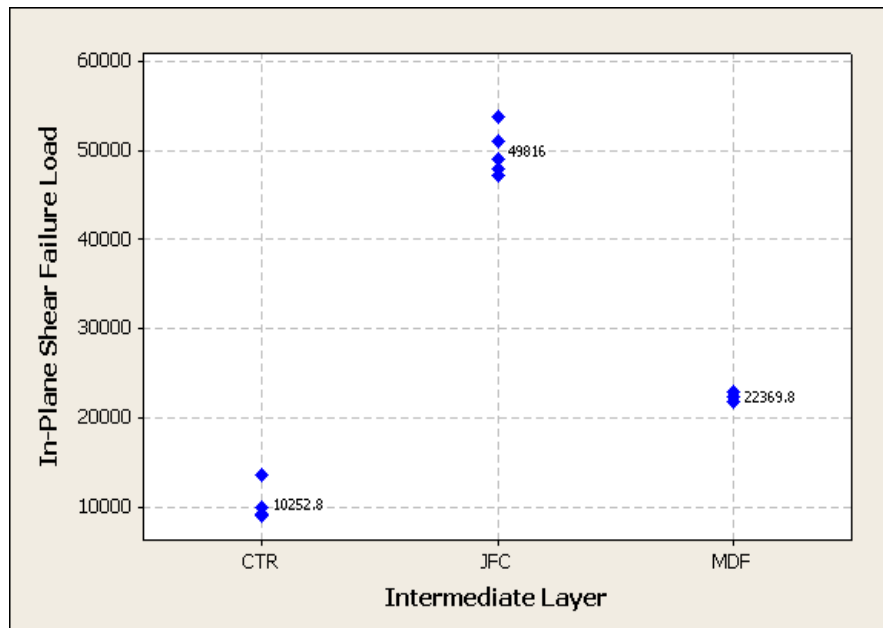


Figure 8.3. Dot-plot diagram for the in-plane shear test results

8.4.2. Analysis and discussions

The experiment was designed as a single factor experiment in which 3 levels of a factor had been examined. The factor refers to the type of intermediate layer used in the sandwich panel. Level 1 and 2 refer to as Jute fibre composite (JFC) and medium density fibre (MDF) while level 0 was a reference or control level (CTR) which was sandwich panels without intermediate layer. For the analysis purpose, the data for Anova are tabulated as follows.

Table 8.17. Tabulated data for analysis of variance (Anova) for in-plane shear test

Factor levels	Observations					Totals	Averages
	1	2	3	4	5		
Level 0 (CTR)	9228	10043	13575	9051	9367	51264	10252.8
Level 1 (JFC)	49006	47921	53834	51127	47192	249080	49816.0
Level 2 (MDF)	21809	22324	22442	22366	22908	111849	22369.8

Table 8.18. The theoretical results of ANOVA for in-plane shear test

Source of variations	Sum of square	Degrees of freedom	Mean square	F ₀
Intermediate layer	4108937296.00	2	2054468648.00	560.73
Error	43967235.60	12	3663936.40	
Total	4152904532.00	14		

As it can be seen in Table 8.17, some important parameters for theoretical calculations can be determined such as replications ($n = 5$), total number of samples ($N = 15$), and number of levels or treatments ($a = 3$). The theoretical results of the analysis of variance for the in-plane shear test are summarized in Table 8.18 while such analysis obtained by statistical software Minitab 15 is presented in Table 8.19.

Table 8.19. Analysis of variance results for in-plane shear test obtained by statistical software Minitab 15

One-way ANOVA: Flexural Load versus Intermediate Layer					
Source	DF	SS	MS	F	P
Intermediate Layer	2	4108937296	2054468648	560.73	0.000
Error	12	43967236	3663936		
Total	14	4152904532			
S = 1914 R-Sq = 98.94% R-Sq(adj) = 98.76%					
Individual 95% CIs For Mean Based on Pooled StDev					
Level	N	Mean	StDev	-----+-----+-----+-----+-----	
0	5	10253	1895	(-*)	
1	5	49816	2692		(-*)
2	5	22370	391		(-*)
				-----+-----+-----+-----+-----	
				12000	24000 36000 48000

Both tables showed that the mean square between treatments was many times larger than the error mean square meaning that the average values of in-plane shear load of each treatment are significantly different. It is also noticeable that the theoretical calculations were comparable to the analysis results obtained by statistical software Minitab 15. The value of F_0 for the in-plane shear test was 560.73, which is much larger than the value obtained from F-distribution table. The F value, obtained by using the significance level of 95% ($\alpha = 0.05$), 3 levels of treatment replications ($a = 3$) and 15 samples ($N = 12$), was 3.89 or can be written as $F_{(0.05;2,12)} = 3.89$. As the value of F_0 was much higher than the value of F table, it can be concluded that the null hypothesis (H_0) should be rejected, and accept the alternative hypothesis (H_1) which stated that there has a significant difference in the treatments means. The inference statement suggests that the in-plane shear load carrying capacity of hybrid sandwich panels with JFC and MDF intermediate layer was significantly higher than the conventional sandwich panels. This statement has a 95% chance of being true, or 5% of not being true, as the significance level used for the analysis was 95%. Based upon the P value, which was much less than 0.005, it can also be concluded that there has factor levels or treatments that have

different means. The P-value for this experiment, as presented in the Table 8.19, was approximately 0.000.

Similar to the previous significance analysis for sandwich panels under flexural load, pairwise comparisons were also conducted in this in-plane shear test results to confirm the decisions drawn from the analysis of variance. The results of Tukey’s, Dunnet’s, and Fisher’s test are presented in the following tables.

Table 8.20. The results of Tukey’s test for in-plane shear test obtained by statistical software Minitab 15

Tukey 95% Simultaneous Confidence Intervals
All Pairwise Comparisons among Levels of Intermediate Layer

Individual confidence level = 97.94%
Intermediate Layer = 0 subtracted from:

Intermediate Layer	Lower	Centre	Upper	
1	36336	39563	42790	(-*)
2	8890	12117	15344	(-*--)

-----+-----+-----+-----+-----
-20000 0 20000 40000

Intermediate Layer = 1 subtracted from:

Intermediate Layer	Lower	Centre	Upper	
2	-30673	-27446	-24219	(*--)

-----+-----+-----+-----+-----
-20000 0 20000 40000

Table 8.20 shows the result of Tukey’s test conducted for the data of in-plane shear test. The comparison of level 0 to level 1 has the confident interval of 36336 for the lower value and 42790 for the upper value, and the critical value of 39563. For level 0 to level 2, the lower and the upper value was 8890 and 15344, respectively. Unlike the previous analysis of variance, the current analysis has negative confident values that appear when the level 2 was compared to the level 0. The lower and upper value was -30673 and -24219, respectively with the centre or critical value of -27446. Although all the confident values were negative, it has a similar meaning with the previous all positive values because they are not containing zero number. The rule for concluding that all levels are different was that whenever the Tukey’s confidence intervals contain zero number, it indicates that the means are not different. In short, it can be concluded that all the treatment means differ as none of confident levels contains zero. The Tukey’s test also suggests that there is a significant different between level 1 and level 2, as they contain only negative numbers or none of confident levels contains zero.

Table 8.21 presents the results of Dunnett’s test for the data of in-plane shear test. It is clearly shown in the table that all confidence intervals include only positive numbers. The lower and upper value of confident intervals for level 1 was 36534 and 42593, respectively. The corresponding vales for level 2 was 9088 and 15146. The critical value of control level was 2.50, which is much lower than the critical value of level 1 and level 2. The critical value for level 1 was 39563 and 12117 for level 2. In short, it can be concluded that the load carrying capacity of level 1and level 2 is much higher than control level.

Table 8.21. The results of Dunnett’s test for in-plane shear test obtained by statistical software Minitab 15

Dunnett's comparisons with a control				
Family error rate = 0.05				
Individual error rate = 0.0278				
Critical value = 2.50				
Control = level (0) of Intermediate Layer				
Intervals for treatment mean minus control mean				
Level	Lower	Centre	Upper	-+-----+-----+-----+-----+
1	36534	39563	42593	(--*--)
2	9088	12117	15146	(--*--)
				-+-----+-----+-----+-----+
				10000 20000 30000 40000

Table 8.22. The results of Fisher’s test for in-plane shear test obtained by statistical software Minitab 15

Fisher 95% Individual Confidence Intervals				
All Pairwise Comparisons among Levels of Intermediate Layer				
Simultaneous confidence level = 88.44%				
Intermediate Layer = 0 subtracted from:				
Intermediate				
Layer	Lower	Centre	Upper	-----+-----+-----+-----+
1	36926	39563	42201	(-*)
2	9479	12117	14755	(*)
				-----+-----+-----+-----+
				-20000 0 20000 40000
Intermediate Layer = 1 subtracted from:				
Intermediate				
Layer	Lower	Centre	Upper	-----+-----+-----+-----+
2	-30084	-27446	-24809	(*-)
				-----+-----+-----+-----+
				-20000 0 20000 40000

The result of Fisher’s test is given in Table 8.22 which shows a similar configuration with the Tukey’s test. The comparison of level 0 to level 1 and level 2 has all positive confident intervals while the comparison of level 1 to level 2 has all negative

numbers. The configuration of the confident values, that only contain positive or negative numbers, indicate that the means are different as they are not including zero number.

8.5. Power Analysis and Determining Sample size

In any experimental design, one of the critical decisions that has to be made is the choice of sample size (Montgomery, 2009). In statistical design of experiment, where Analysis of Variance (Anova) is employed to analysis the result of single factor experimental design, the number of samples is determined prior to conducting the test or checked after running out a preliminary test. The method of determining sample size for analysis of variance is described thoroughly in many respectable statistic books. Generally, different field of research required different way of determining samples. Research in social science normally requires more samples than in engineering science. The required number of samples or replications is depended upon many factors. Kuehl (2000) explained that “the number of replications in a research study affects the precision of estimates for treatment means and the power of statistical tests to detect difference among the means of treatment groups. However, the cost of conducting research studies constrains the number of replications for a reasonably sized study. Thus, replication numbers are determined on the basis of practical constraints that we can assign to the problem”.

The results of power analysis for all the three experimental designs are presented in Table 8.23. Clearly, the statistical power value $(1 - \beta)$ for all experimental arrangements are greater than 0.99 meaning that the results drawn from 4 replications are considered as statistically powerful. The complete analysis and discussions about the power analysis is given in Appendix D.

Table 8.23. Statistical power value of each testing arrangement

	Φ_c (Eq. 3)	Φ_c (Eq. 4)	$(1-\beta)$
Flexural test medium size	7.29	7.25	≥ 0.99
Flexural test large size	6.99	6.94	≥ 0.99
In-plane shear test	18.71	13.65	≥ 0.99

The results of analysis using Minitab software are also included in the appendix. This method is conducted by setting the power level and the desired detection level difference (δ). It is clearly shown in the analysis result that with the target power of 0.8

and a certain level of difference, the required number of sample for flexural test and in-plane shear test is 4 and 5 specimens, respectively. The results of Minitab analysis for flexural test of medium size sample is presented in Figure 8.4. The results for the flexural test of large size sample and the in-plane shear test are provided in Appendix D.

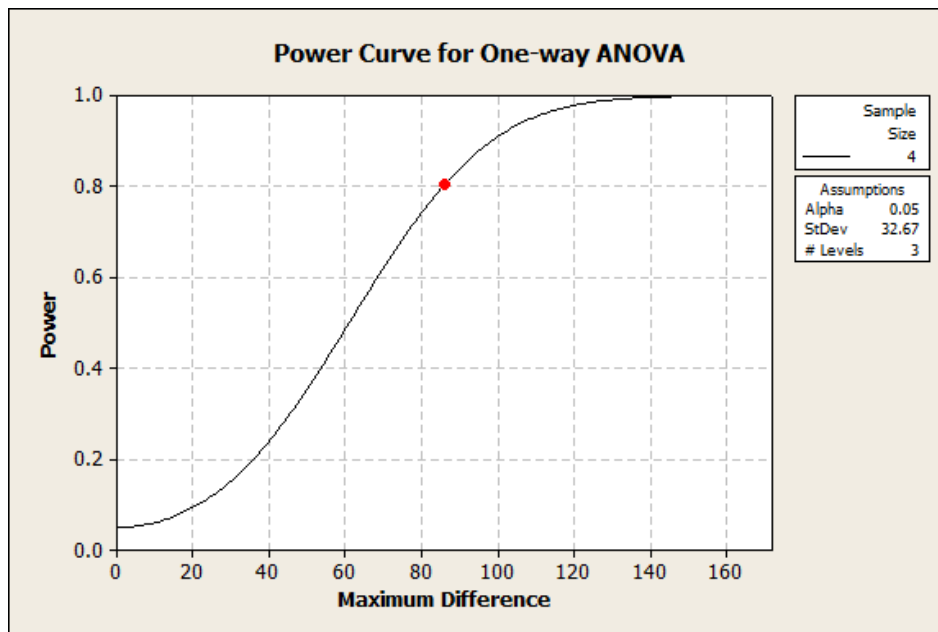


Figure 8.4. The power curve of flexural test with medium scale specimens

8.6. Chapter Conclusions

The significance analysis has been carried out to the data of ultimate load provided from flexural and in-plane shear test of hybrid and conventional sandwich panels. The experiments were designed following the principle of statistical design of experiments and the works reported in this chapter was specifically designed as a single factor experiments. For all experiments, two types of hybrid sandwich panels were compared to the conventional sandwich panels without intermediate layer. The primary conclusion drawn was that the incorporation of intermediate layer has significantly enhanced the load carrying capacity of sandwich panels. More specific outcomes are outlined as follows.

- 1) The value of F_0 for medium scale sandwich panels was much higher than the F value obtained from the F -distribution ($F_{(0.05;2,9)}$). The F_0 was 79.91 while the F -table was only 4.26. It is therefore, the null hypothesis (H_0) should be rejected, meaning that there are significant differences in the treatments means. All

pairwise tests; Tukey's, Dunnet's and Fisher's tests obtained all positive confident intervals that suggests the means of treatments differ.

- 2) The F_0 value for large scale sandwich panels was 73.42, while the F value obtained from the F -distribution table for $F_{(0.05;2,9)}$ was 4.26. The value of F_0 was much higher than the value of F table, accordingly the null hypothesis (H_0) should be rejected, which means that there are a significant difference in the average values of treatments. All pairwise tests also showed all positive confident intervals as observed for medium scale test.
- 3) The value of F_0 for the in-plane shear test was 560.73, which is much larger than the value obtained from F -distribution table. The F value, obtained by using the significance level of 95% ($\alpha = 0.05$), 3 levels of treatment replications ($a = 3$) and 15 samples ($N = 12$), was 3.89. As the value of F_0 was much higher than the value of F table, it can be concluded that the null hypothesis (H_0) should be rejected, and accept the alternative hypothesis (H_1) which stated that there has a significant difference in the treatments means.
- 4) The inference statements suggested that the load carrying capacity of hybrid sandwich panels with JFC and MDF intermediate layer was significantly higher than the conventional sandwich panels.
- 5) The Tukey's test suggests that the load carrying capacity of hybrid sandwich panel with JFC (level 1) and MDF (level 2) intermediate layer is significantly different. All the confident values for medium and large scale flexural test contain only positive numbers, while such values for the in-plane shear test contain all negative numbers. None of them contains zero numbers meaning that the difference is significant.
- 6) All significance analysis have been conducted with the significance level of 95% or $\alpha = 0.05$ meaning that the conclusions drawn have a 95% chance of being true, or 5% of not being true.

CHAPTER 9

SUMMARY, CONCLUSIONS AND RECOMMENDATIONS

9.1. Summary

The purpose of this research was to develop, test and analyse a new developed hybrid sandwich panel with natural fibre composites as an intermediate layer. The new panel was termed a sustainable hybrid sandwich panel. Initially, a review of composite sandwich panels and sustainable green composites was presented in Chapter 2. It was found that upgrading the quality of sandwich panels has been achieved by introducing various new materials for either skins and/or core. Included in these efforts are attempts to develop a lightweight panel for building applications and also to utilise sustainable green materials. However, it was discovered that larger sized components needed to be prepared when the panel was manufactured solely from green materials such as natural fibre composites in order to meet adequate strength. This was at the expense of higher cost. It was also found that the most successful efforts were those involving hybridization concept at both the structural and the constituent levels. Thus, incorporating natural fibre composites as an extra layer in between skins and core to form a hybrid sandwich panel appeared to be a promising solution to the author.

The accumulation of knowledge gained from the literature review has suggested that the properties of natural fibre composites can vary greatly depending upon the raw material used, pre-treatment process and the manufacturing process. In this research, natural fibre composites were prepared using vacuum bagging method, which is a good combination of preparing the raw material using hand lay-up technique and applying a pressure within the vacuum bagging to produce high quality laminates. The composite laminates were prepared with various natural fibres and their mechanical properties had been comparatively assessed to find the best candidates for the intermediate layer. Included in the mechanical properties testing was also medium density fibre (MDF)

panel for further use as an alternative for the intermediate layer of hybrid sandwich panels. The preparation, fibres pre-treatment with chemical processing, manufacturing process, mechanical properties testing and comparative analysis of the experiment results are presented in Chapter 4.

Having selected two types of natural fibre composite laminates as the best candidates for intermediate layer, together with MDF panel, two series of panels' size had been prepared for investigating the flexural behaviour of the panel. The preparation, test and analysis of the flexural behaviour of hybrid sandwich panel were comprehensively described in Chapter 5. A development of a theoretical model for predicting the deflection of hybrid sandwich panels was also highlighted in this chapter. The agreement between the theoretical model and the experimental results was discussed thoroughly. The information gained from the flexural testing provided excellent information about the suitability of natural fibre composites to be used as the intermediate layer of hybrid sandwich panels.

The main concern of wall panel used in building structure is its in-plane shear behaviour. However, there has been a concern about the in-plane shear testing of the panel, which is the scale of the testing. The well established testing method for building panel is a racking test as per ASTM E-72 that might not be suitable for examining the in-plane shear behaviour of panel in the early development stage due to the complexity of the testing set up and the cost. A comprehensive literature review of the existing small and medium scale panel testing was given in Chapter 6. This chapter also includes several experimental trials to obtain the most suitable and convenient way to perform the testing. The actual testing that includes the preparation of specimens, test and analysis the results was comprehensively discussed in Chapter 7. In order to predict the in-plane shear behaviour of the hybrid sandwich panels, theoretical models were proposed for different types of failure mechanisms. The comparison analysis between the theoretical models and the experimental results is also presented as part of this chapter. Lastly, in relation to the statistical experimental design that was applied diligently for all stages of the experimental work, a significance analysis of the experimental results using statistic software Minitab 15 was presented in Chapter 8. The analysis was carried out for the experimental results of both flexural and in-plane shear testing.

9.2. Conclusions

The major findings of this research work can be summarised as follows:

Theoretical Concept and Validation Using Statistical Experimental Design

- 10) The stiffness of a sandwich structure is related to the flexural rigidity of the panel. Introducing an intermediate layer into an ordinary sandwich structure creates a hybrid sandwich panel, increases the flexural rigidity and correspondingly enhances the stiffness. Application of the relevant theory regarding the flexural rigidity and the stiffness of the new hybrid structure has proven the concept.
- 11) The statistical experimental design employed in the preliminary experiment successfully validated the work of Mamalis et al (2008) who stated that the introduction of intermediate layer can significantly enhance the structural behaviour of sandwich panel structure. The result of these preliminary experiments demonstrated the potential of the new hybrid sandwich panel composite to be developed further for potential use as a load-carrying component in buildings.

Characterization of Natural Fibre Composites

- 1) Jute fibre composites and hemp fibre composite laminates were found to be the best two candidates for use in the new composite panel.
- 2) Jute fibre composite laminate possessed the highest average value for almost all the observed mechanical properties in this study. They also have the lowest Poisson ratio. Hemp fibre composite laminate had the most consistent properties except for its flexural properties. It is also important to note that the availability of jute and hemp fibre, especially the types of fibre used in this research. They can be readily obtained in the desired size and volume.
- 3) Composites reinforced with unidirectional sisal fibres might also be an excellent choice for their good observed mechanical properties. However, their availability may prevent their use in a large scale.

Flexural Behaviour

- 1) The load carrying capacity of the hybrid sandwich panels was significantly higher than the conventional sandwich panel.

- 2) Both types of sandwich panels, with or without intermediate layer, behave in a ductile manner by not exhibiting brittle failure. However, there was an obvious change in the load-deflection curve when an intermediate layer was incorporated in the sandwich panels, which was related to the toughness of the material. Hybrid sandwich panels developed a much larger area under the load-deflection curve than the conventional sandwich panels.
- 3) The deflection of the hybrid sandwich panel was slightly larger than those of conventional sandwich panel although they have higher equivalent bending stiffnesses. The introduction of intermediate layer does not contribute to the reduction of the deflection of the hybrid sandwich panel as the main contributor for the total deflection was the shear deformation of the core as mostly determined by the shear modulus and the thickness of the core.
- 4) The proposed model for predicting the deflection of hybrid sandwich panels provided fairly agreement results with the experimental values. The differences range from 3.9% to 35.4%. Most of the sandwich panels showed experimental values lower than the theoretical values. This may be considered as highly desirable in the design.
- 5) The introduction of intermediate layer helps the sandwich panels to sustain larger compressive strain prior to reaching their ultimate loads. This has prevented them from prematurely failing under buckling or indentation.
- 6) The intermediate layer has prevented the occurrence of premature failure mechanisms such as indentation or delamination of skin and core due to compression buckling, resulting in higher flexural ultimate load carrying capacity.

In-Plane Shear Behaviour

- 1) The incorporation of an intermediate layer within the sandwich panel has significantly increased the diagonal load carrying capacity, in-plane shear load and also the shear strength of the sandwich panels.
- 2) Hybrid sandwich panels with a JFC intermediate layer demonstrated excellent strength and stiffness. The panel with the MDF intermediate layer behaved less stiff than the panels with the JFC intermediate layer. The introduction of an

intermediate layer, especially the one that made of natural fibre composites significantly enhanced the load carrying capacity of the sandwich panels.

- 3) Hybrid sandwich panels provided better deformation capability than the conventional sandwich panels. Based upon the tension strains measurement, the deformation capability of hybrid sandwich panels with MDF intermediate layer was 1.6 times higher than the conventional sandwich panels, and 2.4 times higher than the panels with JFC intermediate layer. The enhancement is more significant when the analysis uses the compression strain; the deformation capability of hybrid sandwich panels with MDF intermediate layer is 2.1 times higher than the conventional sandwich panels, and 3.8 times for the panels with the JFC intermediate layer. If the comparison is made under a same load, the hybrid sandwich panels with JFC and MDF intermediate layers are stiffer than the conventional sandwich panel.
- 4) The results of experiment were analysed as per Mohammed et al (2000) and Kuenzi et al (1962). The two methods provided comparable results. The difference between the average results was only about 3.5% for CTR specimens, 4.6% for JFC specimens and 5.5% for MDF specimens
- 5) The Modified Kuenzi Model and Modified Hoff-Mautner Model reasonably predicted the strength of hybrid sandwich panels with the JFC intermediate layer that collapsed under a buckling mechanism. The Modified Mamalis Model successfully predicted the strength of hybrid sandwich panels with MDF intermediate layer that failed due to face wrinkling or delamination between intermediate layer and core. The strength of the sandwich panels without an intermediate layer (CTR) was reasonably predicted by the Classical Euler shear equation.

Significance Analysis

- 1) The analysis clearly found that incorporation of an intermediate layer significantly enhanced the load carrying capacity of sandwich panels.
- 2) The value of F_0 for medium scale sandwich panels was much higher than the F value obtained from the F -distribution ($F_{(0.05;2,9)}$). The F_0 was 79.91 while the F -table was only 4.26. Similarly, the F_0 value for large scale sandwich panels was 73.42, while the F value obtained from the F -distribution table for $F_{(0.05;2,9)}$ was

4.26. Therefore the null hypothesis (H_0) was rejected, meaning that there are significant differences in the treatments. All pairwise tests; Tukey's Dunnet's and Fisher's tests obtained positive confidence intervals suggesting that the means of treatments differ.

- 3) The value of F_0 for the in-plane shear test was 560.73, which is much larger than the value obtained from F-distribution table. The F value, obtained by using the significance level of 95% ($\alpha = 0.05$), 3 levels of treatment replications ($a = 3$) and 15 samples ($N = 12$), was 3.89. As the value of F_0 was much higher than the value of F table, it can be concluded that the null hypothesis (H_0) should be rejected, and accept the alternative hypothesis (H_1) which was that there was a significant difference in the treatments as represented by means.
- 4) The Tukey's test suggests that the load carrying capacity of hybrid sandwich panel with JFC (level 1) and MDF (level 2) intermediate layer is significantly different. All the confident values for medium and large scale flexural test contain only positive numbers, while the values for the in-plane shear test contain all negative numbers. None contain zero numbers meaning that the difference is significant.
- 5) The inference statements suggested that the load carrying capacity of hybrid sandwich panels was significantly higher than the conventional sandwich panels. All significance analysis were conducted with the significance level of 95% or $\alpha = 0.05$ meaning that the conclusions drawn have a 95% chance of being correct.

9.3. Recommendations

The current research work focused on well planned sequential laboratory experimental program. The study included raw material processing to small and medium scale panel testing combined with developing analytical model and also significance analysis using statistical tools. The project has established some essential information about the structural behaviour of the newly developed hybrid sandwich panels. The following aspects could be investigated to further develop the widespread application of this newly developed sandwich panel.

- 1) It is important to undertake racking tests as per ASTM E-72 in order to investigate the in-plane shear behaviour of the sustainable sandwich panel under

a full-scale testing scheme. Collaborative research with the building industry is recommended.

- 2) The durability of the newly developed hybrid sandwich panels is a key aspect that needs to be fully studied prior to full scale application.
- 3) Numerical approach using finite element modelling may also help provide some insight into the contribution of different important parameters. This aspect was beyond the scope of the research reported in this thesis.
- 4) Creep effect in resin could be investigated for long term performance.
- 5) Further research work need to be carried out to investigate the suitability of the hybrid sandwich panels in earthquake prone regions.
- 6) Further research work need to be carried out to investigate fatigue and creep effects in determining the design life of sandwich panels.
- 7) It is also recommended to measure strains in horizontal and vertical directions when conducting in-plane shear test.

It is concluded that the research questions have been successfully addressed. It has been well demonstrated by the author via a well planned laboratory testing program and analysis that the new hybrid sandwich panels are superior.

References

- Abbadi A., Koutsawa Y., Carmasol A., Belouettar S., Azari Z., 2009, Experimental and numerical characterization of honeycomb sandwich composite panels, *Simulation Modelling Practice and Theory*, Vol. 17 (2009) 1533–1547.
- Ahad N.A., Parimin N., Mahmed N., Ibrahim S.S., Nizzam K., Ho Y.M., Effect of chemical treatment on the surface of natural fibre, *Journal of Nuclear and Related Technologies*, Volume 6, No.1, Special edition, 2009.
- Ahmed K.S., Vijayarangan S., 2008, Tensile, flexural and interlaminar shear properties of woven jute and jute-glass fabric reinforced polyester composites *journal of materials processing technology*, 207 (2008), 330–335.
- Aktas A., 2007, Statistical analysis of bearing strength of glass–fibre composite materials, *Journal of Reinforced plastics and composites*, Vol. 26, No. 6/2007.
- Alinia M.M., Dastfan M., Behaviour of thin steel plate shear walls regarding frame members, *Journal of Constructional Steel Research* 62 (2006), 730–738.
- Amaducci S., Gusovious H.J., 2010, Hemp-Cultivation, Extraction and Processing; In Mussig J., 2010, *Industrial Applications of Natural Fibres*, John Wiley and Sons, Ltd., Chichester, West Sussex, PO19 8SQ, United Kingdom.
- Anandjiwala R.D., John M., 2010, Sisal-Cultivation, Extraction and Processing; In Mussig J., 2010, *Industrial Applications of Natural Fibres*, John Wiley and Sons, Ltd., Chichester, West Sussex, PO19 8SQ, United Kingdom.
- Andrews S., 1992, Foam core panels and buildings systems, Cutter Information Corp., Arlington, Mass; in Mullens M.A., Arif M., *Structural Insulated panels: Impact on the residential construction process*, *Journal of Construction Engineering and management*, Volume 132, No 7.
- Antony J., (2003), *Design of experiments for engineers and scientists*, Elsevier Science & technology books.
- Ashby M.F., Brechet Y.J.M., 2003, Designing hybrid material, *Acta Materialia*, 51 (2003) 5801-5821.
- ASTM Standard E 72 (1997), Standard test method of conducting strength test of panels for building constructions, ASTM E 72, ASTM International, Philadelphia, Pa 19103.
- ASTM Standard C 393 (2000), Standard test method for flexural properties of sandwich construction, ASTM C393-00, ASTM International, Philadelphia, Pa 19103.
- ASTM Standard D 5379 M (2005), Standard test method for shear properties of composite materials by the V-Notched beam method, ASTM D 5379 M-05, ASTM International, Philadelphia, Pa 19103.
- ASTM Standard E 564 (2006), Standard practice for static load test for shear resistance of framed walls for buildings, ASTM E 564, ASTM International, Philadelphia, Pa 19103.

References

- ASTM Standard E 519 (2007), Standard test method for diagonal tension (shear) in masonry assemblages, ASTM E 519, ASTM International, Philadelphia, Pa 19103.
- ASTM Standard C 274 (2007), Standard terminology of structural sandwich constructions, ASTM C 274-07, ASTM International, Philadelphia, Pa 19103.
- ASTM Standard D 695 (2008), Standard test method for compressive properties of rigid plastics, ASTM D 695, ASTM International, Philadelphia, Pa 19103.
- Babu M.S., Srikanth G., Biswas S., 2009**, Composite Fabrication by Filament Winding - An Insight, Available from: <http://www.tifac.org>.
- Balzer B., McNabb J., 2008, Significant effect of microwave curing on tensile strength of carbon fiber composites, *Journal of Industrial Technology*, Vol. 24, No. 3, 2008, pp. 2-8.
- Baral N., Cartié D.D.R., Partridge I.K., Baley C., Davies P., Improved impact performance of marine sandwich panels using through thickness reinforcement: Experimental results, *Composites Part B: Engineering*, March 2010, Volume 41, Issue 2, Pages 117-123.
- Beer F.P., Johnston E.R., 1992, *Mechanics of Materials*, McGraw-Hill, England.
- Belmares H., Barrera A., Castillo E., Verheugen V.E., Monjaras M., Patfort G.A., Buequoye E.N., 1981, New composite materials from natural hard fibres, *Ind Eng Chem Prod Res Dev* 1981;20:555; in Mathur V.K., 2006, Composites material from local resources, *Construction and Building Materials*, V.20, p 470-477.
- Benayoune A., Samad A.A.A., Trikha D.N., Ali A.A.A., Ashraborty A.A., 2006, Structural behavior of eccentrically loaded precast sandwich panels, *Construction and Building Materials* 20 (2006), 713-724.
- Berge B., 2009, *The ecology of building materials*, Architect Press, USA.
- Bi W., Coffin D.W., 2006, Racking strength of paperboard based sheathing materials, *BioResources*, 2(1), 3-19.
- Bisanda E.T.N., 2000, Effect of alkali treatment to the adhesion characteristics of sisal fibres, *Applied Composite Materials*, Vol. 7, Nos.5-6, Nov.2000; In Bledzka A.K., Sperber V.E., Faruk O., 2002, *Natural and Wood Fibre Reinforcement in Polymers*, Rapra Review Reports, Volume 13, Number 8, 2002.
- Botaro V.R., Siqueira G., Megiatto J.D., Frollini E., 2010, Sisal fibres treated with NaOH and benzophenonetetracarboxylic dianhydride as reinforcement of phenolic matrix, *Journal of Applied Polymer Science*, Vol. 115, 269–276 (2010).
- Bryan E. L., 1961, Photoelastic evaluation of the panels shear test for plywood, in *Symposium on shear and torsion testing*, ASTM special technical publications No. 289.
- Brinberg D., 1982, Validity concepts in research: an integrative approach, in *Advances in Research Consumer*, Vol. 09.
- British Standard, BS EN ISO 527-2:1996, *Plastics-Determination of tensile properties*, BSI, 389 Chiswick High Road, London.

References

- British Standard, BS EN ISO 14125:1998, Fibre-reinforced plastic composites-determination of flexural properties, BSI, 389 Chiswick High Road, London.
- Burgueno R., Quagliata M.J., Mehta G.M., Mohanty A.K., Misra M., Drzal L.T., 2005, Sustainable cellular biocomposites from natural fibers and unsaturated polyester resin for housing panel applications, *Journal of Polymers and the Environment*, Vol. 13, No. 2, April 2005.
- Cao J., Akkerman R., Boisse P., Chen J., Cheng H.S., de Graaf E.F., Gorczyca J.L., Harrison P., Hivet G, Launay J., Lee W., Liud L., Lomov S.V., LongA., de Luycker E., Morestin F., Padvoiskis J., Peng X.Q., Sherwood J., Stoilova T., Tao X.M., Verpoest I, Willems A., Wiggers J., Yu T.X., Zhu B., 2008, Characterization of mechanical behavior of woven fabrics: Experimental methods and benchmark results, *Composites: Part A* 39 (2008) 1037–1053.
- Cao Y., Sakamoto S., Goda K., 2007, Effects of heat and alkali treatments on mechanical properties of kenaf fibres, 16 th International Conference on composite materials, Kyoto-Japan, 2007.
- Castanie B., Barrau J.J., Jaouen J.P., Rivallant S., 2004, Combined shear/compression structural testing of asymmetric sandwich structure, *Experimental Mechanics*, Vol 4 No 5, pp 461-472.
- Christian S., Billington S., 2009, Sustainable bio composites for construction, *Composites and polycon 2009*, January 15-17, 2009, Tampa FL USA.
- CSULB, 1998, Test for Significance, Available from: <http://www.csulb.edu/~msaintg/ppa696/696stsig.htm>. Accessed: 24/04/2013.
- Davies J.M., 2001, *Lightweight sandwich construction*, Blackwell science, London.
- De-Iorio A., Ianniello D., Iannuzi R., Penta F., 2002, Test methods for composite mechanical characterization, in Found M.S., 2002, *Experimental techniques and design in composite materials 4*, Swets & Zeitlinger, Lisse, ISBN: 90 5809 370 0.
- Deshpande V.S., 2002, *The design of sandwich panels with foam cores*, Lecturing Handout, Cambridge University.
- DIAB, 2001, Sandwich concept, DIAB sandwich book, Available from: www.diabgroup.com.
- Duggal S.K., 2008, *Building Materials*, New Age International Publisher, New Delhi, India.
- Dweib M.A., Hu B., O'Donnell A., Shenton H.W., Wool R.P., 2004, All natural composite sandwich beams for structural applications, *Composite structures* 63 (2004) 147-157.
- Dweib M.A., Hu B., Shenton H.W., Wool R.P., 2006, Bio-based composite roof structure: Manufacturing and processing issues, *Composite Structures* 74 (2006) 379–388.
- Dwivedi U.K., Ghosh A., Chand N., 2007, Abrasive wear behaviour of bamboo powder filled polyester composites, *BioResources*, Vol 2 (4), 693-698.
- Drzal L.T., Mohanty A.K., Burgueno R., Misra M., 2004, *Biobased structural composite materials for housing and infrastructure applications: Opportunities and*

References

- challenges, NSF-PATH Housing Research Agenda Workshop, Proceedings and recommendations, (Syal M.G., Hastak M., Mullens A.A., (2004), 129-140.
- English B., Youngquist J.A., Krzysik A.M., 1994, Lignocellulosic Composites; in: Gilbert R.D., 1994, Cellulosic polymers, blends and composites, Hanser Publishers, New York, USA.
- Ergul. Y, Cengiz D.A., Aleattin K, Hasan G., 2003, Strength and properties of lightweight concrete made with basaltic pumice and fly ash, material Letter, V.57, p 2267-2270.
- Fan H.L., Meng F.H., Yang W., 2007, Sandwich panels with Kagome lattice cores reinforced by carbon fibers, Composite Structures 81 (2007) 533–539.
- Fernandez-Cabo J.L., Majano A.M., Ageo L.S.S., Nieto M.A., 2010, Development of a novel facade sandwich panel with low-density wood fibres core and wood-based panels as faces, Eur. J. Wood Prod. Received: 29 May 2009., © Springer-Verlag 2010.
- Fonseca V. M., Fernandes V. J., de Carvalho L. H., d'Almeida J. R. M., 2004, Evaluation of the mechanical properties of sisal–polyester composites as a function of the polyester matrix formulation, Journal of Applied Polymer Science, Vol. 94, 1209–1217 (2004).
- Gassan J., Bledzki A.K., 1999, Possibilities for improving the mechanical properties of jute/epoxy composites by alkali treatment of fibres, Composites Science and Technology 59 (1999) 1303-1309.
- Gelman A., Stern H., 2006, The difference between significant and not significant is not itself statistically significant, The American Statistician, Vol. 60, No.4, 2006, pp.328-331.
- Gibson L.J., 2000, Mechanical behaviour of metallic foams, Ann Rev Mater Sci 2000;30:191–227; in Styles M., Compston P., Kalyanasundaram S., 2007, The effect of core thickness on the flexural behaviour of aluminium foam sandwich cores, Composite Structures 80 (2007) 532-538.
- Gougeon Brothers, 2010, Vacuum Bagging Techniques, A guide to the principles and practical application of vacuum bagging for laminating composite materials with WEST SYSTEM® Epoxy. Available from: www.westsystem.com.
- Grenestedt J.L., Reany J., Wrinkling of corrugated skin sandwich panels, Composites: Part A 38 (2007) 576–589.
- Groh R, 2013, Fancy a sandwich?, <http://aerospaceengineeringblog.com/sandwich-panel/>.
- Gunsch J., 2013, What is statistical significance?, Available from: www.wisegeek.org. Accessed: 25/04/2013.
- Hanninen T., Hughes M., 2010, Historical, Contemporary and Future Applications; In Mussig J., 2010, Industrial Applications of Natural Fibres, John Wiley and Sons, Ltd., Chichester, West Sussex, PO19 8SQ, United Kingdom.
- Harte A.M., Fleck N.A., Ashby M.F., 2000, Sandwich panel design using aluminium alloy foam, Advanced Engineering Materials, 2000, 2, No. 4.

References

- He M., Hu W., (2008), A study on composite honeycomb sandwich panel structure; *Materials and Design* 29 (2008) 709–713.
- Herrera-Franco P.J., Valadez-González A., 2005, A study of the mechanical properties of short natural-fiber reinforced composites, *Composites: Part B* 36 (2005) 597–608.
- Hicks C.R., 1982, *Fundamental Concepts in the Design of Experiment*, Holt, Rinehart & Winston, Inc., New York-USA.
- Hokens D., Mohanty A K., Misra M., Drzal L.T., 2002, Influence of surface modification and compatibilization on the performance of natural fibre reinforced biodegradable, Thermoplastic Composite Polymer, Volume 43, Number 1. Spring 2002; In Bledzk A.K., Sperber V.E., Faruk O., 2002, *Natural and Wood Fibre Reinforcement in Polymers*, Rapra Review Reports, Volume 13, Number 8, 2002.
- Hong W.K., Park S.C., Kim J.T., Environmental friendly impact of a modularized hybrid construction for high-rise buildings with SMART frames on social and economical aspects, SHB2012 - 8th International Symposium on Sustainable Healthy Buildings, Seoul, Korea, 19 September 2012.
- Horath L., 1995, *Fundamental of materials Science for Technologist*, Prentice Hall, Engelwood Cliffs, New Jersey, Ohio, USA.
- Hossain K.M.A., Wright H.D., 1998, Performance of profiled concrete shear panels, *Journal of Structural Engineering*, Vol 124, No 4.
- Hu B., Dweib M., Wool R.P., Shenton H.W., 2007, Bio-based composite roof for residential construction, *Journal of architectural engineering*, ASCE.
- Icardi U., Ferrero L., (2009), Optimisation of sandwich panels with functionally graded core and faces, *Composite Science and Technology*; 69: 575-585.
- Ismail H., Shuhelmy S., Edyham M.R., 2002, The effects of a silane coupling agent on curing characteristic and mechanical properties of bamboo fibre filled natural rubber composites, *European Polymer Journal*, Vol. 38 (2002), 39-47.
- Ismail N., Peterson R. B., Maasia M. J., Ingham J.M., 2011, Diagonal shear behaviour of unreinforced masonry wallettes strengthened using twisted steel bars, *Constr Build mater* (2011), doi:101016/j.conbuidmat.2011.04.063.
- Ji Y., Plainiotis S., 2006, *Design for Sustainability*. Beijing: China Architecture and Building; In *Form-Based Urban Planning Codes for Trinidad & Tobago: An Exploratory Study - Module 2: Green Design*. Globe Consultants International Ltd - September 2012.
- Jiang D., Shu D., 2005, Local displacement of core in two-layer sandwich composite structure subjected to low velocity impact, *Composite Structure* 71 (2005), 53-60.
- John D.J., 1971, *Shear buckling of isotropic and orthotropic plates; A review*, department of Transport Technology, University of Technology, Loughborough, UK.
- Johnson N.L., Welch B.L., 1939, *Biometrika*, 31, 362-389, in Patel J.K., Patel N.M., Shiyani R.L., Coefficient of variation in field experiments and yardstick thereof- An empirical study, *Current Science*, Vol 81, No 9, 10 November 2001.

References

- Jun Z., Wang X., Chang J., Zheng K., 2008, Optimization of processing variables in wood–rubber composite panel manufacturing technology, *Journal of Bioresource Technology*, Elsevier, Vol. 99, No. 7, 2008, pp.2384-2391.
- Kabir M.M., Islam M.M., Wang H., 2010, Mechanical and thermal properties of untreated and chemically treated jute fibre reinforced composites *International Conference on Mechanical, Industrial and Energy Engineering 2010* 23-24 December, 2010, Khulna, Bangladesh.
- Kampner M., Grenestedt J.L., (2008), On using corrugated skins to carry shear in sandwich beams, *Composite Structures*; 85: 139-148.
- Kaynak, C., Akgul, T., 2001, Open mould process, in *Handbook of composite fabrication*, Akovali, G., 2001, RAPRA technology, Ankara, Turkey.
- Kawasaki T., Zhang M., Kawai S., 1999, Sandwich panel of veneer-overlaid low-density fibreboard, *J Wood Sci* (1999), 45: 91-298.
- Kelly H., 2009, Adaptations of Cementitious Structural Insulated Panels for Multi-storey Construction, A report by The federation of American Scientists for The Charles Pankow Foundation, June 26, 2009.
- Kermany A., 2006, Performance of structural insulated panels, *Proceedings of the Institution of Civil Engineers, Structures and Buildings* 159, p 13-19.
- Khan, M.K., 2006, Compressive and lamination strength of honeycomb sandwich panels with strain energy calculation from ASTM standards, *Proc. IMechE Vol. 220 Part G: J. Aerospace Engineering*.
- Khan R.A., Khan M.A., Zaman H.U., Parvin F., Islam T., Nigar F, Islam R, Saha S., Mustafa A.I., 2012, Fabrication and characterization of jute fabric-reinforced PVC-based composite, *Journal of Thermoplastic Composite Materials*, Vol. 25—February 2012.
- Kim J.J., Rigdon B., 1998, Qualities, Use, and Examples of sustainable Building Materials, national Pollution Prevention Centre, Available from: www.umich.edu.
- Kim Y.Y, Kim J.S., Ha G.J., Kim J.K., 2006, Influence of ECC ductility on the diagonal tension behaviour (shear capacity) of infill panels, *International RILEM workshop on high performance fibre reinforced cementitious composites in structural applications*, RILEM publications SARL.
- Kollar L.P., Springer G.S., 2003, *Mechanics of Composite Structures*, Cambridge University Press, Cambridge, UK.
- Kuehl R.O., *Design of Experiments: Statistical principles of research design and analysis*, Brooks/Cole, CA, USA.
- Kuenzi E.W., 1951, Flexure of structural sandwich construction, United States Department of Agriculture, Forest Products Laboratory, Madison, Wisconsin, USA.
- Kuenzi E. W., Ericksen W.S., Zahn J.J., 1962, Shear stability of flat panels of sandwich structure, Forest Products Laboratory US, Research report No 1560.

References

- Lee S., Munro M., 1986, Evaluation of in-plane shear test methods for advanced composite materials by decision analysis technique, *Jornal of composites*, Vol 17, No 1, January 1986.
- Lewis J., 2003, Housing construction in earthquake-prone places: Perspectives, priorities and projections for development *The Australian Journal of Emergency Management*, Vol. 18 No 2. May 2003
- Li X., Tabil L.G., Panigrahi S., 2007, Chemical treatments of natural fibre for use in natural fibre-reinforced composites: A Review, *J Polym Environ* (2007) 15:25–33.
- Li Y., Mai Y.W., Ye L., 2000, Sisal fibre and its composites: a review of recent developments, *Composites Science and Technology* 60 (2000) 2037-2055.
- Liu Q., Zhao Y., 2007, Effect of Soft Honeycomb Core on Flexural Vibration of Sandwich Panel using Low Order and High Order Shear Deformation Models *Journal of Sandwich Structures and materials*, Vol. 9—January 2007
- Lu T.J., Valdevit L., Evans A.G., 2005, Active cooling by metallic sandwich structures with periodic cores, *Progress in Materials Science* 50 (2005) 789–815.
- Mahfuz H., Islam M.S., Rangari V.K., 2004, Response of sandwich composites with nanophased cores under flexural loading, *Composites: Part B*, 35, 543-550 (2004); in Mirzapour A, Beheshty M.H., Vafayan M., 2005, The response of sandwich panels with rigid polyurethane foam cores under flexural loading, *Iranian Polymer Journal* 14 (12), 2005.
- Malanit P., Barbu M.C., Frühwal A., 2009, The gluability and bonding quality of an asian bamboo (*Dendrocalamus Asper*) for the production of composite lumber, *Journal of Tropical Forest Science* 21(4): 361–368.
- Mamalis A.G., Manolakos D.E., Ioannidis M.B., Papapostolou D.P., Kostazos P.K., Konstantinidis D.G., 2002, On the compression of hybrid sandwich composite panels reinforced with internal tube inserts: experimental, *Composite Structures* 56 (2002) 191–199.
- Mamalis A.G., Spentzas K.N., Manolakos D.E., Pantelis N., Ioannidis M., (2008), Structural impact behavior of an innovative low-cost sandwich panel, *International Journal of Crashworthinnes*, Vol.13, No. 3, June 2008, 231-236.
- Manalo A., Aravinthan T., Karunasena W., Islam M.M., (2009), Flexural behavior of structural fiber composite sandwich beams in flatwise and edgewise positions, *Composite Structures*; doi:10.1016/j.compstruct.2009.09.046.
- Marcari G., Fabbrocino G., 2007, Experimental behaviour and design criteria for FRP in-plane strengthening o tuff walls, *Asia-pacific Conference on FRP in structures (APFIS 2007)*.
- Marshall A.C., 1998, Sandwich Construction; In *Handbook of Composites*, Peters S.T., 1998, Chapman and Hall, London.
- Master I.G., Evans K.E., (1996), Models for the elastic deformation of honeycombs, *Composite Structures*; 35: 403-422.

References

- Mathivanan N.R., Jerald J., Behera P., 2011, Analysis of factors influencing deflection in sandwich panels subjected to low-velocity impact, *Int J Adv Manuf Technol* (2011) 52:433–441.
- Mathur V.K., 2006, Composites material from local resources, *Construction and Building Materials*, V.20, p 470-477.
- Matthews F.L., 2000, Compression, in Hodgkinson J.M., 2000, *Mechanical testing of advanced fibre composites*, Woodhead Publishing Limited, Cambridge, England.
- MCA, 2010, Insulated Metal Panels, Metal Construction Association. Available from: http://www.metalconstruction.org/pubs/pdf/imp_selection_guideline.pdf.
- Mehta G., Mohanty A.K., Thayer K., Misra M. Drzal L.T., 2005, Novel biocomposites sheet molding compounds for low cost housing panel applications, *Journal of Polymers and the Environment*, Vol. 13, No. 2, April 2005.
- Meraghni F., Desrumaux F., Benzeggagh M.L., (1999), Mechanical behavior of cellular core for structural sandwich panel, *Composites: Part A*; 30:767-779.
- Mirzapour A., Beheshty M.H., Vafayan M., 2005, The response of sandwich panels with rigid polyurethane foam cores under flexural loading, *Iranian Polymer Journal* 14 (12), 2005.
- Mishra S., Mishra M., Tripathy S.S., Nayak S.K., 2009, The Influence of Chemical Surface Modification on the performance of sisal-polyester biocomposites, *Polymer Composites*, April 2002, Vol. 23, No. 2.
- Mitra N., 2009, A methodology for improving shear performance of marine grade sandwich composites: Sandwich composite panel with shear key *Compos Struct* (2009), doi:10.1016/j.compstruct.2009.10.005.
- Mohammed U., Lekakou C., Dong I., Bader M.G., 2000, Shear deformation and micromechanics of woven fabrics, *Composites: Part A* 31 (2000) 299–308.
- Montgomery D.C., 2009, *Design and Analysis of Experiment*, John Wiley & Sons Publications, Arizona-USA.
- Montgomery D.C., Runger G.C., 2003, *Applied statistics and probability for engineers*, John Wiley & Sons Publications, Arizona-USA.
- Moreira R.A.S., Rodrigues J.D., (2010), Static and dynamic analysis of soft core sandwich panels with a through-thickness deformation, *Composite Structures*; 92: 201-215.
- Morgenthaler M., Berger L., Feichtinger K., Elkin R., 2005, Dependence of in-plane sandwich shear deformation on core material type and thickness, in Thomson O.T., 2005, *sandwich structures 7: Advancing with sandwich structures and materials*, 441-450, Springer 2005 printed in Netherland.
- Mosalam K.M., Hagerman J., Kelly H., 2008, Seismic evaluation of structural insulated panels, 5th International Engineering and Construction Conference (IECC'5), August 27-29, 2008, Los Angeles, USA
- Mousa M. A., Uddin N., 2010, Debonding of composites structural insulated panels, *Journal of Reinforced Plastic and composites*, 29 (22) 3380-3391 (2010).

References

- Mwaikambo L.Y., Amsell M.P., 2002, Chemical modification of hemp, sisal, jute, and kapok by alkalization, *Journal of Applied Polymer Science* 84, No. 12, June 2002; In Bledzk A.K., Sperber V.E., Faruk O., 2002, *Natural and Wood Fibre Reinforcement in Polymers*, Rapra Review Reports, Volume 13, Number 8, 2002.
- Mwaikambo L.Y., 2006, Review of the history, properties and application of plant fibres, *African Journal of Science and Technology (AJST) Science and Engineering Series* Vol. 7, No. 2, pp. 120 – 133.
- Naidu V.N.P., Reddy G.R., Kumar M.A., Reddy M.M., Khanam P.N., Naidu S.V., 2011, Compressive & impact properties of sisal/glass fibre reinforced hybrid composites, *International Journal of Fibre and Textile Research* 2011; 1(1): 11-14.
- Oksman K., Wallstrom L., Berglund L. A., Toledo F.R.D., 2002, Morphology and mechanical properties of unidirectional sisal-epoxy composite, *Journal of Applied Polymer Science*, Vol. 84, No.13, 24th June 2002, p.2358-65.
- Paudel S.K., Lobovikov M., 2003, Bamboo housing: market potential for low-income groups, *L. Bambbo and Rattan*, Vol. 2., No. 4, pp. 381-396 (2003).
- Pickering K.L., 200), *Properties and performance of natural-fiber composites*, Woodhead Publishing Limited, ISBN: 978-1-84569-267-4.
- Plastermat, 2012, Techno-commercial information on plastic industry, Available from: www.plastemart.com. Accessed 16/10/2012.
- Pogorzelski J A., Firkowicz-Pogorzelska K., 2000, Thermal properties of hemp composite boards to be used in building components, *Natural Polymers and Composites*, Conference Proceedings, Sao Pedro, Brazil, 14th-17th May 2000, p.517-9; In Bledzk A.K., Sperber V.E., Faruk O., 2002, *Natural and Wood Fibre Reinforcement in Polymers*, Rapra Review Reports, Volume 13, Number 8, 2002.
- Pollock T., 1993, *Introduction to Buckling*, Department of Aerospace Engineering, Texas A&M University, College Station,.
- Pothan L.A., George J., Thomas S., 2002, Effect of fibre surface treatments on the fibre matrix interaction in banana fibre reinforced polyester composites, *Composite Interfaces*, Vol. 9, No. 4, pp. 335–353 (2002).
- Prasad A.V.R., Rao K.M., 2011, Mechanical properties of natural fibre reinforced polyester composites: Jowar, sisal and bamboo, *Materials and Design* 32 (2011) 4658–4663.
- Rahman M.S., 2010, Jute – A Versatile Natural Fibre: Cultivation, Extraction and Processing; In Mussig J., 2010, *Industrial Applications of Natural Fibres*, John Wiley and Sons, Ltd., Chichester, West Sussex, PO19 8SQ, United Kingdom.
- Ray D., Sarkar B.K., Rana A.K., Bose N.R., 2001, Effect of alkali treated jute fibres on composite properties, *Bull. Mater. Sci.*, Vol. 24, No. 2, April 2001, pp. 129–135.
- Rajulu A.V., Rao G.B., Devi L.G., 2005, Mechanical properties of short, natural fibre *Hildegardia populifolia*-reinforced styrenated polyester, *Composites Journal of Reinforced plastic and composites*, Vol. 24, No. 4/2005.
- Reardon G.F., 1980, Recommendation for the testing of roofs and walls to resist high wind forces, Technical report, James Cook Cyclone structural testing station.

References

- Reddy E.V.S., Rajulu A.V., Reddy K.H., Reddy G.R., Chemical resistance and tensile properties of glass and bamboo fibres reinforced polyester hybrid composites, *Journal of Reinforced Plastics and Composites*, Vol. 29, No. 14/2010.
- Roca S.V., Nanni A., 2005, Mechanical characteristic of sandwich structure comprised of glass fibre reinforced core: Part 1, *Composites in Construction 2005 – Third International Conference*, Lyon, France, July 11 – 13, 2005.
- Rokbia M., Osmania H., Almadc A., Benseddiq B., 2011, Effect of chemical treatment on flexure properties of natural fiber-reinforced polyester composite, *Procedia Engineering* 10 (2011), 2092–2097.
- Rong M.Z., Zhang M.Q., Liu Y., Yan H.M., Yang G.C., Zeng H.M., 2002, Interfacial interaction in sisal/epoxy composites and its influence on impact performance, *Polymer Composites*, April 2002, Vo. 23. No.2.
- Roscoe J.T., 1979, *Fundamental Research Statistics*, Holt, Rinehart & Winston, Inc., New York-USA.
- Rout J., Tripathy S.S., Nayak S.K., Misra M., Mohanty A.K., 2011, Scanning electron microscopy study of chemically modified coir fibres, *Journal of Applied Polymer Science*, Vol. 79, 1169–1177 (2001).
- Roylance D., 2000, *Beam Displacements*, Department of Materials Science and Engineering, Massachusetts Institute of Technology, Cambridge, USA.
- Russo A., Zuccarello B., 2007, Experimental and numerical evaluation of the mechanical behaviour of GFRP sandwich panels *Composite Structures* 81 (2007) 575–586
- Saha A.K., Das S., Basak R.K., Bhatta D., Mitra B.C., 2000, Improvement of functional properties of jute-based composite by acrylonitrile pretreatment, *Journal of Applied Polymer Science*, Vol 78, 495-506 (2000).
- Salzer I.O., Usmani A.M., 1982, Utilisation of bagasse in new composite building materials, *Ind Eng Chem Prod Res Dev* 1982;21:17–23; In Mathur V.K., 2006, *Composites material from local resources*, *Construction and Building Materials*, V.20, p 470-477.
- Samuel O.D., Agbo S., Adekanye T.A., 2012, Assessing mechanical properties of natural fibre reinforced composites for engineering applications, *Journal of Minerals and Materials Characterization and Engineering*, 2012, 11, 780-784.
- Santa-Maria H., Duarte G., Garib A., 2004, Experimentally investigation of masonry panels externally strengthened with CFRP laminates and fabric to in-plane shear load, 13th World conference on earthquake engineering, Vancouver-Canada, August 1-6, 2004.
- Sastra H. Y., Siregar J. P., Sapuan S., Hamdan M.M., Tensile properties of Arenga pinnata fibre-reinforced epoxy composites, *Polymer-Plastics Technology and Engineering*, 45: 149–155, 2006.
- Satapathy A., Patnaik A., 2010, Analysis of dry sliding wear behaviour of red mud filled polyester composites using the Taguchi Method, 2010, *Journal of Reinforced Plastics and Composites*, Vol. 29, No. 19/2010.

References

- Schwartz-Givli H., Rabinovitch O., Frostig Y., (2007), High order nonlinear contact effects in cyclic loading of delaminated sandwich panel, *Composites: Part B*; 38:86-101.
- Seidl R.J., 1956, Paper-honeycomb cores for structural sandwich panels, Forest Products Laboratory, Forest Service U. S. Department of Agriculture.
- Shahdin A., Mezeix L., Bouver C., Morlier J., Gourinat Y., 2009, Fabrication and mechanical testing of glass fiber entangled sandwich beams: A comparison with honeycomb and foam sandwich beams, *Composite Structures*, Elsevier, Vol. 90, No. 4, 2009, pp.404-412.
- Sharaf T., Shawkat W., Fam A., 2010, Structural performance of sandwich wall panels with different foam core densities in-one-way bending, *Journal of Composite Materials*, Vol. 44, No 19, 2010.
- Shin S., Rice B.P., 2003, Sandwich construction with carbon foam core materials, *Journal of Composite Materials*, Vol. 37. No. 15/2003.
- Silva E.C.N., Walters M.C., Paulino G.H., 2006, Modelling bamboo as a functionally graded material: lessons for the analysis of affordable materials, *J Mater Sci* (2006) 41:6991-7004.
- Singh B., Gupta M., Verma A., 1996, Influence of fibre surface treatment on the properties of sisal-polyester composites, *Polymer Composites*, December 1996, Vol. 17, No. 6.
- Singh B., Gupta M., Verma A., 2000, The durability of jute fibre-reinforced phenolic composites, *Composite Science and Technology* 60 (2000) 581-589.
- Singh B., Gupta M., 2005, Natural Fiber Composites for Building Applications, in Mohanty A.K., Misra M., Drzal L.T., 2005, Natural fibers, biopolymers, and biocomposites, CRC Press, Taylor and Francis Group, USA.
- Singh B., Gupta M., in Mohanty A.K., Misra M., Drzal L.T., 2005, Natural fibers, biopolymers, and biocomposites, CRC Press, Taylor and Francis Group, USA.
- Smith P.M., Walcott M.P., 2006, Opportunities for wood/natural fibre-plastic composites in residential and industrial applications, *Forest Product Journal*, Vol. 56, No. 3, March 2006.
- Somayaji S., 1995, Civil engineering materials, Prentice Hall, Englewood, New Jersey, USA.
- Staiger M.P., Tucker N., 2008, Natural-fibre composites in structural applications; In Pickering K.L., 2008, Properties and performance of natural-fiber composites, Woodhead Publishing Limited, ISBN: 978-1-84569-267-4.
- StatPac, 2013, Statistical Significance, Available from: <http://www.statpac.com/surveys/statistical-significance.htm>. Accessed: 24/4/2013.
- Styles M., Compston P., Kalyanasundaram S., 2007, The effect of core thickness on the flexural behaviour of aluminium foam sandwich cores, *Composite Structures* 80 (2007) 532-538.

References

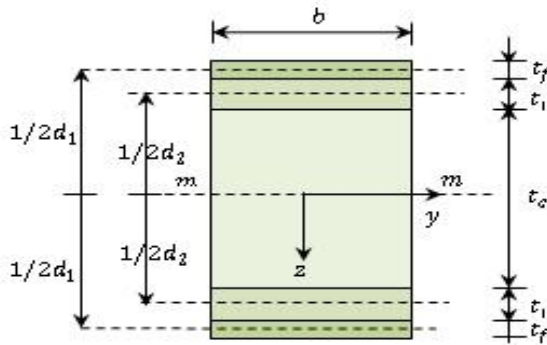
- Suardana N.P.G., Piao Y., Lim J.K., 2011, mechanical properties of hemp fibres and hemp/pp composites: Effects of chemical surface treatment, *Materials Physics and mechanics* 11 (2011) 1-8.
- Suddel B.C., Rosemaund A., 2008, Industrial fibres: recent and current developments, *Proceedings of the symposium on natural fibres, Rome, 20 October 2008*.
- Sun H., Pan N., 2005, Shear deformation analysis for woven fabrics, *Composite Structures* 67 (2005), 317–322.
- Takatani M., Ikeda K., Sakamoto K., Okamoto T., 2008, Cellulose esters as compatibilizers in wood/poly(lactic acid) composite, *J Wood Sci* (2008) 54:54-61. The Japan Wood Research Society.
- Teles R.F., Menezzi C.H.S., Souza F., Souza M.R., 2012, Theoretical and experimental deflections of glued laminated timber beams made from tropical hardwood, *Wood Material Science and Engineering*, 2012, 1-6.
- Thwe M.N., Lio K., 2002, Effects of environmental ageing on the properties of bamboo-glass fibre reinforced polymer matrix hybrid composites, *Composites Part A: Applied Science and Manufacturing*, No 33A, No.1, 2002, p.43-52; In Bledzk A.K., Sperber V.E., Faruk O., 2002, *Natural and Wood Fibre Reinforcement in Polymers*, Rapra Review Reports, Volume 13, Number 8, 2002.
- Ticoalu A., Aravinthan T., Cardona F., 2010, Experimental investigation into gomuti fibres/polyester composites, *Proceeding of the Australasian conference on the mechanics of structures and materials*, 451-456.
- Ticoalu A., Aravinthan T., Cardona F., 2013, A review on the characteristics of gomuti fibre and its composites with thermoset resins, *Journal of Reinforced Plastics and Composites*, Vol. 32(2), 124–136.
- Tissel J.R., 1993, Structural panels shear wall, research report 154-APA
- Tracy J.M., 2000, SIPs overcoming the elements, *Forest Product Journal*, Vol 50 No. 3.
- Uddin M., Kalyankar R.R., 2011, Manufacturing and structural feasibility of natural fiber reinforced polymeric structural insulated panels for panelized construction, *International journal of polymer science*, Volume 2011, No. 7.
- UN-Habitat, 2008, Low-cost sustainable housing, materials building technology in developing countries, Available from: <http://www.unhabitat.org/>
- Vaidya A., Uddin N., Vaidya U., 2010, Structural characterization of composite structural insulated panels for exterior wall application, *Journal of composites for construction*, Volume 14 No 4.
- Van Dam J.E.G., 2008, Environmental benefits of natural fibre production and use, *Proceedings of the symposium on natural fibres, Rome, 20 October 2008*.
- Van Erp G., Rogers D., A highly sustainable fiber composite building panel, *Proceeding of the international on fiber composite in civil engineering: Past-Present-Future*, 1-2 December 2008, USQ, Toowoomba, Qld, Australia.
- Venkateshwarah N., Elayaperumal A., Sathiya G. K., 2012, Prediction of tensile properties of hybrid-natural fiber composites, *Composites Part B: Engineering*, Elsevier, Vol. 43, No. 2, 2012, pp. 793-796.

References

- Wackerley D.D., Mendenhall W., Scheaffer R. L., (2008), *Mathematical statistics with applications*, Thompson Brooks/Cole, USA.
- Wei Z., Zok F.W., Evans A.G., 2006, Design of sandwich panels with prismatic cores, *Journal of Engineering and technology*, April 2006, Vol. 128.
- Weyenberg I.V., Ivens J., Coster A.D., Kino B., Baetens E, Verpoest I., 2003, Influence of processing and chemical treatment of flax fibres on their composites, *Composites Science and Technology* 63 (2003) 1241–1246.
- Winandy J.E., Stark N.M., Clemons C.M., 2004, Considerations in recycling of wood-plastic composites, 5th Global wood and natural fibre composites symposium, April 27-28, 2004, Kassel, Germany.
- Youngquist W.G., Kuenzi E.W., 1961, Shear and Torsion of wood, plywood and sandwich construction at the US Forest Products Laboratory, in *Symposium on shear and torsion testing*, ASTM special technical publications No. 289.
- Zenkert D., (1995), *An introduction to sandwich construction*, Solihull, EMAS.
- Zhou D., Stronge W.J., (2005), Mechanical properties of fibrous core sandwich panels, *International Journal of Mechanical Sciences*; 47: 775-798.
- Zhu B., Yu T.X., Tao X.M., 2007, An experimental study of in-plane large shear deformation of woven fabric composite, *Composites Science and Technology* 67 (2007) 252–261.

Appendix A: Calculation of theoretical deflection

Hybrid sandwich panel's cross section:



Data:

$$\begin{aligned}
 t_f &= 0,5 \text{ mm} \\
 t_i &= 3 \text{ mm} \\
 t_c &= 15 \text{ mm} \\
 E_f &= 68200 \text{ MPa} \\
 E_i &= 4502 \text{ MPa} \\
 E_c &= 7.25 \text{ MPa} \\
 b &= 50 \text{ mm} \\
 L &= 450 \text{ mm} \\
 \nu_c &= 0.35 \\
 \nu_f &= 0.33 \\
 \nu_i &= 0.235
 \end{aligned}$$

Calculation:

$$\begin{aligned}
 d_1 &= 15 + (2 \cdot 3) + (2 \cdot 0.5 \cdot 0.5) = 21.5 \text{ mm} \\
 d_2 &= 15 + (2 \cdot 0.5 \cdot 3) = 18 \text{ mm}
 \end{aligned}$$

Flexural rigidity of the hybrid sandwich panel is given by Equation 3.51 in Chapter 3:

$$(EI)_{eq} = E_f \left[\frac{bt_f^3}{6} + \frac{bt_f d_1^2}{2} \right] + E_i \left[\frac{bt_i^3}{6} + \frac{bt_i d_2^2}{2} \right] + E_c \frac{bt_c^3}{12}$$

➤ Flexural rigidity of the face:

$$\begin{aligned}
 &= 68200 \left[\frac{50 \cdot 0.5^3}{6} + \frac{50 \cdot 0.5 \cdot 21.5^2}{2} \right] \\
 &= 395139167 \text{ Nmm}^2
 \end{aligned}$$

➤ Flexural rigidity of the intermediate layer:

$$\begin{aligned}
 &= 4502 \left[\frac{50 \cdot 3^3}{6} + \frac{50 \cdot 3 \cdot 18^2}{2} \right] \\
 &= 110411550 \text{ Nmm}^2
 \end{aligned}$$

Appendix-A

➤ Flexural rigidity of the core:

$$\begin{aligned} &= 7.25 * \frac{50 * 15^3}{12} \\ &= 101949 \text{ Nmm}^2 \end{aligned}$$

Total flexural rigidity:

$$\begin{aligned} (EI)_{eq} &= 395139167 + 110411550 + 101949 \\ &= 504652670 \text{ Nmm}^2 \end{aligned}$$

Total deflection is defined by Equation 5.10 in Chapter 5:

$$\delta = \frac{23 PL^3}{1296(EI)_{eq}} + \frac{PL}{6(AG)_{eq}}$$

For the calculation of deflection, $P = 1/2 P$. Hence, when checking the deflection at the load (P) of 200 N, the value of P is equal to 100 N.

➤ Deflection due flexure:

$$\begin{aligned} &= \frac{23 * 100 * 450^3}{1296 * 504652670} \\ &= 0.32 \text{ mm} \end{aligned}$$

➤ Deflection due shear:

$$\begin{aligned} &= \frac{100 * 450}{6 * 50 * 18 * 2.69} \\ &= 3.10 \text{ mm} \end{aligned}$$

Finally, the total deflection is:

$$\begin{aligned} \delta_{total} &= 0.32 + 2.48 \\ &= 3.42 \text{ mm} \end{aligned}$$

In the calculation of the deflection of tested panels, the dimensions of the panels may slightly different each other due to cutting and fabrication process. For example, the following calculation is carried out for specimen HFC-1.

SPECIMEN HFC-1:

Data:

$$\begin{aligned}
t_f &= 0,5 \text{ mm} \\
t_i &= 3 \text{ mm} \\
t_c &= 16.55 \text{ mm} \\
E_f &= 68200 \text{ MPa} \\
E_i &= 3048 \text{ MPa} \\
E_c &= 7.25 \text{ MPa} \\
b &= 50.5 \text{ mm} \\
L &= 450 \text{ mm} \\
\nu_c &= 0.35 \\
\nu_f &= 0.33 \\
\nu_i &= 0.39
\end{aligned}$$

Calculation:

$$\begin{aligned}
d_1 &= 16.55 + (2*3) + (2*0.5*0.5) = 23.05 \text{ mm} \\
d_2 &= 16.55 + (2*0.5*3) = 19.55 \text{ mm}
\end{aligned}$$

Flexural rigidity of the hybrid sandwich panel is given by Equation 3.51 in Chapter 3:

$$(EI)_{eq} = E_f \left[\frac{bt_f^3}{6} + \frac{bt_f d_1^2}{2} \right] + E_i \left[\frac{bt_i^3}{6} + \frac{bt_i d_2^2}{2} \right] + E_c \frac{bt_c^3}{12}$$

➤ Flexural rigidity of the face:

$$\begin{aligned}
&= 68200 \left[\frac{50.5 * 0.5^3}{6} + \frac{50.5 * 0.5 * 23.05^2}{2} \right] \\
&= 457536487.1 \text{ Nmm}^2
\end{aligned}$$

➤ Flexural rigidity of the intermediate layer:

$$\begin{aligned}
&= 3048 \left[\frac{50.5 * 3^3}{6} + \frac{50.5 * 3 * 19.55^2}{2} \right] \\
&= 88937864.42 \text{ Nmm}^2
\end{aligned}$$

➤ Flexural rigidity of the core:

$$\begin{aligned}
&= 7.25 \frac{50.5 * 16.55^3}{12} \\
&= 138306..354 \text{ Nmm}^2
\end{aligned}$$

Total flexural rigidity:

$$\begin{aligned}
(EI)_{eq} &= 457536487.1 + 88937864.42 + 138306..354 \\
&= 546612658 \text{ Nmm}^2
\end{aligned}$$

Total deflection is defined by Equation 5.10 in Chapter 5:

$$\delta = \frac{23 PL^3}{1296(EI)_{eq}} + \frac{PL}{6(AG)_{eq}}$$

At the load (P) of 50 N:

➤ Deflection due flexure:

$$\begin{aligned} &= \frac{23 * 50 * 450^3}{1296 * 546612658} \\ &= 0.15 \text{ mm} \end{aligned}$$

➤ Deflection due shear:

$$\begin{aligned} &= \frac{50 * 450}{6 * 50.5 * 16.55 * 2.75} \\ &= 1.67 \text{ mm} \end{aligned}$$

Finally, the total deflection is:

$$\begin{aligned} \delta_{total} &= 0.15 + 1.67 \\ &= 1.82 \text{ mm} \end{aligned}$$

Experimental deflection under the same load:

$$\delta_{exp} = 1.9 \text{ mm}$$

At the load (P) of 100 N:

➤ Deflection due flexure:

$$\begin{aligned} &= \frac{23 * 100 * 450^3}{1296 * 546612658} \\ &= 0.30 \text{ mm} \end{aligned}$$

➤ Deflection due shear:

$$\begin{aligned} &= \frac{100 * 450}{6 * 50.5 * 16.55 * 2.75} \\ &= 3.34 \text{ mm} \end{aligned}$$

$$\begin{aligned} \delta_{total} &= 0.30 + 3.34 \\ &= 3.64 \text{ mm} \end{aligned}$$

$$\delta_{exp} = 3.5 \text{ mm}$$

The difference between theoretical and deflection at P = 50 N is -4.3% and 3.4% at P = 100 N.

Appendix B: Calculation of theoretical shear buckling strength

Modified-Kuenzi Model (Approach 1):

The theoretical buckling shear stress calculation is carried out for hybrid sandwich panel with JFC intermediate layer. The calculation was carried out as per Equation 7.44:

$$q_f = \frac{\pi^2 E_f f_1 f_2 h_1^2}{a^2 \lambda_f (f_1 + f_2)^2} L_{cr} + \frac{\pi^2 E_i i_1 i_2 h_2^2}{a^2 \lambda_i (i_1 + i_2)^2} L_{cr}$$

Data:

f_1	= 0,5 mm
f_2	= 0.5 mm
c	= 25 mm
E_f	= 68200 MPa
E_i	= 4502 MPa
E_c	= 7.25 MPa
a	= 300 mm
b	= 300 mm
ν_c	= 0.35
ν_f	= 0.33
ν_i	= 0.235

The contribution of skins:

➤ *Flexural rigidities (D)*

$$h = c + \frac{f_1 + f_2}{2}$$

$$h = 25 + \frac{(0.5 + 0.5)}{2}$$

$$h = 25.5 \text{ mm}$$

$$D = \frac{E_f}{\lambda_f} \frac{f_1 f_2 h^2}{(f_1 + f_2)}$$

$$D = \frac{68200}{0.89} \frac{0.5 * 0.5 * 25.5^2}{(0.5 + 0.5)}$$

$$D = 12441659.19 \text{ Nmm}$$

➤ *Core shear parameter (S)*

$$S = \frac{\pi^2 f_1 f_2 c E_f}{a^2 \lambda_f \mu_c (f_1 + f_2)}$$

$$S = \frac{\pi^2 * 0.5 * 0.5 * 25 * 68200}{300^2 * 0.89 * 2.685 * (0.5 + 0.5)}$$

$$S = 19.516 > \frac{3/4}{1 + \frac{a^2}{b^2}} = 0.375$$

➤ *Buckling load factor (L_{cr})*

$$L_{cr} = \frac{1}{19.516}$$

$$L_{cr} = 0.051$$

Since the value of L_{cr} is equal to $1/S$ as defined in Equation 7.32, then the buckling stress can be estimated using the following equation:

$$q_f = \frac{h^2 \mu_c}{c(f_1 + f_2)}$$

$$q_f = \frac{25.5^2 * 2.685}{25(0.5 + 0.5)}$$

$$q_f = 69.842 \text{ MPa}$$

The contribution of intermediate layer:

➤ *Flexural rigidities (D)*

$$h = c + \frac{i_1 + i_2}{2}$$

$$h = 19 + \frac{(3 + 3)}{2}$$

$$h = 22 \text{ mm}$$

$$D = \frac{E_i}{\lambda_i} \frac{i_1 i_2 h_i^2}{(i_1 + i_2)}$$

$$D = \frac{4502}{0.91} \frac{3 * 3 * 22^2}{(0.5 + 0.5)}$$

$$D = 3459503.06 \text{ Nmm}$$

Appendix-B

➤ Core shear parameter (S)

$$S = \frac{\pi^2 i_1 i_2 c E_i}{a^2 \lambda_i \mu_i (i_1 + i_2)}$$

$$S = \frac{\pi^2 * 3 * 3 * 19 * 4502}{300^2 * 0.945 * 2.685 * (3 + 3)}$$

$$S = 5.541 > \frac{3/4}{1 + \frac{a^2}{b^2}} = 0.375$$

➤ Buckling load factor (L_{cr})

$$L_{cr} = \frac{1}{5.541}$$

$$L_{cr} = 0.18$$

Since the value of L_{cr} is equal to $1/S$ as defined in Equation 7.32, then the buckling stress can be estimated using the following equation:

$$q_f = \frac{h^2 \mu_c}{c(i_1 + i_2)}$$

$$q_f = \frac{22^2 * 2.685}{19(3 + 3)}$$

$$q_f = 11.4 \text{ MPa}$$

Hence, the total shear buckling stress for hybrid sandwich panel with JFC intermediate layer is:

$$\begin{aligned} q_f &= 69.842 + 11.4 \text{ MPa} \\ &= 78.318 \text{ MPa} \end{aligned}$$

A similar process was conducted for calculating the shear buckling stress of hybrid sandwich panel with MDF intermediate layer. However the result was identical to the above obtained value which means that the existence of different failure modes for that particular panel should be approached with different model. The appropriate approach for predicting the shear buckling of the hybrid sandwich panel with MDF intermediate layer is discussed later in this appendix.

Modified-Kuenzi Model (Approach 2):

The calculation of second approach was carried out as per the following equations:

$$D_{eq} = D_f + D_i$$

$$D_{eq} = S_f + S_i$$

$$q_f = \frac{\pi^2 D_{eq}}{a^2(f_1 + f_2)} L_{cr}$$

Calculations:

➤ *Equivalent flexural rigidities*

$$D_{eq} = 12441659.19 + 3459503$$

$$D_{eq} = 15901162.19$$

➤ *Equivalent core shear parameter*

$$S_{eq} = 19.52 + 5.641$$

$$S_{eq} = 25.157 > \frac{3/4}{1 + \frac{a^2}{b^2}} = 0.375$$

➤ *Buckling load factor (L_{cr})*

$$L_{cr} = \frac{1}{25.157}$$

$$L_{cr} = 0.04$$

The buckling stress can be estimated using the following equation:

$$q_f = \frac{\pi^2 D_{eq}}{a^2(f_1 + f_2)} L_{cr}$$

Hence, the buckling shear stress of sandwich panel with JFC intermediate layer is:

$$q_f = \frac{\pi^2 * 15901162.19}{300^2(0.5 + 0.5)} 0.04$$

$$q_f = 69.245 \text{ MPa}$$

A comprehensive discussion of the results is provided in Chapter 7.

Modified Hoff-Mautner Model:

In this effort, the basic equation obtained by Hoff and Mautner (1945) has been modified by taking into account the contribution of intermediate layer with the following equation:

$$\sigma = 0.5\sqrt[3]{E_f E_c G_c} + 0.5\sqrt[3]{E_i E_c G_c}$$

Calculations:**Data:**

$$\begin{aligned} E_f &= 68200 \text{ MPa} \\ E_i &= 4502 \text{ MPa} \\ E_c &= 7.25 \text{ MPa} \\ G_c &= 2.685 \text{ MPa} \end{aligned}$$

➤ *Contribution of face*

$$\begin{aligned} \sigma &= 0.5\sqrt[3]{E_f E_c G_c} \\ \sigma &= 0.5\sqrt[3]{68200 * 7.25 * 2.685} \\ \sigma &= 54.953 \text{ MPa} \end{aligned}$$

➤ *Contribution of intermediate layer*

$$\begin{aligned} \sigma &= 0.5\sqrt[3]{E_i E_c G_c} \\ \sigma &= 0.5\sqrt[3]{4502 * 7.25 * 2.685} \\ \sigma &= 22.209 \text{ MPa} \end{aligned}$$

Hence, the total shear buckling stress for hybrid sandwich panel with JFC intermediate layer is:

$$\begin{aligned} q_f &= 54.953 + 22.209 \text{ MPa} \\ &= 77.162 \text{ MPa} \end{aligned}$$

Modified Mamalis Model:

The calculation of theoretical shear buckling stress using Modified Mamalis Model is presented as follows (for hybrid panel with MDF intermediate layer):

Data:

$$\begin{aligned} E_f &= 68200 \text{ MPa} \\ E_i &= 2603 \text{ MPa} \\ G_i &= 1038.707 \text{ MPa} \\ L &= \sqrt{2} * 300 = 424 \text{ mm} \end{aligned}$$

The shear buckling stress for hybrid sandwich panel with MDF intermediate layer is:

$$\begin{aligned} \sigma &= \frac{t_i}{L} \sqrt[3]{E_f E_i G_i} \\ \sigma &= \frac{3}{424} \sqrt[3]{68200 * 2603 * 1038.707} \\ \sigma &= 40.27 \text{ MPa} \end{aligned}$$

Appendix C: Theoretical significance calculations

Example calculation of analysis of variance for medium scale sandwich panels:

Table C-1. Tabulated data for analysis of variance for medium scale sandwich panels

Factor levels	Medium Scale				Totals	Averages
	Observations					
	1	2	3	4		
Level 0 (CTR)	321	307	293	302	1223	305.75
Level 1 (JFC)	414	379	378	414	1584	396.25
Level 2 (HFC)	628	579	524	635	2366	591.50

Calculation:

$$SS_T = \sum_{i=1}^3 \sum_{j=1}^4 y_{ij}^2 - \frac{y^2 \dots}{N}$$

$$SS_T = (321)^2 + (307)^2 + \dots + (635)^2 - \left[\frac{5174^2}{12} \right]$$

$$SS_T = 180229.7$$

$$SS_{\text{treatments}} = \frac{1}{n} \sum_{i=1}^3 y_i^2 - \frac{y^2}{N}$$

$$SS_{\text{treatments}} = \frac{1}{4} [(1223)^2 + \dots + (2366)^2] - \left[\frac{5174^2}{12} \right]$$

$$SS_{\text{treatments}} = 170621.2$$

$$SS_E = SS_T - SS_{\text{treatments}}$$

$$SS_E = 180229.7 - 170621.2$$

$$SS_E = 9605.5$$

$$MS_{\text{treatments}} = \frac{SS_{\text{treatments}}}{a-1}$$

$$MS_{\text{treatments}} = \frac{170621.2}{3-1}$$

$$MS_{\text{treatments}} = 85310.58$$

Appendix-C

$$MS_E = \frac{SS_E}{(N - a)}$$

$$MS_E = \frac{9605.5}{(12 - 3)}$$

$$MS_E = 1067.611$$

$$F_0 = \frac{MS_{\text{treatments}}}{MS_E}$$

$$F_0 = \frac{85310.58}{1067.611}$$

$$F_0 = 79.91$$

The theoretical result of the analysis of variance for medium scale sandwich panels is summarized as follows:

Table C-2. The theoretical results of ANOVA for medium scale sandwich panels

Source of variations	Sum of square	Degrees of freedom	Mean square	F ₀
Intermediate layer	170621.20	2	85310.58	79.91
Error	9608.50	9	1067.61	
Total	180229.70	11		

A similar process was conducted to calculate the F₀ value of other experiment results and the results are tabulated as follows:

Table C-3. The theoretical results of ANOVA for large scale sandwich panels

Source of variations	Sum of square	Degrees of freedom	Mean square	F ₀
Intermediate layer	1432098.00	2	716049.10	73.42
Error	87778.75	9	9753.19	
Total	1519877.00	11		

Table C-4. The theoretical results of ANOVA for in-plane shear test

Source of variations	Sum of square	Degrees of freedom	Mean square	F ₀
Intermediate layer	4108937296.00	2	2054468648.00	560.73
Error	43967235.60	12	3663936.40	
Total	4152904532.00	14		

Appendix-C

$$MS_E = \frac{SS_E}{(N - a)}$$

$$MS_E = \frac{9605.5}{(12 - 3)}$$

$$MS_E = 1067.611$$

$$F_0 = \frac{MS_{\text{treatments}}}{MS_E}$$

$$F_0 = \frac{85310.58}{1067.611}$$

$$F_0 = 79.91$$

The theoretical result of the analysis of variance for medium scale sandwich panels is summarized as follows:

Table C-2. The theoretical results of ANOVA for medium scale sandwich panels

Source of variations	Sum of square	Degrees of freedom	Mean square	F ₀
Intermediate layer	170621.20	2	85310.58	79.91
Error	9608.50	9	1067.61	
Total	180229.70	11		

A similar process was conducted to calculate the F₀ value of other experiment results and the results are tabulated as follows:

Table C-3. The theoretical results of ANOVA for large scale sandwich panels

Source of variations	Sum of square	Degrees of freedom	Mean square	F ₀
Intermediate layer	1432098.00	2	716049.10	73.42
Error	87778.75	9	9753.19	
Total	1519877.00	11		

Table C-4. The theoretical results of ANOVA for in-plane shear test

Source of variations	Sum of square	Degrees of freedom	Mean square	F ₀
Intermediate layer	4108937296.00	2	2054468648.00	560.73
Error	43967235.60	12	3663936.40	
Total	4152904532.00	14		

Appendix D: Power Analysis and Determining Sample size

In this appendix, two different approaches in determining the size of samples are presented. The first approach is by conducting statistical power analysis which is the probability that it will correctly lead to the rejection of a false null hypothesis. Power refers to the probability that the test will find a statistically significant difference when such a difference actually exists. It is generally accepted that the power should be 0.8 or greater (<http://meera.snre.umich.edu>). A similar power value also noted by Mazen et al (1985), "a test with a power greater than 0.8 is considered statistically powerful". The second approach is by setting the power level and the desired detection level difference (δ). In this book, the desired detection level difference (δ) is termed as "minimum detectable difference", while in Minitab software it termed as "maximum difference".

According to Paulson (2003), the power of a one-factor, completely randomized Anova is conducted based upon the following equation:

$$\phi_c = \sqrt{\frac{n \sum_{i=1}^a (\mu_i - \mu)^2}{as^2}} \quad \dots\dots\dots (D.1)$$

Where

- ϕ_c : Statistical power value
- n : The replicate sample size
- s^2 : The variance, estimated by MS_E
- a : The number of treatment groups to be tested
- μ : The overall average population "common" value (estimated by $\bar{y} \dots$)
- μ_i : The population average for each treatment group (estimated by $\bar{y}_i \dots$)

Note that,

$$\mu = \frac{\sum_{i=1}^a \mu_i}{a} = \frac{\sum_{i=1}^a \bar{y}_i \cdot}{a} = \bar{y} \dots\dots\dots (D.2)$$

Hence,

$$\phi_c = \sqrt{\frac{n \sum_{i=1}^a (\bar{y}_i - \bar{y} \dots)^2}{a (MS_E)}} \quad \dots\dots\dots (D.3)$$

The power of statistic (ϕ_c) of the experimental results discussed in Chapter 8 can be obtained as follow:

For the flexural test using medium size sample with the following arrangement:

Table D.1. Tabulated data for analysis of variance (Anova) of medium scale specimens

Factor levels	Medium Scale				Totals	Averages
	Observations					
	1	2	3	4		
Level 0 (CTR)	321	307	293	302	1223	305.75
Level 1 (JFC)	414	379	378	414	1584	396.25
Level 2 (HFC)	628	579	524	635	2366	591.50

Table D.2. The theoretical results of Anova for medium scale sandwich panels

Source of variations	Sum of square	Degrees of freedom	Mean square	F ₀
Intermediate layer	170621.20	2	85310.58	79.91
Error	9608.50	9	1067.61	
Total	180229.70	11		

It can be obtained that:

a	:	3
n	:	4
s ²	:	MS _E = 1067.61
MS _{treatments}	:	85310.58
α	:	0.05
v ₁	:	a-1 = 2
v ₂	:	a(n-1) = 9
Stdv	:	32.67

Calculation:

$$\sum_{i=1}^a (\bar{y}_i - \bar{y} \dots)^2 = (305.75 + 431.16)^2 + (396.25 - 431.16)^2 + (591.5 \pm 431.16)^2$$

$$\sum_{i=1}^a (\bar{y}_i - \bar{y} \dots)^2 = 42655.28$$

$$\phi_c = \sqrt{\frac{4 * 42655.28}{4 * 1067.61}}$$

$$= 7.29$$

From the tabled power value (Paulson, 2003), when v₁ = 2, v₂ = 9, α = 0.05, and φ_c = 7.29, the statistic power value (1 - β) is greater than 0.99. This result clearly shows that 4 replications for each level of factor are sufficient to draw a significance inference. The calculation process may also use the following equation:

$$\begin{aligned} \phi_c &= \sqrt{\frac{(a - 1)(MS_{\text{treatments}} - MS_E)}{a (MS_E)}} \dots\dots\dots (D.4) \\ &= \sqrt{\frac{(3 - 1)(85310.58 - 1067.61)}{3 (1067.61)}} \\ &= 7.25 \end{aligned}$$

Using the same process with the previous method, it is clear that “an n of 4” is sufficient. The testing arrangement and the results of Anova for flexural test in large scale and in-plane shear test are presented in the following tables:

Table D.3. Tabulated data for analysis of variance (Anova) of large scale specimens

Large Scale						
Factor levels	Observations				Totals	Averages
	1	2	3	4		
Level 0 (CTR)	489	572	518	407	1986	496.50
Level 1 (JFC)	898	751	842	738	3229	807.25
Level 2 (MDF)	1241	1537	1275	1281	5334	1333.50

Table D.4. The theoretical results of Anova for large scale sandwich panels

Source of variations	Sum of square	Degrees of freedom	Mean square	F ₀
Intermediate layer	1432098.00	2	716049.10	73.42
Error	87778.75	9	9753.19	
Total	1519877.00	11		

Table D.5. Tabulated data for analysis of variance (Anova) of the in-plane shear test

Factor levels	Observations					Totals	Averages
	1	2	3	4	5		
Level 0 (CTR)	9228	10043	13575	9051	9367	51264	10252.8
Level 1 (JFC)	49006	47921	53834	51127	47192	249080	49816.0
Level 2 (MDF)	21809	22324	22442	22366	22908	111849	22369.8

Table D.6. The theoretical results of ANOVA for in-plane shear test

Source of variations	Sum of square	Degrees of freedom	Mean square	F ₀
Intermediate layer	4108937296.00	2	2054468648.00	560.73
Error	43967235.60	12	3663936.40	
Total	4152904532.00	14		

The analysis results obtained by Equation 3 and 4 for all experimental arrangements are tabulated as follow:

Table D.7. Statistical power value of each testing arrangement

	Φ_c (Eq. 3)	Φ_c (Eq. 4)	(1- β)
Flexural test medium size	7.29	7.25	≥ 0.99
Flexural test large size	6.99	6.94	≥ 0.99
In-plane shear test	18.71	13.65	≥ 0.99

Clearly, the statistical power value (1 – β) for all experimental arrangements are greater than 0.99 meaning that the results drawn from 4 replications are considered as statistically powerful.

The second approach is by setting the power level and the desired detection level difference (δ). The process of determining sample size using this approach is available in Minitab software. As suggested above, the power should be 0.8 or greater. The desired detection level difference or the minimum/maximum detectable difference can be obtained as per Equation D.4 (Paulson, 2003).

$$\delta = \sqrt{\frac{2as^2 \phi_c^2}{n}} \dots\dots\dots (D.5)$$

For the flexural test using medium size sample, the following data are obtained:

a	:	3
n	:	4
s ²	:	MS _E = 1067.61
MS _{treatments}	:	85310.58
α	:	0.05
v ₁	:	a-1 = 2
v ₂	:	a(n-1) = 9
Stdv	:	32.67
1- β	:	0.80
β	:	0.20

From the tabled power value, when v₁= 2, v₂ = 9, α = 0.05, and (1 – β) = 0.8, the ϕ_c = 2.15. Using Equation D.5, the desired detection level difference can be obtained as follow:

$$\delta = \sqrt{\frac{2 * 3 * 1067.61 * (2.15)^2}{4}}$$

$$= 86$$

Appendix-D

Now, all the above obtained values are inserted in the ‘power sample size’ analysis in Minitab 15 as presented in Figure D.1. The results of the analysis are presented in Figure D.2 and Table D.8.

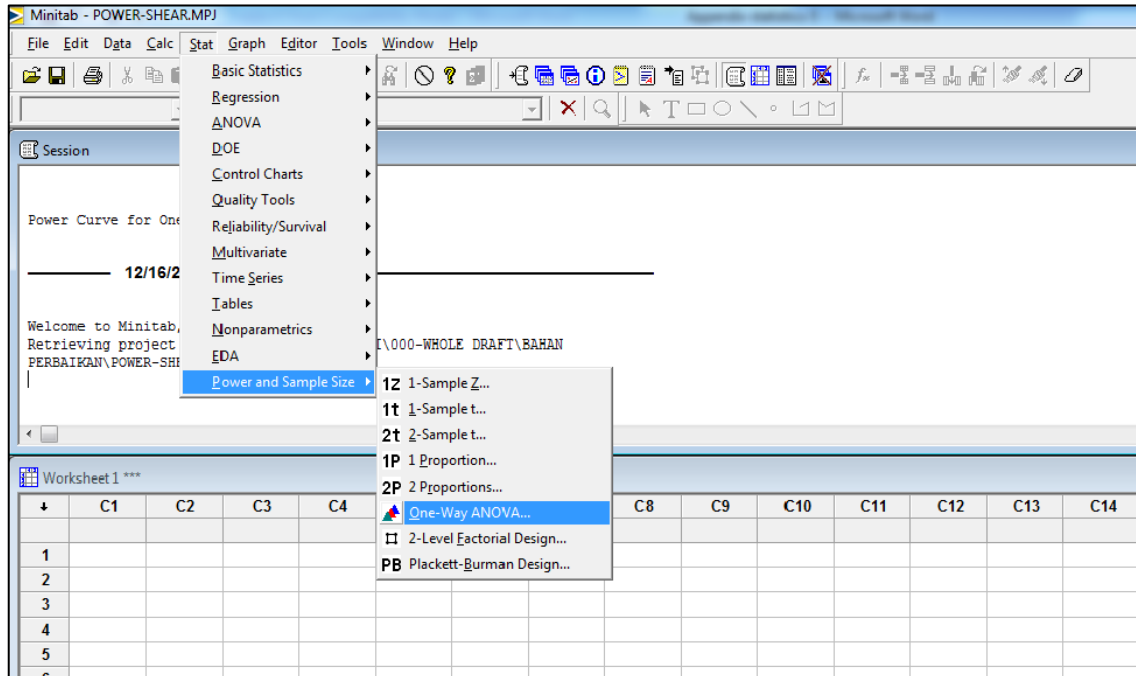


Figure D.1. Conducting power and sample size analysis in Minitab 15

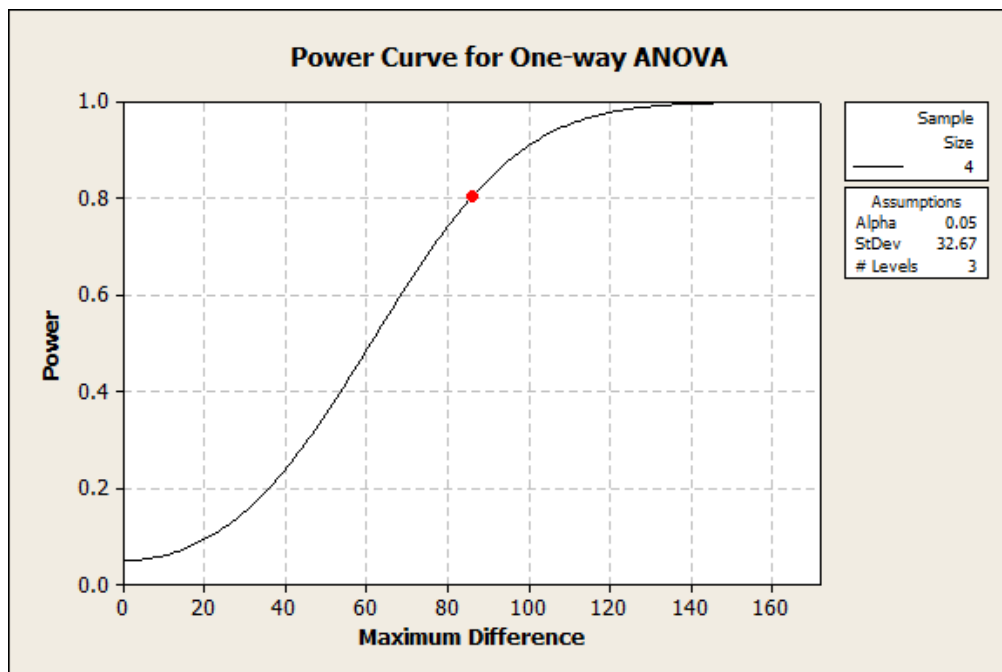


Figure D.2. The power curve for one-way Anova of flexural test with medium scale specimens

Table D.8. The script of power and sample size analysis of the flexural test with medium scale specimens using Minitab software

Power and Sample Size				
One-way ANOVA				
Alpha = 0.05 Assumed standard deviation = 32.67 Number of Levels = 3				
	Sample	Target		Maximum
SS Means	Size	Power	Actual Power	Difference
3698	4	0.8	0.804608	86
The sample size is for each level.				

It clearly shown on the above table that with the target power of 0.8 and the desired detection level difference of 86, the required number of sample or the sample size is 4 units or 4 replications. The analysis results for the flexural test of large scale specimens and in-plane shear test are presented in the following figures.

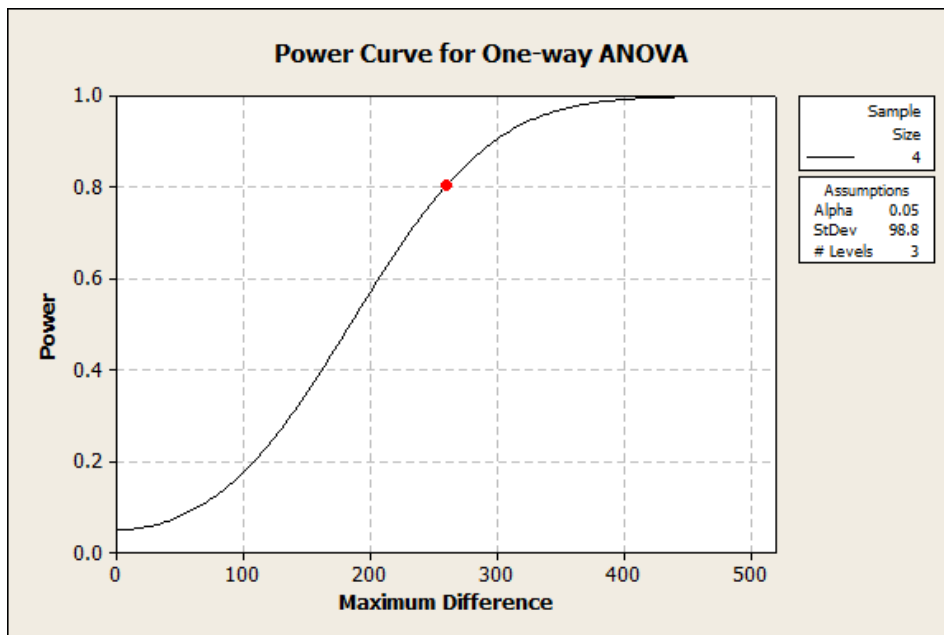


Figure D.3. The power curve for one-way Anova of flexural test with large scale specimens

Table D.9. The script of power and sample size analysis of the flexural test with large scale specimens using Minitab software

Power and Sample Size					
One-way ANOVA					
Alpha = 0.05 Assumed standard deviation = 98.8 Number of Levels = 3					
SS Means	Sample Size	Target Power	Actual Power	Maximum Difference	
33800	4	0.8	0.804358	260	
The sample size is for each level.					

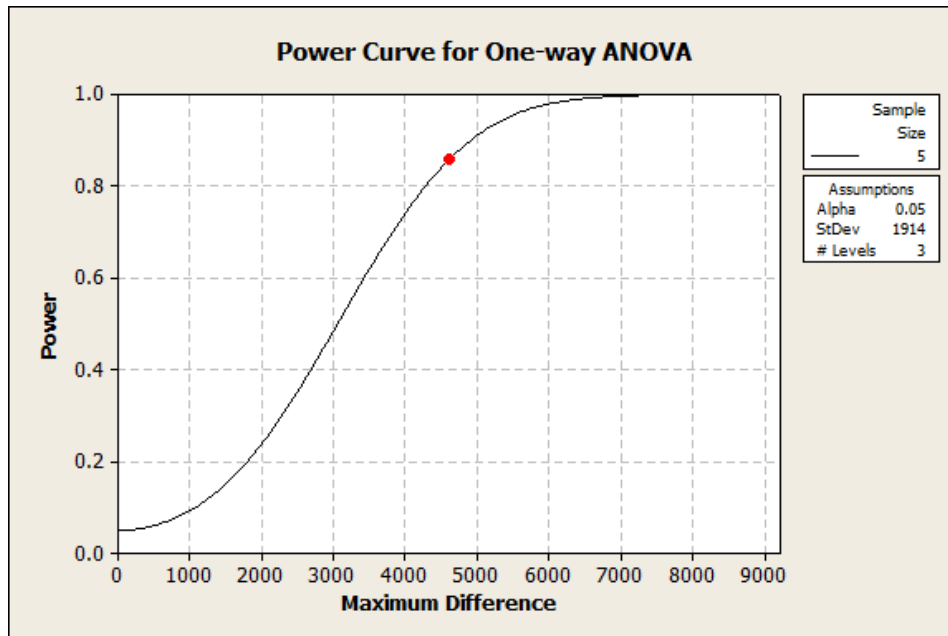
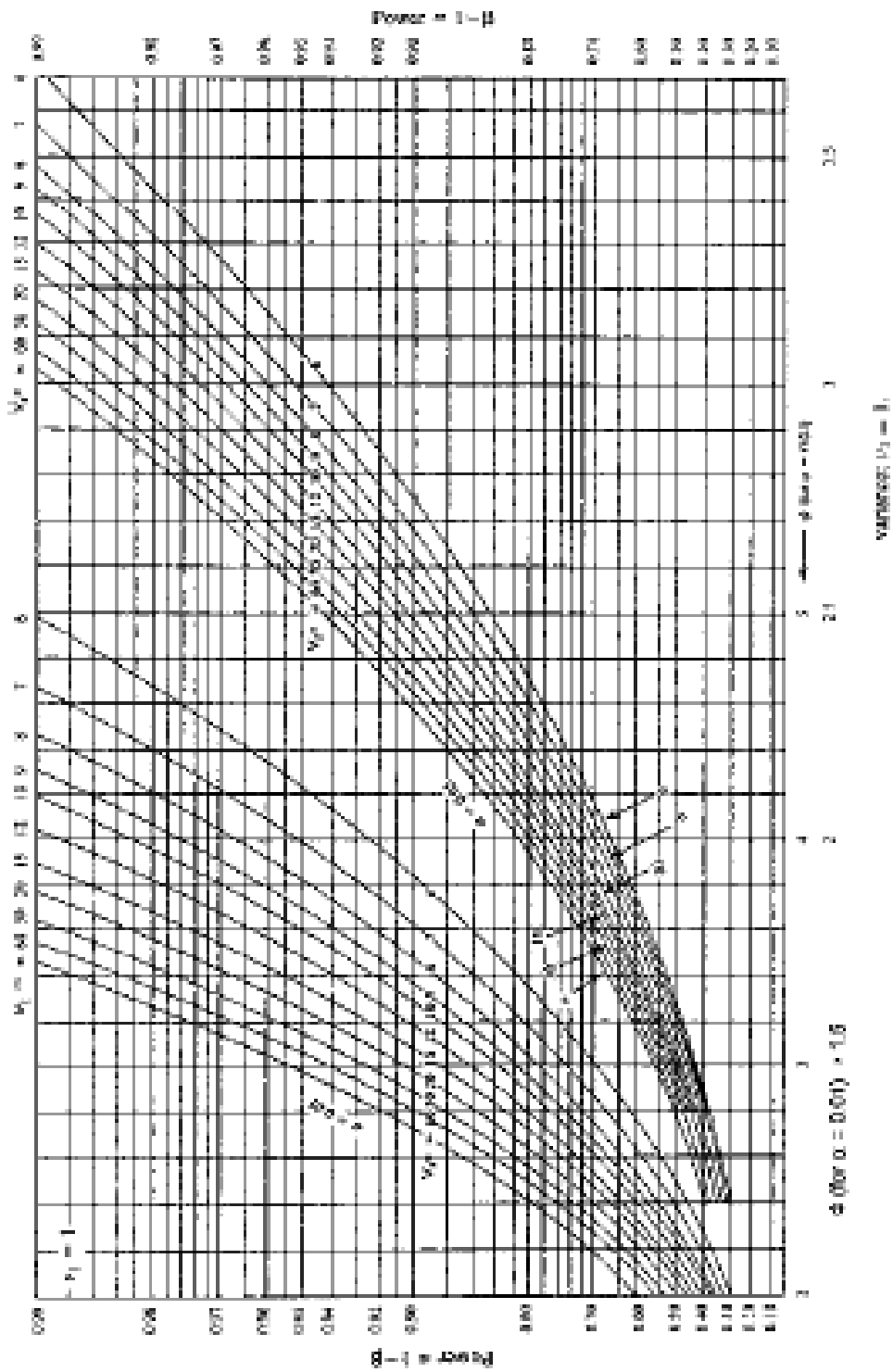


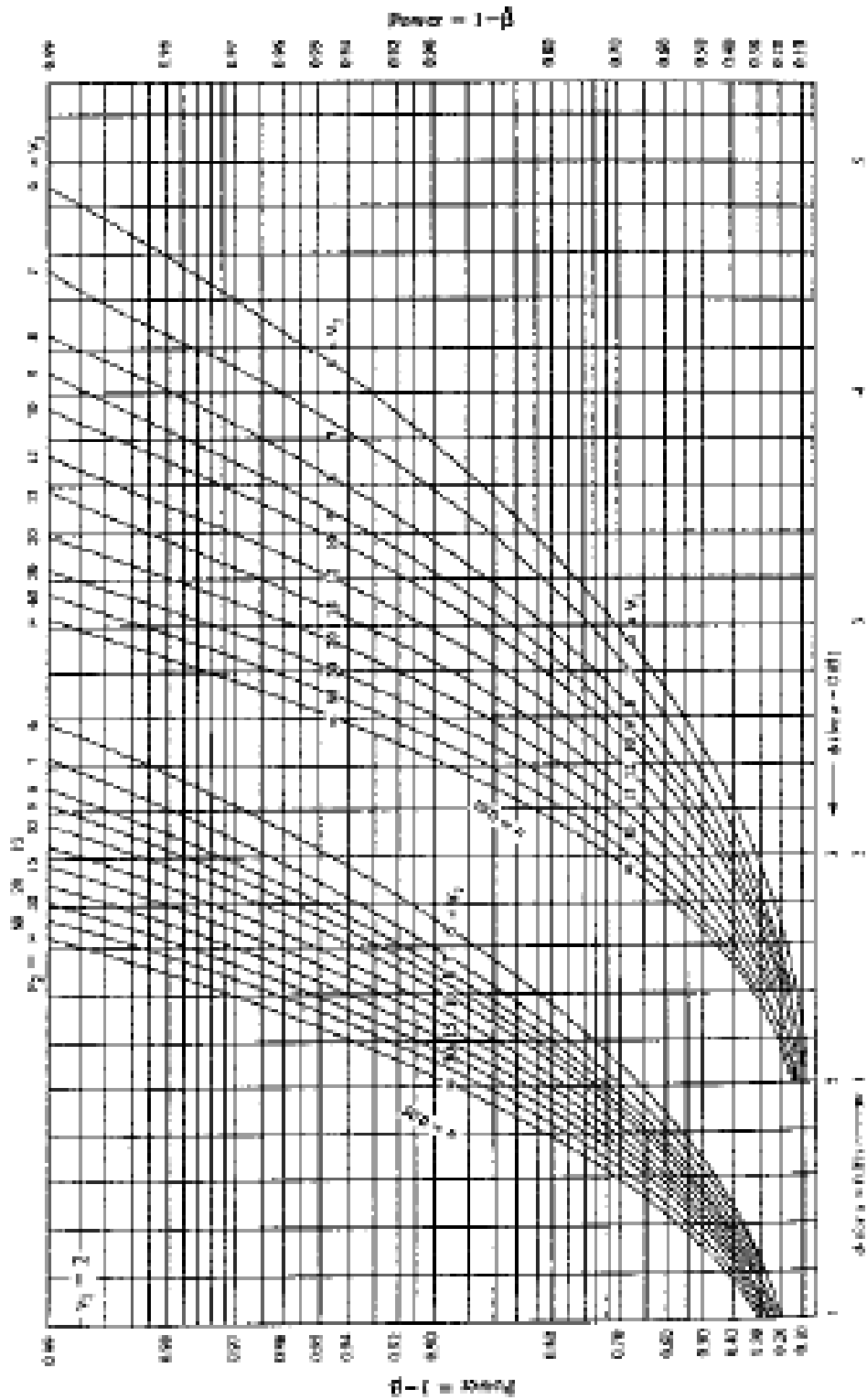
Figure D.4. The power curve for one-way Anova of in-plane shear test

Table D.10. The script of power and sample size analysis of the In-plane shear test

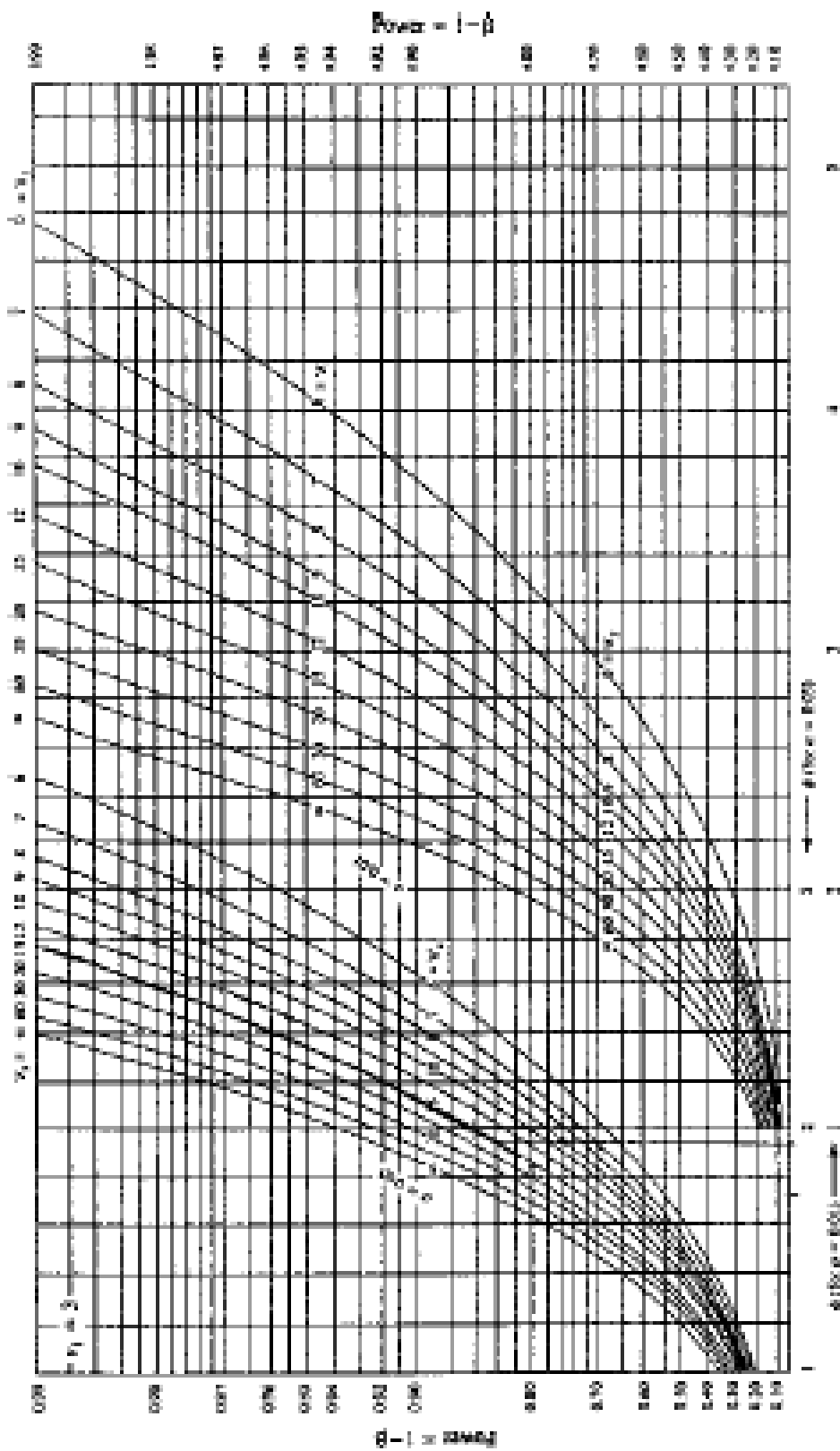
Power and Sample Size					
One-way ANOVA					
Alpha = 0.05 Assumed standard deviation = 1914 Number of Levels = 3					
SS Means	Sample Size	Target Power	Actual Power	Maximum Difference	
10639885	5	0.8	0.858193	4613	
The sample size is for each level.					



A.4.1. Power and sample size in analysis of variance; $r_1=1$.



A.4.2. Power and sample size in analysis of variance; $r_1=2$.



A.4.3. Power and sample size in analysis of variance; $r_1=3$.